

CHRIS CHAPMAN

Fundamentals of Seismic Wave Propagation

The background of the cover features an abstract geometric diagram illustrating seismic wave propagation. It consists of several intersecting lines and curves. A series of parallel horizontal lines are intersected by several diagonal lines that slope upwards from left to right. Some of these diagonal lines are solid, while others are dashed. A prominent dashed line forms a V-shape, opening upwards, with its vertex located in the lower right quadrant. The overall color scheme is a gradient of warm tones, ranging from deep reds and oranges to bright yellows, with a pattern of overlapping circles in the background.

CAMBRIDGE

FUNDAMENTALS OF SEISMIC
WAVE PROPAGATION:
Solutions to Exercises

CHRIS H. CHAPMAN

Schlumberger Cambridge Research
Copyright © C.H. Chapman, 2008.

This document contains solutions to the exercises in *Fundamentals of Seismic Wave Propagation* with cross-references to equations and the bibliography in the text. Solutions for the programming exercises are provided in Matlab (Matlab is a trademark of MathWorks, Inc.). These programs have been written to be simple, and straightforward to read and understand. They are not necessarily particularly efficient, nor do they contain all the desirable features that would check parameters and handle special cases. The plots are simple without cosmetic additions. It would be easy to include these extras features but often they require a disproportionate amount of code and complication. For brevity, these extras are omitted.

This version contains errata, addenda and revisions to 3 January 2008.

2

Basic wave propagation

2.1

Confirm that the standard, simple algebraic expression (2.5.20) for the travel time along a circular arc, reduces to the numerically robust expression (2.5.23). In turn show that this reduces to the vector expression (2.5.34).

The standard results we need are

$$\frac{d}{dx} \tanh^{-1} x = \frac{1}{1-x^2} \quad \text{and} \quad \tanh^{-1} x = \frac{1}{2} \ln \left(\frac{1+x}{1-x} \right).$$

Confirming expression (2.5.20) by differentiation

$$\frac{d}{d\psi} \tanh^{-1}(\sin \psi) = \frac{\cos \psi}{1 - \sin^2 \psi} = \sec \psi.$$

Confirming expression (2.5.22)

$$\tanh^{-1}(\sin \psi) = \frac{1}{2} \ln \left(\frac{1 + \sin \psi}{1 - \sin \psi} \right) = \frac{1}{2} \ln \frac{(1 + \sin \psi)^2}{1 - \sin^2 \psi} = \ln \left(\frac{1 + \sin \psi}{\cos \psi} \right).$$

Now

$$\frac{1 + \sin \psi}{\cos \psi} = \frac{\left(\cos \frac{\psi}{2} + \sin \frac{\psi}{2} \right)^2}{\cos^2 \frac{\psi}{2} - \sin^2 \frac{\psi}{2}} = \frac{\cos \frac{\psi}{2} + \sin \frac{\psi}{2}}{\cos \frac{\psi}{2} - \sin \frac{\psi}{2}} = \frac{1 + \tan \frac{\psi}{2}}{1 - \tan \frac{\psi}{2}},$$

so the definite integral is

$$\begin{aligned} \Delta T &= \frac{1}{|c'|} \ln \frac{(1 + \sin \psi_1) \cos \psi_0}{(1 + \sin \psi_0) \cos \psi_1} \\ &= \frac{1}{|c'|} \ln \frac{\left(1 + \tan \frac{\psi_1}{2} \right) \left(1 - \tan \frac{\psi_0}{2} \right)}{\left(1 - \tan \frac{\psi_1}{2} \right) \left(1 + \tan \frac{\psi_0}{2} \right)} \end{aligned}$$

$$= \frac{1}{|c'|} \ln \left(\frac{1+y}{1-y} \right) = \frac{2}{|c'|} \tanh^{-1} y,$$

where

$$\begin{aligned} y &= \frac{\tan \frac{\psi_1}{2} - \tan \frac{\psi_0}{2}}{1 - \tan \frac{\psi_1}{2} \tan \frac{\psi_0}{2}} \\ &= \frac{\sin \frac{\psi_1}{2} \cos \frac{\psi_0}{2} - \cos \frac{\psi_1}{2} \sin \frac{\psi_0}{2}}{\cos \frac{\psi_1}{2} \cos \frac{\psi_0}{2} - \sin \frac{\psi_1}{2} \sin \frac{\psi_0}{2}} = \frac{\sin \frac{\psi_1 - \psi_0}{2}}{\cos \frac{\psi_1 + \psi_0}{2}} \\ &= \frac{2 \sin \frac{\psi_1 - \psi_0}{2} \cos \frac{\psi_1 - \psi_0}{2}}{2 \cos \frac{\psi_1 + \psi_0}{2} \cos \frac{\psi_1 - \psi_0}{2}} = \frac{\sin(\psi_1 - \psi_0)}{\cos \psi_0 + \cos \psi_1}, \end{aligned}$$

confirming expression (2.5.24).

Finally

$$\begin{aligned} y &= \frac{R |c'| \sin(\psi_1 - \psi_0)}{R |c'| \cos \psi_0 + R |c'| \cos \psi_1} \\ &= \frac{R |c'| |\hat{\mathbf{p}}_0 \times \Delta \hat{\mathbf{p}}|}{c_0 + c_1} \end{aligned}$$

as the angle between the ray directions $\hat{\mathbf{p}}_0$ and $\hat{\mathbf{p}}_1$ is $\psi_1 - \psi_0$, and $c = R |c'| \cos \psi$ from the linear velocity function ($R \cos \psi$ is the ‘vertical’ distance from zero velocity at the arc centre). Using expression (2.5.33) in the numerator

$$R \hat{\mathbf{p}}_0 \times \Delta \hat{\mathbf{p}} = \hat{\mathbf{p}}_0 \times (\hat{\mathbf{j}} \times \Delta \mathbf{x}) = \hat{\mathbf{j}} (\hat{\mathbf{p}}_0 \cdot \Delta \mathbf{x}) - \Delta \mathbf{x} (\hat{\mathbf{p}}_0 \cdot \hat{\mathbf{j}}),$$

using the standard expansion for the triple vector cross product. As $\hat{\mathbf{p}}_0$ and $\hat{\mathbf{j}}$ are perpendicular, the final term is zero, and we obtain result (2.5.34). The expression

$$\Delta T = \frac{2}{|c'|} \tanh^{-1} y = \frac{2}{|c'|} \tanh^{-1} \left(\frac{|c'| \hat{\mathbf{p}}_0 \cdot \Delta \mathbf{x}}{c_0 + c_1} \right),$$

is simpler than most that have appeared in the literature.

2.2

Examples of other two-parameter velocity functions for which algebraic results are known are $c(r) = a - br^2$ (a circular ray) and $c(z) = a \exp(bz)$. Obtain algebraic expressions for the range and travel time for a ray in these velocity functions.

Show that $c(z) = a \exp(bz)$ is equivalent to $c(r) = ar^b$ via the Earth

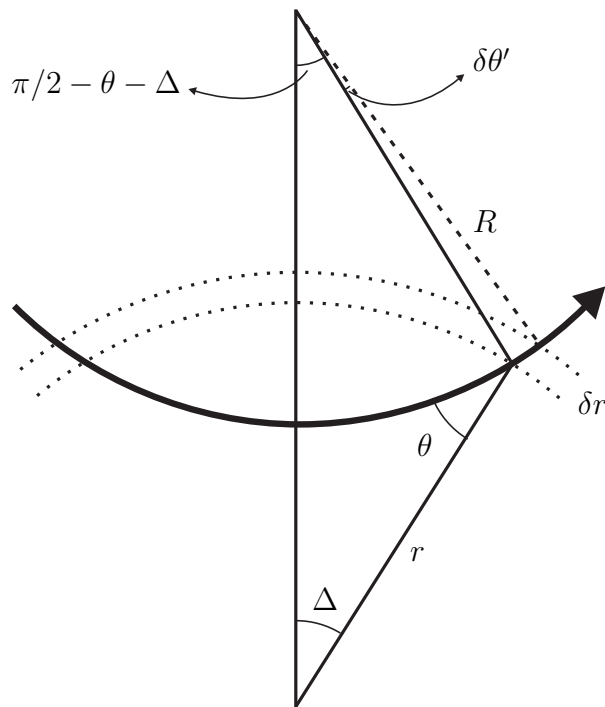
flattening transformation (this velocity distribution is sometimes known as the Mohorovičić velocity function).

Further reading: The constant gradient functions in velocity (Section 2.5.2.1) and slowness-squared (Section 2.5.2.2) can be generalized to constant gradient functions of $c^{-n}(z)$ or $\ln(c(z))$. These have been discussed by Červený (2001, Section 3.7).

The velocity function $c(r) = a - br^2$ in a spherical Earth is discussed by Bullen (1963, pp. 122–3). We follow a similar approach. We denote the conserved Bullen parameter (2.3.31) by

$$p' = r_0 p_\Delta = \frac{r \sin \theta(r)}{c(r)}.$$

Consider a ray arc between radii r and $r + \delta r$ (see figure).



A circular ray arc in a spherical model.

Even if the medium were homogeneous and the ray straight, the angle θ

would decrease by

$$\delta\theta = -\tan\theta \frac{\delta r}{r}.$$

In an inhomogeneous medium, we would have (by differentiating the expression for p')

$$r \cos\theta \delta\theta = \left(p' \frac{dc}{dr} - \sin\theta \right) \delta r,$$

and the extra change in angle

$$\delta\theta' = \frac{p'}{r \cos\theta} \left| \frac{dc}{dr} \right| \delta r,$$

is the angle subtended by the arc at the centre of curvature (see figure). The arc length is $\delta s = \sec\theta \delta r = R \delta\theta'$ so the radius of curvature is

$$R = \frac{\delta s}{\delta\theta'} = -\frac{r}{p'} \frac{dr}{dc}.$$

If the velocity is $c(r) = a - br^2$, this reduces to

$$R = \frac{1}{2p'b},$$

a constant, so the ray is circular.

Measuring the angular range Δ from the line joining the centre of the Earth to the centre of the ray arc, and applying the sine rule to the triangle formed by the centres and the ray point, we have

$$\frac{\sin\Delta}{R} = \frac{\cos(\theta + \Delta)}{r}.$$

Rearranging we have

$$\Delta = \tan^{-1} \left(\frac{\cot\theta}{\nu} \right),$$

where

$$\nu(r) = \frac{2a}{c(r)} - 1.$$

Knowing the radius r , we can calculate the velocity $c(r)$ and $\nu(r)$, and for a given ray parameter p' , the angle $\theta(r)$. Hence we can calculate the range, Δ .

Comparing expressions (2.3.14), (2.3.27) and (2.3.31), we have that

$$p' = \frac{dT}{d\Delta},$$

for the differential of the travel-time function at fixed radius. Thus differentiating the above result for Δ (ν is fixed)

$$\begin{aligned} dT &= p' d\Delta \\ &= \frac{r \sin \theta}{c} \frac{\nu}{\nu^2 + \cot^2 \theta} \operatorname{cosec}^2 \theta d\theta. \end{aligned}$$

Integrating this, we obtain

$$T = \frac{r}{c\sqrt{\nu^2 - 1}} \ln \left(\frac{\nu + \sqrt{\nu^2 - 1} \cos \theta}{\nu - \sqrt{\nu^2 - 1} \cos \theta} \right).$$

It is possible to substitute for $\cos \theta$ in terms of Δ and reduce to a travel-time function, $T(\Delta)$, which is sometimes useful.

If $c(z) = a \exp(bz)$, then

$$q^2(p, z) = a^{-2} e^{-2bz} - p^2.$$

Thus

$$q dq = -b a^{-2} e^{-2bz} dz = -b(q^2 + p^2) dz.$$

Thus expression (2.3.7) reduces to

$$X = \int \frac{p}{q} dz = -\frac{1}{b} \int \frac{p}{q^2 + p^2} dq = \left\| \frac{1}{b} \tan^{-1} \left(\frac{q}{p} \right) \right\|,$$

and expression (2.3.8) to

$$T = \int \frac{1}{c^2 q} dz = -\frac{1}{b} \int \frac{1}{q} dq = \left\| \frac{1}{b} \ln q \right\|.$$

Using expressions (2.3.29) and (2.3.30)

$$c(r) = \frac{r}{r_0} c(z) = \frac{r}{r_0} a e^{bz} = \frac{r}{r_0} a e^{br_0 \ln(r/r_0)} = \frac{r}{r_0} a \left(\frac{r}{r_0} \right)^{br_0} = a' r^{b'},$$

where

$$a' = \frac{a}{r_0^{1+br_0}} \quad \text{and} \quad b' = 1 + br_0.$$

Hence $c(z) = a \exp(bz)$ and $c(r) = a' r^{b'}$ are equivalent.

2.3

Many two-parameter velocity functions are known with algebraic results (see the previous exercise) which can be used to approximate a general discretized velocity function. However, these suffer from the disadvantage that the function dX/dp has singularities due to each gradient discontinuity (see Figure 2.24). A three-parameter velocity function, $c^{-2}(z) = a + bz + cz^2$, a parabolic layer, has been discussed by Červený (2001, Section 3.7) — see also Kravtsov and Orlov (1990), and references therein. This has the advantage that, in principle at least, gradient continuity can be obtained. Obtain the algebraic results for this function.

With $c^{-2}(z) = a + bz + cz^2$, we have for expression (2.3.15)

$$\begin{aligned}\tau &= \int \left(a + bz + cz^2 - p^2 \right)^{1/2} dz \\ &= \int \left(\left(\sqrt{c}z + \frac{b}{2\sqrt{c}} \right)^2 + \left(a - \frac{b^2}{4c} - p^2 \right) \right)^{1/2} dz.\end{aligned}$$

Letting

$$x = \sqrt{c}z + \frac{b}{2\sqrt{c}},$$

we have

$$\tau = \frac{1}{\sqrt{c}} \int \left(x^2 + A \right)^{1/2} dx,$$

where

$$A = a - \frac{b^2}{4c} - p^2.$$

If $A > 0$, let $x = A^{1/2} \sinh \theta$ and

$$\tau = \frac{A}{\sqrt{c}} \int \cosh^2 \theta d\theta = \frac{A}{4\sqrt{c}} (\sinh 2\theta + 2\theta)|.$$

Similarly if $A < 0$, let $x = (-A)^{1/2} \cosh \theta$ and

$$\tau = \frac{(-A)}{\sqrt{c}} \int \sinh^2 \theta d\theta = \frac{A}{4\sqrt{c}} (\sinh 2\theta - 2\theta)|.$$

The range and travel-time functions can then be obtained using expressions (2.3.16) and (2.3.17).

2.4

Programming exercise: Figures 2.18 to 2.28 were drawn using a relative simple Matlab program. Write a program to compute the travel-time functions in which it is easy to change the velocity function and type of ray.

Hint: The ray can be defined using a structure array (struct) which defines the sequence of ray segments — the type, depth limits, etc. The integrals can all be calculated using the function quad where the required integrand function is passed as an argument. The velocity function — the model — can be defined by a function whose name is known to the integrand routines.

The model is defined by a function returning the slowness and slowness gradient, and by defining a global variable with the function name. The slowness and its gradient can then be computed for the model using the eval statement. Thus a model with a linear velocity function can be defined by

```
function [ u, dudz ] = linear( z )
% LINEAR = slowness and gradient at z values
%           for a linear velocity a+bz

% For internal use in tt_integrals for Exercise 2.4
%
% INPUT:  z          = z values
%
% GLOBAL: layer      = layer in model
%          raytype    = ray type flag P or S
%          aa         = velocity at z=0
%          bb         = velocity gradient
%
% OUTPUT: u          = slownesses
%          dudz       = slowness gradients
%
% Note:
% model parameters must be in global;
% function name is global variable model;
% z coordinates are measured upwards.
%
global layer raytype aa bb
%
u      = 1./(aa+bb*z);
```

```
dudz = -bb*u.*u;
return
```

and the code

```
global model
model = 'linear';
eval([ '[ u, dudz ] = ' model '( z );' ] );
```

used to define and query the model for the travel-time integrals. In general, the code for the model function will be more complicated and will need to discriminate depth range (**layer**) and ray types (**raytype**). The model parameters are global variables. A simple function

```
function q = verticalslowness( u )
% VERTICALSLOWNESS = vertical slowness (2.3.10) for
%                      slowness values u

% For internal use in tt_integrals for Exercise 2.4
%
global p                      % horizontal slowness
%
q = sqrt((u-p).*(u+p));
return
```

computes the vertical slowness, $q(p, z)$ (2.3.10). The horizontal slowness, p (2.3.9), is a global variable.

The following are three functions that return the integrands of the range (2.3.7), time (2.3.8) and intercept-time (2.3.15) integrals. The model name and horizontal slowness, p , are global variables.

```
function dx = range( z )
% RANGE = range integrand (2.3.7) at z values

% For internal use in tt_integrals for Exercise 2.4
%
global p model
%
eval([ '[ u, dudz ] = ' model '( z );' ] );
dx = p./vertical_slowness( u );
return

function dt = time( z )
```

```

% TIME = time integrand (2.3.8) at z values

% For internal use in tt_integrals for Exercise 2.4
%
global model
%
eval([ '[ u, dudz ] = ' model '( z );' ] );
dt = u.^2./ vertical_slowness( u );
return

function dtau = tau( z )
% TAU = time integrand (2.3.15) at z values

% For internal use in tt_integrals for Exercise 2.4
%
global model
%
eval([ '[ u, dudz ] = ' model '( z );' ] );
dtau = vertical_slowness( u );
return

```

If a turning point exists in the depth range we must detect this, revise the range of the integral so the lower limit is the turning point, and change the variable of integration to remove the singularity. To detect a turning point, we simply compare the slowness with the horizontal slowness. A turning point must exist if the following function returns a negative value.

```

function ump = turning( z )
% TURNING = 1/v(z) - p at z value

% For internal use in tt_integrals for Exercise 2.4
%
global p model
%
eval([ '[ u, dudz ] = ' model '( z );' ] );
ump = u-p;
return

```

If a turning point, $z(p)$, exists, we change the variable of integration to

$$y = (z - z(p))^{1/2},$$

so

$$dz = 2y dy = 2(z - z(p))^{1/2} dy.$$

The following functions provide the range, time and intercept-time integrands with respect to the variable y (removing the singularity of the range and time integrals, and making the intercept integrand approximately linear). The turning point is a global variable.

```
function dx = turnrange( y )
% TURNRANGE = range integrand (2.3.7) at y values with
%           variable change to y=sqrt(z-zp)

% For internal use in ttintegrals for Exercise 2.4
%
global p zp model
%
dx = zeros(size(y));
for i = 1:length(y)
    z = zp+y(i)^2;
    eval([ ' [ u, dudz ] = ' model '( z );' ]);
    if y(i) > 0.
        dx(i) = 2*y(i)*p/verticalslowness( u );
    else
        dx(i) = sqrt(2*p/dudz );           % l'Hopital rule at zp
    end
end
return

function dt = turntime( y )
% TURNTIME = time integrand (2.3.8) at y values with
%           variable change to y=sqrt(z-zp)

% For internal use in ttintegrals for Exercise 2.4
%
global zp model
%
dt = zeros(size(y));
for i = 1:length(y)
    z = zp+y(i)^2;
    eval([ ' [ u, dudz ] = ' model '( z );' ]);
    if y(i) > 0.
```



```

    dt(i) = 2*y(i)*u^2/verticalslowness( u );
else
    dt(i) = u*sqrt(2*u/dudz);    % l'Hopital rule at zp
end
end
return

function dtau = turntau( y )
% TURNTAU = tau integrand (2.3.15) at y values with
%          variable change to y=sqrt(z-zp)

% For internal use in ttintegrals for Exercise 2.4
%
global zp model
%
z = zp+y.^2;
eval([ '[ u, dudz ] = ' model '( z );' ] );
dtau = 2*y.*verticalslowness( u );
return

```

Using the above functions, the following function integrates the range (2.3.7), time (2.3.8) and intercept-time (2.3.15) integrals for a ray segment that may end at a turning point. It is assumed that only one turning point can exist and that it is at the lower limit of the ray.

```

function [ dx, dt, dtau ] = ttsegment( z )
% TTSEGMENT = travel-time integrals for segment

% INPUT:  z(2)          = depths defining segment
%
% OUTPUT: dx            = range integral for segment
%          dt            = time integral for segment
%          dtau          = intercept time integral for segment
%
% Note:
% for use by tt_integrals;
% z may be larger array but just max and min used;
% segment integrals always positive whatever z order;
% z must be vertically upwards with possible turning point
% at bottom of segment (not top);
%

```

```

global zp
% depth limits of segment for positive contribution
zmin=min(z);
zmax=max(z);
% turning point above top of layer so no contribution
if turning( zmax ) < 0.
    dx =0.;
    dt =0.;
    dtau=0.;
% no turning point
elseif turning( zmin ) > 0.
    dx = quad( @range, zmin, zmax );
    dt = quad( @time, zmin, zmax );
    dtau = quad( @tau, zmin, zmax );
% turning point within layer
else
    zp = fzero( @turning, z );
    y2 = sqrt(zmax-zp);
    dx = quad( @turnrange, 0., y2 );
    dt = quad( @turntime, 0., y2 );
    dtau = quad( @turntau, 0., y2 );
end
return

```

The following function then combines multiple segments for multiple values of the horizontal slowness.

```

function [ x, t, tau ] = ttintegrals( hslow , segment )
% TTINTEGRALS = travel-time integrals for rays defined by
%               segment for horizontal slownesses hslow

% INPUT:  hslow      = horizontal slownesses
%         segment    = struct defining ray segments
%
% OUTPUT: x          = ranges
%         t          = times
%         tau        = intercept times
%
global p layer raytype
%
x = zeros(size(hslow)); t = x; tau = x;

```

```

% loop over horizontal slownesses
for i = 1:length(hslow)
    p = hslow(i);
    % loop over ray segments
    for j=1:length(segment)
        % set layer and raytype which may be used in model
        layer = segment(j).layer;
        raytype = segment(j).raytype;
        % do travel-time integrals for segment
        [ dx, dt, dtau ] = ...
            ttsegment( [segment(j).zstart segment(j).zend] );
        x(i) = x(i)+dx;
        t(i) = t(i)+dt;
        tau(i) = tau(i)+dtau;
    end
end
return

```

Finally, here is a simple main program in the constant gradient model with reflections and turning rays. For more complicated rays in a more complicated model, just the model function and the specification of the ray segments need elaborating.

```

function Exercise24
% Exercise 2.4
%
% set up model functions and model parameters
global model
% example for linear gradient
model='linear';
% simple example with velocity increasing from 1 to 2
global aa bb
aa = 1;
bb = -1;
za = 0;
zb = -1;
% slowness range
eval([ '[ pa, dudz ] = ' model '( za );' ]);
eval([ '[ pb, dudz ] = ' model '( zb );' ]);
% define sequence of ray segments
% zstart and zend are start and end depth ranges

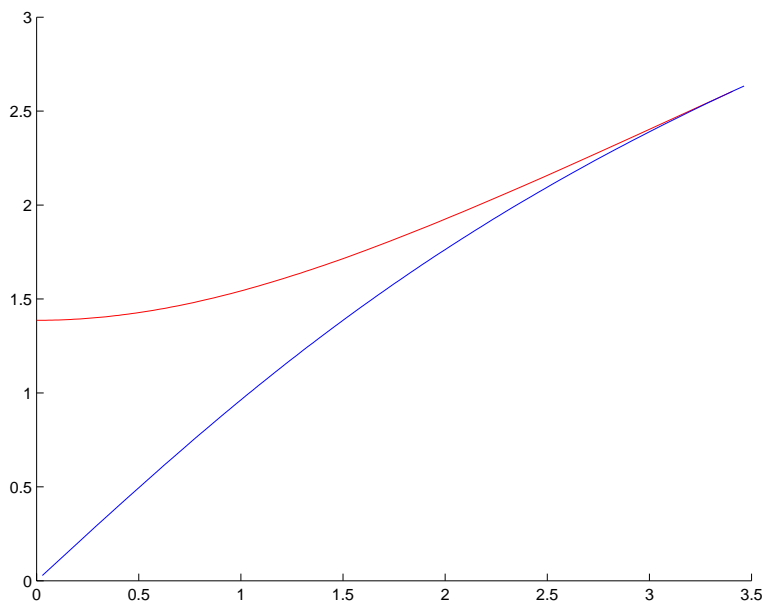
```

```

% raytype defines velocity to use (P or S), layer defines
% layer in model
% example for reflection from zb, with source and receiver
% at za, or if slowness greater than slowness at zb, a
% turning ray
segment(1) = struct( ...
    'zstart',za,'zend',zb,'raytype',1,'layer',1);
segment(2) = struct( ...
    'zstart',zb,'zend',za,'raytype',1,'layer',1);
% set of horizontal slownesses
reflections = linspace( 0, 0.9999*pb, 100 );
turnings = linspace( 1.0001*pb, 0.9999*pa, 100 );
% compute travel-time integrals
[ xr tr taur ] = ttintegrals( reflections, segment );
[ xt tt taut ] = ttintegrals( turnings, segment );
% plot travel times
figure
hold
plot( xr, tr, 'r' )
plot( xt, tt, 'b' )
print -depsc2 exercise2_4.eps
return

```

This produces the simple travel-time plot:



Travel-time curves for turning rays (blue) and reflections (red) in a layer with velocity $c = 1 - z$, where $z_S = z_R = 0$ and an interface exists at $z = -1$.

These programs have not been written to be efficient — many calculations are repeated in different integrals, and full advantage of Matlab arrays is not taken. Using `quad` to perform the integrals numerically often ignores efficient analytic methods. However, the program can be used for a wide variety of models and rays.

2.5

Evaluate the ray integrals (2.3.7), (2.3.8) and (2.3.12) (remaining valid for (2.3.26)) for a medium with a linear velocity function (see Section 2.5.2). Show algebraically that the ray path is an arc of a circle.

For algebraic simplicity, we shift the depth origin so it lies where $c(z)$ would be zero, i.e. the velocity-depth function is $c(z) = c'z$. The physical medium exists for $z > 0$ if $c' > 0$, and for $z < 0$ if $c' < 0$.

The travel-time integral (2.3.7) is then

$$T(p) = \oint \frac{dz}{c^2 q} = \oint \frac{dz}{c' z (1 - (c' p z)^2)^{1/2}} = \frac{1}{2c'} \log \left(\frac{1 - cq}{1 + cq} \right) \Big|,$$

where $cq = (1 - c^2 p^2)^{1/2}$. Note that the logarithm is negative and decreases to zero at the turning point $z = 1/c'p$ (but the definite integral for a positive z range, is positive, of course).

The range integral (2.3.8) is

$$X(p) = \oint \frac{p dz}{q} = \oint \frac{c' p z dz}{(1 - (c' p z)^2)^{1/2}} = - \frac{cq}{c' p} \Big|.$$

We can differentiate this directly to obtain the geometrical spreading (2.3.12)

$$\frac{dX}{dp} = \frac{1}{cc' p^2 q} \Big|.$$

The indefinite function for the range function $-cq/c'p$ is zero at the turning point, i.e. $-cq/c'p$ is the range measured from the turning point, so the turning point does not contribute to this differential, and this expression for dX/dp remains valid with a turning point (2.3.26) provided the turning-point limit is omitted.

Measuring the horizontal range from the turning point, where $z = 1/c'p$, we have

$$X^2(p) + z^2 = \left(\frac{cq}{c'p} \right)^2 + z^2 = \frac{1}{(c'p)^2},$$

i.e. a circle of radius $1/c'p$.

3

Transforms

3.1

The results in Table 3.1 can be found in many textbooks, but confirm the proofs from first principles. What assumptions are necessary for each result?

Fourier transform: a (naive) proof of the Fourier transform is usually developed from the Fourier series. The complex Fourier series for a function of period T is defined as

$$f(t) = \sum_{n=-\infty}^{\infty} c_n e^{-i\omega_n t},$$

where $\omega_n = 2\pi n/T$ (the sign is taken to be consistent with our choice in the Fourier transform). As $T \rightarrow \infty$, the frequency step, $\Delta\omega = 2\pi/T$ tends to zero, and the infinite sum of terms in the Fourier series becomes an integral with the coefficients, c , becoming functions of the continuous variable, ω . The coefficients of the series are given by

$$c_m = \frac{1}{T} \int_{-T/2}^{T/2} f(t') e^{i\omega_m t'} dt' = \frac{\Delta\omega}{2\pi} \int_{-T/2}^{T/2} f(t') e^{i\omega_m t'} dt',$$

which can be proved by evaluating the integral of the series, when only the term $n = m$ is non-zero. Substituting in the series we have

$$f(t) = \sum_{n=-\infty}^{\infty} \frac{\Delta\omega}{2\pi} \int_{-T/2}^{T/2} f(t') e^{i\omega_n t'} dt' e^{-i\omega_n t}.$$

In the limit $T \rightarrow \infty$, $\Delta\omega \rightarrow 0$ and the summation becomes an integral, i.e.

$$\sum_{n=-\infty}^{\infty} \frac{\Delta\omega}{2\pi} g(\omega_n) e^{-i\omega_n t} \rightarrow \frac{1}{2\pi} \int_{-\infty}^{\infty} g(\omega) e^{-i\omega t} d\omega,$$

where

$$g(\omega) = \int_{-T/2}^{T/2} f(t') e^{i\omega_n t'} dt' \rightarrow \int_{-\infty}^{\infty} f(t') e^{i\omega_n t'} dt'$$

Hence we can define a transform pair

$$f(t) = \frac{1}{2\pi} \int_{-\infty}^{\infty} f(\omega) e^{-i\omega t} d\omega \quad \text{and} \quad f(\omega) = \int_{-\infty}^{\infty} f(t) e^{i\omega t} dt.$$

This proof assumes the infinite integrals exist. A more rigorous proof can be found in Zygmund (1988)[†].

Convolution: taking the Fourier transform of the convolution integral

$$f(t) = \int_{-\infty}^{\infty} g(t') f(t - t') dt',$$

we have

$$\begin{aligned} f(\omega) &= \int_{-\infty}^{\infty} \int_{-\infty}^{\infty} g(t') h(t - t') dt' e^{i\omega t} dt \\ &= \int_{-\infty}^{\infty} \int_{-\infty}^{\infty} g(t') e^{i\omega t'} h(t'') e^{i\omega t''} dt' dt'', \end{aligned}$$

where $t'' = t - t'$. The Jacobian of the variable change is unity, and the double integral over the complete plane still applies. Thus

$$f(\omega) = \int_{-\infty}^{\infty} g(t') e^{i\omega t'} dt' \int_{-\infty}^{\infty} h(t'') e^{i\omega t''} dt'' = g(\omega) h(\omega).$$

This proof assumes that the various transforms exist.

Hilbert Transform: the inverse Fourier transform of the spectrum $f(\omega) = -i \operatorname{sgn}(\omega)$ is

$$\begin{aligned} f(t) &= \frac{1}{2\pi} \int_{-\infty}^{\infty} -i \operatorname{sgn}(\omega) e^{-i\omega t} d\omega \\ &= \frac{i}{2\pi} \int_{-\infty}^0 e^{-i\omega t} d\omega - \frac{i}{2\pi} \int_0^{\infty} e^{-i\omega t} d\omega \\ &= -\frac{1}{2\pi t} e^{-i\omega t} \Big|_{-\infty}^0 + \frac{1}{2\pi t} e^{-i\omega t} \Big|_0^{\infty} \\ &= -\frac{1}{\pi t}. \end{aligned}$$

Hence, using the convolution theorem, the inverse Fourier transform of $g(\omega) = -i \operatorname{sgn}(\omega) f(\omega)$ is

$$g(t) = -\frac{1}{\pi} \int_{-\infty}^{\infty} \frac{f(t')}{t - t'} dt',$$

[†] Zygmund, A., 1988. *Trigonometric Series*, 2nd edn, Cambridge: Cambridge University Press.

where to avoid the singularity, the integral is taken as the Cauchy principal value. This proof assumes that the convolution integral exists.

Analytic times series: taking the Fourier transforms of $F(t) = f(t) + i\bar{f}(t)$, we have

$$F(\omega) = f(\omega) + i(-i \operatorname{sgn}(\omega))f(\omega) = 2H(\omega)f(\omega),$$

directly.

Shift rule: taking the Fourier transform of the shift function $f(t+a)$

$$\int_{-\infty}^{\infty} f(t+a) e^{i\omega t} dt = e^{-i\omega a} \int_{-\infty}^{\infty} f(t') e^{i\omega t'} dt' = f(\omega) e^{-i\omega a},$$

where $t' = t+a$. The shift is normally taken to be real. If complex, it assumes that the shift causes no singularities to cross the real axis of integration.

Scaling rule: taking the inverse Fourier transform of $f(a\omega)$ (and assuming a is real and positive),

$$\frac{1}{2\pi} \int_B f(a\omega) e^{-i\omega t} d\omega = \frac{1}{2\pi} \int_B f(\omega') e^{-i\omega'(t/a)} \frac{d\omega'}{a} = f(t/a)/a,$$

where the dummy variable of integration is $\omega' = a\omega$. If a is negative, the algebra is the same but the direction of the ω' integral is reversed so

$$\frac{1}{2\pi} \int_B f(a\omega) e^{-i\omega t} d\omega = -f(t/a)/a.$$

Hence the inverse transform of $f(a\omega)$ is $f(t/a)/|a|$, if a is real and non-zero.

Derivative: as in the text (3.1.26)

$$\begin{aligned} \left(\frac{\partial f}{\partial t}\right)(\omega) &= \int_{-\infty}^{\infty} \frac{\partial f}{\partial t} e^{i\omega t} dt = f(t) e^{i\omega t} \Big|_{-\infty}^{\infty} - \int_{-\infty}^{\infty} i\omega f(t) e^{i\omega t} dt \\ &= -i\omega f(\omega) \end{aligned}$$

provided $f(t) e^{i\omega t} \rightarrow 0$ as $t \rightarrow \infty$ ($f(-\infty) = 0$, from causality). Applying n times, we obtain

$$\partial_t^n f(t) \longrightarrow (-i\omega)^n f(\omega),$$

where the conditions at infinity must apply to derivatives up to $\partial_t^{n-1} f(t)$.

Integration: similarly integrating by parts

$$\begin{aligned} \left(\int_{-\infty}^t f(t') dt'\right)(\omega) &= \int_{-\infty}^{\infty} e^{i\omega t} \left(\int_{-\infty}^t f(t') dt'\right) dt \\ &= \frac{e^{i\omega t}}{i\omega} \int_{-\infty}^t f(t') dt' \Big|_{-\infty}^{\infty} - \int_{-\infty}^{\infty} \frac{e^{i\omega t}}{i\omega} f(t) dt \\ &= (-i\omega)^{-1} f(\omega), \end{aligned}$$

assuming $\int_{-\infty}^{\infty} f(t') dt' = 0$, i.e. the D.C. level is zero. Applying n times we obtain

$$\int^t \dots \int^{t_2} f(t_1) dt_1 \dots dt_n \longrightarrow (-i\omega)^{-n} f(\omega),$$

assuming the D.C. levels of the function and its $(n-1)$ integrals are zero.

3.2

Several useful Fourier transforms are given in Appendix B. Confirm these results.

Dirac delta function: the Fourier transform of the Dirac delta function follows from its definition

$$\int_{-\infty}^{\infty} \delta(t) f(t) dt = f(0),$$

so

$$\int_{-\infty}^{\infty} \delta(t) e^{i\omega t} dt = 1.$$

The inverse Fourier transform of $\exp(-|\omega|b)$ is easily evaluated

$$\begin{aligned} \frac{1}{2\pi} \int_{-\infty}^{\infty} e^{-|\omega|b-i\omega t} d\omega &= \frac{1}{2\pi} \int_{-\infty}^0 e^{\omega b-i\omega t} d\omega + \frac{1}{2\pi} \int_0^{\infty} e^{-\omega b-i\omega t} d\omega \\ &= \frac{1}{2\pi} \left. \frac{e^{\omega b-i\omega t}}{b-it} \right|_{-\infty}^0 - \frac{1}{2\pi} \left. \frac{e^{-\omega b-i\omega t}}{b-it} \right|_0^{\infty} \\ &= \frac{1}{2\pi} \left(\frac{1}{b-it} + \frac{1}{b+it} \right) \\ &= \frac{1}{\pi} \frac{b}{b^2+t^2}. \end{aligned}$$

The other results in Appendix B.1 can then be derived using the results in Table 3.1.

Inverse square roots: the Fourier transform of the inverse square root, $\lambda(t)$ (B.2.1) is evaluated

$$\int_{-\infty}^{\infty} \frac{H(t)}{t^{1/2}} e^{i\omega t} dt = 2 \int_0^{\infty} e^{i\omega y^2} dy = \left(\frac{\pi}{|\omega|} \right)^{1/2} e^{i \operatorname{sgn}(\omega) \pi/4},$$

using $t = y^2$ and the standard result (D.1.11). This result agrees with the result (B.2.2) for $\lambda(\omega)$. The other results in Appendix B.2 can then be derived using the results in Table 3.1.

Exponentials and inverse square roots: rather than prove the result for the inverse Fourier transform of the modified Bessel function of order $1/2$ (B.3.1), we find the inverse Fourier transform of

$$\left(\frac{2\pi}{\omega}\right)^{1/2} e^{\pm i\pi/4} e^{-b\omega}$$

(with $\omega > 0$) using the convolution theorem ((3.1.16) and (3.1.17)). The spectrum is the product of an exponential (B.1.4) and inverse square root ((B.2.2) or (B.2.4)). Thus for results (B.3.3) and (B.3.3) we have

$$\begin{aligned} \int_B \left(\frac{2\pi}{\omega}\right)^{1/2} e^{+i\pi/4} e^{-b\omega - i\omega t} d\omega &= 2^{1/2} \lambda(t) * \frac{b}{\pi(t^2 + b^2)} \\ \int_B \left(\frac{2\pi}{\omega}\right)^{1/2} e^{-i\pi/4} e^{-b\omega - i\omega t} d\omega &= 2^{1/2} \bar{\lambda}(t) * \frac{b}{\pi(t^2 + b^2)}. \end{aligned}$$

The first case with the positive sign gives

$$\begin{aligned} \int_{-\infty}^t \frac{2^{1/2}b}{\pi} \frac{d\tau}{(\tau^2 + b^2)(t - \tau)^{1/2}} &= \frac{2^{1/2}b}{\pi} \int_0^\infty \frac{dx}{((t - x)^2 + b^2) x^{1/2}} \\ &= \frac{2^{3/2}b}{\pi} \int_0^\infty \frac{dy}{y^4 - 2ty^2 + t^2 + b^2}, \end{aligned}$$

where $\tau = t - x = t - y^2$.

This is a standard integral with a quadratic in y^2 in the denominator. The denominator has no real roots as

$$B^2 - 4AC = 4t^2 - 4(t^2 + b^2) < 0,$$

and the indefinite integral is

$$\begin{aligned} \int \frac{dz}{Az^4 + Bz^2 + C} &= \frac{1}{4Aq^3 \sin(2\alpha)} \left(\sin \alpha \ln \left(\frac{z^2 + 2qz \cos \alpha + q^2}{z^2 - 2qz \cos \alpha + q^2} \right) \right. \\ &\quad \left. + 2 \cos \alpha \tan^{-1} \left(\frac{z^2 - q^2}{2qz \sin \alpha} \right) \right) \end{aligned}$$

where $q = (C/A)^{1/4}$ and $\cos(2\alpha) = -B/2\sqrt{AC}$ (Gradshteyn and Ryzhik, 1980, §2.161 (1) — although complicated, given the result, it can be confirmed by differentiation). The definite integral is then

$$\int_0^\infty \frac{dz}{Az^4 + Bz^2 + C} = \frac{\pi \cos \alpha}{2Aq^3 \sin 2\alpha}.$$

Now $A = 1$, $B = -2t$ and $C = t^2 + b^2$ so $q = (t^2 + b^2)^{1/4}$ and $\tan(2\alpha) = b/t$.

Thus

$$\cos \alpha = \left(\frac{\cos 2\alpha + 1}{2} \right)^{1/2} = \frac{\left(t + (t^2 + b^2)^{1/2} \right)^{1/2}}{2^{1/2}(t^2 + b^2)^{1/4}},$$

and the convolution integral reduces to

$$\frac{2^{3/2}b}{\pi} \int_0^\infty \frac{dy}{y^4 - 2ty^2 + t^2 + b^2} = \frac{\left(t + (t^2 + b^2)^{1/2} \right)^{1/2}}{(t^2 + b^2)^{1/2}},$$

i.e. result (B.3.3). The Hilbert transform result (B.3.4) is obtained in a very similar fashion.

Bessel and Hankel functions: with special functions it is always difficult to know where to start — which definition of the Bessel function is fundamental? We start with integral representations of the Bessel functions

$$\begin{aligned} J_0(x) &= \frac{2}{\pi} \int_0^\infty \sin(x \cosh \theta) d\theta \\ Y_0(x) &= -\frac{2}{\pi} \int_0^\infty \cos(x \cosh \theta) d\theta, \end{aligned}$$

with $x > 0$ (Abramowitz and Stegun, 1965, §9.1.23), modified forms of the Parseval's integral (8.2.13). These can be found in various textbooks.

Thus

$$\begin{aligned} \int_0^\infty J_0(a\omega) e^{-i\omega t} d\omega &= \frac{2}{\pi} \int_0^\infty \int_0^\infty \sin(a\omega \cosh \theta) e^{-i\omega t} d\theta d\omega \\ &= \frac{1}{i\pi} \int_0^\infty \int_0^\infty \left(e^{i\omega(a \cosh \theta - t)} - e^{-i\omega(a \cosh \theta + t)} \right) d\omega d\theta \\ &= -\frac{1}{\pi} \int_0^\infty \left(\frac{e^{i\omega(a \cosh \theta - t)}}{a \cosh \theta - t} + \frac{e^{-i\omega(a \cosh \theta + t)}}{a \cosh \theta + t} \right) \Big|_0^\infty d\theta \\ &= \frac{1}{\pi} \int_0^\infty \left(\frac{1}{a \cosh \theta - t} + \frac{1}{a \cosh \theta + t} \right) d\theta. \end{aligned}$$

These are known integrals. The indefinite results are

$$\begin{aligned} \int \frac{dz}{a \cosh z + b} &= -\frac{1}{(a^2 - b^2)^{1/2}} \sin^{-1} \left(\frac{a + b \cosh z}{b + a \cosh z} \right) \\ &= \frac{1}{(b^2 - a^2)^{1/2}} \ln \left(\frac{a + b + \sqrt{b^2 - a^2} \tanh(z/2)}{a + b - \sqrt{b^2 - a^2} \tanh(z/2)} \right), \end{aligned}$$

when $a^2 > b^2$ and $a^2 < b^2$, respectively (Gradshteyn and Ryzhik, 1980,

§2.443 (3) — as the results are known, they can be confirmed by differentiation). Then the definite results are

$$\begin{aligned} \int_0^\infty \frac{dz}{a \cosh z + b} &= \frac{2}{(a^2 - b^2)^{1/2}} \tan^{-1} \left(\frac{(a^2 - b^2)^{1/2}}{a + b} \right) \\ &= \frac{1}{(b^2 - a^2)^{1/2}} \ln \left(\frac{a + b + \sqrt{b^2 - a^2}}{a + b - \sqrt{b^2 - a^2}} \right), \end{aligned}$$

(Gradshteyn and Ryzhik, 1980, §3.513 (2)) when $a^2 > b^2$ and $a^2 < b^2$, respectively.

Thus if $t^2 < a^2$

$$\begin{aligned} \int_0^\infty J_0(a\omega) e^{-i\omega t} d\omega &= \frac{2}{\pi(a^2 - t^2)^{1/2}} \left(\tan^{-1} \frac{(a^2 - t^2)^{1/2}}{a - t} + \tan^{-1} \frac{(a^2 - t^2)^{1/2}}{a + t} \right) \\ &= \frac{1}{(a^2 - t^2)^{1/2}}, \end{aligned}$$

using the standard formula (Abramowitz and Stegun, 1965, §4.4.34) to combine two inverse tangents (and the argument of the single inverse tangent is infinite — or immediately as the arguments of the two inverse tangents are reciprocal). If $t^2 > a^2$

$$\begin{aligned} \int_0^\infty J_0(a\omega) e^{-i\omega t} d\omega &= \frac{1}{\pi(t^2 - a^2)^{1/2}} \ln \left(\frac{a - t + (t^2 - a^2)^{1/2}}{a - t - (t^2 - a^2)^{1/2}} \cdot \frac{a + t + (t^2 - a^2)^{1/2}}{a + t - (t^2 - a^2)^{1/2}} \right) \\ &= \frac{i}{(t^2 - a^2)^{1/2}}, \end{aligned}$$

as the argument of the logarithm reduces to -1 . This confirms (B.4.7) and (B.4.8).

Similarly

$$\int_0^\infty Y_0(a\omega) e^{-i\omega t} d\omega = \frac{i}{\pi} \int_0^\infty \left(\frac{1}{a \cosh \theta - t} - \frac{1}{a \cosh \theta + t} \right) d\theta.$$

Thus

$$\begin{aligned} \int_0^\infty Y_0(a\omega) e^{-i\omega t} d\omega &= \frac{2i}{\pi(a^2 - t^2)^{1/2}} \left(\tan^{-1} \frac{(a^2 - t^2)^{1/2}}{a - t} - \tan^{-1} \frac{(a^2 - t^2)^{1/2}}{a + t} \right) \end{aligned}$$

$$= \frac{2i}{\pi(a^2 - t^2)^{1/2}} \sin^{-1} \left(\frac{t}{a} \right),$$

if $t^2 < a^2$, and

$$\begin{aligned} & \int_0^\infty Y_0(a\omega) e^{-i\omega t} d\omega \\ &= \frac{i}{\pi(t^2 - a^2)^{1/2}} \ln \left(\frac{a - t + (t^2 - a^2)^{1/2}}{a - t - (t^2 - a^2)^{1/2}} \cdot \frac{a + t - (t^2 - a^2)^{1/2}}{a + t + (t^2 - a^2)^{1/2}} \right) \\ &= \frac{i}{\pi(t^2 - a^2)^{1/2}} \ln \left(- \frac{(t - (t^2 - a^2)^{1/2})^2}{a^2} \right) \\ &= \frac{2i}{\pi(t^2 - a^2)^{1/2}} \ln \left(\frac{t - (t^2 - a^2)^{1/2}}{a} \right) - \frac{1}{(t^2 - a^2)^{1/2}}, \end{aligned}$$

if $t^2 > a^2$, confirming results (B.4.9) and (B.4.10).

With these results we can obtain the inverse Fourier transforms of the Bessel and Hankel functions.

3.3

Evaluate the Radon transform as defined in equation (3.4.18) for the function $f(t, x) = A(x) \delta(t - T(x))$. Approximate this about the singularities, and show that the original function is recovered when substituted in the inverse transform (3.4.19).

Substitute $f(t, x) = A(x) \delta(t - T(x))$ in definition (3.4.18)

$$g(\tau, p) = - \frac{1}{2^{1/2}\pi} \frac{d}{dt} \bar{\lambda}(\tau) * \int_{-\infty}^{\infty} A(x) \delta(\tau - T(x) + px) dx.$$

Defining

$$\tilde{T}(p, x) = T(x) - px,$$

this can be rewritten

$$g(\tau, p) = - \frac{1}{2^{1/2}\pi} \frac{d}{dt} \bar{\lambda}(\tau) * \oint A(x) \delta(\tau - \tilde{T}) \left(\frac{dx}{d\tilde{T}} \right) d\tilde{T},$$

where the integral is written \oint to indicate it is over all ranges of \tilde{T} mapped by $x = -\infty$ to ∞ . In general, this will consist of several segments, some in the positive direction when $d\tilde{T}/dx > 0$, and some in the negative direction when $d\tilde{T}/dx < 0$ (in general, unless $\tilde{T}(p, x)$ is a monotonic function of x ,

the integral will have multiple branches each ending at the points where $d\tilde{T}/dx = 0$). For a given τ and p , we can solve the equation

$$\tau = \tilde{T}(p, x),$$

for value(s) of x . At these points, the delta function contributes to the integral and we obtain

$$g(\tau, p) = -\frac{1}{2^{1/2}\pi} \frac{d}{dt} \bar{\lambda}(\tau) * \sum_{\tau=\tilde{T}(p,x)} \left(\frac{A(x)}{|\partial\tilde{T}/\partial x|} \right),$$

where the summation is over solutions of the equation $\tau = \tilde{T}$ with the value(s) of x substituted. The modulus of the derivative is obtained as when the gradient is negative, the integral is in the negative direction (clearly in the original integral, $\delta(t - T(x)) dx \geq 0$). This technique for evaluating the Radon transform is clearly equivalent to that used for the WKB seismogram (Section 8.4.1).

The above result is singular when

$$\frac{\partial\tilde{T}}{\partial x} = \frac{dT}{dx} - p = 0,$$

i.e.

$$p = \frac{dT}{dx} = p(x), \quad \text{say.}$$

Expanding about a stationary point at x_0

$$\begin{aligned} \tilde{T} &\simeq \tilde{T}(x_0) + \frac{1}{2} \frac{\partial^2 \tilde{T}}{\partial x^2} (x - x_0)^2 \\ &= \tilde{T}_0 + \frac{1}{2} \left(\frac{dp}{dx} \right)_0 (x - x_0)^2 \end{aligned}$$

(subscript $_0$ indicates values at x_0). Assuming $(dp/dx)_0 > 0$, two solutions of $\tau = \tilde{T}$ exist for $\tau > \tilde{T}_0$ at

$$x = x_0 \pm \sqrt{\frac{2(\tau - \tilde{T}_0)}{(dp/dx)_0}}.$$

Substituting these two solutions in the Radon transform we obtain

$$\begin{aligned} g(\tau, p) &\simeq -\frac{1}{2^{1/2}\pi} \frac{d}{dt} \bar{\lambda}(\tau) * \frac{2A_0}{\sqrt{2(dp/dx)_0(t - \tilde{T}_0)}} \\ &= -A(p) \sqrt{dx/dp} \bar{\delta}(t - \tilde{T}(p)), \end{aligned}$$

as $\lambda(t) * \lambda(t) = \pi H(t)$, with

$$\begin{aligned} A(p) &= A(x(p)) \\ \tilde{T}(p) &= \tilde{T}(p, x(p)), \end{aligned}$$

and $x(p)$ is the inverse function of $p(x)$. If $(dp/dx)_0 < 0$, the two solutions of $\tau = \tilde{T}$ are for $\tau < \tilde{T}_0$ and the algebra is similar and the final result is the Hilbert transform. In general there may be more than one singularity and these can be summed in the final result.

Substituting this approximate Radon transform in the inverse transform (3.4.19), we have

$$f(t, x) \simeq \frac{1}{2^{1/2}\pi} \frac{d}{dt} \lambda(t) * \int_{-\infty}^{\infty} A(p) \sqrt{dx/dp} \, \delta(t - \tilde{T}(p) - px) \, dp.$$

Defining

$$\tilde{\tilde{T}}(x, p) = \tilde{T}(p) + px,$$

we obtain

$$f(t, x) = - \frac{1}{2^{1/2}\pi} \frac{d}{dt} \bar{\lambda}(t) * \sum_{t=\tilde{\tilde{T}}} \frac{A(p) \sqrt{dx/dp}}{\left| \partial \tilde{\tilde{T}} / \partial p \right|},$$

where for a given t and x , the points in the summation are where $t = \tilde{\tilde{T}}$ which can be solved for p . Again the terms in the summation will be singular when

$$\frac{\partial \tilde{\tilde{T}}}{\partial p} = 0 = \frac{d\tilde{T}}{dp} + x = x - x(p),$$

which can be solve for p . Expanding around a stationary point at p_0 ,

$$\tilde{\tilde{T}} \simeq \tilde{\tilde{T}}_0 + \frac{1}{2} \frac{\partial^2 \tilde{\tilde{T}}}{\partial p^2} (p - p_0)^2,$$

and the summation can be evaluated as before. The second derivative is

$$\frac{\partial^2 \tilde{\tilde{T}}}{\partial p^2} = - \frac{dx}{dp},$$

so where if we had a minimum in \tilde{T} before ($\partial^2 \tilde{T} / \partial x^2 = dp/dx > 0$), we now have a maximum in $\tilde{\tilde{T}}$ ($\partial^2 \tilde{\tilde{T}} / \partial x^2 = -dx/dp < 0$). Thus we find

$$f(t, x) = A(p(x)) \delta(t - \tilde{\tilde{T}}(x, p(x))) = A(x) \delta(x - T(x)),$$

as $\bar{\lambda}(t) * \bar{\lambda}(t) = -\pi H(t)$ and $A(p(x)) = A(x)$ and $\tilde{\tilde{T}}(x, p(x)) = T(x)$, the original functions.

4

Review of continuum mechanics and elastic waves

4.1

Various other elastic parameters are used to describe isotropic, elastic media apart from the Lamé parameters, λ and μ :

a) *If a solid is compressed by a hydrostatic pressure, then the bulk modulus, κ is defined as minus the ratio of the hydrostatic pressure to the dilatation, e.g. $\kappa = -P/\theta$ where $\sigma_{xx} = \sigma_{yy} = \sigma_{zz} = -P$. Show that*

$$\kappa = \lambda + \frac{2}{3}\mu.$$

b) *If a solid is stretched with just one non-zero normal stress component, e.g. stretching a wire where the sides are unconstrained, then Young's modulus, E , is defined as the ratio of the stress to the same strain component, e.g. $E = \sigma_{xx}/e_{xx}$ with $\sigma_{yy} = \sigma_{zz} = 0$. Show that*

$$E = \frac{\mu(3\lambda + 2\mu)}{\lambda + \mu}.$$

c) *With the same experiment as in part b), Poisson's ratio, ν , is defined as minus the ratio of the transverse strain and the longitudinal strain, e.g. $\nu = -e_{yy}/e_{xx}$. Show that*

$$\nu = \frac{\lambda}{2(\lambda + \mu)} = \frac{\alpha^2 - 2\beta^2}{2(\alpha^2 - \beta^2)}.$$

a) The isotropic constitutive relation is (4.4.50)

$$\sigma_{ij} = \lambda \theta \delta_{ij} + 2\mu e_{ij}.$$

For hydrostatic pressure, $\sigma_{xx} = \sigma_{yy} = \sigma_{zz} = -P$ and by symmetry $e_{xx} =$

$e_{xx} = e_{xx} = \theta/3$. Thus

$$-P = \lambda \theta + 2\mu \theta/3 = \left(\lambda + \frac{2}{3}\mu\right) \theta.$$

Thus

$$\kappa = -P/\theta = \lambda + \frac{2}{3}\mu.$$

c) For the stretching in the x direction, we have by symmetry $e_{yy} = e_{zz}$ and for the unconstrained sides

$$\sigma_{yy} = \sigma_{zz} = 0 = \lambda(e_{xx} + 2e_{yy}) + 2\mu e_{yy}.$$

Poisson's ratio is then defined as

$$\nu = -\frac{e_{yy}}{e_{xx}} = \frac{\lambda}{2(\lambda + \mu)},$$

solving the above equation.

b) For the stretching stress

$$\sigma_{xx} = \lambda(e_{xx} + 2e_{yy}) + 2\mu e_{xx},$$

and substituting for e_{yy} from above

$$\sigma_{xx} = \lambda \left(1 - \frac{\lambda}{\lambda + \mu}\right) e_{xx} + 2\mu e_{xx} = \frac{\mu(3\lambda + 2\mu)}{\lambda + \mu} e_{xx}.$$

Thus

$$E = \frac{\sigma_{xx}}{e_{xx}} = \frac{\mu(3\lambda + 2\mu)}{\lambda + \mu}.$$

4.2

Show that if a plane wave

$$\mathbf{u} = \mathbf{g} e^{i\omega \hat{\mathbf{p}} \cdot \mathbf{x}/c - i\omega t},$$

where $\hat{\mathbf{p}}$ is the normalized phase direction and c the phase velocity, propagates in a general, homogeneous anisotropic medium described by the matrices \mathbf{c}_{jk} (4.4.39), then the polarization, \mathbf{g} , and phase velocity, c , must satisfy the eigen-equation

$$(\hat{p}_j \hat{p}_k \mathbf{c}_{jk}/\rho) \mathbf{g} = c^2 \mathbf{g}.$$

This is commonly called the Christoffel equation (see Section 5.3.2). As the matrix $\hat{\mathbf{\Gamma}} = \hat{p}_j \hat{p}_k \mathbf{c}_{jk}/\rho$ is symmetric the eigenvalues are real and the non-degenerate eigenvectors are orthogonal.

Show that for an isotropic medium, the solutions reduce to the longitudinal P and the degenerate transverse S waves, with phase velocities given by equations (4.5.60) and (4.5.61).

Substituting the plane wave

$$\mathbf{u} = \mathbf{g} e^{i\omega \hat{\mathbf{p}} \cdot \mathbf{x}/c - i\omega t},$$

in the constitutive equation (4.4.36), we obtain

$$\mathbf{t}_j = \frac{i\omega \hat{p}_k}{c} \mathbf{c}_{jk} \mathbf{g} e^{i\omega \hat{\mathbf{p}} \cdot \mathbf{x}/c - i\omega t}.$$

Then substituting in the equation of motion (4.5.35) (with zero body forces), we have

$$-\omega^2 \mathbf{g} e^{i\omega \hat{\mathbf{p}} \cdot \mathbf{x}/c - i\omega t} = -\frac{1}{\rho} \frac{\omega^2 \hat{p}_j \hat{p}_k}{c^2} \mathbf{c}_{jk} \mathbf{g} e^{i\omega \hat{\mathbf{p}} \cdot \mathbf{x}/c - i\omega t}.$$

Hence

$$(\hat{p}_j \hat{p}_k \mathbf{c}_{jk}/\rho) \mathbf{g} = c^2 \mathbf{g}.$$

For an isotropic medium, we can simplify the algebra by taking $\hat{\mathbf{p}}$ in any convenient direction. Let us take $\hat{\mathbf{p}} = \hat{\mathbf{k}}$, i.e. $\hat{p}_1 = \hat{p}_2 = 0$ and $\hat{p}_3 = 1$. Then with the matrices (4.4.55) and (4.4.56), the Christoffel matrix reduces to

$$\hat{\mathbf{\Gamma}} = \hat{p}_j \hat{p}_k \mathbf{c}_{jk}/\rho = \begin{pmatrix} \mu/\rho & 0 & 0 \\ 0 & \mu/\rho & 0 \\ 0 & 0 & (\lambda + 2\mu)/\rho \end{pmatrix} = \begin{pmatrix} \beta^2 & 0 & 0 \\ 0 & \beta^2 & 0 \\ 0 & 0 & \alpha^2 \end{pmatrix},$$

and the eigen-equation has solutions $c^2 = \beta^2$ and $c^2 = \alpha^2$ as in equations (4.5.60) and (4.5.61).

4.3

Using the results of the previous question, show that for a transversely isotropic medium with an x_3 axis of symmetry (TIV), the eigenvalues (squared phase velocities) are given by

$$\rho c^2 = C_{66} \sin^2 \phi + C_{44} \cos^2 \phi$$

or

$$\rho c^2 = \frac{1}{2} (C_{44} + C_{33} \cos^2 \phi + C_{11} \sin^2 \phi)$$

$$\pm \sqrt{[(C_{33} - C_{44}) \cos^2 \phi - (C_{11} - C_{44}) \sin^2 \phi]^2 + 4a^2 \cos^2 \phi \sin^2 \phi},$$

where $\hat{\mathbf{p}} = (\sin \phi, 0, \cos \phi)$ is the phase direction (so the polar angle from the symmetry axis is ϕ), and

$$a = C_{13} + C_{44}.$$

Show that the corresponding polarizations are

$$\hat{\mathbf{g}} = \begin{pmatrix} 0 \\ 1 \\ 0 \end{pmatrix},$$

which is commonly called the *qSH* wave, and

$$\hat{\mathbf{g}} = \text{sgn} \begin{pmatrix} 2a\hat{p}_1\hat{p}_3 \\ 0 \\ (C_{33} - C_{44})\hat{p}_3^2 - (C_{11} - C_{44})\hat{p}_1^2 \pm \left[((C_{33} - C_{44})\hat{p}_3^2 - (C_{11} - C_{44})\hat{p}_1^2)^2 + 4\hat{p}_1^2\hat{p}_3^2 a^2 \right]^{1/2} \end{pmatrix}.$$

The wave with the upper sign in the phase velocity and polarization is commonly called the *qP* wave, and the lower sign *qSV*.

As a TIV medium is axially symmetric, we can take $\hat{p}_2 = 0$ so $\hat{p}_1 = \sin \phi$ and $\hat{p}_3 = \cos \phi$ where ϕ is the angle from the symmetry axis. With the matrices (4.4.62), the Christoffel matrix is

$$\hat{\mathbf{\Gamma}} = \begin{pmatrix} A_{11}\hat{p}_1^2 + A_{44}\hat{p}_3^2 & 0 & a'\hat{p}_1\hat{p}_3 \\ 0 & A_{66}\hat{p}_1^2 + A_{44}\hat{p}_3^2 & 0 \\ a'\hat{p}_1\hat{p}_3 & 0 & A_{44}\hat{p}_1^2 + A_{33}\hat{p}_3^2 \end{pmatrix},$$

where

$$a' = A_{13} + A_{44},$$

and $A_{ij} = C_{ij}/\rho$. This separates into a 2×2 system (the first and third rows and columns) and a scalar system (the second row and column).

For the scalar system, the eigenvector is

$$\hat{\mathbf{g}} = \begin{pmatrix} 0 \\ 1 \\ 0 \end{pmatrix},$$

and eigenvalue

$$c^2 = A_{66}\hat{p}_1^2 + A_{44}\hat{p}_3^2,$$

or

$$\rho c^2 = C_{66} \sin^2 \phi + C_{44} \cos^2 \phi.$$

As the polarization is perpendicular to the $\hat{p}_1 - \hat{p}_3$ propagation plane, this is known as the qSH wave.

For the polarization in the propagation plane, the system is 2×2 . For the eigenvalue, we obtain (Musgrave, 1970, (8.2.7) and (8.2.1))

$$A_{11}A_{44}\hat{p}_1^4 + A_{33}A_{44}\hat{p}_3^4 + A\hat{p}_1^2\hat{p}_3^2 - c^2(A_{11} + A_{44})\hat{p}_1^2 - c^2(A_{33} + A_{44})\hat{p}_3^2 + c^4 = 0,$$

where

$$A = A_{11}A_{33} + A_{44}^2 - a'^2.$$

This is a quadratic in c^2 and the solution reduces to

$$c^2 = \frac{1}{2} \left(A_{44} + A_{33}\hat{p}_3^2 + A_{11}\hat{p}_1^2 \pm \sqrt{[(A_{33} - A_{44})\hat{p}_3^2 - (A_{11} - A_{44})\hat{p}_1^2]^2 + 4a'^2\hat{p}_1^2\hat{p}_3^2} \right),$$

or

$$\begin{aligned} \rho c^2 &= \frac{1}{2} \left(C_{44} + C_{33} \cos^2 \phi + C_{11} \sin^2 \phi \right. \\ &\quad \left. \pm \sqrt{[(C_{33} - C_{44}) \cos^2 \phi - (C_{11} - C_{44}) \sin^2 \phi]^2 + 4a^2 \cos^2 \phi \sin^2 \phi} \right), \end{aligned}$$

where

$$a = C_{13} + C_{44}.$$

With the positive sign, the phase velocity is higher and we have the qP wave; with the lower sign, the qSV wave.

Note that the qSH velocity depends on two parameters, A_{44} and A_{66} , and the phase direction, while the qP and qSV velocities depend on four parameters, A_{11} , A_{33} , A_{44} and A_{13} , and the phase direction (A_{44} is common to all). We return to this in Exercise 4.5.

From the first row of the Christoffel equation, we have

$$(A_{11}\hat{p}_1^2 + A_{44}\hat{p}_3^2 - c^2)g_1 + a\hat{p}_1\hat{p}_3g_3 = 0,$$

so

$$\frac{g_3}{g_1} = \frac{c^2 - A_{11}\hat{p}_1^2 - A_{44}\hat{p}_3^2}{a\hat{p}_1\hat{p}_3},$$

and substituting for c^2 we obtain the result for the polarization.

4.4

Verify that if the elastic parameters of two TIV media are equal, except for the substitution

$$C_{13} \rightarrow -C_{13} - 2C_{44},$$

then the phase velocities are identical, but the polarizations differ. Physically, the anomalous negative value for C_{13} is extremely unlikely with very unusual polarizations (verify by numerical example), but it is possible (Helbig and Schoenberg, 1987).

The above expressions for the phase velocity are quadratic in the variable a (or a'), i.e. substituting $-a$ for a makes no difference. The only place where C_{13} enters is in the factor a . That is

$$a = C_{13} + C_{44} \rightarrow -a = -C_{13} - C_{44},$$

or equivalently

$$C_{13} \rightarrow -C_{13} - 2C_{44},$$

will not alter the phase velocity. However, this substitution alters the sign of the g_1 component of the polarization.

We illustrate this result numerically with a Matlab program. For TI media, it is straightforward to solve the Christoffel equation (Exercises 4.2 and 4.3, or see Section 5.7.1). For a given phase direction, $\hat{\mathbf{p}}$, the following function computes the phase velocities, c , the group velocities, \mathbf{V} (see Section 5.3) and the polarizations, \mathbf{g} (Exercise 4.2):

```
function [ PhaseSlow, GroupVel, Polar ] = ...
    TISurfaces( dir , TI, nu )
% TISurfaces = anisotropic phase slowness, group velocity
%               and polarization for qP, qSH and qSV for
%               general TI medium using Voigt parameters

% INPUT:
%       dir(3)      = phase direction (normalised)
%       TI.Cjk      = TI squared-velocity parameters
%       nu          = symmetry axis (normalised)
%
```

```

% OUTPUT:
%      PhaseSlow(3)      = phase slownesses
%      GroupVel(3,3)     = group velocities
%      Polar(3,3)        = normalized polarizations
%
% Note:
% TI are squared velocity parameters A_jk (not C_jk);
% dir and symmetry axis must be unit vectors;
% results order qP, qSH and qSV which may not correspond to
% qP, qS1 and qS2 in AnisoSurfaces.
%
%
GroupVel = zeros(3,3); Polar = GroupVel;
%
cs = dot(dir,nu);
tmp = cross(nu,dir);
ss = norm(tmp);
% special cases
% on axis
if ss == 0
    PhaseSlow(3) = 1/sqrt(TI.C44);
    PhaseSlow(2) = 1/sqrt(TI.C44);
    PhaseSlow(1) = 1/sqrt(TI.C33);
    GroupVel(:,3) = sqrt(TI.C44)*dir;
    GroupVel(:,2) = sqrt(TI.C44)*dir;
    GroupVel(:,1) = sqrt(TI.C33)*dir;
    % polarizations degenerate
    Polar(:,1) = dir;
    % tmp from smallest component cannot be parallel
    % to Polar(:,1)
    if abs(dir(1)) < abs(dir(2))
        if abs(dir(1)) < abs(dir(3)) tmp=[1 0 0]';
        else tmp=[0 0 1]'; end
    else
        if abs(dir(2)) < abs(dir(3)) tmp=[0 1 0]';
        else tmp=[0 0 1]'; end
    end
    % orthonormalize
    Polar(:,2) = tmp-dot(tmp,Polar(:,1))*Polar(:,1);
    Polar(:,2) = Polar(:,2)/norm(Polar(:,2));

```



```

    Polar(:,3) = cross(Polar(:,2),Polar(:,1));
    return
% on equator
elseif cs == 0
    PhaseSlow(3) = 1/sqrt(TI.C44);
    PhaseSlow(2) = 1/sqrt(TI.C66);
    PhaseSlow(1) = 1/sqrt(TI.C11);
    GroupVel(:,3) = sqrt(TI.C44)*dir;
    GroupVel(:,2) = sqrt(TI.C66)*dir;
    GroupVel(:,1) = sqrt(TI.C11)*dir;
    Polar(:,3) = nu;
    Polar(:,2) = cross(nu,dir);
    Polar(:,1) = dir;
    return
end
% qSH (5.7.23), (5.7.21), (5.7.25) and (5.7.26)
Polar(:,2) = tmp/ss;
pn = cross(Polar(:,2),nu);
cq = cs*cs;
sq = 1-cq;
PhaseSlow(2) = 1/sqrt(TI.C66*sq+TI.C44*cq);
GroupVel(:,2) = PhaseSlow(2)*(TI.C66*ss*pn+TI.C44*cs*nu);
% qP and qSV phase slowness (5.7.34)
aa = TI.C13+TI.C44;
A = TI.C11*TI.C33+(TI.C44-aa)*(TI.C44+aa);
xx = (TI.C33-TI.C44)*cq-(TI.C11-TI.C44)*sq;
yy = xx*xx+4*cq*sq*aa*aa;
zz = sqrt(yy);
vv = TI.C44+TI.C33*cq+TI.C11*sq;
PhaseSlow(3) = 1/sqrt(.5*(vv-zz));
PhaseSlow(1) = 1/sqrt(.5*(vv+zz));
% qP and qSV group velocities (5.7.36) and (5.7.37)
p1 = ss*PhaseSlow(1);
p3 = cs*PhaseSlow(1);
p1s = p1*p1;
p3s = p3*p3;
vv = (TI.C11+TI.C44)*p1s+(TI.C33+TI.C44)*p3s-2;
GroupVel(:,1) = ...
    (p1*(2*TI.C11*TI.C44*p1s+A*p3s-TI.C11-TI.C44)/vv)*pn+...
    (p3*(A*p1s+2*TI.C33*TI.C44*p3s-TI.C33-TI.C44)/vv)*nu;

```

```

p1 = ss*PhaseSlow(3);
p3 = cs*PhaseSlow(3);
p1s = p1*p1;
p3s = p3*p3;
vv = (TI.C11+TI.C44)*p1s+(TI.C33+TI.C44)*p3s-2;
GroupVel(:,3) = ...
    (p1*(2*TI.C11*TI.C44*p1s+A*p3s-TI.C11-TI.C44)/vv)*pn+...
    (p3*(A*p1s+2*TI.C33*TI.C44*p3s-TI.C33-TI.C44)/vv)*nu;
% qP and qSV polarizations (5.7.35)
vv = 2*aa*cs*ss;
Polar(:,3) = (zz-xx)*nu-vv*pn;
Polar(:,3) = Polar(:,3)/norm(Polar(:,3));
Polar(:,1) = vv*pn+(xx+zz)*nu;
Polar(:,1) = Polar(:,1)/norm(Polar(:,1));
if cs < 0 Polar(:,1) = -Polar(:,1); end
return

```

A main program that uses this function for the Green Horn shale (Jones and Wang, 1981) and the equivalent anomalous TI medium is

```

function Exercise44
% Exercise 4.4
%
% uses Green Horn shale (Jones and Wang, 1981) properties to
% compute phase, group and polarizations for a TI medium using
% function TISurfaces. Units are Gpa and Mg/m^3.
%
density = 2.42;
TI = struct( ...
    'C11',34.3, 'C33',22.7, 'C44',5.4, 'C66',10.6, 'C13',10.7 );
% squared-velocity parameters
TI.C11 = TI.C11/density;
TI.C13 = TI.C13/density;
TI.C33 = TI.C33/density;
TI.C44 = TI.C44/density;
TI.C66 = TI.C66/density;
% polarization length
gg = .04;
% overplot all results
% note phase slowness curves overplot but polarizations differ
figure

```

```

hold on
% loop over normal and anomalous TI
linetype = ' ';
for k=1:2
    % results for one quadrant
    symmetry_axis = [ 0 0 1 ]';
    for j=1:91
        theta=(j-1)*pi/180;
        ct = cos(theta);
        st = sin(theta);
        direction = [ ct 0 st ]';
        [ PhaseSlow, GroupVel, Polar ] = ...
            TISurfaces( direction , TI, symmetry_axis );
        qSVx(j) = ct*PhaseSlow(1);
        qSVz(j) = st*PhaseSlow(1);
        qSHx(j) = ct*PhaseSlow(2);
        qSHz(j) = st*PhaseSlow(2);
        qPx(j) = ct*PhaseSlow(3);
        qPz(j) = st*PhaseSlow(3);
        % plot polarization
        if ( rem(j,5) == 1 )
            plot( [ qSVx(j) qSVx(j) ], [ qSVz(j) qSVz(j) ], 'b.')
            plot( [ qSHx(j) qSHx(j) ], [ qSHz(j) qSHz(j) ], 'r.')
            plot( [ qPx(j) qPx(j) ], [ qPz(j) qPz(j) ], 'k.')
            %
            plot( [ qSVx(j) qSVx(j)+gg*Polar(1,1) ], ...
                [ qSVz(j) qSVz(j)+gg*Polar(3,1) ], ...
                ['b' linetype], 'LineWidth', 2)
            plot( [ qPx(j) qPx(j)+gg*Polar(1,3) ], ...
                [ qPz(j) qPz(j)+gg*Polar(3,3) ], ...
                ['k' linetype], 'LineWidth', 2)
        end
    end
end
% plot phase surfaces
plot( qSVx, qSVz, 'b' )
plot( qSHx, qSHz, 'r' )
plot( qPx, qPz, 'k' )
% convert to anomalous TI
TI.C13 = -TI.C13-2*TI.C44;
linetype = ':';

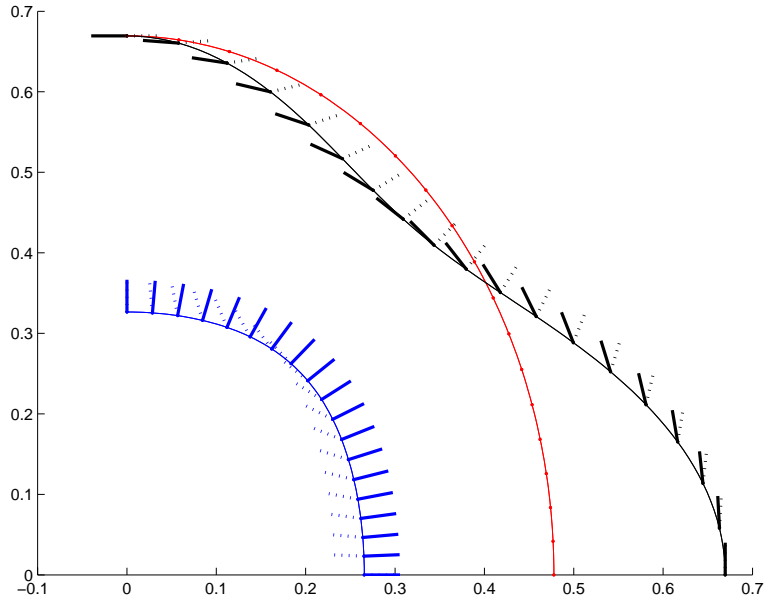
```

```

end
print -depsc2 exercise4_4.eps
return

```

This produces the following simple plot of the slowness surfaces (which are coincident for the normal and anomalous media), and polarizations (which are not):



One quadrant of the slowness surfaces for the Green Horn shale (Jones and Wang, 1981). The units are s/km. The short solid, thick lines illustrate the polarization directions for the qP (blue) and qSV (black) waves at various points on the slowness surfaces (they are of constant length). Also illustrated with dotted lines are the polarization directions for the anomalous TI media with the same slowness surfaces.

4.5

A TIV material is conveniently described by two axial velocities

$$\begin{aligned}\alpha_0 &= \sqrt{C_{33}/\rho} \\ \beta_0 &= \sqrt{C_{44}/\rho},\end{aligned}$$

and three dimensionless parameters

$$\begin{aligned}\delta &= \frac{(C_{13} + C_{44})^2 - (C_{33} - C_{44})^2}{2C_{33}(C_{33} - C_{44})} \\ \epsilon &= \frac{C_{11} - C_{33}}{2C_{33}} \\ \gamma &= \frac{C_{66} - C_{44}}{2C_{44}}.\end{aligned}$$

These useful parameters were introduced by Thomsen (1986). Verify that the elastic parameters, C_{ij} , can be determined from these, except for an arbitrary sign in the equation for C_{13} (see previous exercise). The anomalous negative sign is normally ignored. In a general TI medium, two additional parameters are needed to specify the direction of the symmetry axis, e.g. the spherical polar angles, for a total of seven parameters.

Show that if the dimensionless parameters are small (compared with unity), the phase velocities (see the previous exercises) can be approximated by

$$\begin{aligned}c_{qSH} &= \beta_0(1 + \gamma \sin^2 \phi) \\ c_{qSV} &= \beta_0 \left(1 + \frac{\alpha_0^2}{\beta_0^2} (\epsilon - \delta) \sin^2 \phi \cos^2 \phi \right) \\ c_{qP} &= \alpha_0(1 + \delta \sin^2 \phi \cos^2 \phi + \epsilon \sin^4 \phi).\end{aligned}$$

To first order, the polarizations are in the phase direction and transverse, i.e. as in an isotropic medium. See Thomsen (1986) for more details.

If the 5 parameters are α_0 , β_0 , δ , ϵ and γ , we can obtain the Voigt parameters as

$$\begin{aligned}C_{33} &= \rho \alpha_0^2 \\ C_{44} &= \rho \beta_0^2 \\ C_{11} &= (1 + 2\epsilon)C_{33} \\ C_{66} &= (1 + 2\gamma)C_{44},\end{aligned}$$

and

$$C_{13} = \pm \sqrt{(C_{33} - C_{44} + 2\delta C_{33})(C_{33} - C_{44})} - C_{44},$$

where normally we take the positive sign. If the anisotropy is weak, the results for δ can be simplified to

$$\delta \simeq \frac{C_{13} + 2C_{44} - C_{33}}{C_{33}},$$

and

$$C_{13} \simeq (1 + \delta)C_{33} - 2C_{44},$$

corresponding to the positive sign.

In Exercise 4.3, we have an exact expression for the phase velocities. We now substitute the weak approximations for the elastic parameters and approximate the square roots by the binomial expansion. For qSH waves we have

$$\begin{aligned} c_{qSH}^2 &= A_{66} \sin^2 \phi + A_{44} \cos^2 \phi \\ &= \beta_0^2 (1 + 2\gamma \sin^2 \phi). \end{aligned}$$

Thus

$$c_{qSH} \simeq \beta_0 (1 + \gamma \sin^2 \phi).$$

The first term in the expression for qSV and qP squared phase velocity is

$$A_{44} + A_{33} \cos^2 \phi + A_{11} \sin^2 \phi = \alpha_0^2 + \beta_0^2 + 2\epsilon\alpha_0^2 \sin^2 \phi.$$

The argument of the square root is

$$\begin{aligned} &\left[(A_{33} - A_{44})\hat{p}_3^2 - (A_{11} - A_{44})\hat{p}_1^2 \right]^2 + 4a'^2 \hat{p}_1^2 \hat{p}_3^2 \\ &\simeq (\alpha_0^2 - \beta_0^2)^2 + 4\alpha_0^2 (\alpha_0^2 - \beta_0^2) \left((2\delta - \epsilon) \cos^2 \phi \sin^2 \phi + \epsilon \sin^4 \phi \right). \end{aligned}$$

Thus

$$\begin{aligned} &\sqrt{\left[(A_{33} - A_{44})\hat{p}_3^2 - (A_{11} - A_{44})\hat{p}_1^2 \right]^2 + 4a'^2 \hat{p}_1^2 \hat{p}_3^2} \\ &\simeq (\alpha_0^2 - \beta_0^2) + 2\alpha_0^2 \left((2\delta - \epsilon) \cos^2 \phi \sin^2 \phi + \epsilon \sin^4 \phi \right). \end{aligned}$$

Adding these expressions

$$\begin{aligned} c_{qP}^2 &\simeq \frac{1}{2} \left(2\alpha_0^2 + 2\epsilon\alpha_0^2 \sin^2 \phi + 2(2\delta - \epsilon)\alpha_0^2 \sin^2 \phi \cos^2 \phi + 2\epsilon\alpha_0^2 \sin^4 \phi \right) \\ &= \alpha_0^2 (1 + 2\delta \cos^2 \phi \sin^2 \phi + 2\epsilon \sin^4 \phi). \end{aligned}$$

Hence

$$c_{qP} \simeq \alpha_0 (1 + \delta \cos^2 \phi \sin^2 \phi + \epsilon \sin^4 \phi).$$

Similarly, subtracting the expressions

$$\begin{aligned} c_{qSV}^2 &\simeq \frac{1}{2} \left(2\beta_0^2 + 2\epsilon\alpha_0^2 \sin^2 \phi - 2(2\delta - \epsilon)\alpha_0^2 \sin^2 \phi \cos^2 \phi - 2\epsilon\alpha_0^2 \sin^4 \phi \right) \end{aligned}$$

$$= \beta_0^2 + 2(\epsilon - \delta)\alpha_0^2 \cos^2 \phi \sin^2 \phi.$$

Hence

$$c_{qSV} \simeq \beta_0 \left(1 + \frac{\alpha_0^2}{\beta_0^2} (\epsilon - \delta) \cos^2 \phi \sin^2 \phi \right).$$

In Exercise 4.3, we commented that the exact expressions for the qP and qSV velocities depend on four parameters, A_{11} , A_{33} , A_{44} and A_{13} , and the phase direction. In the weak approximation, this number is reduced. The qP velocity depends on three parameters, α_0 , δ and ϵ , which using the weak approximation for δ , is equivalent to three parameters A_{11} , A_{33} and $A_{13} + 2A_{44}$. Equivalently, we can consider the three parameters as the deviation of the velocity from isotropy on the axis (A_{33}), on the equator (A_{11}), and at 45 degrees to the axis ($A_{13} + 2A_{44}$) (Chapman and Miller, 1996)[†]. The qSV velocity depends on only two parameters, β_0 and $(\epsilon - \delta)\alpha_0^2/\beta_0^2$, again the latter describing the anisotropy of the velocity at 45 degrees.

4.6

Further reading: Interpreting general anisotropic elastic parameters is difficult. If all 21 parameters are non-zero, is the medium in fact one with a high-order of symmetry, e.g. TI, but with tilted axes or planes of symmetry? In other words, would a simple rotation reduce the number of non-zero parameters significantly? This question has been addressed by several authors who develop decompositions that do not depend on the coordinate system. A useful review is by Baerheim (1993), who compares his results with those by earlier authors (Backus, 1970 and Cowin, 1989, 1993). The general results are too complicated to be included here and the paper by Baerheim (1993) is suggested for further reading.

One particularly useful result is for the mean-squared velocities, averaged over all directions. This can be used to define an isotropic medium that approximates an anisotropic medium. Defining the dilatational modulus tensor

$$D_{ij} = c_{ijkk},$$

and the Voigt tensor

$$V_{ij} = c_{ikjk},$$

[†] Chapman, C.H. and Miller, D.E., 1996. Velocity sensitivity in transversely isotropic media, *Geophys. Prosp.*, **44**, 525–49

the mean squared P and S velocities are

$$\begin{aligned}\overline{\alpha^2} &= \left(\text{tr}(\mathbf{D}) + 2 \text{tr}(\mathbf{V}) \right) / 15\rho \\ \overline{\beta^2} &= \left(3 \text{tr}(\mathbf{V}) - \text{tr}(\mathbf{D}) \right) / 30\rho.\end{aligned}$$

Show that in isotropic media, these expressions reduce to

$$\begin{aligned}\overline{\alpha^2} &= \alpha^2 \\ \overline{\beta^2} &= \beta^2;\end{aligned}$$

in transversely isotropic media to

$$\begin{aligned}\overline{\alpha^2} &= \frac{8C_{11} + 3C_{33} + 8C_{44} + 4C_{31}}{15\rho} \\ \overline{\beta^2} &= \frac{C_{11} + C_{33} + 6C_{44} + 5C_{66} - 2C_{13}}{15\rho},\end{aligned}$$

and in general anisotropic media to

$$\begin{aligned}\overline{\alpha^2} &= \frac{3(C_{11} + C_{22} + C_{33}) + 4(C_{44} + C_{55} + C_{66}) + 2(C_{23} + C_{31} + C_{12})}{15\rho} \\ \overline{\beta^2} &= \frac{(C_{11} + C_{22} + C_{33}) + 3(C_{44} + C_{55} + C_{66}) - (C_{23} + C_{31} + C_{12})}{15\rho}.\end{aligned}$$

In a weak transversely isotropic medium (see previous exercise), show that the results are

$$\begin{aligned}\overline{\alpha^2} &= \alpha_0^2 \left(1 + \frac{16}{15}\epsilon + \frac{4}{15}\delta \right) \\ \overline{\beta^2} &= \beta_0^2 \left(1 + \frac{2}{3}\gamma + \frac{2}{15}(\epsilon - \delta) \frac{\alpha_0^2}{\beta_0^2} \right).\end{aligned}$$

Show that these two results agree with averaging the approximate squared velocities given in the previous exercise over a sphere, and averaging the two shear wave velocities.

From the definitions

$$\begin{aligned}D_{ij} &= c_{ijkl} \\ V_{ij} &= c_{ikjk},\end{aligned}$$

we obtain

$$\text{tr}(\mathbf{D}) = (c_{1111} + c_{1122} + c_{1133}) + (c_{2211} + c_{2222} + c_{2233}) +$$

$$\begin{aligned}
& (c_{3311} + c_{3322} + c_{3333}) \\
&= (C_{11} + C_{22} + C_{33}) + 2(C_{23} + C_{31} + C_{12}) \\
\text{tr}(\mathbf{V}) &= (c_{1111} + c_{1212} + c_{1313}) + (c_{2121} + c_{2222} + c_{2323}) + \\
& (c_{3131} + c_{3232} + c_{3333}) \\
&= (C_{11} + C_{22} + C_{33}) + 2(C_{44} + C_{55} + C_{66}).
\end{aligned}$$

Then for general anisotropy

$$\begin{aligned}
\overline{\alpha^2} &= \left(\text{tr}(\mathbf{D}) + 2 \text{tr}(\mathbf{V}) \right) / 15\rho = \\
& \frac{3(C_{11} + C_{22} + C_{33}) + 4(C_{44} + C_{55} + C_{66}) + 2(C_{23} + C_{31} + C_{12})}{15\rho} \\
\overline{\beta^2} &= \left(3 \text{tr}(\mathbf{V}) - \text{tr}(\mathbf{D}) \right) / 30\rho = \\
& \frac{(C_{11} + C_{22} + C_{33}) + 3(C_{44} + C_{55} + C_{66}) - (C_{23} + C_{31} + C_{12})}{15\rho}.
\end{aligned}$$

Simplifying to transversely isotropic media with $C_{11} = C_{22}$, $C_{31} = C_{23}$, $C_{44} = C_{55}$ and $C_{12} = C_{11} - 2C_{66}$, these reduce to

$$\begin{aligned}
\overline{\alpha^2} &= \frac{3(2C_{11} + C_{33}) + 4(2C_{44} + C_{66}) + 2(2C_{31} + C_{11} - 2C_{66})}{15\rho} \\
&= \frac{8C_{11} + 3C_{33} + 8C_{44} + 4C_{31}}{15\rho} \\
\overline{\beta^2} &= \frac{(2C_{11} + C_{33}) + 3(2C_{44} + C_{66}) - (2C_{31} + C_{11} - 2C_{66})}{15\rho} \\
&= \frac{C_{11} + C_{33} + 6C_{44} + 5C_{66} - 2C_{31}}{15\rho}.
\end{aligned}$$

Finally in isotropic media with $C_{11} = C_{33} = \rho\alpha^2$, $C_{44} = C_{66} = \rho\beta^2$ and $C_{31} = \rho(\alpha^2 - 2\beta^2)$, these reduce to

$$\begin{aligned}
\overline{\alpha^2} &= \frac{8\alpha^2 + 3\alpha^2 + 8\beta^2 + 4(\alpha^2 - 2\beta^2)}{15} = \alpha^2 \\
\overline{\beta^2} &= \frac{\alpha^2 + \alpha^2 + 6\beta^2 + 5\beta^2 - 2(\alpha^2 - 2\beta^2)}{15} = \beta^2.
\end{aligned}$$

In order to take the spherical average of the expressions in Exercise 4.5, we integrate over surface elements on a sphere, i.e.

$$\frac{1}{4\pi} \int_0^{2\pi} \int_0^\pi \dots \sin \phi \, d\phi \, d\psi = \frac{1}{2} \int_0^\pi \dots \sin \phi \, d\phi,$$

as the velocity is azimuthally symmetric, where ψ is the azimuthal angle. Now

$$c_{qP}^2 \simeq \alpha_0^2 (1 + 2\delta \cos^2 \phi \sin^2 \phi + 2\epsilon \sin^4 \phi),$$

so

$$\overline{c_{qP}^2} \simeq \alpha_0^2 \left(1 + \delta \int_0^\pi \cos^2 \phi \sin^3 \phi \, d\phi + \epsilon \int_0^\pi \sin^5 \phi \, d\phi \right).$$

We need

$$\begin{aligned} I_n &= \int_0^\pi \sin^n \phi \, d\phi \\ &= I_{n-2} - \int_0^\pi \left(\sin^{n-2} \phi \cos \phi \right) \cos \phi \, d\phi \\ &= I_{n-2} - \frac{\sin^{n-1} \phi}{n-1} \cos \phi \Big|_0^\pi - \int_0^\pi \frac{\sin^{n-1} \phi}{n-1} \sin \phi \, d\phi \\ &= I_{n-2} - \frac{1}{n-1} I_n, \end{aligned}$$

integrating by parts. Thus

$$I_n = \frac{n-1}{n} I_{n-2},$$

and we have

$$\begin{aligned} I_1 &= 2 \\ I_3 &= \frac{2}{3} I_1 = \frac{4}{3} \\ I_5 &= \frac{4}{5} I_3 = \frac{16}{15}, \end{aligned}$$

etc. Thus

$$\begin{aligned} \overline{c_{qP}^2} &\simeq \alpha_0^2 \left(1 - \frac{16}{15} \delta + \frac{4}{3} \delta + \frac{16}{15} \epsilon \right) \\ &= \alpha_0^2 \left(1 + \frac{16}{15} \epsilon + \frac{4}{15} \delta \right), \end{aligned}$$

which agrees with the $\overline{\alpha^2}$ given. For the qSH velocity we have

$$c_{qSH}^2 \simeq \beta_0^2 (1 + 2\gamma \sin^2 \phi).$$

Hence

$$\begin{aligned} \overline{c_{qSH}^2} &\simeq \beta_0^2 (1 + \gamma \int_0^\pi \sin^3 \phi \, d\phi) \\ &= \beta_0^2 \left(1 + \frac{4}{3} \gamma \right). \end{aligned}$$

Similarly for the qSV velocity

$$c_{qSV}^2 \simeq \beta_0^2 \left(1 + 2 \frac{\alpha_0^2}{\beta_0^2} (\epsilon - \delta) \sin^2 \phi \cos^2 \phi \right).$$

Hence

$$\begin{aligned}\overline{c_{qSV}^2} &\simeq \beta_0^2 \left(1 + \frac{\alpha_0^2}{\beta_0^2} (\epsilon - \delta) \int_0^\pi \sin^3 \phi \cos^2 \phi \, d\phi \right) \\ &= \beta_0^2 \left(1 + \frac{4}{15} \frac{\alpha_0^2}{\beta_0^2} (\epsilon - \delta) \right).\end{aligned}$$

Taking the average of these

$$\frac{1}{2} (\overline{c_{qSH}^2} + \overline{c_{qSV}^2}) = \beta_0^2 \left(1 + \frac{2}{3} \gamma + \frac{2}{15} \frac{\alpha_0^2}{\beta_0^2} (\epsilon - \delta) \right),$$

which agrees with the $\overline{\beta^2}$ given.

4.7

Confirm that the two-dimensional result (4.5.84) or (4.5.85) can be derived from the equivalent three-dimensional results by dividing the line source into infinitesimal point elements and integrating along the line (see Figure 4.16).

Further reading: See, for instance, Hudson (1980, Section 2.5).

The point force, Green function is (4.5.71)

$$\begin{aligned}\underline{\mathbf{u}}(t, \mathbf{x}_R; \mathbf{x}_S) &= \frac{\delta(t - R/\alpha)}{4\pi\rho\alpha^2 R} \hat{\mathbf{R}} \hat{\mathbf{R}}^T + \frac{\delta(t - R/\beta)}{4\pi\rho\beta^2 R} (\mathbf{I} - \hat{\mathbf{R}} \hat{\mathbf{R}}^T) \\ &+ \frac{t}{4\pi\rho R^3} \left(H(t - R/\alpha) - H(t - R/\beta) \right) (3\hat{\mathbf{R}} \hat{\mathbf{R}}^T - \mathbf{I}),\end{aligned}$$

where to avoid confusion with the cylindrical system we have denoted the radial vector by $\hat{\mathbf{R}}$. In the cylindrical system, we use the unit vectors $\hat{\mathbf{r}}$, $\hat{\phi}$ and $\hat{\mathbf{z}}$. We consider a line source along the z axis and decompose it into point sources from $z = -\infty$ to ∞ . For convenience, we measure the position of a point source by the angle χ between the symmetry plane through the receiver (z constant) and the line joining the receiver to the elementary source, i.e.

$$\hat{\mathbf{R}}^T \hat{\mathbf{r}} = \cos \chi,$$

and

$$\hat{\mathbf{R}} = \cos \chi \hat{\mathbf{r}} - \sin \chi \hat{\mathbf{z}}.$$

In order to integrate elementary point sources along the line, we can use

independent variables z , χ or R . We have

$$\begin{aligned} dz &= r \sec^2 \chi d\chi \\ d\chi &= \frac{r dR}{R(R^2 - r^2)^{1/2}}. \end{aligned}$$

First we consider a line source with the force $\hat{\mathbf{r}}$. Integrating the point sources we have

$$\begin{aligned} \mathbf{u} &= \int_{-\infty}^{\infty} \left(\frac{\delta(t - R/\alpha)}{4\pi\rho\alpha^2 R} \cos \chi (\cos \chi \hat{\mathbf{r}} - \sin \chi \hat{\mathbf{z}}) \right. \\ &\quad + \frac{\delta(t - R/\beta)}{4\pi\rho\beta^2 R} (\hat{\mathbf{r}} - \cos \chi (\cos \chi \hat{\mathbf{r}} - \sin \chi \hat{\mathbf{z}})) \\ &\quad + \frac{t}{4\pi\rho R^3} (H(t - R/\alpha) - H(t - R/\beta)) \\ &\quad \left. \times (3 \cos \chi (\cos \chi \hat{\mathbf{r}} - \sin \chi \hat{\mathbf{z}}) - \hat{\mathbf{r}}) \right) dz \\ &= \frac{r \hat{\mathbf{r}}}{2\pi\rho} \int_0^{\pi/2} \left(\frac{\delta(t - R/\alpha)}{\alpha^2 R} \cos^2 \chi + \frac{\delta(t - R/\beta)}{\beta^2 R} \sin^2 \chi \right. \\ &\quad \left. + \frac{t}{R^3} (H(t - R/\alpha) - H(t - R/\beta)) (3 \cos^2 \chi - 1) \right) \sec^2 \chi d\chi \\ &= \frac{r \hat{\mathbf{r}}}{2\pi\rho} \int_r^{\infty} \left(\frac{\delta(t - R/\alpha)r}{\alpha^2 R^2 (R^2 - r^2)^{1/2}} + \frac{\delta(t - R/\beta)(R^2 - r^2)^{1/2}}{\beta^2 R^2 r} \right. \\ &\quad \left. + \frac{t(3r^2 - R^2)}{R^4 r (R^2 - r^2)^{1/2}} (H(t - R/\alpha) - H(t - R/\beta)) \right) dR, \end{aligned}$$

retaining the symmetric part in half the range, and changing variables of integration. The first two terms contribute at $R = \alpha t$ and $R = \beta t$, respectively. The final term contributes in the range $R = \beta t$ to αt (assuming these are in the range $R = r$ to ∞). Thus we obtain

$$\begin{aligned} \mathbf{u} &= \frac{r^2 \hat{\mathbf{r}}}{2\pi\rho\alpha^4 t^2 (t^2 - r^2/\alpha^2)^{1/2}} + \frac{(t^2 - r^2/\beta^2)^{1/2} \hat{\mathbf{z}}}{2\pi\rho\beta^2 t^2} \\ &\quad + \frac{t \hat{\mathbf{r}}}{2\pi\rho} \int_{\beta t}^{\alpha t} \frac{3r^2 - R^2}{R^4 (R^2 - r^2)^{1/2}} dR. \end{aligned}$$

To evaluate the final integral, we need

$$\begin{aligned} \int \frac{dx}{x^2(x^2 - a^2)^{1/2}} &= \frac{(x^2 - a^2)^{1/2}}{a^2 x} \\ \int \frac{dx}{x^4(x^2 - a^2)^{1/2}} &= \frac{(x^2 - a^2)^{1/2}}{a^4 x} - \frac{(x^2 - a^2)^{3/2}}{3a^4 x^3}. \end{aligned}$$

Then

$$\begin{aligned}
\mathbf{u} &= \frac{r^2 \hat{\mathbf{r}}}{2\pi\rho\alpha^4 t^2 (t^2 - r^2/\alpha^2)^{1/2}} + \frac{(t^2 - r^2/\beta^2)^{1/2} \hat{\mathbf{z}}}{2\pi\rho\beta^2 t^2} \\
&\quad + \frac{t(R^2 - r^2)^{1/2}(R^2 + r^2) \hat{\mathbf{r}}}{2\pi\rho r^2 R^3} \Big|_{\beta t}^{\alpha t} \\
&= \frac{\hat{\mathbf{r}}}{2\pi\rho r^2} \left(\frac{r^2/\alpha^2}{(t^2 - r^2/\alpha^2)^{1/2}} + (t^2 - r^2/\alpha^2)^{1/2} - (t^2 - r^2/\beta^2)^{1/2} \right).
\end{aligned}$$

This agrees with the line source, Green function (4.5.84) with a source $\hat{\mathbf{r}}$.

For a line source with force $\hat{\phi}$, we have $\hat{\mathbf{R}}^T \hat{\phi} = 0$, so the integrated point sources become

$$\begin{aligned}
\mathbf{u} &= \int_{-\infty}^{\infty} \left(\frac{\delta(t - R/\beta)}{4\pi\rho\beta^2 R} \hat{\phi} \right. \\
&\quad \left. - \frac{t}{4\pi\rho R^3} (H(t - R/\alpha) - H(t - R/\beta)) \hat{\phi} \right) dz \\
&= \frac{r\hat{\phi}}{2\pi\rho} \int_0^{\pi/2} \left(\frac{\delta(t - R/\beta)}{\beta^2 R} \right. \\
&\quad \left. - \frac{t}{R^3} (H(t - R/\alpha) - H(t - R/\beta)) \right) \sec^2 \chi d\chi \\
&= \frac{\hat{\phi}}{2\pi\rho} \int_r^{\infty} \left(\frac{\delta(t - R/\beta)}{\beta^2 (R^2 - r^2)^{1/2}} \right. \\
&\quad \left. - \frac{t}{R^2 (R^2 - r^2)^{1/2}} (H(t - R/\alpha) - H(t - R/\beta)) \right) dR \\
&= \frac{\hat{\phi}}{2\pi\rho} \left(\frac{1}{\beta^2 (t^2 - r^2/\beta^2)^{1/2}} - t \int_{\beta t}^{\alpha t} \frac{dR}{R^2 (R^2 - r^2)^{1/2}} \right) \\
&= \frac{\hat{\phi}}{2\pi\rho r^2} \left(\frac{r^2/\beta^2}{(t^2 - r^2/\beta^2)^{1/2}} - (t^2 - r^2/\alpha^2)^{1/2} + (t^2 - r^2/\beta^2)^{1/2} \right),
\end{aligned}$$

in agreement with the line source, Green function (4.5.84) with a source $\hat{\phi}$.

Finally we consider a line source with force $\hat{\mathbf{z}}$, so we have $\hat{\mathbf{R}}^T \hat{\mathbf{z}} = -\sin \chi$, and

$$\begin{aligned}
\mathbf{u} &= \int_{-\infty}^{\infty} \left(-\frac{\delta(t - R/\alpha)}{4\pi\rho\alpha^2 R} \sin \chi (\cos \chi \hat{\mathbf{r}} - \sin \chi \hat{\mathbf{z}}) \right. \\
&\quad + \frac{\delta(t - R/\beta)}{4\pi\rho\beta^2 R} (\hat{\mathbf{z}} - \sin \chi (\cos \chi \hat{\mathbf{r}} - \sin \chi \hat{\mathbf{z}})) \\
&\quad \left. + \frac{t}{4\pi\rho R^3} (H(t - R/\alpha) - H(t - R/\beta)) \right) dz
\end{aligned}$$

$$\begin{aligned}
& \times \left(-3 \sin \chi (\cos \chi \hat{\mathbf{r}} - \sin \chi \hat{\mathbf{z}}) - \hat{\mathbf{z}} \right) dz \\
& = \frac{r \hat{\mathbf{z}}}{2\pi\rho} \int_0^{\pi/2} \left(\frac{\delta(t - R/\alpha)}{\alpha^2 R} \sin^2 \chi + \frac{\delta(t - R/\beta)}{\beta^2 R} \cos^2 \chi \right. \\
& + \left. \frac{t}{R^3} \left(H(t - R/\alpha) - H(t - R/\beta) \right) (3 \sin^2 \chi - 1) \right) \sec^2 \chi d\chi \\
& = \frac{r \hat{\mathbf{z}}}{2\pi\rho} \int_r^\infty \left(\frac{\delta(t - R/\alpha)(R^2 - r^2)^{1/2}}{\alpha^2 R^2 r} + \frac{\delta(t - R/\beta)r}{\beta^2 R^2 (R^2 - r^2)^{1/2}} \right. \\
& \quad \left. + \frac{t(2R^2 - 3r^2)}{R^4 r (R^2 - r^2)^{1/2}} \left(H(t - R/\alpha) - H(t - R/\beta) \right) \right) dR.
\end{aligned}$$

The first two terms contribute at $R = \alpha t$ and $R = \beta t$, respectively. The final term contributes in the range $R = \beta t$ to αt (assuming these are in the range r to ∞). Thus we obtain

$$\begin{aligned}
\mathbf{u} & = \frac{(t^2 - r^2/\alpha^2)^{1/2} \hat{\mathbf{z}}}{2\pi\rho\alpha^2 t^2} + \frac{r^2 \hat{\mathbf{z}}}{2\pi\rho\beta^4 t^2 (t^2 - r^2/\beta^2)^{1/2}} \\
& + \frac{t \hat{\mathbf{z}}}{2\pi\rho} \int_{\beta t}^{\alpha t} \frac{2R^2 - 3r^2}{R^4 (R^2 - r^2)^{1/2}} dR.
\end{aligned}$$

Using the integrals given above, this reduces to

$$\begin{aligned}
\mathbf{u} & = \frac{(t^2 - r^2/\alpha^2)^{1/2} \hat{\mathbf{z}}}{2\pi\rho\alpha^2 t^2} + \frac{r^2 \hat{\mathbf{z}}}{2\pi\rho\beta^4 t^2 (t^2 - r^2/\beta^2)^{1/2}} \\
& - \frac{\hat{\mathbf{z}}}{2\pi\rho} \left(\frac{(t^2 - r^2/\alpha^2)^{1/2}}{\alpha^2 t^2} - \frac{(t^2 - r^2/\beta^2)^{1/2}}{\beta^2 t^2} \right) \\
& = \frac{\hat{\mathbf{z}}}{2\pi\rho\beta^2 (t^2 - r^2/\beta^2)^{1/2}},
\end{aligned}$$

in agreement with the line source, Green function (4.5.84) with a source $\hat{\mathbf{z}}$.

Combining the results for sources $\hat{\mathbf{r}}$, $\hat{\phi}$ and $\hat{\mathbf{z}}$, we confirm the complete line source, Green function (4.5.84). Although the above algebra for the construction of a line source from elementary point sources is straightforward, there are some interesting features. For instance for the source $\hat{\mathbf{z}}$, the far-field of the P waves from symmetric elementary point sources appears not to cancel. However, because the P radiation pattern is zero on the symmetry plane (Figure 4.14), the far-field from all the elementary point sources only contributes a near-field term. This cancels with the near-field terms from the elementary point sources, and the final result contains no P wave (as expected, by symmetry). Alternative derivations of Green function (4.5.84) can be found in Hudson (1980, Section 2.5). The time derivative

of his equation (2.34) gives the result for a $\hat{\mathbf{z}}$ source (source (2.35) has a time function $H(t)$ rather than $\delta(t)$). Equation (2.36) gives the results for sources $\hat{\mathbf{r}}$ and $\hat{\phi}$.

4.8

Prove the general form of an isotropic fourth-order tensor (4.4.45) (Jeffreys, 1931).

We follow closely the proofs in Chapter VII of Jeffreys (1931, pp. 66–70). For completeness we consider tensors up to fourth order.

For a tensor to be isotropic, its components must retain the same values however the axes are rotated. We consider a rotation as described by $\delta\theta$ (4.2.5) or the anti-symmetric tensor, ξ .

There are no isotropic tensors of first order. Applying the anti-symmetric tensor ξ_{ip} (4.2.4) to rotate a first-order tensor \mathbf{u} , we have

$$u'_i = (\delta_{ip} - \xi_{ip})u_p = u_i - \xi_{ip}u_p,$$

and this can be equal to u_i only if $\xi_{ip}u_p = 0$ for all admissible values of ξ_{ip} . Thus

$$\begin{aligned}\xi_{12}u_2 - \xi_{31}u_3 &= 0 \\ -\xi_{12}u_1 + \xi_{23}u_3 &= 0 \\ \xi_{31}u_1 - \xi_{23}u_2 &= 0,\end{aligned}$$

and these equations are only satisfied for any ξ_{23} , ξ_{31} and ξ_{12} if

$$u_1 = u_2 = u_3 = 0.$$

If u_{ij} is a second-order, isotropic tensor then

$$\begin{aligned}u'_{ij} &= (\delta_{ip} - \xi_{ip})(\delta_{jq} - \xi_{jq})u_{pq} \\ &= u_{ij} - \xi_{ip}u_{pj} - \xi_{jq}u_{iq},\end{aligned}\tag{4.1}$$

to first order, for all values of i and j . Hence

$$\xi_{ip}u_{pj} + \xi_{jq}u_{iq} = 0.$$

Take $i = 1$ and $j = 2$ and we have

$$\xi_{12}u_{22} - \xi_{31}u_{32} - \xi_{12}u_{11} + \xi_{23}u_{13} = 0.$$

Therefore $u_{23} = u_{32} = 0$ and $u_{11} = u_{22}$. By symmetry $u_{ij} = 0$ if $i \neq j$, and $u_{11} = u_{22} = u_{33}$. If $i = j = 1$, we have

$$\xi_{12}u_{21} - \xi_{31}u_{31} + \xi_{12}u_{12} - \xi_{31}u_{13} = 0,$$

which is satisfied as every term is zero. Hence the only isotropic tensors of second order are a scalar multiple of δ_{ij} .

If u_{ijk} is an third-order, isotropic tensor then

$$u'_{ijk} = (\delta_{ip} - \xi_{ip})(\delta_{jq} - \xi_{jq})(\delta_{kr} - \xi_{kr})u_{pqr},$$

and for all values of i, j and k

$$\xi_{ip}u_{pjk} + \xi_{jq}u_{iqk} + \xi_{kr}u_{ijr} = 0.$$

Take $i = j = 1$ and

$$\xi_{12}u_{21k} - \xi_{31}u_{31k} + \xi_{12}u_{12k} - \xi_{31}u_{13k} + \xi_{k1}u_{111} + \xi_{k2}u_{112} + \xi_{k3}u_{113} = 0.$$

Now put $k = 2$, then

$$\begin{aligned} u_{212} + u_{122} &= u_{111} \\ u_{312} + u_{132} &= 0 \\ u_{113} &= 0. \end{aligned}$$

From the last equation, and by symmetry, $u_{ijk} = 0$ if two i, j, k are equal and the third unequal. Then by the first equation, $u_{ijk} = 0$ if all indices are equal. And the second equation shows that

$$u_{ijk} = -u_{jik}.$$

If we put $k = 1$ in the above equation, i.e. $i = j = k$, every term vanishes so it holds. Finally in the general equation, if i, j and k are all different, u_{pjk} is zero unless $p = i$ and then $\xi_{ip} = 0$. Thus the general equation holds. It follows that the only third-order, isotropic tensors are scalar multiples of ϵ_{ijk} .

Finally for an isotropic, fourth-order tensor u_{ijkl} we have

$$\xi_{ip}u_{pjkl} + \xi_{jq}u_{iqkl} + \xi_{kr}u_{ijrl} + \xi_{ls}u_{ijks} = 0.$$

There are four cases to consider: **(a)** two equal indices and the other two unequal; **(b)** three equal; **(c)** two equal and the other two equal but different; and **(d)** all four different.

Case (a): take $i = j = 1, k = 2$ and $l = 3$. Then

$$\begin{aligned} &\xi_{12}u_{2123} - \xi_{31}u_{3123} + \xi_{12}u_{1223} - \xi_{31}u_{1323} \\ &- \xi_{12}u_{1113} + \xi_{23}u_{1133} + \xi_{31}u_{1121} - \xi_{23}u_{1122} = 0. \end{aligned}$$

Hence

$$\begin{aligned} u_{2123} + u_{1223} - u_{1113} &= 0 \\ u_{3123} + u_{1323} - u_{1121} &= 0 \\ u_{1133} - u_{1122} &= 0. \end{aligned}$$

Other instances of case **(a)** can be obtained by interchanging indices that are not equal and by permuting axes. Thus the final relation gives

$$u_{1133} = u_{1122} = u_{2233} = u_{2211} = u_{3322} = u_{3311},$$

and also

$$\begin{aligned} u_{1313} &= u_{1212} = u_{2323} = u_{2121} = u_{3232} = u_{3131} \\ u_{3113} &= u_{2112} = u_{3223} = u_{1221} = u_{2332} = u_{1331}. \end{aligned}$$

Case (b): take $i = j = k = 1$ and $l = 2$. Then

$$\begin{aligned} \xi_{12}u_{2112} - \xi_{31}u_{3112} + \xi_{12}u_{1212} - \xi_{31}u_{1312} \\ + \xi_{12}u_{1122} - \xi_{31}u_{1132} - \xi_{12}u_{1111} + \xi_{23}u_{1113} = 0. \end{aligned}$$

The last term shows $u_{1113} = 0$ and therefore by interchanging indices, all components of case (b) are zero. Also from the coefficient of ξ_{31}

$$u_{3112} + u_{1312} + u_{1132} = 0.$$

But in the first result for class **(a)** the last term vanishes, so

$$u_{2123} + u_{1223} = 0.$$

Similarly interchanging indices

$$u_{1312} + u_{3112} = 0,$$

so

$$u_{1132} = 0,$$

and all coefficients of case **(a)** are zero. Finally from the coefficient of ξ_{12} we have

$$u_{1111} = u_{2112} + u_{1212} + u_{1122},$$

relating components of class **(d)** to three of type **(c)**.

No further information is obtained by transforming components of cases **(c)** and **(d)**. For if $i = j = 1$ and $k = l = 2$, replacing i or j by p will give a zero component unless $p = 1$ and then the factor ξ_{ip} or ξ_{jp} is zero. The transformation relationship holds automatically. Similarly if $i = j = k = l$.

Above we have three groups of six equal components that need not be zero:

$$\begin{aligned} u_{1133} &= u_{1122} = u_{2233} = u_{2211} = u_{3322} = u_{3311} = \lambda \\ u_{1313} &= u_{1212} = u_{2323} = u_{2121} = u_{3232} = u_{3131} = \mu \\ u_{3113} &= u_{2112} = u_{3223} = u_{1221} = u_{2332} = u_{1331} = \nu, \end{aligned}$$

where λ , μ and ν are arbitrary constants. It is then self-evident that all the above results satisfy

$$u_{ijkl} = \lambda \delta_{ij} \delta_{kl} + \mu \delta_{ik} \delta_{jl} + \nu \delta_{il} \delta_{jk},$$

the most general form of a fourth-order, isotropic tensor.

4.9

The dipole, explosion and double-couple results have only been given for the far-field radiation patterns. Investigate the near-field terms by differentiating the exact point source results (see, for instance, Aki and Richards (1980, 2002) or Pujol (2003) for details). Are the signals exactly zero on the node planes?

The Green force dyadic is (4.5.71)

$$\begin{aligned} \underline{\mathbf{u}}(t, \mathbf{x}_R; \mathbf{x}_S) &= \frac{\delta(t - R/\alpha)}{4\pi\rho\alpha^2 R} \hat{\mathbf{r}} \hat{\mathbf{r}}^T + \frac{\delta(t - R/\beta)}{4\pi\rho\beta^2 R} (\mathbf{I} - \hat{\mathbf{r}} \hat{\mathbf{r}}^T) \\ &+ \frac{t}{4\pi\rho R^3} \{H(t - R/\alpha) - H(t - R/\beta)\} (3\hat{\mathbf{r}} \hat{\mathbf{r}}^T - \mathbf{I}), \end{aligned}$$

or

$$\begin{aligned} 4\pi\rho u_{jk}(t, \mathbf{x}_R; \mathbf{x}_S) &= \hat{r}_j \hat{r}_k \frac{\delta(t - R/\alpha)}{\alpha^2 R} \\ &+ (\delta_{jk} - \hat{r}_j \hat{r}_k) \frac{\delta(t - R/\beta)}{\beta^2 R} \\ &+ (3\hat{r}_j \hat{r}_k - \delta_{jk}) \frac{H(t - R/\alpha) - H(t - R/\beta)}{R^3} t, \end{aligned}$$

where \hat{r}_i are the direction cosines (components of $\hat{\mathbf{r}}$).

Using $\boldsymbol{\xi}$ for the source location and \mathbf{x} for the receiver (to avoid further subscripts), we have $\mathbf{r} = \mathbf{x} - \boldsymbol{\xi}$ so $R^2 = (x_k - \xi_k)(x_k - \xi_k)$ and

$$\frac{\partial R}{\partial \xi_i} = -\frac{x_i - \xi_i}{R} = -\hat{r}_i,$$

as $\hat{r}_j = (x_j - \xi_j)/R$. Also differentiating \hat{r}_j , we have

$$\frac{\partial \hat{r}_j}{\partial \xi_i} = -\frac{x_j - \xi_j}{R^2} \frac{\partial R}{\partial \xi_i} - \frac{\delta_{ij}}{R} = \frac{\hat{r}_i \hat{r}_j - \delta_{ij}}{R}.$$

Applying these operators, it is now just a lot of terms! Thus

$$\begin{aligned} \frac{\partial}{\partial \xi_i} \hat{r}_j \hat{r}_k \frac{\delta(t - R/\alpha)}{R} &= (3\hat{r}_i \hat{r}_j \hat{r}_k - \hat{r}_j \delta_{ik} - \hat{r}_k \delta_{ij}) \frac{\delta(t - R/\alpha)}{R^2} \\ &\quad + \hat{r}_j \hat{r}_k \frac{\delta_{,i}(t - R/\alpha)}{R}, \end{aligned}$$

where we use the shorthand $\delta_{,i} = \partial \delta / \partial \xi_i$. Next

$$\begin{aligned} \frac{\partial}{\partial \xi_i} (\delta_{jk} - \hat{r}_j \hat{r}_k) \frac{\delta(t - R/\beta)}{R} &= \\ &(\hat{r}_i \delta_{jk} + \hat{r}_j \delta_{ki} + \hat{r}_k \delta_{ij} - 3\hat{r}_i \hat{r}_j \hat{r}_k) \frac{\delta(t - R/\beta)}{R^2} \\ &\quad + (\delta_{jk} - \hat{r}_j \hat{r}_k) \frac{\delta_{,i}(t - R/\beta)}{R}. \end{aligned}$$

Finally

$$\begin{aligned} \frac{\partial}{\partial \xi_i} (3\hat{r}_j \hat{r}_k - \delta_{jk}) \frac{H(t - R/\alpha) - H(t - R/\beta)}{R^3} t &= \\ 3(5\hat{r}_i \hat{r}_j \hat{r}_k - \hat{r}_i \delta_{jk} - \hat{r}_j \delta_{ki} - \hat{r}_k \delta_{ij}) \frac{H(t - R/\alpha) - H(t - R/\beta)}{R^4} t & \\ + (3\hat{r}_j \hat{r}_k - \delta_{jk}) \left(\frac{\delta(t - R/\alpha)}{\alpha^2} - \frac{\delta(t - R/\beta)}{\beta^2} \right) \frac{\hat{r}_i}{R^2}, & \end{aligned}$$

where in the final term we use

$$\frac{\partial}{\partial \xi_i} H(t - R/c) t = -t \delta(t - R/c) (R/c)_{,i} = \delta(t - R/c) \frac{R \hat{r}_i}{c^2},$$

as we can set $t = R/c$ outside the delta function. Gathering up the various terms, we obtain

$$\begin{aligned} 4\pi \rho u_{jk,i}(t, \mathbf{x}_R; \mathbf{x}_S) &= \\ \hat{r}_i \hat{r}_j \hat{r}_k \frac{\dot{\delta}(t - R/\alpha)}{\alpha^3 R} & \\ + (\delta_{jk} - \hat{r}_j \hat{r}_k) \hat{r}_i \frac{\dot{\delta}(t - R/\beta)}{\beta^3 R} & \\ + (6\hat{r}_i \hat{r}_j \hat{r}_k - \hat{r}_i \delta_{jk} - \hat{r}_j \delta_{ki} - \hat{r}_k \delta_{ij}) \frac{\delta(t - R/\alpha)}{\alpha^2 R^2} & \\ - (6\hat{r}_i \hat{r}_j \hat{r}_k - 2\hat{r}_i \delta_{jk} - \hat{r}_j \delta_{ki} - \hat{r}_k \delta_{ij}) \frac{\delta(t - R/\beta)}{\beta^2 R^2} & \end{aligned}$$

$$+ 3(5\hat{r}_i\hat{r}_j\hat{r}_k - \hat{r}_i\delta_{jk} - \hat{r}_j\delta_{ki} - \hat{r}_k\delta_{ij}) \frac{H(t - R/\alpha) - H(t - R/\beta)}{R^4} t.$$

The first two terms agree with the far-field approximation used in expression (4.6.17). The other terms are the near field.

In both the force and moment Green functions, the near-field terms are non-zero on the nodes of the far-field terms.

4.10

Further reading: The homogeneous, far-field radiation pattern has been given here for an isotropic medium (4.5.75). Lighthill (1960), Buchwald (1959) and Burridge (1967) have investigated the equivalent result in an anisotropic medium. The result, while more complicated to derive, is remarkably similar, i.e. in the frequency domain

$$\underline{\mathbf{u}}(\omega, \mathbf{x}_R; \mathbf{x}_S) \simeq \frac{e^{i\omega \mathbf{p} \cdot (\mathbf{x}_R - \mathbf{x}_S)}}{4\pi\rho |\mathbf{V}| K^{1/2}(\mathbf{p}) R} \hat{\mathbf{g}} \hat{\mathbf{g}}^T,$$

where $K(\mathbf{p})$ is the Gaussian curvature of the slowness surface at \mathbf{p} , and \mathbf{V} is the ray (group) velocity. See, for instance, Burridge (1967, Section 6.7). This result is useful in anisotropic ray theory (see Section 5.4.2 and Kendall, Guest and Thomson, 1992).

4.11

Further reading: We have only developed the stress and strain tensors, and the elastic constitutive equations and equations of motion in cartesian coordinates. For some problems, the equations in cylindrical or spherical coordinates are useful. These results can be found in several textbooks, for instance, the classic book by Love (1944) or the more modern treatments by Fung (1965) or Takeuchi and Saito (1972).

As the full development can be found in textbooks, we just quote the useful results.

Cylindrical polar coordinates: denoting the cylindrical coordinates by r (cylindrical radius), ϕ (azimuthal angle) and z (axial coordinate), the strain components are

$$e_{rr} = \frac{\partial u_r}{\partial r}$$

$$\begin{aligned}
e_{\phi\phi} &= \frac{1}{r} \frac{\partial u_\phi}{\partial \phi} + \frac{u_r}{r} \\
e_{zz} &= \frac{\partial u_z}{\partial z} \\
e_{\phi z} &= \frac{1}{2} \left(\frac{\partial u_\phi}{\partial z} + \frac{1}{r} \frac{\partial u_z}{\partial \phi} \right) \\
e_{zr} &= \frac{1}{2} \left(\frac{\partial u_z}{\partial r} + \frac{\partial u_r}{\partial z} \right) \\
e_{r\phi} &= \frac{1}{2} \left(\frac{1}{r} \frac{\partial u_r}{\partial \phi} + \frac{\partial u_\phi}{\partial r} - \frac{u_\phi}{r} \right).
\end{aligned}$$

The equations of motion are

$$\begin{aligned}
\rho \frac{\partial v_r}{\partial t} &= f_r + \frac{1}{r} \frac{\partial}{\partial r} (r \sigma_{rr}) + \frac{1}{r} \frac{\partial \sigma_{r\phi}}{\partial \phi} + \frac{\partial \sigma_{zr}}{\partial z} - \frac{\sigma_{\phi\phi}}{r} \\
\rho \frac{\partial v_\phi}{\partial t} &= f_\phi + \frac{1}{r} \frac{\partial}{\partial r} (r \sigma_{r\phi}) + \frac{1}{r} \frac{\partial \sigma_{\phi\phi}}{\partial \phi} + \frac{\partial \sigma_{\phi z}}{\partial z} + \frac{\sigma_{r\phi}}{r} \\
\rho \frac{\partial v_z}{\partial t} &= f_z + \frac{1}{r} \frac{\partial}{\partial r} (r \sigma_{zr}) + \frac{1}{r} \frac{\partial \sigma_{\phi z}}{\partial \phi} + \frac{\partial \sigma_{zz}}{\partial z}.
\end{aligned}$$

Note the derivative terms on the right-hand side are $\text{div}(\mathbf{t}_r)$, $\text{div}(\mathbf{t}_\phi)$ and $\text{div}(\mathbf{t}_z)$, respectively.

Spherical coordinates: denoting the spherical coordinates by r (spherical radius), θ (co-latitude angle) and ϕ (azimuthal angle), the strain components are

$$\begin{aligned}
e_{rr} &= \frac{\partial u_r}{\partial r} \\
e_{\theta\theta} &= \frac{1}{r} \frac{\partial u_\theta}{\partial \theta} + \frac{u_r}{r} \\
e_{\phi\phi} &= \frac{1}{r \sin \theta} \frac{\partial u_\phi}{\partial \phi} + \frac{u_r}{r} + \frac{\cot \theta}{r} u_\theta \\
e_{\theta\phi} &= \frac{1}{2} \left(\frac{1}{r \sin \theta} \frac{\partial u_\theta}{\partial \phi} + \frac{1}{r} \frac{\partial u_\phi}{\partial \theta} - \frac{\cot \theta}{r} u_\phi \right) \\
e_{\phi r} &= \frac{1}{2} \left(\frac{\partial u_\phi}{\partial r} + \frac{1}{r \sin \theta} \frac{\partial u_r}{\partial \phi} - \frac{u_\phi}{r} \right) \\
e_{r\theta} &= \frac{1}{2} \left(\frac{1}{r} \frac{\partial u_r}{\partial \theta} + \frac{\partial u_\theta}{\partial r} - \frac{u_\theta}{r} \right).
\end{aligned}$$

The equations of motion are

$$\begin{aligned}
\rho \frac{\partial v_r}{\partial t} &= f_r + \frac{1}{r^2} \frac{\partial}{\partial r} (r^2 \sigma_{rr}) \\
&+ \frac{1}{r \sin \theta} \frac{\partial}{\partial \theta} (\sin \theta \sigma_{r\theta}) + \frac{1}{r \sin \theta} \frac{\partial \sigma_{\phi r}}{\partial \phi} - \frac{1}{r} (\sigma_{\theta\theta} + \sigma_{\phi\phi})
\end{aligned}$$

$$\begin{aligned}
\rho \frac{\partial v_\theta}{\partial t} &= f_\theta + \frac{1}{r^2} \frac{\partial}{\partial r} (r^2 \sigma_{r\theta}) \\
&\quad + \frac{1}{r \sin \theta} \frac{\partial}{\partial \theta} (\sin \theta \sigma_{\theta\theta}) + \frac{1}{r \sin \theta} \frac{\partial \sigma_{\theta\phi}}{\partial \phi} + \frac{1}{r} (\sigma_{r\theta} - \sigma_{\phi\phi} \cot \theta) \\
\rho \frac{\partial v_\phi}{\partial t} &= f_\phi + \frac{1}{r^2} \frac{\partial}{\partial r} (r^2 \sigma_{\phi r}) \\
&\quad + \frac{1}{r \sin \theta} \frac{\partial}{\partial \theta} (\sin \theta \sigma_{\theta\phi}) + \frac{1}{r \sin \theta} \frac{\partial \sigma_{\phi\phi}}{\partial \phi} + \frac{1}{r} (\sigma_{\phi r} + \sigma_{\theta\phi} \cot \theta).
\end{aligned}$$

Note the derivative terms on the right-hand side are $\text{div}(\mathbf{t}_r)$, $\text{div}(\mathbf{t}_\theta)$ and $\text{div}(\mathbf{t}_\phi)$, respectively.

4.12

Muir (personal communication, 2003) has pointed out that although the Voigt notation is compact (Section 4.4.2), many of the awkward factors of 2 or $\sqrt{2}$, e.g. equation (4.4.14), can be avoided if we retain all 9 components in the stress and strain vectors. Writing a stress vector as

$$\boldsymbol{\sigma} = \begin{pmatrix} \mathbf{t}_1 \\ \mathbf{t}_2 \\ \mathbf{t}_3 \end{pmatrix},$$

and similarly for a strain vector, the constitutive equation can be written

$$\boldsymbol{\sigma} = \mathbf{C} \mathbf{e} = \begin{pmatrix} \mathbf{c}_{11} & \mathbf{c}_{12} & \mathbf{c}_{13} \\ \mathbf{c}_{21} & \mathbf{c}_{22} & \mathbf{c}_{23} \\ \mathbf{c}_{31} & \mathbf{c}_{32} & \mathbf{c}_{33} \end{pmatrix} \mathbf{e},$$

where the 3×3 sub-matrices of the 9×9 matrix \mathbf{C} are defined in equations (4.4.36) to (4.4.39).

The symmetry of the stress and strain tensors are imposed by the equality of rows and elements in the matrix \mathbf{C} . Although this makes the matrix \mathbf{C} singular, show by numerical example or otherwise, that the compliance matrix \mathbf{S} can be obtained from the generalized inverse of the stiffness matrix \mathbf{C} .

It should also be commented that Muir (personal communication, 2003) suggested an alternative order for the components of the stress and strain vectors that emphasizes symmetries in the matrix \mathbf{C} for symmetric media, i.e. isotropic, transversely isotropic, etc.

To illustrate the stiffness matrix \mathbf{C} and corresponding compliance matrix

\mathbf{S} , we introduce a general purpose routine which converts from the Voigt notation C_{ij} (4.4.12) to the matrix notation \mathbf{c}_{jk} (4.4.37):

```
function matrices = cMatrices( Voigt )
% cMatrices = form 3x3 c_jk matrices (4.4.37) from Voigt
% notation, i.e. definitions (4.4.39)

% INPUT:
%      Voigt.Cjk      = Voigt elastic parameters
%
% OUTPUT:
%      matrices.cjk    = 3x3 matrices c_jk
%
matrices = ...
    struct('c11', [ Voigt.C11, Voigt.C16, Voigt.C15 ;...
                    Voigt.C16, Voigt.C66, Voigt.C56 ;...
                    Voigt.C15, Voigt.C56, Voigt.C55 ],...
          'c22', [ Voigt.C66, Voigt.C26, Voigt.C26 ;...
                    Voigt.C26, Voigt.C22, Voigt.C24 ;...
                    Voigt.C46, Voigt.C24, Voigt.C44 ],...
          'c33', [ Voigt.C55, Voigt.C45, Voigt.C35 ;...
                    Voigt.C45, Voigt.C44, Voigt.C34 ;...
                    Voigt.C35, Voigt.C34, Voigt.C33 ],...
          'c23', [ Voigt.C56, Voigt.C46, Voigt.C36 ;...
                    Voigt.C25, Voigt.C24, Voigt.C23 ;...
                    Voigt.C45, Voigt.C44, Voigt.C34 ],...
          'c31', [ Voigt.C15, Voigt.C56, Voigt.C55 ;...
                    Voigt.C14, Voigt.C46, Voigt.C45 ;...
                    Voigt.C13, Voigt.C36, Voigt.C35 ],...
          'c12', [ Voigt.C16, Voigt.C12, Voigt.C14 ;...
                    Voigt.C66, Voigt.C26, Voigt.C46 ;...
                    Voigt.C56, Voigt.C25, Voigt.C45 ] );
return
```

This function is used in further exercises in Chapter 5 and 6. The Voigt notation is convenient for user input and display, while the matrix notation is more suitable for computations.

For illustrative purposes, we consider an isotropic, Poisson solid with Lamé parameters $\lambda = \mu = 1$. The following program displays the 9×9 stiffness matrix \mathbf{C} and the corresponding 9×9 compliance matrix \mathbf{S} obtained

using the Moore-Penrose pseudoinverse. The Moore-Penrose pseudoinverse is defined such that

$$\begin{aligned}\mathbf{CSC} &= \mathbf{C} \\ \mathbf{SCS} &= \mathbf{S},\end{aligned}$$

and \mathbf{CS} and \mathbf{SC} are Hermitian.

```
function Exercise412
% Exercise 4.12
%
% Moore-Penrose pseudoinverse of 9x9 matrix C
%
% use a very simple isotropic Poisson solid as example with
% mu = lambda = 1, so stiffnesses are 1, 1 and 3, and
% compliances are 2/5, 1/4 and -1/10 from equations (4.4.53)
% through (4.4.58)
L=1;
G=1;
% fluid example
% G=0;
A=L+2*G;
Poisson = struct( ...
    'C11',A,'C12',L,'C13',L,'C14',0,'C15',0,'C16',0,...
    'C22',A,'C23',L,'C24',0,'C25',0,'C26',0,...
    'C33',A,'C34',0,'C35',0,'C36',0,...
    'C44',G,'C45',0,'C46',0,...
    'C55',G,'C56',0,...
    'C66',G);
%
cjk = cMatrices( Poisson );
% make the 9x9 matrix C
C = zeros(9,9);
C(1:3,1:3) = cjk.c11;
C(1:3,4:6) = cjk.c12;
C(1:3,7:9) = cjk.c31';
C(4:6,1:3) = cjk.c12';
C(4:6,4:6) = cjk.c22;
C(4:6,7:9) = cjk.c23;
C(7:9,1:3) = cjk.c31;
C(7:9,4:6) = cjk.c23';
```



```

C(7:9,7:9) = cjk.c33;
C
% take Moore-Penrose pseudoinverse
S = pinv(C)
return

```

The output for the matrix \mathbf{C} is

3	0	0		0	1	0		0	0	1
0	1	0		1	0	0		0	0	0
0	0	1		0	0	0		1	0	0

0	1	0		1	0	0		0	0	0
1	0	0		0	3	0		0	0	1
0	0	0		0	0	1		0	1	0

0	0	1		0	0	0		1	0	0
0	0	0		0	0	1		0	1	0
1	0	0		0	1	0		0	0	3

and for the matrix \mathbf{S} is

0.40	0	0		0	-0.10	0		0	0	-0.10
0	0.25	0		0.25	0	0		0	0	0
0	0	0.25		0	0	0		0.25	0	0

0	0.25	0		0.25	0	0		0	0	0
-0.10	0	0		0	0.40	0		0	0	-0.10
0	0	0		0	0	0.25		0	0.25	0

0	0	0.25		0	0	0		0.25	0	0
0	0	0		0	0	0.25		0	0.25	0
-0.10	0	0		0	-0.10	0		0	0	0.40

which can be recognized as agreeing with results (4.4.57) and (4.4.58). This even works for a fluid when the analytic results (4.4.57) and (4.4.58) break down. For example with bulk modulus $\kappa = 1$, the stiffness matrix \mathbf{C} is

1	0	0	0	1	0	0	0	1
0	0	0	0	0	0	0	0	0
0	0	0	0	0	0	0	0	0
0	0	0	0	0	0	0	0	0
1	0	0	0	1	0	0	0	1

$$\begin{array}{ccccccccc}
0 & 0 & 0 & 0 & 0 & 0 & 0 & 0 & 0 \\
0 & 0 & 0 & 0 & 0 & 0 & 0 & 0 & 0 \\
0 & 0 & 0 & 0 & 0 & 0 & 0 & 0 & 0 \\
1 & 0 & 0 & 0 & 1 & 0 & 0 & 0 & 1
\end{array}$$

and the Moore-Penrose pseudoinverse gives the compliance matrix $\mathbf{S} = \mathbf{C}/9$, which corresponds to a compressibility $k = 1$, and the equation $e_{11} = -kP/3$, etc. (4.4.4).

4.13

Determine the compliance matrix \mathbf{S} for a TIV medium, i.e. the equivalent of (4.4.54) from (4.4.53) for isotropic media, but for (4.4.60) for TIV media (see Nye, 1957).

Isotropic Media: In isotropic media, the Voigt matrix has the form (4.4.53)

$$\mathbf{C} = \begin{pmatrix} \lambda + 2\mu & \lambda & \lambda & 0 & 0 & 0 \\ \lambda & \lambda + 2\mu & \lambda & 0 & 0 & 0 \\ \lambda & \lambda & \lambda + 2\mu & 0 & 0 & 0 \\ 0 & 0 & 0 & \mu & 0 & 0 \\ 0 & 0 & 0 & 0 & \mu & 0 \\ 0 & 0 & 0 & 0 & 0 & \mu \end{pmatrix},$$

and the compliance matrix has the same symmetries (4.4.54). As is well known, the elastic stiffnesses can be written (4.4.49)

$$c_{ijkl} = \lambda \delta_{ij} \delta_{kl} + \mu(\delta_{ik} \delta_{jl} + \delta_{il} \delta_{jk}),$$

and the compliances as

$$s_{ijkl} = \bar{\lambda} \delta_{ij} \delta_{kl} + \bar{\mu}(\delta_{ik} \delta_{jl} + \delta_{il} \delta_{jk}),$$

where (4.4.54)

$$\begin{aligned}
\bar{\lambda} &= -\frac{\lambda}{2\mu(3\lambda + 2\mu)} \\
\bar{\mu} &= \frac{1}{4\mu}.
\end{aligned}$$

It is readily verified that

$$\bar{\lambda} + 2\bar{\mu} = \frac{\lambda + \mu}{\mu(3\lambda + 2\mu)}.$$

TIV Media: In TIV media, the Voigt matrix has the form (4.4.60)

$$\mathbf{C} = \begin{pmatrix} \lambda_{\perp} + 2\mu_{\perp} & \lambda_{\perp} & \nu & 0 & 0 & 0 \\ \lambda_{\perp} & \lambda_{\perp} + 2\mu_{\perp} & \nu & 0 & 0 & 0 \\ \nu & \nu & \lambda_{\parallel} + 2\mu_{\parallel} & 0 & 0 & 0 \\ 0 & 0 & 0 & \mu_{\parallel} & 0 & 0 \\ 0 & 0 & 0 & 0 & \mu_{\parallel} & 0 \\ 0 & 0 & 0 & 0 & 0 & \mu_{\perp} \end{pmatrix},$$

and the compliance matrix must have the same symmetries with five parameters, $\bar{\lambda}_{\perp}$, $\bar{\mu}_{\perp}$, $\bar{\lambda}_{\parallel}$, $\bar{\mu}_{\parallel}$ and $\bar{\nu}$. Nye (1957, p. 147) has given expressions for the relationships between the compliances and stiffnesses. The results are (remembering that Nye (1957, p. 134) has introduced factors of 2 and 4 in the compliance terms to make the relationship between compliance and stiffness, and *vice versa*, symmetrical)

$$\begin{aligned} \bar{\lambda}_{\perp} &= \frac{\lambda_{\parallel} + 2\mu_{\parallel}}{2c} - \frac{1}{4\mu_{\perp}} \\ \bar{\mu}_{\perp} &= \frac{1}{4\mu_{\perp}} \\ \bar{\lambda}_{\parallel} &= \frac{2(\lambda_{\perp} + \mu_{\perp})}{c} - \frac{1}{2\mu_{\parallel}} \\ \bar{\mu}_{\parallel} &= \frac{1}{4\mu_{\parallel}} \\ \bar{\nu} &= -\frac{\nu}{c}, \end{aligned}$$

where

$$c = 2(\lambda_{\parallel} + 2\mu_{\parallel})(\lambda_{\perp} + \mu_{\perp}) - 2\nu^2.$$

It is straightforward to confirm that this reduces to the isotropic result, in particular that $\bar{\lambda}_{\perp} = \bar{\lambda}_{\parallel} = \bar{\nu} = \bar{\lambda}$.

5

Asymptotic ray theory

5.1

Confirm that in equation (5.3.20) the terms due to derivatives of the polarizations, $\partial \hat{\mathbf{g}}_I / \partial p_i$, cancel as the polarizations are normalized.

By differentiating the eigen-equation (5.3.14), show that the partial derivative of the polarization is

$$\frac{\partial \hat{\mathbf{g}}_I}{\partial p_k} = \sum_{\nu \neq I} \left(\frac{2p_j \hat{\mathbf{g}}_\nu^T \mathbf{a}_{jk}^S \hat{\mathbf{g}}_I}{1 - G_\nu} \right) \hat{\mathbf{g}}_\nu,$$

where the summation is for values of ν different from I (we assume non-degeneracy), and \mathbf{a}_{jk}^S is the symmetric part of \mathbf{a}_{jk} , i.e. $\mathbf{a}_{jk}^S = (\mathbf{a}_{jk} + \mathbf{a}_{kj})/2$.

Using the above result, obtain an expression for the partial derivatives $\partial V_i / \partial p_j$ required for the elements of matrix \mathbf{R} in equation (5.2.20). Confirm that it reduces to the isotropic result, $\mathbf{R} = \alpha^2 \mathbf{I}$ (5.2.21).

With the definition (5.3.18) of the Hamiltonian, i.e.

$$H_I(\mathbf{x}, \mathbf{p}) = \frac{1}{2} p_j p_k \hat{\mathbf{g}}_I^T \mathbf{a}_{jk} \hat{\mathbf{g}}_I,$$

the derivative required for equation (5.3.20) is

$$\frac{\partial H_I}{\partial p_i} = p_k \hat{\mathbf{g}}_I^T \mathbf{a}_{ik}^S \hat{\mathbf{g}}_I + \frac{1}{2} p_j p_k \frac{\partial \hat{\mathbf{g}}_I^T}{\partial p_i} \mathbf{a}_{jk} \hat{\mathbf{g}}_I + \frac{1}{2} p_j p_k \hat{\mathbf{g}}_I^T \mathbf{a}_{jk} \frac{\partial \hat{\mathbf{g}}_I}{\partial p_i},$$

where

$$\mathbf{a}_{jk}^S = \frac{1}{2} (\mathbf{a}_{jk} + \mathbf{a}_{kj}),$$

the symmetric part of \mathbf{a}_{jk} . As the polarization is normalized, i.e. $\hat{\mathbf{g}}_I^T \hat{\mathbf{g}}_I = 1$, we must have

$$\hat{\mathbf{g}}_I^T \frac{\partial \hat{\mathbf{g}}_I}{\partial p_i} = 0,$$

and the derivative of the polarization is orthogonal to the polarization. Now $p_j p_k \mathbf{a}_{jk} \hat{\mathbf{g}}_I = \hat{\mathbf{g}}_I$ from the eigen-equation (5.3.11), so

$$\frac{\partial H_I}{\partial p_i} = p_k \hat{\mathbf{g}}_I^T \mathbf{a}_{ik}^S \hat{\mathbf{g}}_I + \frac{1}{2} \frac{\partial \hat{\mathbf{g}}_I^T}{\partial p_i} \hat{\mathbf{g}}_I + \frac{1}{2} \hat{\mathbf{g}}_I^T \frac{\partial \hat{\mathbf{g}}_I}{\partial p_i} = p_k \hat{\mathbf{g}}_I^T \mathbf{a}_{ik}^S \hat{\mathbf{g}}_I.$$

Thus the derivatives of the polarizations do not contribute to equation (5.3.20).

In the eigen-equation (5.3.14), $G_I = 1$ for the required solution and $G_J = c_J^2/c_I^2$, etc. for the others. Differentiating with respect to p_k , we obtain

$$2p_j \mathbf{a}_{jk}^S \hat{\mathbf{g}}_I + (\mathbf{\Gamma} - \mathbf{I}) \frac{\partial \hat{\mathbf{g}}_I}{\partial p_k} = \mathbf{0}.$$

Expanding the partial derivative of the polarization in terms of the orthogonal polarizations

$$\frac{\partial \hat{\mathbf{g}}_I}{\partial p_i} = g_J \hat{\mathbf{g}}_J + g_K \hat{\mathbf{g}}_K = g_\nu \hat{\mathbf{g}}_\nu,$$

say, where J and K are the indices not equal to I , we obtain

$$2p_j \mathbf{a}_{jk}^S \hat{\mathbf{g}}_I + (\mathbf{\Gamma} - \mathbf{I}) g_\nu \hat{\mathbf{g}}_\nu = \mathbf{0} = 2p_j \mathbf{a}_{jk}^S \hat{\mathbf{g}}_I + g_\nu (G_\nu - 1) \hat{\mathbf{g}}_\nu.$$

Thus

$$g_\nu = \frac{2p_j \hat{\mathbf{g}}_\nu^T \mathbf{a}_{jk}^S \hat{\mathbf{g}}_I}{1 - G_\nu},$$

and

$$\frac{\partial \hat{\mathbf{g}}_I}{\partial p_k} = \sum_{\nu \neq I} \left(\frac{2p_j \hat{\mathbf{g}}_\nu^T \mathbf{a}_{jk}^S \hat{\mathbf{g}}_I}{1 - G_\nu} \right) \hat{\mathbf{g}}_\nu,$$

where we assume non-degeneracy.

For elements of the matrix \mathbf{R} (5.2.20), we need

$$\frac{\partial^2 H_I}{\partial p_j \partial p_k} = \frac{\partial V_j}{\partial p_k} = \hat{\mathbf{g}}_I^T \mathbf{a}_{jk}^S \hat{\mathbf{g}}_I + p_\ell \left(\frac{\partial \hat{\mathbf{g}}_I^T}{\partial p_k} \mathbf{a}_{j\ell}^S \hat{\mathbf{g}}_I + \hat{\mathbf{g}}_I^T \mathbf{a}_{j\ell}^S \frac{\partial \hat{\mathbf{g}}_I}{\partial p_k} \right).$$

The second term on the right-hand side is

$$\begin{aligned} p_\ell \left(\frac{\partial \hat{\mathbf{g}}_I^T}{\partial p_k} \mathbf{a}_{j\ell}^S \hat{\mathbf{g}}_I + \hat{\mathbf{g}}_I^T \mathbf{a}_{j\ell}^S \frac{\partial \hat{\mathbf{g}}_I}{\partial p_k} \right) &= 2p_\ell \hat{\mathbf{g}}_I^T \mathbf{a}_{j\ell}^S \frac{\partial \hat{\mathbf{g}}_I}{\partial p_k} \\ &= 2p_\ell \hat{\mathbf{g}}_I^T \mathbf{a}_{j\ell}^S \sum_{\nu \neq I} \left(\frac{2p_m \hat{\mathbf{g}}_\nu^T \mathbf{a}_{mk}^S \hat{\mathbf{g}}_I}{1 - G_\nu} \right) \hat{\mathbf{g}}_\nu \\ &= \sum_{\nu \neq I} \frac{(2p_\ell \hat{\mathbf{g}}_I^T \mathbf{a}_{j\ell}^S \hat{\mathbf{g}}_\nu)(2p_m \hat{\mathbf{g}}_I^T \mathbf{a}_{mk}^S \hat{\mathbf{g}}_\nu)}{1 - G_\nu} \end{aligned}$$

$$= \sum_{\nu \neq I} \frac{4\hat{p}_\ell \hat{p}_m (\hat{\mathbf{g}}_I^T \mathbf{a}_{\ell j}^S \hat{\mathbf{g}}_\nu) (\hat{\mathbf{g}}_I^T \mathbf{a}_{mk}^S \hat{\mathbf{g}}_\nu)}{c_I^2 - c_\nu^2}.$$

Hence

$$\frac{\partial^2 H_I}{\partial p_j \partial p_k} = \frac{\partial V_j}{\partial p_k} = \hat{\mathbf{g}}_I^T \mathbf{a}_{jk}^S \hat{\mathbf{g}}_I + \sum_{\nu \neq I} \frac{4\hat{p}_\ell \hat{p}_m (\hat{\mathbf{g}}_I^T \mathbf{a}_{\ell j}^S \hat{\mathbf{g}}_\nu) (\hat{\mathbf{g}}_I^T \mathbf{a}_{mk}^S \hat{\mathbf{g}}_\nu)}{c_I^2 - c_\nu^2}.$$

In isotropic media, we can check the result for P as it is non-degenerate. Let us take $\hat{\mathbf{p}} = \hat{\mathbf{g}}_I = \hat{\mathbf{k}} = \hat{\mathbf{i}}_3$, say ($I = 3$). The matrices \mathbf{a}_{jk} for isotropic media are

$$\mathbf{a}_{11} = \begin{pmatrix} \alpha^2 & 0 & 0 \\ 0 & \beta^2 & 0 \\ 0 & 0 & \beta^2 \end{pmatrix} \quad \text{and} \quad \mathbf{a}_{23} = \begin{pmatrix} 0 & 0 & 0 \\ 0 & 0 & \alpha^2 - 2\beta^2 \\ 0 & \beta^2 & 0 \end{pmatrix},$$

etc. The matrix with the jk element $\hat{\mathbf{g}}_I^T \mathbf{a}_{jk} \hat{\mathbf{g}}_I$ is

$$\left(\hat{\mathbf{g}}_I^T \mathbf{a}_{jk} \hat{\mathbf{g}}_I \right) = \left(\hat{\mathbf{i}}_3^T \mathbf{a}_{jk} \hat{\mathbf{i}}_3 \right) = \begin{pmatrix} \beta^2 & 0 & 0 \\ 0 & \beta^2 & 0 \\ 0 & 0 & \alpha^2 \end{pmatrix}$$

We also need $\hat{\mathbf{g}}_I^T \mathbf{a}_{jk}^S \hat{\mathbf{g}}_\nu$:

$$\begin{aligned} \hat{\mathbf{g}}_I^T \mathbf{a}_{33}^S \hat{\mathbf{g}}_\nu &= \hat{\mathbf{i}}_3^T \mathbf{a}_{33}^S \hat{\mathbf{i}}_\nu &= 0 \\ \hat{\mathbf{g}}_I^T \mathbf{a}_{32}^S \hat{\mathbf{g}}_\nu &= \hat{\mathbf{i}}_3^T \mathbf{a}_{32}^S \hat{\mathbf{i}}_\nu &= 0 \quad \text{if } \nu = 1 \\ & &= (\alpha^2 - \beta^2)/2 \quad \text{if } \nu = 2 \\ \hat{\mathbf{g}}_I^T \mathbf{a}_{31}^S \hat{\mathbf{g}}_\nu &= \hat{\mathbf{i}}_3^T \mathbf{a}_{31}^S \hat{\mathbf{i}}_\nu &= 0 \quad \text{if } \nu = 2 \\ & &= (\alpha^2 - \beta^2)/2 \quad \text{if } \nu = 1, \end{aligned}$$

so

$$\hat{\mathbf{g}}_I^T \mathbf{a}_{3j}^S \hat{\mathbf{g}}_\nu = \frac{\alpha^2 - \beta^2}{2} \delta_{j\nu}.$$

Thus

$$\begin{aligned} \sum_{\nu \neq 3} \frac{4\hat{p}_\ell \hat{p}_m (\hat{\mathbf{g}}_I^T \mathbf{a}_{\ell j}^S \hat{\mathbf{g}}_\nu) (\hat{\mathbf{g}}_I^T \mathbf{a}_{mk}^S \hat{\mathbf{g}}_\nu)}{c_I^2 - c_\nu^2} &= \sum_{\nu \neq 3} \frac{4 \left(\frac{\alpha^2 - \beta^2}{2} \right)^2 \delta_{j\nu} \delta_{k\nu}}{\alpha^2 - \beta^2} \\ &= (\alpha^2 - \beta^2) \sum_{\nu \neq 3} \delta_{j\nu} \delta_{k\nu}, \end{aligned}$$

where $\ell = m = 3$ are the non-zero contributors. The matrix with this as the

jk element is

$$\left(\sum_{\nu \neq 3} \frac{4\hat{p}_\ell \hat{p}_m (\hat{\mathbf{g}}_I^T \mathbf{a}_{\ell j}^S \hat{\mathbf{g}}_\nu) (\hat{\mathbf{g}}_I^T \mathbf{a}_{mk}^S \hat{\mathbf{g}}_\nu)}{c_I^2 - c_\nu^2} \right) = \begin{pmatrix} \alpha^2 - \beta^2 & 0 & 0 \\ 0 & \alpha^2 - \beta^2 & 0 \\ 0 & 0 & 0 \end{pmatrix}.$$

Combining with the above matrix $(\hat{\mathbf{g}}_I^T \mathbf{a}_{jk}^S \hat{\mathbf{g}}_I)$, we obtain

$$\left(\frac{\partial^2 H_I}{\partial p_j \partial p_k} \right) = \alpha^2 \mathbf{I} = \mathbf{R},$$

as required (5.2.21).

5.2

Show that in isotropic media

$$\nabla^2 T = \frac{1}{cJ} \frac{d}{dT} \left(\frac{J}{c} \right),$$

where T is the travel time, J is the ray tube cross-section and c is the velocity.

From the definitions (5.1.6) and (5.1.14), we have

$$\nabla^2 T = \nabla \cdot \mathbf{p} = \nabla \cdot \left(\frac{\mathbf{V}}{c^2} \right).$$

From equations (5.2.14) and (5.2.15),

$$\frac{d}{dT} \ln D = \nabla \cdot \mathbf{V} = \frac{d}{dT} \ln(cJ).$$

But

$$\nabla \cdot \left(\frac{\mathbf{V}}{c^2} \right) = \frac{1}{c^2} \nabla \cdot \mathbf{V} - \frac{2}{c^3} \mathbf{V} \cdot \nabla c = \frac{1}{c^2} \nabla \cdot \mathbf{V} - \frac{2}{c^3} \frac{dc}{dT}.$$

Combining these results we obtain

$$\nabla^2 T = \frac{J'}{c^2 J} - \frac{c'}{c^3} = \frac{1}{cJ} \frac{d}{dT} \left(\frac{J}{c} \right).$$

5.3

Show that in isotropic media, the transport equation, e.g. equation (5.2.10) can be written

$$\frac{dv^{(0)}}{dT} + \frac{1}{2} \left(c^2 \nabla^2 T + \frac{d}{dT} \ln(\rho c^2) \right) v^{(0)} = 0$$

(which can be found in classic developments, e.g. Červený and Hron, 1980).

From Exercise 5.2:

$$\nabla \cdot \mathbf{V} = c^2 \nabla \cdot \left(\frac{\mathbf{V}}{c^2} \right) + \frac{2}{c} \frac{dc}{dT} = c^2 \nabla^2 T + \frac{d}{dT} \ln c^2.$$

Substituting in equation (5.2.10) and expanding

$$\frac{d}{dT} \ln \rho + \frac{2}{v^{(0)}} \frac{dv^{(0)}}{dT} = -c^2 \nabla^2 T - \frac{d}{dT} \ln c^2,$$

and hence

$$\frac{dv^{(0)}}{dT} + \frac{1}{2} \left(c^2 \nabla^2 T + \frac{d}{dT} \ln(\rho c^2) \right) v^{(0)} = 0.$$

5.4

Show that in isotropic media, the matrix \mathbf{M} (defined in equation (5.2.47)), satisfies a Riccati differential equation

$$\frac{d\mathbf{M}}{dT} + c^2 \mathbf{M}^2 = \mathbf{C},$$

where the matrix \mathbf{C} is defined in equation (5.2.22).

Definition (5.2.47) is

$$\mathbf{M} = \mathbf{P}_{pp} \mathbf{P}_{xp}^{-1}.$$

Differentiating we have

$$\frac{d\mathbf{M}}{dT} = \frac{d\mathbf{P}_{pp}}{dT} \mathbf{P}_{xp}^{-1} - \mathbf{P}_{pp} \left(\mathbf{P}_{xp}^{-1} \frac{d\mathbf{P}_{xp}}{dT} \mathbf{P}_{xp}^{-1} \right),$$

using the result $(\mathbf{A}^{-1})' = -\mathbf{A}^{-1} \mathbf{A}' \mathbf{A}^{-1}$ for the derivative of an inverse matrix (6.7.3). As the propagator matrix \mathbf{P} (5.2.24) satisfies the differential equation (5.2.19) with matrix (5.2.21), this becomes

$$\frac{d\mathbf{M}}{dT} = (\mathbf{C} \mathbf{P}_{xp}) \mathbf{P}_{xp}^{-1} - \mathbf{P}_{pp} \mathbf{P}_{xp}^{-1} \left(c^2 \mathbf{P}_{pp} \right) \mathbf{P}_{xp}^{-1} = \mathbf{C} - c^2 \mathbf{M}^2.$$

Hence

$$\frac{d\mathbf{M}}{dT} + c^2 \mathbf{M}^2 = \mathbf{C}.$$

5.5

If a wavefront has principal radii of curvature r_1 and r_2 , show that

$$\nabla \cdot \hat{\mathbf{p}} = \frac{1}{r_1} + \frac{1}{r_2} = K,$$

say, in isotropic media as $\hat{\mathbf{p}}$ is normal to the wavefront (this result is equivalent to equation (5.6.11) — also proved result (5.6.10)). $K = \text{tr}(\mathbf{K})$ is the curvature of the wavefront, where matrix \mathbf{K} is defined in equation (5.2.48). Show that this is consistent with the differential equation

$$\frac{dJ}{ds} = JK,$$

where J is the ray tube cross-section and s the ray length.

Consider a wavefront with principal radii of curvature r_1 and r_2 . Measure positions on the wavefront in terms of the angles θ_1 and θ_2 subtended at the centres of curvature in the principal directions. Then an elementary area on the wavefront is $r_1 r_2 d\theta_1 d\theta_2$. Consider the volume formed when the wavefront propagates a distance dr . Then applying the divergence theorem to the volume between the wavefronts, we have

$$\begin{aligned} \int \nabla \cdot \hat{\mathbf{p}} dV &= \int \hat{\mathbf{p}} \cdot d\mathbf{S} \\ &\simeq (r_1 + dr)(r_2 + dr) d\theta_1 d\theta_2 - r_1 r_2 d\theta_1 d\theta_2 \\ &\simeq (r_1 + r_2) dr d\theta_1 d\theta_2. \end{aligned}$$

But $dV = dr(r_1 d\theta_1)(r_2 d\theta_2)$, so

$$\nabla \cdot \hat{\mathbf{p}} = \frac{r_1 + r_2}{r_1 r_2} = \frac{1}{r_1} + \frac{1}{r_2} = K = \text{tr}(\mathbf{K}),$$

where \mathbf{K} is the curvature matrix (equation (5.2.46) gives $\delta\hat{\mathbf{p}} = \mathbf{K} \delta\mathbf{x}$ on the wavefront). This result is equivalent to equation (5.6.11) as $\hat{\mathbf{p}} = \hat{\mathbf{g}}_3$. But

$$\begin{aligned} \nabla \cdot \hat{\mathbf{p}} &= \nabla \cdot (c\mathbf{p}) = c \nabla^2 T + \frac{1}{c^2} \frac{dc}{dT} \\ &= \frac{1}{J} \frac{d}{dT} \left(\frac{J}{c} \right) + \frac{1}{c^2} \frac{dc}{dT} = \frac{1}{cJ} \frac{dJ}{dT} = \frac{1}{J} \frac{dJ}{ds}, \end{aligned}$$

using the result of Exercise 5.2 and $ds = c dT$. Hence

$$\frac{dJ}{ds} = JK.$$

In order to prove result (5.6.10), we consider the divergence theorem

$$\int (\nabla \cdot \hat{\mathbf{g}}_\nu) dV = \int \hat{\mathbf{g}}_\nu \cdot d\mathbf{S},$$

in a volume formed by a ray tube and two wavefronts. The polarization, $\hat{\mathbf{g}}_\nu$, is transverse so the surface integrals on the wavefronts are zero. The integrals on the sides of the ray tube are just signed areas (as $\hat{\mathbf{g}}_\nu$ is a unit vector normal to the side). Opposite sides approximately cancel — the only contribution is from area changes due to changes in the ray arc lengths due to velocity gradients in the wavefront. Thus if the volume in the divergence theorem is $ds dg_1 dg_2$, where $ds = V dT$ is the ray arc length, and dg_ν the tube width in the direction of the polarization $\hat{\mathbf{g}}_\nu$, then in this direction, the arc length increases to $ds + (\hat{\mathbf{g}}_\nu \cdot \nabla V) dg_\nu dT$ due to the change in velocity (to keep dT fixed — no summation over ν). Thus the area increase is $(\hat{\mathbf{g}}_\nu \cdot \nabla V)/V dg_1 dg_2 ds$, and cancelling the volume in the divergence theorem, we obtain result (5.6.10)

$$\nabla \cdot \hat{\mathbf{g}}_\nu = \frac{1}{V} (\hat{\mathbf{g}}_\nu \cdot \nabla V).$$

5.6

Confirm the isotropic polarization results at the end of Section 5.5 (equations (5.5.6) to (5.5.9)).

Using results (4.4.55) and (4.4.56), we have

$$p_j \mathbf{c}_{j1} = \begin{pmatrix} (\lambda + 2\mu)p_1 & \mu p_2 & \mu p_3 \\ \lambda p_2 & \mu p_1 & 0 \\ \lambda p_3 & 0 & \mu p_1 \end{pmatrix}.$$

For equation (5.5.6) with $k = 1$, we have

$$p_j \mathbf{c}_{j1} = (\lambda + \mu)p_1 \mathbf{I} + \mu \begin{pmatrix} \mathbf{p}^T \\ \mathbf{0} \\ \mathbf{0} \end{pmatrix} + \lambda \begin{pmatrix} 0 & 0 & 0 \\ p_2 & -p_1 & 0 \\ p_3 & 0 & -p_1 \end{pmatrix},$$

so

$$p_j \mathbf{c}_{j1} \hat{\mathbf{g}}_3 = (\lambda + \mu)p_1 \hat{\mathbf{g}}_3 + \frac{\mu}{c} \hat{\mathbf{i}}_1 + 0,$$

as $\mathbf{p} = \hat{\mathbf{g}}_3/c$. Thus for an arbitrary index k , we obtain result (5.5.6).

For equation (5.5.7) with $k = 1$, the transpose of the above matrix gives

$$p_j \mathbf{c}_{1j} = 2\mu p_1 \mathbf{I} + \lambda \begin{pmatrix} \mathbf{p}^\top \\ \mathbf{0} \\ \mathbf{0} \end{pmatrix} + \mu \begin{pmatrix} 0 & 0 & 0 \\ p_2 & -p_1 & 0 \\ p_3 & 0 & -p_1 \end{pmatrix},$$

so

$$p_j \mathbf{c}_{1j} \hat{\mathbf{g}}_3 = 2\mu p_1 \hat{\mathbf{g}}_3 + \frac{\lambda}{c} \hat{\mathbf{i}}_1 + 0.$$

Thus for an arbitrary index k , we obtain result (5.5.7).

For equation (5.5.8) with $k = 1$, we have

$$p_j \mathbf{c}_{j1} = \mu p_1 \mathbf{I} + \lambda \begin{pmatrix} \mathbf{p} & \mathbf{0} & \mathbf{0} \end{pmatrix} + \mu \begin{pmatrix} \mathbf{p}^\top \\ 0 \\ 0 \end{pmatrix},$$

so

$$p_j \mathbf{c}_{j1} \hat{\mathbf{g}}_\nu = \mu p_1 \hat{\mathbf{g}}_\nu + \lambda (\hat{\mathbf{i}}_1^\top \hat{\mathbf{g}}_\nu) \mathbf{p} + 0,$$

as $\mathbf{p}^\top \hat{\mathbf{g}}_\nu = 0$. Thus for an arbitrary index k , we obtain result (5.5.8).

Finally for equation (5.5.9) with $k = 1$, we have

$$p_j \mathbf{c}_{1j} = \mu p_1 \mathbf{I} + \mu \begin{pmatrix} \mathbf{p} & \mathbf{0} & \mathbf{0} \end{pmatrix} + \lambda \begin{pmatrix} \mathbf{p}^\top \\ 0 \\ 0 \end{pmatrix},$$

so

$$p_j \mathbf{c}_{1j} \hat{\mathbf{g}}_\nu = \mu p_1 \hat{\mathbf{g}}_\nu + \mu (\hat{\mathbf{i}}_1^\top \hat{\mathbf{g}}_\nu) \mathbf{p} + 0.$$

Thus for an arbitrary index k , we obtain result (5.5.9).

Thus in isotropic media we have

$$\begin{aligned} \mathbf{Z}_k^\top \hat{\mathbf{g}}_3 &= p_j \mathbf{c}_{jk} \hat{\mathbf{g}}_3 = (\lambda + 2\mu) p_k \hat{\mathbf{g}}_3 + \frac{\mu}{c} \hat{\mathbf{i}}_k \\ \mathbf{Z}_k \hat{\mathbf{g}}_3 &= p_j \mathbf{c}_{kj} \hat{\mathbf{g}}_3 = 2\mu p_k \hat{\mathbf{g}}_3 + \frac{\lambda}{c} \hat{\mathbf{i}}_k \\ \mathbf{Z}_k^\top \hat{\mathbf{g}}_\nu &= p_j \mathbf{c}_{jk} \hat{\mathbf{g}}_\nu = \mu p_k \hat{\mathbf{g}}_\nu + \lambda (\hat{\mathbf{g}}_\nu \cdot \hat{\mathbf{i}}_k) \mathbf{p} \\ \mathbf{Z}_k \hat{\mathbf{g}}_\nu &= p_j \mathbf{c}_{kj} \hat{\mathbf{g}}_\nu = \mu p_k \hat{\mathbf{g}}_\nu + \mu (\hat{\mathbf{g}}_\nu \cdot \hat{\mathbf{i}}_k) \mathbf{p}, \end{aligned}$$

where $\mathbf{p} = \hat{\mathbf{g}}_3/\alpha$ or $\hat{\mathbf{g}}_3/\beta$ for P or S rays. The second and fourth results, (5.5.7) and (5.5.9), give the traction vectors, \mathbf{t}_k (5.3.24), and are equivalent to the constitutive relationship (4.4.51).

5.7

Confirm that the expressions in Section 5.7.1 for a transversely isotropic medium reduce to those for an isotropic medium.

In an isotropic medium, if p_1 is real, then p_3 is either real or imaginary. Demonstrate that this is not necessarily so in transversely isotropic media, and that p_3 may be complex.

In an isotropic medium we have $A_{11} = A_{33} = \alpha^2$, $A_{44} = A_{66} = \beta^2$ and $A_{13} = \alpha^2 - 2\beta^2$. Thus in expression (5.7.32) for an isotropic medium we have

$$\begin{aligned} a &= \alpha^2 - \beta^2 \\ A &= 2\alpha^2\beta^2 \\ 2B &= \alpha^2 + \beta^2 - 2\alpha^2\beta^2p_1^2. \end{aligned}$$

Thus the factor in the square root is

$$4B^2 - 4A_{33}A_{44}(A_{11}p_1^2 - 1)(A_{44}p_1^2 - 1) = (\alpha^2 - \beta^2)^2,$$

so

$$p_3^2 = \frac{\alpha^2 + \beta^2 - 2\alpha^2\beta^2p_1^2 \pm (\alpha^2 - \beta^2)}{2\alpha^2\beta^2} = \frac{1}{\alpha^2} - p_1^2 \quad \text{or} \quad \frac{1}{\beta^2} - p_1^2,$$

i.e. expression (2.3.3). It is straightforward to show that other expressions in Section 5.7.1 reduce to the equivalent isotropic result.

Note that p_3^2 is necessarily real in isotropic media if p_1 is real (the factor in the square root is independent of p_1 and always positive), although it may be positive or negative, so p_3 may be real or imaginary but not complex. This is not necessarily so in TI media.

The factor in the square root in expression (5.7.32) is

$$\begin{aligned} 4B^2 - 4A_{33}A_{44}(A_{11}p_1^2 - 1)(A_{44}p_1^2 - 1) &= (A^2 - 4A_{11}A_{33}A_{44}^2)p_1^4 + \\ &+ (4A_{33}A_{44}(A_{11} + A_{44}) - 2A(A_{33} + A_{44}))p_1^2 + (A_{33} - A_{44})^2. \end{aligned}$$

At $p_1^2 = 0$, this is obviously positive. The coefficients of p_1^4 and p_1^2 are zero for isotropic media and the expression is independent of p_1 . Note that these coefficients are zero from the subtraction of two equal terms. It is possible to vary A_{13} slightly, making a TI medium, so that the coefficient of p_1^4 is negative, i.e. by increasing A_{13} so $A^2 < 4A_{11}A_{33}A_{44}^2$. This is clearly possible as the only energy constraint is that $A_{13}^2 < A_{33}(A_{11} - A_{66})$. This constraint is well satisfied in isotropic media so there is plenty of room to increase A_{13} , decrease A and make the coefficient of p_1^4 negative. If this is done, for

large enough p_1 the factor in the square root will become negative and p_3^2 complex. Then p_3 will be complex not purely imaginary.

5.8

If a ray-tracing program is available for two- or three-dimensional models, set up a model with random velocity variations. Trace rays through this model and confirm numerically the dynamic reciprocity results, e.g. result (5.2.36), and the KMAH index (it is assumed that the ray-tracing program is good enough to satisfy kinematic reciprocity!).

5.9

Programming exercise: Write a computer program to compute the slowness surfaces and wavefronts for an anisotropic, homogeneous medium, e.g. Figure 5.9, together with the polarization vectors, e.g. given the slowness direction $\hat{\mathbf{p}}$, compute the vector slowness, \mathbf{p} , the ray velocity, \mathbf{V} , and the polarization, $\hat{\mathbf{g}}$. Try the program for realistic values of the anisotropic parameters (from, for instance, Musgrave, 1970).

Hint: Although given the slowness direction, $\hat{\mathbf{p}}$, the solution for the slowness reduces to a cubic polynomial, it is better to find the slowness from the eigen-equation, (5.3.11). The 3×3 Christoffel matrix is symmetric and so three, real eigenvalues are guaranteed, whereas rounding errors may make the solutions of a cubic polynomial complex (especially near the degenerate, isotropic case).

Using the function `cMatrices` from Exercise 4.12 to form the matrices \mathbf{c}_{jk} , it is then straightforward to form the 3×3 Christoffel matrix, $\hat{\Gamma}$ (5.3.15):

```
function Gamma = Christoffel( direction , aMatrices )
% Christoffel = form 3x3 Christoffel matrix (5.3.15)

% INPUT:
%       direction(3)      = phase direction
%       aMatrices.cjk     = squared-velocity matrices a_jk
%
% OUTPUT:
%       Gamma(3,3)        = Christoffel matrix (5.3.15)
```

```

%
% Note:
% assumes direction is unit vector and aMatrices are density
% normalized, and Christoffel matrix is normalized accordingly.
%
Gamma = ...
    direction(1)*direction(1)*aMatrices.c11 +...
    direction(2)*direction(2)*aMatrices.c22 +...
    direction(3)*direction(3)*aMatrices.c33 +...
    direction(2)*direction(3)*(aMatrices.c23 +aMatrices.c23')+...
    direction(3)*direction(1)*(aMatrices.c31 +aMatrices.c31')+...
    direction(1)*direction(2)*(aMatrices.c12 +aMatrices.c12');
return

```

and to solve the eigen-equation (5.3.16) for the phase velocities, c_I , and polarizations, $\hat{\mathbf{g}}_I$:

```

function [ PhaseSlow, GroupVel, Polar ] = ...
    AnisoSurfaces( direction , aMatrices )
% AnisoSurfaces = anisotropic phase slowness, group velocity
%                 and polarization vectors in order of
%                 decreasing velocity (P, S1, S2)

% INPUT:
%       direction (3)      = phase direction
%       aMatrices.cjk      = squared-velocity matrices a_jk
%
% OUTPUT:
%       PhaseSlow(3)       = phase slownesses
%       GroupVel(3,3)      = group velocities
%       Polar(3,3)        = normalized polarizations
%
% Note:
% solutions are sorted according to ascending phase slowness;
% for multiple directions this may not give the continuous
% surfaces, and may give problems with plotting
% (phase slowness surface plots should be OK except for right at
% crossing point, but group velocity surface may be seriously
% wrong when points are joined. Check by just plotting points,
% solve by resorting according to other criterion,
% e.g. polarization)

```

```

%
% Christoffel matrix (5.3.15)
Gamma = Christoffel( direction , aMatrices );
% solve eigen-equation (5.3.16)
% columns of V are normalized polarizations
% diagonal elements of D are squared phase velocities
[ V, D ] = eig( Gamma );
[ PhaseSlow, ix ] = sort( 1./sqrt(diag(D)') );
%
GroupVel = zeros(3,3); Polar = GroupVel;
for j=1:3
    v = PhaseSlow(j);
    g = V(:,ix(j));
    Polar(:,j) = g;
    % group velocity (5.3.20)
    GroupVel(1,j) = g'*(direction(1)*aMatrices.c11+...
                        direction(2)*aMatrices.c12+...
                        direction(3)*aMatrices.c31')*g*v;
    GroupVel(2,j) = g'*(direction(1)*aMatrices.c12'+...
                        direction(2)*aMatrices.c22 +...
                        direction(3)*aMatrices.c23)*g*v;
    GroupVel(3,j) = g'*(direction(1)*aMatrices.c31'+...
                        direction(2)*aMatrices.c23'+...
                        direction(3)*aMatrices.c33)*g*v;
end
return

```

This routine also computes the group velocities, \mathbf{V}_I (5.3.20).

The following program computes results for Green Horn shale (Jones and Wang, 1981). The results are the same as in Exercise 4.4 and Figure 5.13 except that the roots are ordered by slowness, qP , $qS1$ and $qS2$, rather than polarization, qP , qSH and qSV . The program also reproduces the results for iron (Figure 5.15).

```

function Exercise59
% Exercise 5.9
%
% Solve Christoffel's equation (5.3.11)
%
% use Green Horn shale (Jones and Wang, 1981) as an example
% (see Exercise 4.4). Units are Gpa and Mg/m^3

```

```

density = 2.42;
GreenHorn = struct( ...
    'C11',34.3,'C12',13.1,'C13',10.7,'C14', 0,'C15', 0,'C16',0,...
        'C22',34.3,'C23',10.7,'C24', 0,'C25', 0,'C26',0,...
        'C33',22.7,'C34', 0,'C35', 0,'C36',0,...
        'C44',5.4,'C45', 0,'C46',0,...
        'C55',5.4,'C56',0,...
        'C66',10.6);

%
cjk = cMatrices( GreenHorn );
sqrtrho = sqrt(density);
%
for j=1:91
    theta=(j-1)*pi/180;
    % introduce density factor
    ct = cos(theta);
    st = sin(theta);
    direction = [ ct 0 st ]';
    [ PhaseSlow, GroupVel, Polar ] = ...
        AnisoSurfaces( direction , cjk );
    qS2x(j) = sqrtrho*ct*PhaseSlow(1);
    qS2z(j) = sqrtrho*st*PhaseSlow(1);
    qS1x(j) = sqrtrho*ct*PhaseSlow(2);
    qS1z(j) = sqrtrho*st*PhaseSlow(2);
    qPx(j) = sqrtrho*ct*PhaseSlow(3);
    qPz(j) = sqrtrho*st*PhaseSlow(3);
end
% plot phase surfaces
figure
hold on
plot( qS2x, qS2z, 'b' )
plot( qS1x, qS1z, 'r' )
plot( qPx, qPz, 'k' )
print -depsc2 exercise5_9a.eps
%
% second example with iron (cubic) see Shearer and
% Chapman (1988), p.580. Units are (km/s)^2.
%
iron=struct( ...
    'C11',29.64,'C12',17.71,'C13',17.71,'C14', 0,'C15', 0,'C16',0,...

```



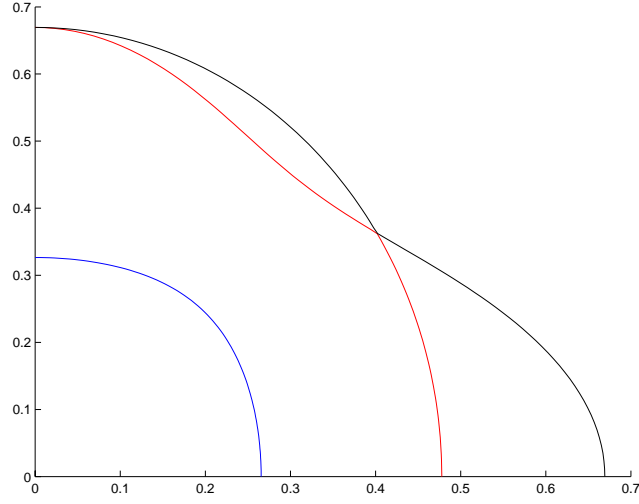
```

'C22',29.64,'C23',17.71,'C24',    0,'C25',    0,'C26',0,...
      'C33',29.64,'C34',    0,'C35',    0,'C36',0,...
      'C44',14.78,'C45',    0,'C46',0,...
      'C55',14.78,'C56',0,...
      'C66',14.78);

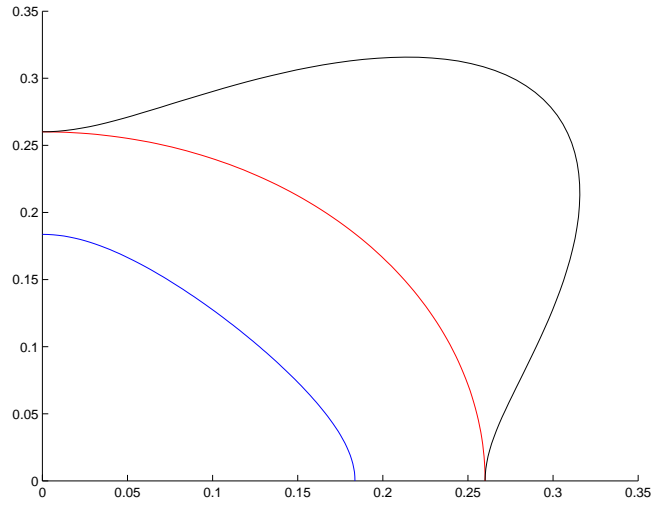
%
cjk = cMatrices( iron );
%
for j=1:91
    theta=(j-1)*pi/180;
    ct = cos(theta);
    st = sin(theta);
    direction = [ ct 0  st ]';
    [ PhaseSlow, GroupVel, Polar ] = ...
        AnisoSurfaces( direction , cjk );
    qS2x(j) = ct*PhaseSlow(1);
    qS2z(j) = st*PhaseSlow(1);
    qS1x(j) = ct*PhaseSlow(2);
    qS1z(j) = st*PhaseSlow(2);
    qPx(j)  = ct*PhaseSlow(3);
    qPz(j)  = st*PhaseSlow(3);
end
% plot phase surfaces
figure
hold on
plot( qS2x, qS2z, 'b' )
plot( qS1x, qS1z, 'r' )
plot( qPx,  qPz,  'k' )
print -depsc2 exercise5_9b.eps
return

```

The results are shown in the following figures:



The slowness surfaces for Green Horn shale (Jones and Wang, 1981). These are coloured with qP blue, qS_1 red, and qS_2 black.



The slowness surfaces for iron. These are coloured with qP blue, qS_1 red, and qS_2 black.

5.10

Further reading: The dependence of the Hamiltonian, $H_I(\mathbf{x}, \mathbf{p})$ (5.3.18), on the slowness, \mathbf{p} , occurs explicitly in the Christoffel matrix, $\Gamma = p_j p_k \mathbf{a}_{jk}$, and implicitly in the polarization, $\hat{\mathbf{g}}_I$, through the solution of the eigen-equation

(5.3.26). Alternatively, using standard matrix methods, it can be written explicitly in terms of the slowness.

The matrix

$$\mathbf{G}(G) = G\mathbf{I} - \mathbf{\Gamma} ,$$

in equation (5.3.14) is known as the characteristic matrix of matrix $\mathbf{\Gamma}$. Its determinant,

$$\Gamma(G) = |\mathbf{G}(G)| = |G\mathbf{I} - \mathbf{\Gamma}| ,$$

is the characteristic function or polynomial in G , and

$$\Gamma(G) = 0 ,$$

is the characteristic equation, cf. equation (5.3.17). The roots, G_I , of the characteristic equation are the eigenvalues of the matrix $\mathbf{\Gamma}$.

Denoting the adjoint (5.4.24) of the characteristic matrix, \mathbf{G} , by

$$\mathbf{G}^\dagger(G) = \text{adj} \left(\mathbf{G}(G) \right) ,$$

we have

$$\mathbf{G}(G)\mathbf{G}^\dagger(G) = \Gamma(G)\mathbf{I} ,$$

and

$$\mathbf{G}(G_I)\mathbf{G}^\dagger(G_I) = 0 ,$$

for an eigenvalue. Provided G_I is not a degenerate root, $\mathbf{G}(G_I)$ is simply degenerate, and as $\mathbf{G}^\dagger(G_I)$ is not null, it is of unit rank. It can be expanded in terms of the left and right eigenvectors of matrix $\mathbf{\Gamma}$ (this is a specialization of the well-known singular value decomposition (SVD, e.g. Golub and Loan, 1996; Riley, Hobson and Bence, 2002, Chapter 8), where any matrix can be expanded as an outer product of its left and right singular vectors). As the matrix $\mathbf{\Gamma}$ is symmetric, the left and right singular vectors are the eigenvectors and

$$\mathbf{G}^\dagger(G_I) = \text{tr} \left(\mathbf{G}^\dagger(G_I) \right) \hat{\mathbf{g}}_I \hat{\mathbf{g}}_I^\text{T} .$$

Červený (1972) has used this result in the kinematic ray equations (5.3.20) and (5.3.21). The Hamiltonian (5.3.18) becomes

$$H_I(\mathbf{x}, \mathbf{p}) = \frac{1}{2} p_j p_k a_{ijkl} G_{il} / G_{mm} ,$$

where G_{il} are elements of the matrix $\mathbf{G}^\dagger(1)$ (Červený, 1972, used the symbol

D_{il}). The elements of $\mathbf{G}^\dagger(G)$ are simply

$$\begin{aligned} G_{11}^\dagger(G) &= (\Gamma_{22} - G)(\Gamma_{33} - G) - \Gamma_{23}^2 \\ G_{23}^\dagger(G) &= \Gamma_{12}\Gamma_{31} - \Gamma_{23}(\Gamma_{11} - G) , \end{aligned}$$

etc. with cyclic permutations, or generally

$$G_{jk}^\dagger(G) = \frac{1}{2} \epsilon_{jil} \epsilon_{krs} (\Gamma_{ir} - G\delta_{ir})(\Gamma_{ls} - G\delta_{ls}) ,$$

where ϵ_{jil} is the Levi-Civita symbol.

This result expresses the Hamiltonian, $H_I(\mathbf{x}, \mathbf{p})$, explicitly in terms of the slowness without the polarizations. However, this is not necessary in order to obtain the differentials with respect to slowness (see Exercise 5.1), and the polarizations will probably be known from the solution of the Christoffel equation (see Exercise 5.9), e.g. for equations (5.3.20) and (5.3.21), anyway.

5.11

Further reading: In anisotropic media, the KMAH index, σ , may decrease instead of increase at a caustic. Klimeš (1997), Bakker (1998) and Garmany (2000) give details of when this occurs (for a more general description, see Lewis, 1965).

5.12

Show that the kinematic ray equations in general anisotropic media, (5.3.20) and (5.3.21), can be rewritten (Zhu, Gray and Wang, 2005)

$$\begin{aligned} \frac{d\mathbf{x}}{dT} &= \mathbf{V} \\ \frac{d\mathbf{p}}{dT} &= -\nabla \ln c. \end{aligned}$$

In a recent abstract, Zhu, Gray and Wang (2005) have developed an alternative expression for the kinematic ray equations in anisotropic media. Apart from being a simpler, more elegant and unifying expression, it clarifies the dependence of the equations on the appropriate parameters, and in

media where the Christoffel equation can be solved analytically, simplifies computations.

The kinematic ray equations (5.3.20) and (5.3.21) are

$$\begin{aligned}\frac{dx_i}{dT} &= \frac{\partial H}{\partial p_i} \\ \frac{dp_i}{dT} &= -\frac{\partial H}{\partial x_i},\end{aligned}$$

where the Hamiltonian is given by (5.3.18)

$$H(\mathbf{x}, \mathbf{p}) = \frac{1}{2} a_{ijkl} p_i p_k \hat{g}_j \hat{g}_l.$$

The first equation is, of course, the definition of the ray (group) velocity (5.3.23)

$$V_i = \frac{\partial H}{\partial p_i} = a_{ijkl} p_k \hat{g}_j \hat{g}_l,$$

but the second kinematic ray equation involves spatial derivatives of the density normalized elastic parameters, a_{ijkl} (5.3.21). But the Hamiltonian and its spatial derivative are homogeneous of degree 2 in the slowness, i.e.

$$\begin{aligned}H(\mathbf{x}, \mathbf{p}) &= \frac{1}{c^2(\mathbf{x}, \hat{\mathbf{p}})} H(\mathbf{x}, \hat{\mathbf{p}}) \\ \frac{\partial}{\partial x_i} H(\mathbf{x}, \mathbf{p}) &= \frac{1}{2} \frac{\partial a_{ijkl}}{\partial x_i} p_j p_m \hat{g}_k \hat{g}_l = \frac{1}{c^2(\mathbf{x}, \hat{\mathbf{p}})} \frac{\partial}{\partial x_i} H(\mathbf{x}, \hat{\mathbf{p}}).\end{aligned}$$

As we have (5.3.19)

$$H(\mathbf{x}, \mathbf{p}) = \frac{1}{2},$$

on the ray, we can combine these equations to give

$$\frac{\partial}{\partial x_i} H(\mathbf{x}, \mathbf{p}) = \frac{1}{c} \frac{\partial c}{\partial x_i}.$$

Thus the kinematic ray equations can be written

$$\begin{aligned}\frac{d\mathbf{x}}{dT} &= \mathbf{V} \\ \frac{d\mathbf{p}}{dT} &= -\nabla \ln c.\end{aligned}$$

These equations are completely analogous to the acoustic equations (5.1.14) and (5.1.15). Note that the spatial derivatives of the phase velocity are calculated for fixed phase direction, $\hat{\mathbf{p}}$.

These equations are a simple, unified way to write the kinematic ray equations in anisotropic media. It appears that Zhu, Gray and Wang (2005) are the first to write the second equation as above. The equations indicate that the kinematic ray results only depend on the appropriate parameters — the group velocity and phase velocity of the appropriate ray type. In the original equation (5.3.21) this property is not obvious as all elastic parameters appear to contribute. This result is important in analyzing the sensitivity of travel times to media properties, i.e. in tomography. It also means that in media where the group and phase velocity can be found from simple analytic expressions, e.g. weak or normal TI media (Exercises 4.3, 4.5 and Section 5.7.1), computations are more straightforward and efficient.

Finally, the above results simplify the dynamic ray equations. The matrix of the dynamic ray equations (5.2.20)

$$\mathbf{D} = \begin{pmatrix} \mathbf{T}^\top & \mathbf{R} \\ -\mathbf{S} & -\mathbf{T} \end{pmatrix},$$

has elements

$$\begin{aligned} T_{ij} &= \frac{\partial^2 H}{\partial x_i \partial p_j} = \frac{\partial V_j}{\partial x_i} \\ R_{ij} &= \frac{\partial^2 H}{\partial p_i \partial p_j} = \frac{\partial V_i}{\partial p_j} \\ S_{ij} &= \frac{\partial^2 H}{\partial x_i \partial x_j} = \frac{\partial^2 \ln c}{\partial x_i \partial x_j}. \end{aligned}$$

6

Rays at an interface

6.1

Programming exercise: Write a computer program to solve Snell's law for an anisotropic medium. (Finding the slowness vectors is more complicated than the Exercise 5.9 in Chapter 5. Given the slowness direction, $\hat{\mathbf{p}}$, and finding the slowness, was equivalent to solving a cubic polynomial or finding the eigenvalues of a symmetric 3×3 matrix, whereas given the interface slowness, \mathbf{p}_\perp , and finding the normal slowness component, p_n , is equivalent to solving a sextic polynomial or finding the eigenvalues of a non-symmetric 6×6 matrix.)

Hint: The simplest method is probably to use a library routine to solve the eigen-equation (6.3.14).

Further reading: Burridge (1970, Section 5) and van der Hijden (1987, Section 6.3) discuss an alternative method for identifying the direction of propagation of the eigen-solutions based on the analytic continuation of the slowness component, p_n , rather than the sign of the group velocity component, V_n .

Using the function `cMatrices` in Exercise 4.12 to define the matrices \mathbf{c}_{jk} (4.4.39), the following function solves the eigen-equation (6.3.14):

```
function [ oSlow, polarizations, tractions ] = ...  
    AnisoEigen( p, rho, cjk )  
% AnisoEigen = anisotropic eigenvectors  
  
% INPUT:  
%      p(2)                = horizontal slowness (px,py)  
%      rho                 = density  
%      cjk                 = c_jk matrices from c_Matrices
```

```

%
% OUTPUT:
%      oSlow(1,6)          = normal slownesses
%      polarizations(3,6) = matrix of polarizations
%      tractions(3,6)      = matrix of tractions
%
% Note:
% cjk are elastic parameter matrices c_jk;
% columns 1 to 3 are in positive direction; 4 to 6 negative;
% use in conjunction with functions AnisoCoeffs;
% special cases (e.g. zero normal group velocity, fluid
% media, free surface) are not covered (shift by small
% numerical factor);
% no advantage of material symmetry taken (e.g. isotropy -
% use IsoEigen)
%
% differential matrix (6.3.15) to (6.3.17)
% in the matrix A, unit(A_11) and unit(A_22) = 1/velocity,
% unit(A_21) = density, unit(A_12) = 1/density*velocity^2
% so A_21 multiplied and A_12 divided by impedance to make
% unit(A) = 1/velocity. No compensation is needed to
% eigenvectors as traction is recalculated.
% RMS P velocity used for impedance (see Exercise 4.6)
A = zeros(6,6);
meansc = (3*(cjk.c11(1,1)+cjk.c22(2,2)+cjk.c33(3,3))+...
          4*(cjk.c22(3,3)+cjk.c33(1,1)+cjk.c11(2,2))+...
          2*(cjk.c23(2,3)+cjk.c31(3,1)+cjk.c12(1,2)))/15;
Z = sqrt(rho*meansc);
ic33 = inv(cjk.c33);
A(4:6,4:6) = -(p(1)*cjk.c31'+p(2)*cjk.c23)*ic33;
A(1:3,1:3) = A(4:6,4:6)';
A(1:3,4:6) = -ic33*Z;
A(4:6,1:3) = (p(1)*p(1)*(cjk.c11-cjk.c31'*ic33*cjk.c31)+...
              p(2)*p(2)*(cjk.c22-cjk.c23*ic33*cjk.c23')+...
              p(1)*p(2)*(cjk.c12-cjk.c31'*ic33*cjk.c23'+...
              cjk.c12'-cjk.c23*ic33*cjk.c31)-...
              rho*eye(3,3))/Z;
% solve eigen-equation (6.3.14)
[ w, pn ] = eig(A);
% extract results - note tractions recomputed after

```



```

% ordering and normalizations
po = zeros(3,6); polarizations = po; tractions = po;
os = zeros(1,6); oSlow = os;
for m = 1:6
    os(1,m) = pn(m,m);
    po(:,m) = w(1:3,m);
end
% order and degenerate cases
[ oSlow, polarizations ] = TidyEigen( p, cjk, rho, os, po );
% tractions t3 = -Z3 v (5.3.24) = -p_k c_3k v (5.3.22)
pc12 = p(1)*cjk.c31+p(2)*cjk.c23';
for m = 1:6
    tractions(:,m) = -(pc12+oSlow(m)*cjk.c33)* ...
        polarizations(:,m);
end
return

```

It uses a function `TidyEigen` to handle degenerate eigenvalues, to choose the signs of the eigenvectors according to the isotropic definitions, (6.3.51) to (6.3.53), to group the eigen-solutions according to their propagation direction (from the normal component of group velocity), to order them according to the phase slowness (by decreasing real and increasing imaginary part for waves propagating in positive direction, and vice versa in the negative direction), and to normalize the polarizations according to equation (6.3.29).

```

function [ oSlow, polarizations ] =...
    TidyEigen( p, cjk, rho, in_oSlow, in_polarizations )
% TidyEigen = order and orthonormalize eigenvectors
% as revised for Addenda and Errata, 15 November 2004

% INPUT:
%      p(2)                = horizontal slowness
%      cjk                 = struct of matrices c_jk
%      rho                 = density
%      in_oSlow(1,6)       = normal slownesses
%      in_polarizations(3,6) = matrix of polarizations
%
%
% OUTPUT:
%      oSlow(1,6)          = normal slownesses
%      polarizations(3,6)  = matrix of polarizations

```

```

%
% Note:
% for internal use in Aniso_Eigen.
%
% algorithm:
% (1) first normalize polarization and order by phase slowness
%     (negative qS will be 1/2 and positive qS will be 5/6);
% (2) orthogonalizing degenerate qS eigenvectors making qSH and
%     qSV (will be appropriate for isotropic but may not be
%     correct for other degeneracies when qS1=qS2);
% (3) make signs of eigenvectors as like isotropic as possible;
% (4) compute normal group velocity for normalization and
%     ordering;
% (5) divide into positive and negative solutions using
%     normal group velocity;
% (6) order real eigenvalues by decreasing slowness magnitude,
%     and complex by increasing imag magnitude;
% (7) energy flux normalize;
% (8) if qS degenerate, make 1 and 4 like qSV.
%
% storage
os = in_oSlow; po = in_polarizations;
oSlow = os; polarizations = po;
%
for m = 1:6
    os(m) = in_oSlow(1,m);
    % normalize (not using norm as without conjugate)
    po(:,m) = in_polarizations(:,m)/...
        sqrt(in_polarizations(:,m)'*in_polarizations(:,m));
end
% interface vectors
pnorm = p(1)^2+p(2)^2;
if ( pnorm == 0 )
    ll = [ 1 0 0 ]';
    hh = [ 0 1 0 ]';
else
    ll = [ p(1) p(2) 0 ]'/sqrt(pnorm);
    hh = [ -p(2) p(1) 0 ]'/sqrt(pnorm);
end
% handle degeneracies and modifications to polarisations

```

```

% first (must be done first as group velocity depends on
% polarisations) order eigenvalues with increasing real(os)
% to get degeneracies together (use io to index order,
% rather than swapping)
io = 1:6;
for m = 1:5
    for n = m+1:6
        if ( real(os(io(n))) < real(os(io(m))) )
            tmp = io(n); io(n) = io(m); io(m) = tmp; end %swap
        end
    end
end
% degenerate eigenvalues (particularly isotropic)
% assumes degeneracies are largest slownesses (qS)
j = 1; % most negative slownesses
k = 2;
% two cases for down-going and up-going
for m = 1:2
    % degenerate equal eigenvalues
    if ( abs(os(io(j))-os(io(k))) < 1.e-6*abs(os(io(j))) )
        os(io(k)) = os(io(j));
        % find normal to degenerate polarizations
        pol1 = real( po(:,io(j)) );
        pol2 = real( po(:,io(k)) );
        % normal to degeneracy plane
        normal = cross( pol1, pol2 );
        normal = normal/norm(normal);
        fnorm = normal(1)^2+normal(2)^2;
        % degenerate plane is interface
        if ( fnorm == 0 )
            % in slowness plane (qSV) and normal to it (qSH)
            po(:,io(j)) = ll;
            po(:,io(k)) = hh;
            % general orientation of degenerate plane
        else
            % horizontal orthogonal to normal (qSH)
            po(:,io(k)) = [ -normal(2) normal(1) 0 ]'/sqrt(fnorm);
            po(:,io(j)) = cross( normal, po(:,io(k)) );
        end
    end
end
%
```

```

j = 6;                % most positive slownesses
k = 5;
end
% try and make signs of polarizations compatible (like
% isotropic)
% qSH should be in direction of cross( k, p )
% qP and qSV should have dot( pol, p ) > 0
%
if ( abs(po(3,io(1))) > abs(po(3,io(2))) )
    % 2 is qSH, 1 qSV
    if ( dot( po(:,io(2)), hh ) < 0 )
        po(:,io(2)) = -po(:,io(2)); end
    if ( dot( po(:,io(1)), ll ) < 0 )
        po(:,io(1)) = -po(:,io(1)); end
else
    % 1 is qSH, 2 qSV
    if ( dot( po(:,io(1)), hh ) < 0 )
        po(:,io(1)) = -po(:,io(1)); end
    if ( dot( po(:,io(2)), ll ) < 0 )
        po(:,io(2)) = -po(:,io(2)); end
end
% 3 and 4 are qP
if ( dot( po(:,io(3)), ll ) < 0 )
    po(:,io(3)) = -po(:,io(3)); end
if ( dot( po(:,io(4)), ll ) < 0 )
    po(:,io(4)) = -po(:,io(4)); end
%
if ( abs(po(3,io(5))) > abs(po(3,io(6))) )
    % 6 is qSH, 5 qSV
    if ( dot( po(:,io(6)), hh ) < 0 )
        po(:,io(6)) = -po(:,io(6)); end
    if ( dot( po(:,io(5)), ll ) < 0 )
        po(:,io(5)) = -po(:,io(5)); end
else
    % 5 is qSH, 6 qSV
    if ( dot( po(:,io(5)), hh ) < 0 )
        po(:,io(5)) = -po(:,io(5)); end
    if ( dot( po(:,io(6)), ll ) < 0 )
        po(:,io(6)) = -po(:,io(6)); end
end
end

```

```

% normal component of group velocity (5.3.20)
pc12 = p(1)*cjk.c31+p(2)*cjk.c23';
for m = 1:6
    m2 = pc12+oSLOW(1,m)*cjk.c33;
    group(m) = po(:,m)'*m2*po(:,m)/rho;
end

% final ordering using group for up-down separation
% and on real and imaginary phase slowness
nRp = 0; nRn = 0; nCp = 0; nCn = 0;
for m = 1:6
    if      imag(group(m)) > 0, nCp=nCp+1;iCp(nCp)=m;
    elseif imag(group(m)) < 0, nCn=nCn+1;iCn(nCn)=m;
    elseif real(group(m)) > 0, nRp=nRp+1;iRp(nRp)=m;
    else      nRn=nRn+1;iRn(nRn)=m;
    end
end

% order Real positive (Rp) decreasing
for m=1:nRp-1
    for n=m+1:nRp
        if real(os(iRp(m))) < real(os(iRp(n)))
            tmp = iRp(m); iRp(m)=iRp(n); iRp(n)=tmp; end
        end
    end
end

% make qSV first if degenerate
if (nRp > 2) && (real(os(iRp(1))) == real(os(iRp(2))))
    if abs(po(3,iRp(1))) < abs(po(3,iRp(2)))
        tmp=iRp(1); iRp(1)=iRp(2); iRp(2)=tmp; end
    end

% order Complex positive (Cp) increasing
for m=1:nCp-1
    for n=m+1:nCp
        if imag(os(iCp(m))) > imag(os(iCp(n)))
            tmp = iCp(m); iCp(m)=iCp(n); iCp(n)=tmp; end
        end
    end
end

% order Real hegative (Rn) increasing
for m=1:nRn-1
    for n=m+1:nRn

```

```

        if real(os(iRn(m))) > real(os(iRn(n)))
            tmp = iRn(m); iRn(m)=iRn(n); iRn(n)=tmp; end
        end
    end
% make qSV first if degenerate
if (nRn > 2) && (real(os(iRn(1))) == real(os(iRn(2))))
    if abs(po(3,iRn(1))) < abs(po(3,iRn(2)))
        tmp=iRn(1); iRn(1)=iRn(2); iRn(2)=tmp; end
    end
% order Complex negative (Cn) decreasing
for m=1:nCn-1
    for n=m+1:nCn
        if imag(os(iCn(m))) > imag(os(iCn(n)))
            tmp = iCn(m); iCn(m)=iCn(n); iCn(n)=tmp; end
        end
    end
end

% transfer to output
k = 1;
for m=1:nRp
    oSlow(k) = os(iRp(m));
    polarizations(:,k) = po(:,iRp(m))/sqrt( 2*rho*group(iRp(m)));
    k = k+1;
end
for m=1:nCp
    oSlow(k) = os(iCp(m));
    polarizations(:,k) = po(:,iCp(m))/sqrt( 2*rho*group(iCp(m)));
    k = k+1;
end
for m=1:nRn
    oSlow(k) = os(iRn(m));
    polarizations(:,k) = po(:,iRn(m))/sqrt(-2*rho*group(iRn(m)));
    k = k+1;
end
for m=1:nCn
    oSlow(k) = os(iCn(m));
    polarizations(:,k) = po(:,iCn(m))/sqrt(-2*rho*group(iCn(m)));
    k = k+1;
end
return

```

For the sake of completeness, we include a specialized version of **AnisoEigen** for isotropic media:

```
function [ oSlow, polarizations, tractions ] = ...
    IsoEigen( p, iso )
% IsoEigen = isotropic eigenvectors

% INPUT:
%       p                = horizontal slowness
%       iso.Alpha        = P velocity
%       iso.Beta         = S velocity
%       iso.Rho          = density
%
% OUTPUT:
%       oSlow(6)         = normal slownesses
%       polarizations(3,6) = matrix of polarizations
%       tractions(3,6)    = matrix of tractions
%
% Note:
% the order of the eigenvectors is SV, SH and P;
% columns 1 to 3 are in positive direction; 4 to 6 negative;
% use in conjunction with functions Zoeppritz and AnisoCoeffs;
% the important features of the eigenvectors are the
% energy-flux normalization, and that the interface component
% displacement is positive (with p positive). Thus for the P
% waves, the normal components are in the propagation direction,
% and the SV normal components are opposite to the propagation
% direction.
%
polarizations = zeros(3,6); tractions = polarizations;
oSlow = zeros(1,6);
% fluid
if ( iso.Beta == 0 )
    qa = sqrt((1/iso.Alpha-p)*(1/iso.Alpha+p));
    w3 = sqrt(.5/(iso.Rho*qa));
    % equations (6,3,53)
    polarizations(1,3) = w3*p;
    polarizations(1,6) = polarizations(1,3);
    polarizations(3,3) = w3*qa;
    polarizations(3,6) = -polarizations(3,3);
```

```

    tractions(3,3) = -w3*iso.Rho;
    tractions(3,6) = tractions(3,3);
    %
    oSlow(1,3) = qa;
    oSlow(1,6) = -qa;
% solid
else
    qa = sqrt((1/iso.Alpha-p)*(1/iso.Alpha+p));
    qb = sqrt((1/iso.Beta-p)*(1/iso.Beta+p));
    mu = iso.Rho*iso.Beta^2;
    % definition (6.3.54)
    Omega = qb*qb-p*p;
    % normalizations (6.3.55) to (6.3.57)
    w1 = sqrt(.5/(iso.Rho*qb));
    w2 = sqrt(.5/(mu*qb));
    w3 = sqrt(.5/(iso.Rho*qa));
    % equations (6.3.51)
    polarizations(1,1) = w1*qb;
    polarizations(1,4) = polarizations(1,1);
    polarizations(3,1) = -w1*p;
    polarizations(3,4) = -polarizations(3,1);
    tractions(1,1) = -w1*mu*Omega;
    tractions(1,4) = -tractions(1,1);
    tractions(3,1) = w1*2*mu*p*qb;
    tractions(3,4) = tractions(3,1);
    % equations (6.3.52)
    polarizations(2,2) = w2;
    polarizations(2,5) = polarizations(2,2);
    tractions(2,2) = -w2*mu*qb;
    tractions(2,5) = -tractions(2,2);
    % equations (6,3,53)
    polarizations(1,3) = w3*p;
    polarizations(1,6) = polarizations(1,3);
    polarizations(3,3) = w3*qa;
    polarizations(3,6) = -polarizations(3,3);
    tractions(1,3) = -w3*2*mu*p*qa;
    tractions(1,6) = -tractions(1,3);
    tractions(3,3) = -w3*mu*Omega;
    tractions(3,6) = tractions(3,3);
    %

```



```

oSlow(1,1) = qb;
oSlow(1,2) = qb;
oSlow(1,3) = qa;
oSlow(1,4) = -qb;
oSlow(1,5) = -qb;
oSlow(1,6) = -qa;
end
return

```

The following program uses `AnisoEigen` to solve Snell's law for Green Horn shale (Jones and Wang, 1981) used in Exercises 4.4 and 5.9 and Figure 5.13.

```

function Exercise61
% Exercise 6.1
%
% Solve Snell's law
%
% use Green Horn shale (Jones and Wang, 1981) as an example
% (see Exercise 4.4). Units are Gpa and Mg/m^3
density = 2.42;
GreenHorn = struct( ...
'C11',34.3,'C12',13.1,'C13',10.7,'C14', 0,'C15', 0,'C16',0,...
'C22',34.3,'C23',10.7,'C24', 0,'C25', 0,'C26',0,...
'C33',22.7,'C34', 0,'C35', 0,'C36',0,...
'C44',5.4,'C45', 0,'C46',0,...
'C55',5.4,'C56',0,...
'C66',10.6);
%
cjk = cMatrices( GreenHorn );
sqrtrho = sqrt(density);
% repeat Exercise 5.9 to display results
for j=1:91
    theta=(j-1)*pi/180;
    % introduce density factor
    ct = cos(theta);
    st = sin(theta);
    direction = [ ct 0 st ]';
    [ PhaseSlow, GroupVel, Polar ] = ...
        AnisoSurfaces( direction , cjk );
    qS2x(j) = sqrtrho*ct*PhaseSlow(1);
end

```

```

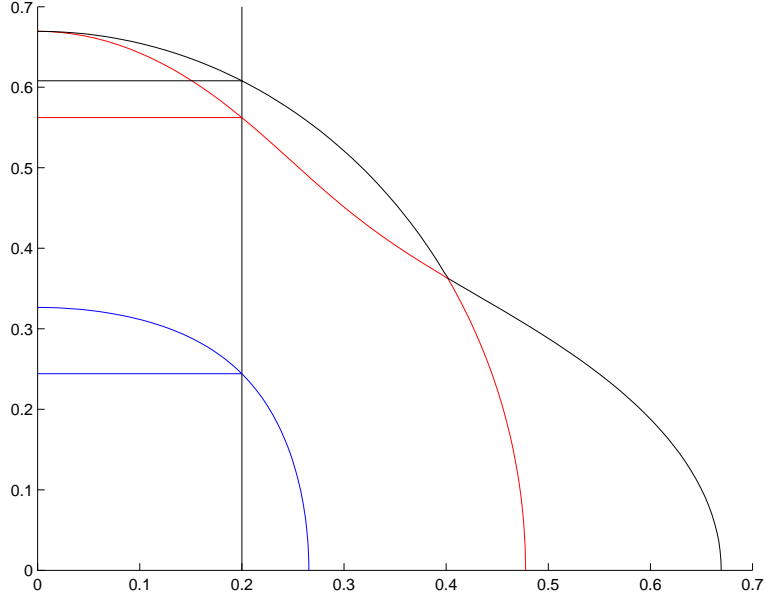
    qS2z(j) = sqrtrho*st*PhaseSlow(1);
    qS1x(j) = sqrtrho*ct*PhaseSlow(2);
    qS1z(j) = sqrtrho*st*PhaseSlow(2);
    qPx(j)  = sqrtrho*ct*PhaseSlow(3);
    qPz(j)  = sqrtrho*st*PhaseSlow(3);
end
% plot phase surfaces
% note here roots are ordered by phase slowness
figure
hold on
plot( qS2x, qS2z, 'b' )
plot( qS1x, qS1z, 'r' )
plot( qPx,  qPz,  'k' )
%
% now do Snell's law for px = .2
px=.2;
%
[ oSlow, polarizations, tractions ] = ...
    AnisoEigen( [ px 0 ], density, cjk );
% note here roots are ordered by normal group velocity
% (which differs from phase slowness order)
plot( [ .2 .2 ], [ 0 .7 ], 'k' )
plot( [ 0 .2 ], [ oSlow(3) oSlow(3) ], 'b' )
plot( [ 0 .2 ], [ oSlow(2) oSlow(2) ], 'r' )
plot( [ 0 .2 ], [ oSlow(1) oSlow(1) ], 'k' )
print -depsc2 exercise6_1.eps
return

```

The results for the normal slownesses p_n (6.3.14) are confirmed in a repeat of the plot in Exercise 5.9.

The routine `TidyEigen` uses the normal component of the group velocity V_n to discriminate the propagation direction of the eigenvectors. Burridge (1970, Section 5) and van der Hijden (1987, Section 6.3) discuss an alternative method based on the analytic continuation of the slowness eigenvalues, p_n . They give detailed arguments concerning the Riemann surfaces and singularities of the function $p_n(\mathbf{p}_\perp)$ — here we just summarize the more important results using our notation.

We assume that the coordinate system has been rotated into an interface basis, e.g. equations (6.0.1) and (6.0.2), so that the slowness component normal to the interface is $p_3 = p_n$. We consider a general cross-section of



The slowness surfaces for Green Horn shale (Jones and Wang, 1981) with solutions for p_3 for $p_1 = 0.2$. These are coloured with qP blue, qS_1 red, and qS_2 black.

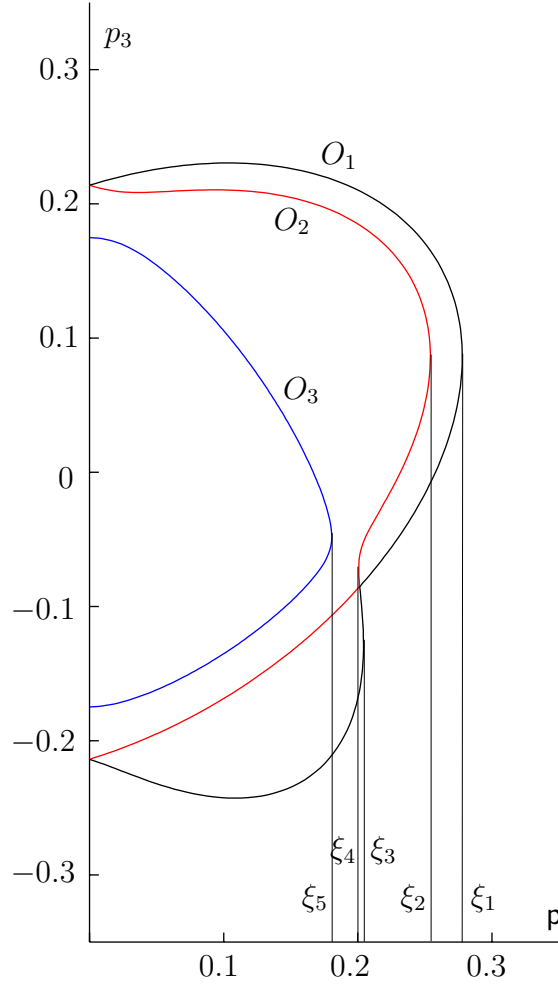
the slowness surfaces defined by an angle χ such that

$$\begin{aligned} p_1 &= p \cos \chi \\ p_2 &= p \sin \chi. \end{aligned}$$

In the interfaces basis (6.0.1), $\chi = 0$ but in general we consider any real angle. Note that $\mathbf{p} = |\mathbf{p}_\perp|$ is not to be confused with $p = |\mathbf{p}|$. For fixed χ , we study the six solutions $p_3^n(\mathbf{p})$ with $n = \pm 1, \pm 2$ and ± 3 . The solutions $p_3^n(\mathbf{p})$ can be found by solving the Christoffel equation (5.3.17) or the eigenvalue equation (6.3.14) (both leading to a sixth-order polynomial with six solutions). Our task is to associate the solutions with positive n with waves propagating in the positive x_3 direction, and *vice versa*.

The positive definite, strain energy function (4.4.32) means that the cross-section of the slowness surfaces (χ fixed) consists of three nested ovals (an oval is topologically like a circle but not necessarily convex) enclosing the origin. Note that the curves have point symmetry through the origin (as slowness terms are all second order in equation (5.3.17)). We label the curves O_j , $j = 1, 2$ and 3 in order of decreasing slowness (corresponding to the ordering used in the text for the eigenvectors \mathbf{W}). Note that in general, the index n of the solutions does not correspond to the index j of the oval

— one oval may have multiple solutions. The curves have branch points at $\mathbf{p} = \pm \xi_m$ where $dp_3/d\mathbf{p} = \pm\infty$, again ordered in decreasing order with $m = 1$ to M . In the simplest cases, e.g. isotropy, the oval and branch point indices, j and m , correspond, but in general $M \geq 3$ and they do not. This is illustrate in the figure for α -quartz as used in Figure 5.8 in the main text (p. 168) where $M = 5$ (in this example $\chi = \pi/2$).



Similar to Figure 5.8 but illustrating the branch points. The $p_2 - p_3$ cross-section of the three slowness surfaces O_j for α -quartz ($\chi = \pi/2$ in this cross-section) for $\mathbf{p} \geq 0$ is shown. The figure is based on the elastic constants from Bechmann (1958) as used by Shearer and Chapman (1988, p. 579). See also Figure 10.2.1(i) in Musgrave (1970). Branch points at $\mathbf{p} = \xi_m$ with $m = 1$ to 5 are indicated.

This figure was produced using the code

```
function Exercise61a
% Exercise 6.1a
% added to Addenda and Errata, 15 November 2004
% C12 corrected from c13 to c12 (note figures do not
% alter significantly), 17 May 2007
%
% slowness surfaces for trigonal alpha-quartz as used in
% Figure 5.8 (see Figure 10.2.1 in Musgrave, 1970).
% Shearer, P.M. and Chapman, C.H., 1988.
% Ray tracing in anisotropic media with a linear gradient,
% Geophys. J., 94, 575-580.
% Bechmann, R., 1958. Elastic and piezoelectric constants
% of alpha-quartz, Phys. Rev., 110, 1060-1061.
% Musgrave (1970, p. 130 and 282, density ~ 2.67 and
% axis in Figure 10.2.1 (i) is reversed)
% Density normalized so units km2 s-2
%
c11 = 32.73;           % from Shearer and Chapman (1988)
c33 = 40.45;
c12 = 2.64;
c13 = 4.49;
c44 = 21.86;
c14 = -6.76;          % sign as Bechmann not Musgrave
%
quartz=struct( ...
'C11',c11,'C12',c12,'C13',c13,'C14', c14,'C15', 0,'C16',0,...
        'C22',c11,'C23',c13,'C24',-c14,'C25', 0,'C26',0,...
        'C33',c11,'C34', 0,'C35', 0,'C36',0,...
        'C44', c44,'C45', 0,'C46',0,...
        'C55',c44,'C56',c14,...
        'C66',.5*(c11-c12));
%
cjk = cMatrices( quartz );
% modified from Exercise 5.9
for j=1:181
    theta=(j-91)*pi/180;
    ct = cos(theta);
    st = sin(theta);
```

```

direction = [ 0 ct st ]';      % Figure 10.2.1 (i)
% direction = [ ct 0 st ]';    % Figure 10.2.1 (ii)
% direction = [ ct st 0 ]';    % Figure 10.2.1 (iii)
[ PhaseSlow, GroupVel, Polar ] = ...
    AnisoSurfaces( direction , cjk );
sx1(j) = ct*PhaseSlow(1);
sz1(j) = st*PhaseSlow(1);
sx2(j) = ct*PhaseSlow(2);
sz2(j) = st*PhaseSlow(2);
sx3(j) = ct*PhaseSlow(3);
sz3(j) = st*PhaseSlow(3);
end
figure
hold on
plot( sx1, sz1, 'b' )
plot( sx2, sz2, 'r' )
plot( sx3, sz3, 'k' )
% units are km/s
axis ([0 .35 -.35 .35])
axis equal
axis manual
print -depsc2 exercise6_1a.eps
return

```

which uses the routine **AnisoSurfaces** given in the *Solutions to Exercises* for Exercise 5.9.

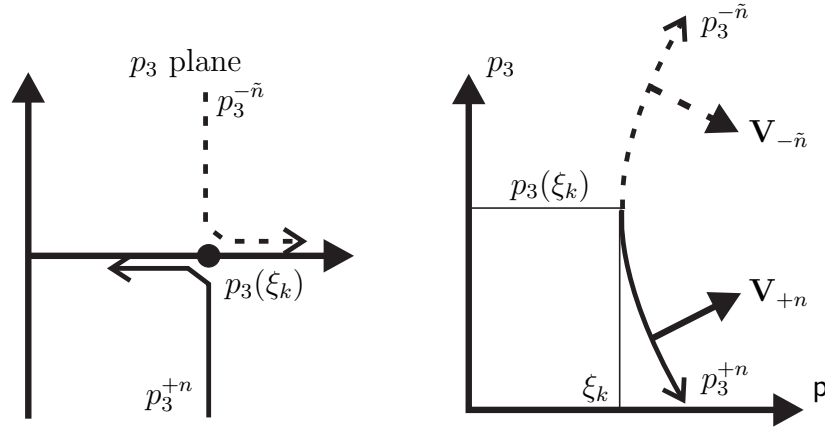
At a branch point, two solutions p_3^n coincide. As the product of all eigenvalues is the determinant of the matrix **A** (6.3.14), differentiating with respect to **p**, it is clear that for one solution $dp_3^n/d\mathbf{p} = +\infty$, while for the other $dp_3^{-\tilde{n}}/d\mathbf{p} = -\infty$ (with n and \tilde{n} having the same sign), i.e. the two solutions have indices of opposite sign — near the branch point, the propagation direction has the opposite sign to the gradient — but not necessarily the same value. For $-\xi_M < \mathbf{p} < \xi_M$ between the branch points and the origin, a line $\mathbf{p} = \text{constant}$ must intersect each oval in two points, as there must be six solutions. At $\mathbf{p} = 0$, there will be three positive-negative pairs of solutions for $p_3(\mathbf{p})$ (from the point symmetry, or the quadratic nature of the Christoffel equation). The propagation direction is the same as the sign of the solution, i.e.

$$p_3^{-1}(0) \leq p_3^{-2}(0) \leq p_3^{-3}(0) < 0 < p_3^3(0) \leq p_3^2(0) \leq p_3^1(0).$$

Let us define

$$\bar{p}_i = p_i / \mathbf{p},$$

so $\bar{p}_1 = \cos \chi$ and $\bar{p}_2 = \sin \chi$ are real. Suppose \mathbf{p} is positive imaginary. It is obvious that $p_3(\mathbf{p})$ cannot be purely real or imaginary but must be complex. If $\text{Im}(\mathbf{p}) > 0$, then $\text{Im}(\bar{p}_3^{+n}) < 0$ and $\text{Im}(\bar{p}_3^{-\tilde{n}}) > 0$ (n positive), and *vice versa* when $\text{Im}(\mathbf{p}) < 0$. $\text{Im}(\bar{p}_3^{\pm n})$ differ in sign unless $\text{Im}(\mathbf{p}) = 0$. Let us consider a branch cut at $\mathbf{p} = \xi_m$ on the real axis, where two solutions p_3^{+n} and $p_3^{-\tilde{n}}$ coalesce and are real for $\mathbf{p} > \xi_k$ (n and \tilde{n} are positive but not necessarily equal) as illustrated in the figure.



The behaviour of the slowness \mathbf{p} near a branch point: on the left, the solutions in the complex p_3 plane as \mathbf{p} increases past a branch point at ξ_k ; and on the right, the slowness surface $p_3(\mathbf{p})$ near the branch point $p_3(\mathbf{p} = \xi_k)$. In both figures, the solution propagating in the negative direction is indicated with a dashed line.

Consider \mathbf{p} with a small, positive imaginary part passing the branch point. For $\text{Re}(\mathbf{p}) < \xi_k$, $\text{Im}(p_3^{+n}) < 0$ and $\text{Im}(p_3^{-\tilde{n}}) > 0$. As \mathbf{p} passes the branch point, these solutions approach the real axis at $p_3(\xi_k)$. As \mathbf{p} passes the branch point on the left, the solutions for p_3 turn to the left. Hence $\text{Re}(p_3^{+n}) < p_3(\xi_k)$ and decreases, while $\text{Re}(p_3^{-\tilde{n}}) > p_3(\xi_k)$ and increases. As $dp_3^{+n}/d\mathbf{p} < 0$ it continues as the solution propagating in the positive direction, and $dp_3^{-\tilde{n}}/d\mathbf{p} > 0$ continues in the negative direction (as these gradients define the direction of the group velocity vector, \mathbf{V}). This behaviour is illustrated in the figure. A similar argument applies at branch cuts when the solutions are real for $\mathbf{p} < \xi_k$.

Burridge (1970) and van der Hijden (1987) have discussed in some detail

the possible singularities of $p_3(\mathbf{p})$. Only the branch points on the real axis are significant, so we have omitted other details.

Thus as $\text{Im}(\bar{p}_3^{\pm n})$ differ in sign unless $\text{Im}(\mathbf{p}) = 0$, analytic continuity of the solutions from $\mathbf{p} = 0$ (where they are clearly identifiable), allows us to identify the solutions if $\text{Im}(\mathbf{p}) \neq 0$. Taking $\text{Im}(\mathbf{p}) > 0$ and small, we can identify the positive and negative propagating solutions with $\text{Im}(p_3^{+n}) < 0$ and $\text{Im}(p_3^{-n}) > 0$, respectively. A simple modification of the code and figure given above illustrates the algorithm. The code becomes

```
function Exercise61b
% Exercise 6.1b
% added to Addenda and Errata, 15 November 2004
% C12 corrected from c13 to c12 (note figures do not
% alter significantly), 17 May 2007
%
% illustrate algorithm for finding propagation direction
%
% slowness surfaces for trigonal alpha-quartz as used in
% Figure 5.8 (p_2 - p_3 crossection of slowness surface)
% Shearer, P.M. and Chapman, C.H., 1988.
% Ray tracing in anisotropic media with a linear gradient,
% Geophys. J., 94, 575-580.
% Bechmann, R., 1958. Elastic and piezoelectric constants
% of alpha-quartz, Phys. Rev., 110, 1060-1061.
% Musgrave (1970, p. 130, 136 and 282, density ~ 2.67 and
% axis in Figure 10.2.1 (i) is reversed)
% Density normalized so units km^2 s^-2
%
c11 = 32.73;           % from Shearer and Chapman (1988)
c33 = 40.45;
c12 = 2.64;
c13 = 4.49;
c44 = 21.86;
c14 = -6.76;          % sign as Bechmann not Musgrave
%
quartz=struct( ...
'C11',c11,'C12',c12,'C13',c13,'C14', c14,'C15', 0,'C16',0,...
'C22',c11,'C23',c13,'C24',-c14,'C25', 0,'C26',0,...
'C33',c11,'C34', 0,'C35', 0,'C36',0,...
'C44', c44,'C45', 0,'C46',0,...
```



```

'C55',c44,'C56',c14,...
'C66',.5*(c11-c12));

%
cjk = cMatrices( quartz );
% modified from Exercise 5.9
figure
hold on
% loop over 3 slowness surfaces - blue, red and black
cols = [ 'b' 'r' 'k' ];
for n=1:3
    cnt = 0;                % point counter
    dir = +1;               % direction indicators
    % start from py = 0 which is always dir==+1
    % lots of detail to accurately pick up reversals
    for j=91:-.1:-91
        theta=(j-1)*pi/180;
        ct = cos(theta);
        st = sin(theta);
        % Figure 10.2.1 (i) in Musgrave (1970)
        direction = [ 0 ct st ]';
        % find n-th slowness surface
        [ PhaseSlow, GroupVel, Polar ] = ...
            AnisoSurfaces( direction , cjk );
        py = ct*PhaseSlow(n);
        pz = st*PhaseSlow(n);
        % solve for p_z with slightly positive imaginary p_y
        cp = complex( py, 1.e-8 );
        [ oSlow, polarizations, tractions ] = ...
            AnisoEigen( [ 0 cp ], 1, cjk );
        [ c k ] = min(abs(oSlow-pz));
        % change of propagation direction
        % from positive to negative direction
        if ( imag(oSlow(k)) > 0 && dir > 0 )
            % plot positive direction with solid line
            if ( cnt>0 ) plot( ppy(1:cnt), ppz(1:cnt), cols(n) ), end
            dir = -1; cnt = 1;
        % from negative to positive direction
        elseif ( imag(oSlow(k)) < 0 && dir < 0 )
            % plot negative direction with dashed line
            plot( ppy(1:cnt), ppz(1:cnt), [ cols(n) '--' ] )

```

```

        dir = +1; cnt = 1;
    % continue in same direction
    else
        cnt =cnt+1;
    end
    ppy(cnt) = py;
    ppz(cnt) = pz;
end
% finish
if ( dir > 0 )
    plot( ppy(1:cnt), ppz(1:cnt), cols(n) )
else
    plot( ppy(1:cnt), ppz(1:cnt), [ cols(n)  '--' ] )
end
end
% units are km/s
axis ([0 .35 -.35 .35])
axis equal
axis manual
print -depsc2 exercise6_1b.eps
return

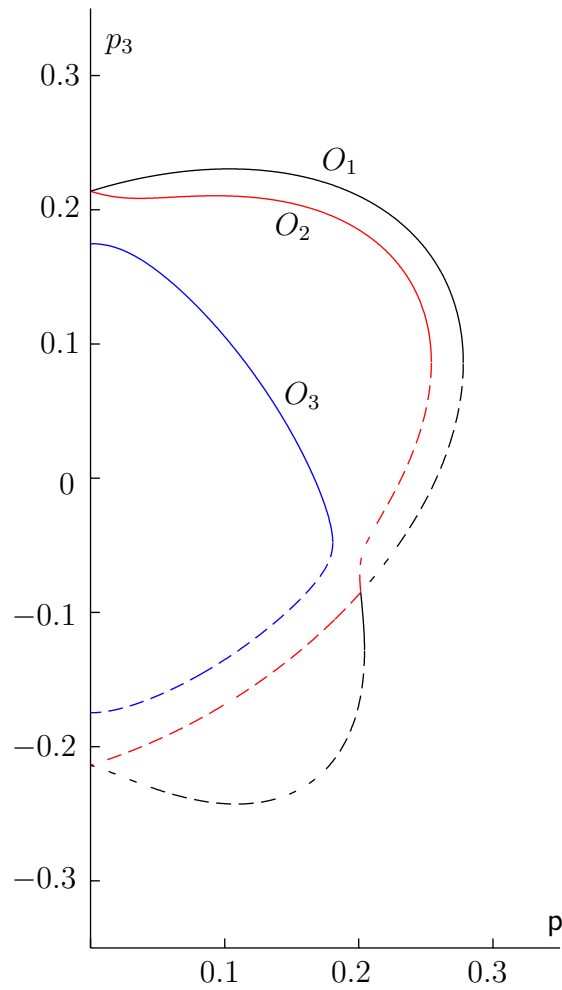
```

which uses routines **AnisoSurfaces** from Exercise 5.9 and **AnisoEigen** from Exercise 6.1. The figure, a modification of the previous figure, illustrates the results, indicating the solutions propagating in a positive direction by solid lines, and the solutions propagating in a negative direction by dashed lines. Note, in particular, the section with $\xi_4 < p < \xi_3$ propagating in the positive direction with $p_3 < 0$.

6.2

Programming exercise: Using the results of the previous question (or otherwise), compute the eigenvectors, \mathbf{w} , of the matrix, \mathbf{A} (6.3.14). Confirm numerically that with the normalization (6.3.29), the eigenvectors satisfy the orthonormality condition (6.3.33).

Using the functions from Exercise 6.1 in the following program, the orthonormality (6.3.29) is confirmed as the printed output is the matrix $-\mathbf{I}_3$ (defined in equation (0.1.5)).



As the previous figure but with the solutions propagating in a positive direction indicated by a solid line, and the solutions propagating in a negative direction by a dashed line. Note, in particular, the section with $\xi_4 < p < \xi_3$ propagating in the positive direction.

```
function Exercise62
% Exercise 6.2
%
% Solve eigen-equation (6.3.14) and check
% orthonormality (6.3.33)
%
% first check orthonormality for an isotropic medium
```

```

px=.2;
isotropic = struct( 'Alpha', sqrt(3), 'Beta', 1, 'Rho', 1.5 );
[ oSlow, polarizations, tractions ] = ...
    IsoEigen( px, isotropic );
%
orthonormal = zeros(6,6);
for m=1:6
    for n=1:6
        orthonormal(m,n) = -tractions(:,m)'*polarizations(:,n) ...
            -polarizations(:,m)'*tractions(:,n);
    end
end
orthonormal
% now check for anisotropic (TI) medium
% use Green Horn shale (Jones and Wang, 1981) as an example
% (see Exercise 4.4). Units are Gpa and Mg/m^3
density = 2.42;
GreenHorn = struct( ...
    'C11',34.3,'C12',13.1,'C13',10.7,'C14', 0,'C15', 0,'C16',0,...
    'C22',34.3,'C23',10.7,'C24', 0,'C25', 0,'C26',0,...
    'C33',22.7,'C34', 0,'C35', 0,'C36',0,...
    'C44',5.4,'C45', 0,'C46',0,...
    'C55',5.4,'C56',0,...
    'C66',10.6);
%
cjk = cMatrices( GreenHorn );
% solve eigen-equation (6.3.14) for p = .2
%
[ oSlow, polarizations, tractions ] = ...
    AnisoEigen( [ px 0 ], density, cjk );
%
orthonormal = zeros(6,6);
for m=1:6
    for n=1:6
        orthonormal(m,n) = -tractions(:,m)'*polarizations(:,n) ...
            -polarizations(:,m)'*tractions(:,n);
    end
end
orthonormal
return

```

6.3

Programming exercise: Using the results of the previous question (or otherwise), compute the reflection/transmission coefficients (6.3.23) with (6.3.34) for anisotropic media. Confirm the reciprocity (6.3.42) numerically. Confirm numerically that for isotropic media, the results agree with expressions (6.3.60) with (6.3.61) and (6.3.62).

Comment: The sign of the coefficients depends on the sign of the eigenvectors. A computer program for solving the eigen-equation (6.3.14) may give the eigenvectors with arbitrary signs. If the eigenvector signs are not chosen consistently in the two media, the reciprocity result may have sign inconsistencies. It is vital to remember that reflection/transmission coefficients only have meaning when given together with the eigenvectors.

Using the function `AnisoEigen` from Exercise 6.1 in each medium, the following function computes the matrix (6.3.23) of reflection/transmission coefficients.

```
function Rmatrix = AnisoCoeffs( pol1, trc1, pol2, trc2 )
% AnisoCoeffs = anisotropic reflection/transmission
%               coefficients

% INPUT:
%       pol1(3,6)      = polarizations in medium 1
%       trc1(3,6)      = tractions in medium 1
%       pol2(3,6)      = polarizations in medium 2
%       pol2(3,6)      = tractions in medium 2
%
% OUTPUT:
%       Rmatrix(6,6)    = full matrix of coefficients
%
% Note:
% the Rmatrix corresponds to equation (6.3.23);
% first 3 columns correspond to waves incident from medium 1;
% last 3 columns correspond to waves incident from medium 2;
% first 3 rows correspond to waves generate in medium 1;
% last 3 rows correspond to waves generate in medium 2;
```

```

% waves are ordered as in eigenvectors;
% the eigenvectors are defined in equation (6.3.29);
% thus writing Rmatrix = ( T_11 T_12 ) with 3x3 sub-matrices,
%               ( T_21 T_22 )
% T_11 are reflections in medium 1, T_21 are transmissions
% from medium 1 to 2, T_12 are transmissions from medium 2
% to 1, and T_22 are reflections in medium 2;
% the eigenvectors are given by function Aniso_Eigen.
%
% matrix Q = I_3 W_1^T I_2 W_2 equation (6.3.34)
Q11 = zeros(3,3); Q12=Q11; Q21=Q11; Q22=Q11;
for m = 1:3
    for n = 1:3
        Q11(m,n) = -Dot( pol1(:,m ),trc2(:,n ) )...
                    -Dot( trc1(:,m ),pol2(:,n ) );
        Q12(m,n) = -Dot( pol1(:,m ),trc2(:,n+3) )...
                    -Dot( trc1(:,m ),pol2(:,n+3) );
        Q21(m,n) =  Dot( pol1(:,m+3),trc2(:,n ) )...
                    +Dot( trc1(:,m+3),pol2(:,n ) );
        Q22(m,n) =  Dot( pol1(:,m+3),trc2(:,n+3) )...
                    +Dot( trc1(:,m+3),pol2(:,n+3) );
    end
end
% coefficients (6.3.23)
Rmatrix=zeros(6,6);
Rmatrix(4:6,1:3) = inv(Q22);           % T_21
Rmatrix(1:3,1:3) = Q12*Rmatrix(4:6,1:3); % T_11
Rmatrix(1:3,4:6) = Q11-Rmatrix(1:3,1:3)*Q21; % T_12
Rmatrix(4:6,4:6) = -Rmatrix(4:6,1:3)*Q21; % T_22
return

```

In isotropic media, the coefficients can be computed directly using expressions (6.3.60), (6.3.61) and (6.3.62).

```

function Rmatrix = Zoeppritz( p, iso1, iso2)
% Zoeppritz = Zoeppritz reflection/transmission coefficients

% INPUT:
%      p          = horizontal slowness
%      iso1.Alpha  = medium 1 P velocity
%      iso1.Beta   = medium 1 S velocity

```

```

%      iso1.Rho      = medium 1 density
%      iso2.Alpha    = medium 2 P velocity
%      iso2.Beta     = medium 2 S velocity
%      iso2.Rho      = medium 2 density
%
% OUTPUT:
%      Rmatrix(6,6)   = full matrix of coefficients
%
% Note:
% the Rmatrix corresponds to equation (6.3.23);
% first 3 columns correspond to waves incident from medium 1;
% last 3 columns correspond to waves incident from medium 2;
% first 3 rows correspond to waves generate in medium 1;
% last 3 rows correspond to waves generate in medium 2;
% the waves are ordered SV, SH and P;
% the SH and P-SV entries in Rmatrix are zero;
% the eigenvectors are defined in equations (6.3.51)-(6.3.53);
% the normalization is defined in equations (6.3.55)-(6.3.57);
% the coefficients are defined by equations (6.3.60)-(6.3.62);
% thus writing Rmatrix = ( T_11 T_12 ) with 3x3 sub-matrices,
%                      ( T_21 T_22 )
% T_11 are reflections in medium 1, T_21 are transmissions
% from medium 1 to 2, T_12 are transmissions from medium 2 to
% 1, and T_22 are reflections in medium 2;
% Rmatrix obviously contains redundant information due to
% reciprocity (6.3.63), zero entries and interchanging media;
% the eigenvectors are given by function Iso_Eigen;
% the important features of the eigenvectors are the
% energy-flux normalization, and that the interface component
% displacement is positive (with p positive). Thus for the P
% waves, the normal components are in the propagation direction,
% and the SV normal components are opposite to the propagation
% direction.
%
Rmatrix=zeros(6,6);
r1 = iso1.Rho;
r2 = iso2.Rho;
p2=p*p;
%
% free surface

```

```

if ( r1 == 0 )
    % free-fluid
    if ( iso2.Beta == 0 )
        % equation (6.4.2)
        Rmatrix(6,6) = -1;
    % free-solid
    else
        qa2 = sqrt((1/iso2.Alpha-p)*(1/iso2.Alpha+p));
        qb2 = sqrt((1/iso2.Beta-p)*(1/iso2.Beta+p));
        % definition (6.3.54)
        Omega2 = qb2*qb2-p2;
        % definition (6.4.6)
        DeltaPV = 4*p2*qa2*qb2+Omega2^2;
        % equations (6.4.5)
        Rmatrix(6,6) = (4*p2*qa2*qb2-Omega2^2)/DeltaPV;
        Rmatrix(4,4) = - Rmatrix(6,6);
        Rmatrix(4,6) = 4*p*Omega2*sqrt(qa2*qb2)/DeltaPV;
        Rmatrix(6,4) = Rmatrix(4,6);
        Rmatrix(5,5) = 1;
    end
elseif ( r2 == 0 )
    if ( iso1.Beta == 0 )
        Rmatrix(3,3) = -1;
    else
        qa1 = sqrt((1/iso1.Alpha-p)*(1/iso1.Alpha+p));
        qb1 = sqrt((1/iso1.Beta-p)*(1/iso1.Beta+p));
        Omega1 = qb1*qb1-p2;
        DeltaPV = 4*p2*qa1*qb1+Omega1^2;
        Rmatrix(3,3) = (4*p2*qa1*qb1-Omega1^2)/DeltaPV;
        Rmatrix(1,1) = - Rmatrix(3,3);
        Rmatrix(1,3) = 4*p*Omega1*sqrt(qa1*qb1)/DeltaPV;
        Rmatrix(3,1) = Rmatrix(1,3);
        Rmatrix(2,2) = 1;
    end
% fluid
elseif ( iso1.Beta == 0 )
    % fluid-fluid
    if ( iso2.Beta == 0 )
        qa1 = sqrt((1/iso1.Alpha-p)*(1/iso1.Alpha+p));
        qa2 = sqrt((1/iso2.Alpha-p)*(1/iso2.Alpha+p));

```



```

DeltaA = r2*qa1+r1*qa2;
% equations (6.3.7) and (6.3.8)
Rmatrix(3,3) = (r2*qa1-r1*qa2)/DeltaA;
Rmatrix(6,6) = -Rmatrix(3,3);
Rmatrix(3,6) = 2*sqrt(r1*r2*qa1*qa2)/DeltaA;
Rmatrix(6,3) = Rmatrix(3,6);
% fluid-solid
else
    qa1 = sqrt((1/iso1.Alpha-p)*(1/iso1.Alpha+p));
    qa2 = sqrt((1/iso2.Alpha-p)*(1/iso2.Alpha+p));
    qb2 = sqrt((1/iso2.Beta-p)*(1/iso2.Beta+p));
    Omega2 = qb2*qb2-p2;
    Fa1 = sqrt(2*r1*qa1);
    Fa2 = sqrt(2*r2*qa2);
    Fb2 = sqrt(2*r2*qb2);
    % equation (6.5.9)
    DeltaPV = 4*p2*qa2*qb2+Omega2^2+r1*qa2/(r2*iso2.Beta^4*qa1);
    % equations (6.5.8)
    Rmatrix(3,3) = (4*p2*qa2*qb2+Omega2^2-...
        r1*qa2/(r2*iso2.Beta^4*qa1))/DeltaPV;
    Rmatrix(4,4) = (-4*p2*qa2*qb2+Omega2^2+...
        r1*qa2/(r2*iso2.Beta^4*qa1))/DeltaPV;
    Rmatrix(6,6) = (4*p2*qa2*qb2-Omega2^2+...
        r1*qa2/(r2*iso2.Beta^4*qa1))/DeltaPV;
    Rmatrix(3,6) = Fa1*Fa2*Omega2/(qa1*r2*iso2.Beta^2*DeltaPV);
    Rmatrix(6,3) = Rmatrix(3,6);
    Rmatrix(4,6) = 2*p*Fa2*Fb2*Omega2/(r2*DeltaPV);
    Rmatrix(6,4) = Rmatrix(4,6);
    Rmatrix(3,4) = -2*p*Fa1*Fb2*qa2/ ...
        (qa1*r2*iso2.Beta^2*DeltaPV);
    Rmatrix(4,3) = Rmatrix(3,4);
    Rmatrix(5,5) = 1;
end
% solid-fluid
elseif ( iso2.Beta == 0 )
    qa1 = sqrt((1/iso1.Alpha-p)*(1/iso1.Alpha+p));
    qb1 = sqrt((1/iso1.Beta-p)*(1/iso1.Beta+p));
    qa2 = sqrt((1/iso2.Alpha-p)*(1/iso2.Alpha+p));
    Omega1 = qb1*qb1-p2;
    Fa1 = sqrt(2*r1*qa1);

```

```

Fb1 = sqrt(2*r1*qb1);
Fa2 = sqrt(2*r2*qa2);
% equation (6.5.9)
DeltaPV = 4*p2*qa1*qb1+Omega1^2+...
          r2*qa1/(r1*iso1.Beta^4*qa2);
Rmatrix(6,6) = (4*p2*qa1*qb1+Omega1^2-...
               r2*qa1/(r1*iso1.Beta^4*qa2))/DeltaPV;
Rmatrix(1,1) = (-4*p2*qa1*qb1+Omega1^2+...
               r2*qa1/(r1*iso1.Beta^4*qa2))/DeltaPV;
Rmatrix(3,3) = (4*p2*qa1*qb1-Omega1^2+...
               r2*qa1/(r1*iso1.Beta^4*qa2))/DeltaPV;
Rmatrix(3,6) = Fa1*Fa2*Omega1/(qa2*r1*iso1.Beta^2*DeltaPV);
Rmatrix(6,3) = Rmatrix(3,6);
Rmatrix(1,3) = 2*p*Fa1*Fb1*Omega1/(r1*DeltaPV);
Rmatrix(3,1) = Rmatrix(1,3);
Rmatrix(6,1) = -2*p*Fa2*Fb1*qa1/ ...
               (qa2*r1*iso1.Beta^2*DeltaPV);
Rmatrix(1,6) = Rmatrix(6,1);
Rmatrix(2,2) = 1;
% solid-solid
else
% vertical slownesses (6.2.8) and (6.2.9)
qa1 = sqrt((1/iso1.Alpha-p)*(1/iso1.Alpha+p));
qa2 = sqrt((1/iso2.Alpha-p)*(1/iso2.Alpha+p));
qb1 = sqrt((1/iso1.Beta-p)*(1/iso1.Beta+p));
qb2 = sqrt((1/iso2.Beta-p)*(1/iso2.Beta+p));
% definitions (6.3.62)
Aap = r2*qa1+iso1.Rho*qa2;
Abp = r2*qb1+r1*qb2;
Aam = r2*qa1-r1*qa2;
Abm = r2*qb1-r1*qb2;
mu1 = r1*iso1.Beta^2;
mu2 = r2*iso2.Beta^2;
B1 = mu1-mu2;
B2 = -B1;
C1p = 2*p*(B1*(p2+qa1*qb1)-r1);
C1m = 2*p*(B1*(p2-qa1*qb1)-r1);
C2p = 2*p*(B2*(p2+qa2*qb2)-r2);
C2m = 2*p*(B2*(p2-qa2*qb2)-r2);
D = p2*(r1+r2)^2;

```

```

E1 = r1-2*p2*B1;
E2 = r2-2*p2*B2;
Fa1 = sqrt(2*r1*qa1);
Fa2 = sqrt(2*r2*qa2);
Fb1 = sqrt(2*r1*qb1);
Fb2 = sqrt(2*r2*qb2);
Gbp = mu1*qb1+mu2*qb2;
Gbm = mu1*qb1-mu2*qb2;
Hb1 = sqrt(2*mu1*qb1);
Hb2 = sqrt(2*mu2*qb2);
% denominators (6.3.61)
DeltaPV = Aap*Abp-C1p*C2p+D;
DeltaH = Gbp;
% non-zero coefficients (6.3.60)
Rmatrix(3,3) = (Aam*Abp+C1m*C2p-D)/DeltaPV;      %P1P1
Rmatrix(6,6) = (-Aam*Abp+C1p*C2m-D)/DeltaPV;      %P2P2
Rmatrix(1,1) = (-Aap*Abm-C1m*C2p+D)/DeltaPV;      %V1V1
Rmatrix(4,4) = (Aap*Abm-C1p*C2m+D)/DeltaPV;      %V2V2
Rmatrix(3,6) = Fa1*Fa2*(qb1*E2+qb2*E1)/DeltaPV;   %P2P1
Rmatrix(6,3) = Rmatrix(3,6);                      %P1P2
Rmatrix(1,4) = Fb1*Fb2*(qa1*E2+qa2*E1)/DeltaPV;   %V2V1
Rmatrix(4,1) = Rmatrix(1,4);                      %V1V2
Rmatrix(1,3) = -p*Fa1*Fb1*(2*qa2*qb2*E1*B2+...
               E2*(E2-r1))/(r1*DeltaPV);          %P1V1
Rmatrix(3,1) = Rmatrix(1,3);                      %V1P1
Rmatrix(4,6) = -p*Fa2*Fb2*(2*qa1*qb1*E2*B1+...
               E1*(E1-r2))/(r2*DeltaPV);          %P2V2
Rmatrix(6,4) = Rmatrix(4,6);                      %V2P2
Rmatrix(3,4) = -p*Fa1*Fb2*(2*B2*qb1*qa2+...
               E1-r2)/DeltaPV;                    %V2P1
Rmatrix(4,3) = Rmatrix(3,4);                      %P1V2
Rmatrix(1,6) = -p*Fa2*Fb1*(2*B1*qb2*qa1+...
               E2-r1)/DeltaPV;                    %P2V1
Rmatrix(6,1) = Rmatrix(1,6);                      %V1P2
Rmatrix(2,2) = Gbm/DeltaH;                        %H1H1
Rmatrix(5,5) = -Gbm/DeltaH;                      %H2H2
Rmatrix(2,5) = Hb1*Hb2/DeltaH;                   %H2H1
Rmatrix(5,2) = Rmatrix(2,5);                      %H1H2
end
return

```

These are compared for the isotropic media used in Figure 6.8 at one slowness.

```
function Exercise63a
% Exercise 6.3 - first example
%
% compute reflection/transmission coefficients using
% (6.3.23) or (6.3.60), (6.3.61) and (6.3.31)
%
% a slowness value
px = .2;
%
a1 = sqrt(3);
b1 = 1;
r1 = 1;
a2 = 1.270*a1;
b2 = a2/2;
r2 = 1.072*r1;
iso1 = struct( 'Alpha', a1, 'Beta', b1, 'Rho', r1 );
iso2 = struct( 'Alpha', a2, 'Beta', b2, 'Rho', r2 );
% make cjk matrices for isotropic media
c11 = r1*a1*a1;
c44 = r1*b1*b1;
c13 = c11-2*c44;
aniso = struct( ...
'C11',c11,'C12',c13,'C13',c13,'C14', 0,'C15', 0,'C16',0,...
'C22',c11,'C23',c13,'C24', 0,'C25', 0,'C26',0,...
'C33',c11,'C34', 0,'C35', 0,'C36',0,...
'C44',c44,'C45', 0,'C46',0,...
'C55',c44,'C56',0,...
'C66',c44);

cjk1 = cMatrices( aniso );
c11 = r2*a2*a2;
c44 = r2*b2*b2;
c13 = c11-2*c44;
aniso = struct( ...
'C11',c11,'C12',c13,'C13',c13,'C14', 0,'C15', 0,'C16',0,...
'C22',c11,'C23',c13,'C24', 0,'C25', 0,'C26',0,...
'C33',c11,'C34', 0,'C35', 0,'C36',0,...
'C44',c44,'C45', 0,'C46',0,...
```

```

                                'C55',c44,'C56',0,...
                                'C66',c44);

cjk2 = cMatrices( aniso );
%
% with Zoeppritz (6.3.60), (6.3.61) and (6.3.31)
rt = Zoeppritz( px, iso1, iso2 )
% (6.3.23) using (6.3.51), (6.3.52) and (6.3.53)
[ os1, pol1, trc1 ] = IsoEigen( px, iso1 );
[ os2, pol2, trc2 ] = IsoEigen( px, iso2 );
Rmatrix = AnisoCoeffs( pol1, trc1, pol2, trc2 )
% (6.3.23) using (6.3.14) with (6.3.29)
[ os1, pol1, trc1 ] = AnisoEigen( [ px 0 ], r1, cjk1 );
[ os2, pol2, trc2 ] = AnisoEigen( [ px 0 ], r2, cjk2 );
Rmatrix = AnisoCoeffs( pol1, trc1, pol2, trc2 )
return

```

The results from function `Zoeppritz` and `AnisoCoeffs` using `IsoEigen` or `AnisoEigen` all agree and are

-0.0629	0	-0.0413	0.9966	0	0.0325
0	-0.0800	0	0	0.9968	0
-0.0413	0	0.1532	-0.0284	0	0.9869
0.9966	0	-0.0284	0.0602	0	0.0479
0	0.9968	0	0	0.0800	0
0.0325	0	0.9869	0.0479	0	-0.1504

In the final case using `AnisoEigen`, the equality depends on function `TidyEigen` reproducing the order and signs of the eigen-solutions.

Finally we give results for coefficients from an isotropic/TI medium. The main program is

```

function Exercise63b
% Exercise 6.3 - second example
%
% compute reflection/transmission coefficients using
% (6.3.23) for isotropic/TI
%
% a slowness value
px = .2;
% an isotropic medium
a1 = sqrt(3);
b1 = 1;

```

```

r1 = 1;
iso1 = struct( 'Alpha', a1, 'Beta', b1, 'Rho', r1 );
% a TI medium - Green Horn shale (Jones and Wang, 1981)
% (see Exercise 4.4). Units are Gpa and Mg/m^3
r2 = 2.42;
GreenHorn = struct( ...
    'C11',34.3,'C12',13.1,'C13',10.7,'C14', 0,'C15', 0,'C16',0,...
    'C22',34.3,'C23',10.7,'C24', 0,'C25', 0,'C26',0,...
    'C33',22.7,'C34', 0,'C35', 0,'C36',0,...
    'C44',5.4,'C45', 0,'C46',0,...
    'C55',5.4,'C56',0,...
    'C66',10.6);

%
cjk2 = cMatrices( GreenHorn );
%
[ os1, pol1, trc1 ] = IsoEigen( px, iso1 );
[ os2, pol2, trc2 ] = AnisoEigen( [ px 0 ], r2, cjk2 );
Rmatrix = AnisoCoeffs( pol1, trc1, pol2, trc2 )
return

```

and the results

-0.3948	-0.0000	-0.2581	-0.0000	0.8499	0.2349
-0.0000	-0.5403	-0.0000	0.8415	-0.0000	0.0000
-0.2581	0.0000	0.5675	-0.0000	-0.1591	0.7655
-0.0000	0.8415	0.0000	0.5403	0.0000	-0.0000
0.8499	-0.0000	-0.1591	-0.0000	0.2219	0.4507
0.2349	-0.0000	0.7655	-0.0000	0.4507	-0.3946

6.4

In anisotropic media with up-down symmetry, e.g. isotropic, TIV, orthorhombic or generally monoclinic, the eigen-system (6.3.14) must reduce to a third-order system for p_n^2 , i.e. the eigenvalues of equation (6.3.14) must occur in positive-negative pairs, symmetric about the horizontal plane of symmetry. Obtain the third-order system, and demonstrate that it gives the known results for isotropic and transversely isotropic media (Section 5.7.1).

In anisotropic elastic media with up-down symmetry, i.e. the slowness sur-

faces are symmetric under reflection in the horizontal plane, say the $x - y$ plane, the eigen-system (6.3.14)

$$\mathbf{A}\mathbf{w} = p_n \mathbf{w},$$

must have some special structure. In particular, we expect the eigenvalues to be positive and negative pairs, and the equation to reduce from sixth order to a cubic in p_n^2 . Up-down symmetry applies in isotropic, TIV, orthorhombic media and more generally in monoclinic anisotropic media. It is necessary to solve the eigen-system for Snell's law at interfaces, and for ray tracing in 1D media, so analyzing the structure of the equations in up-down symmetric media is important.

In monoclinic media with a horizontal, reflection symmetry plane, elastic parameters where the vertical index appears an *odd* number of times must be zero. Thus in the Voigt notation (4.4.13), the elastic parameter 6×6 matrix must be of the form

$$\mathbf{C} = \begin{pmatrix} C_{11} & C_{12} & C_{13} & 0 & 0 & C_{16} \\ C_{12} & C_{22} & C_{23} & 0 & 0 & C_{26} \\ C_{13} & C_{23} & C_{33} & 0 & 0 & C_{36} \\ 0 & 0 & 0 & C_{44} & 0 & 0 \\ 0 & 0 & 0 & 0 & C_{55} & 0 \\ C_{16} & C_{26} & C_{36} & 0 & 0 & C_{66} \end{pmatrix}.$$

Isotropic media (4.4.53) and TIV media (4.4.59) are obviously special cases of a monoclinic medium. The 3×3 stiffness matrices \mathbf{c}_{jk} (4.4.39) are

$$\begin{aligned} \mathbf{c}_{11} &= \begin{pmatrix} C_{11} & C_{16} & 0 \\ C_{16} & C_{66} & 0 \\ 0 & 0 & C_{55} \end{pmatrix} & \mathbf{c}_{22} &= \begin{pmatrix} C_{66} & C_{26} & 0 \\ C_{26} & C_{22} & 0 \\ 0 & 0 & C_{44} \end{pmatrix} \\ \mathbf{c}_{33} &= \begin{pmatrix} C_{55} & 0 & 0 \\ 0 & C_{44} & 0 \\ 0 & 0 & C_{33} \end{pmatrix} & \mathbf{c}_{23} &= \begin{pmatrix} 0 & 0 & C_{36} \\ 0 & 0 & C_{23} \\ 0 & C_{44} & 0 \end{pmatrix} \\ \mathbf{c}_{31} &= \begin{pmatrix} 0 & 0 & C_{55} \\ 0 & 0 & 0 \\ C_{13} & C_{36} & 0 \end{pmatrix} & \mathbf{c}_{12} &= \begin{pmatrix} C_{16} & C_{12} & 0 \\ C_{66} & C_{26} & 0 \\ 0 & 0 & 0 \end{pmatrix}. \end{aligned}$$

The matrix \mathbf{A} is constructed from these parameter matrices, and if it is divided into four 3×3 sub-matrices $\mathbf{A}_{\mu\nu}$

$$\mathbf{A} = \begin{pmatrix} \mathbf{A}_{11} & \mathbf{A}_{12} \\ \mathbf{A}_{21} & \mathbf{A}_{22} \end{pmatrix}$$

we obtain (6.3.15), (6.3.16) and (6.3.17)

$$\begin{aligned}\mathbf{A}_{22} &= \mathbf{A}_{11}^T = -p_\eta \mathbf{c}_{\eta 3} \mathbf{c}_{33}^{-1} \\ \mathbf{A}_{12} &= -\mathbf{c}_{33}^{-1} \\ \mathbf{A}_{21} &= p_\eta p_\nu \mathbf{c}_{\eta \nu} - \rho \mathbf{I} - p_\eta p_\nu \mathbf{c}_{\eta 3} \mathbf{c}_{33}^{-1} \mathbf{c}_{3\nu},\end{aligned}\tag{6.1}$$

with summations over indices 1 and 2. Thus in monoclinic media we have

$$\begin{aligned}\mathbf{A}_{12} &= -\begin{pmatrix} 1/C_{55} & 0 & 0 \\ 0 & 1/C_{44} & 0 \\ 0 & 0 & 1/C_{33} \end{pmatrix} \\ \mathbf{A}_{22} &= \mathbf{A}_{11}^T = -\begin{pmatrix} 0 & 0 & (p_1 C_{13} + p_2 C_{36})/C_{33} \\ 0 & 0 & (p_1 C_{36} + p_2 C_{23})/C_{33} \\ p_1 & p_2 & 0 \end{pmatrix}.\end{aligned}$$

Matrix \mathbf{A}_{21} has many more terms but is constructed from matrices \mathbf{I} , \mathbf{c}_{11} , \mathbf{c}_{22} , \mathbf{c}_{12} and

$$\begin{aligned}\mathbf{c}_{13} \mathbf{c}_{33}^{-1} \mathbf{c}_{31} &= \begin{pmatrix} C_{13}^2/C_{33} & C_{13} C_{36}/C_{33} & 0 \\ C_{13} C_{36}/C_{33} & C_{36}^2/C_{33} & 0 \\ 0 & 0 & C_{55} \end{pmatrix} \\ \mathbf{c}_{23} \mathbf{c}_{33}^{-1} \mathbf{c}_{32} &= \begin{pmatrix} C_{36}^2/C_{33} & C_{23} C_{36}/C_{33} & 0 \\ C_{23} C_{36}/C_{33} & C_{23}^2/C_{33} & 0 \\ 0 & 0 & C_{44} \end{pmatrix} \\ \mathbf{c}_{13} \mathbf{c}_{33}^{-1} \mathbf{c}_{32} &= (\mathbf{c}_{23} \mathbf{c}_{33}^{-1} \mathbf{c}_{31})^T = \begin{pmatrix} C_{13} C_{36}/C_{33} & C_{13} C_{23}/C_{33} & 0 \\ C_{36}^2/C_{33} & C_{23} C_{36}/C_{33} & 0 \\ 0 & 0 & 0 \end{pmatrix}.\end{aligned}$$

The important thing is that although there are lots of terms, all these matrices and therefore \mathbf{A}_{21} are of the form

$$\mathbf{A}_{21} = \begin{pmatrix} \times & \times & 0 \\ \times & \times & 0 \\ 0 & 0 & \times \end{pmatrix},$$

where the cross indicates a non-zero element. Overall the matrix \mathbf{A} has the form

$$\mathbf{A} = \begin{pmatrix} 0 & 0 & \times & \times & 0 & 0 \\ 0 & 0 & \times & 0 & \times & 0 \\ \times & \times & 0 & 0 & 0 & \times \\ \times & \times & 0 & 0 & 0 & \times \\ \times & \times & 0 & 0 & 0 & \times \\ 0 & 0 & \times & \times & \times & 0 \end{pmatrix}.$$

Noting where the zero elements are, we interchange the third and sixth rows and columns in the eigen-system, corresponding to v_3 and σ_{33} , which can be achieved by pre- and post-multiplying by the matrix

$$\mathbf{I}_{36} = \begin{pmatrix} 1 & 0 & 0 & 0 & 0 & 0 \\ 0 & 1 & 0 & 0 & 0 & 0 \\ 0 & 0 & 0 & 0 & 0 & 1 \\ 0 & 0 & 0 & 1 & 0 & 0 \\ 0 & 0 & 0 & 0 & 1 & 0 \\ 0 & 0 & 1 & 0 & 0 & 0 \end{pmatrix},$$

and obtain a modified eigen-system

$$\mathbf{A}' \mathbf{w}' = p_n \mathbf{w}',$$

where

$$\mathbf{A}' = \mathbf{I}_{36} \mathbf{A} \mathbf{I}_{36} = \begin{pmatrix} \mathbf{0} & \mathbf{A}'_{12} \\ \mathbf{A}'_{21} & \mathbf{0} \end{pmatrix},$$

with the diagonal 3×3 blocks zero, and

$$\mathbf{w}' = \mathbf{I}_{36} \mathbf{w} = \begin{pmatrix} v_1 \\ v_2 \\ \sigma_{33} \\ \sigma_{13} \\ \sigma_{23} \\ v_3 \end{pmatrix} = \begin{pmatrix} \mathbf{w}'_1 \\ \mathbf{w}'_2 \end{pmatrix}, \text{ say.}$$

The sub-matrices are

$$\begin{aligned} \mathbf{A}'_{12} &= \begin{pmatrix} A_{14} & A_{15} & A_{13} \\ A_{24} & A_{25} & A_{23} \\ A_{64} & A_{65} & A_{63} \end{pmatrix} \\ \mathbf{A}'_{21} &= \begin{pmatrix} A_{41} & A_{42} & A_{46} \\ A_{51} & A_{52} & A_{56} \\ A_{31} & A_{32} & A_{36} \end{pmatrix}. \end{aligned}$$

The eigen-system can be expanded as

$$\begin{aligned} \mathbf{A}'_{12} \mathbf{w}'_2 &= p_n \mathbf{w}'_1 \\ \mathbf{A}'_{21} \mathbf{w}'_1 &= p_n \mathbf{w}'_2, \end{aligned}$$

and hence

$$\begin{aligned} (\mathbf{A}'_{12} \mathbf{A}'_{21}) \mathbf{w}'_1 &= p_n^2 \mathbf{w}'_1 \\ (\mathbf{A}'_{21} \mathbf{A}'_{12}) \mathbf{w}'_2 &= p_n^2 \mathbf{w}'_2. \end{aligned}$$

These two eigen-systems are equivalent as both \mathbf{A}'_{12} and \mathbf{A}'_{21} are symmetric (as $A_{15} = A_{24} = 0$, $A_{42} = A_{51}$ from elements of matrix \mathbf{A}_{21} , and $A_{13} = A_{64}$, $A_{23} = A_{65}$, $A_{46} = A_{31}$ and $A_{56} = A_{32}$ as $\mathbf{A}_{22} = \mathbf{A}_{11}^T$). The matrix $\mathbf{A}'_{12}\mathbf{A}'_{21}$ has right-eigenvector \mathbf{w}'_1 and left-eigenvector \mathbf{w}'_2 ; for the matrix $\mathbf{A}'_{12}\mathbf{A}'_{21}$, the roles of the eigenvectors are reversed.

Thus we have reduced the sixth-order eigen-system to a third-order system for the eigenvalues p_n^2 . Hence, the original eigenvalues must be in positive and negative pairs. In the eigenvectors, \mathbf{w}' , the second part, \mathbf{w}'_2 , changes sign with p_n . These results agree with the physical requirements in media with up-down symmetry. There is always a sign ambiguity in the definition of eigenvectors. The signs can always be chosen to be consistent with the above rule that \mathbf{w}'_1 does not change sign but \mathbf{w}'_2 changes sign with p_n . Note that the signs in definitions (6.3.5), (6.3.51), (6.3.52) and (6.3.53) are consistent with this rule.

Isotropic case (2 parameters): The matrix \mathbf{A} in an isotropic medium is given by equation (6.3.47). Thus the sub-matrices are

$$\begin{aligned}\mathbf{A}'_{12} &= - \begin{pmatrix} 1/\mu & 0 & p \\ 0 & 1/\mu & 0 \\ p & 0 & \rho \end{pmatrix} \\ \mathbf{A}'_{21} &= \begin{pmatrix} \eta p^2 - \rho & 0 & -p\lambda/(\lambda + 2\mu) \\ 0 & \mu p^2 - \rho & 0 \\ -p\lambda/(\lambda + 2\mu) & 0 & -1/(\lambda + 2\mu) \end{pmatrix},\end{aligned}$$

where η is defined in equation (6.3.48). The 3×3 matrix for the eigenvalues p_n^2 is

$$\mathbf{A}'_{12}\mathbf{A}'_{21} = \begin{pmatrix} \frac{\rho}{\mu} - \frac{3\lambda+4\mu}{\lambda+2\mu}p^2 & 0 & \frac{\lambda+\mu}{\mu(\lambda+2\mu)}p \\ 0 & \frac{\rho}{\mu} - p^2 & 0 \\ 2p(\rho - 2\mu p^2) \frac{\lambda+\mu}{\lambda+2\mu} & 0 & \frac{\rho+\lambda p^2}{\lambda+2\mu} \end{pmatrix}.$$

Although the *SH* eigenvalue is obvious, the *P-SV* result is not obvious but straightforward algebra shows

$$\left| \mathbf{A}'_{12}\mathbf{A}'_{21} - p_n^2 \mathbf{I} \right| = \left(\frac{\rho}{\mu} - p^2 - p_n^2 \right)^2 \left(\frac{\rho}{\lambda + 2\mu} - p^2 - p_n^2 \right) = 0,$$

giving the expected eigenvalues.

TIV case (5 parameters): From the matrix \mathbf{A} (6.3.64), the sub-matrices are

$$\mathbf{A}'_{12} = - \begin{pmatrix} 1/C_{44} & 0 & p \\ 0 & 1/C_{44} & 0 \\ p & 0 & \rho \end{pmatrix}$$

$$\mathbf{A}'_{21} = \begin{pmatrix} p^2(C_{11} - C_{13}^2/C_{33}) - \rho & 0 & -p C_{13}/C_{33} \\ 0 & p^2 C_{66} - \rho & 0 \\ -p C_{13}/C_{33} & 0 & -1/C_{33} \end{pmatrix}.$$

The eigen-matrix is

$$\mathbf{A}'_{12}\mathbf{A}'_{21} = \begin{pmatrix} \frac{\rho}{C_{44}} + p^2 \frac{C_{13}^2 + C_{13}C_{44} - C_{11}C_{33}}{C_{33}C_{44}} & 0 & p \frac{C_{13} + C_{44}}{C_{33}C_{44}} \\ 0 & \frac{\rho}{C_{44}} - p^2 \frac{C_{66}}{C_{44}} & 0 \\ p^3 \frac{C_{13}^2 - C_{11}C_{33}}{C_{33}} + \rho p \frac{C_{13} + C_{33}}{C_{33}} & 0 & \frac{\rho}{C_{33}} + p^2 \frac{C_{13}}{C_{33}} \end{pmatrix}.$$

After some algebra, the eigenvalue equation can be reduced to

$$\left| \mathbf{A}'_{12}\mathbf{A}'_{21} - p_n^2 \mathbf{I} \right| = \frac{1}{A_{33}A_{44}} \left(\frac{1}{A_{44}} - p^2 \frac{A_{66}}{A_{44}} - p_n^2 \right) \left[A_{33}A_{44}p_n^4 - Bp_n^2 + (A_{11}p^2 - 1)(A_{44}p^2 - 1) \right],$$

where B is defined by equation (5.7.33) with (5.7.31) and (5.7.20), and just here $A_{ij} = C_{ij}/\rho$ are the density-normalized elastic parameters not elements of the matrix \mathbf{A} . Clearly the qSH root agrees with result (5.7.24), and the qP - qSV roots from the quadratic for p_n^2 agree with solutions (5.7.32).

monoclinic (12 parameters): We discuss the general monoclinic system next with 12 parameters, as in the simpler orthorhombic medium only 3 more parameters are zero. The general 3×3 matrices of elastic parameters (4.4.39) have been given above. The sub-matrices \mathbf{A}_{11} and \mathbf{A}_{22} (6.3.15) and \mathbf{A}_{12} (6.3.16) of the matrix \mathbf{A} have been given above and the elements of the sub-matrix \mathbf{A}_{21} (6.3.17) are

$$\begin{aligned} A_{41} &= p_1^2(C_{11} - C_{13}^2/C_{33}) + p_2^2(C_{66} - C_{36}^2/C_{33}) \\ &\quad + 2p_1p_2(C_{16} - C_{13}C_{36}/C_{33}) - \rho \\ A_{52} &= p_1^2(C_{66} - C_{36}^2/C_{33}) + p_2^2(C_{22} - C_{23}^2/C_{33}) \\ &\quad + 2p_1p_2(C_{26} - C_{23}C_{36}/C_{33}) - \rho \\ A_{63} &= -\rho \\ A_{51} &= A_{42} = p_1^2(C_{16} - C_{13}C_{36}/C_{33}) + p_2^2(C_{26} - C_{23}C_{36}/C_{33}) \\ &\quad + p_1p_2(C_{12} + C_{66} - C_{13}C_{23}/C_{33} - C_{36}^2/C_{33}) \\ A_{61} &= A_{62} = A_{43} = A_{53} = 0. \end{aligned}$$

The matrices of the third-order system are

$$\mathbf{A}'_{12} = - \begin{pmatrix} 1/C_{55} & 0 & p_1 \\ 0 & 1/C_{44} & p_2 \\ p_1 & p_2 & \rho \end{pmatrix}$$

$$\mathbf{A}'_{21} = \begin{pmatrix} A_{41} & A_{51} & -(p_1 C_{13} + p_2 C_{36})/C_{33} \\ A_{51} & A_{52} & -(p_1 C_{36} + p_2 C_{23})/C_{33} \\ -(p_1 C_{13} + p_2 C_{36})/C_{33} & -(p_1 C_{36} + p_2 C_{23})/C_{33} & -1/\rho \end{pmatrix},$$

where the 3 long elements in the upper-left 2×2 have not been repeated. It is easily checked that these results reduce to the isotropic and TIV results.

To find the eigenvalues of the third-order system we need to expand and solve

$$|\mathbf{A}'_{12}\mathbf{A}'_{21} - p_n^2 \mathbf{I}| = 0.$$

This reduces to a cubic, but having found the matrices \mathbf{A}'_{12} and \mathbf{A}'_{21} algebraically there is little point in proceeding further as the algebra does not simplify. It is straightforward to find the coefficients of the cubic numerically. An analytic solution is available for a cubic. Although this used to be textbook stuff, it is perhaps less well known now. The procedure is:

consider the cubic in its standard form

$$x^3 + px^2 + qx + r = 0.$$

This can be reduced to

$$y^3 + 3Qy - 2R = 0,$$

where

$$\begin{aligned} y &= x + \frac{p}{3} \\ 3Q &= q - \frac{1}{3}p^2 \\ 2R &= \frac{p}{3} \left(q - \frac{2p^2}{9} \right) - r. \end{aligned}$$

We define a discriminant

$$D = Q^3 + R^2.$$

If $D > 0$, there is one real root, and if $D \leq 0$ there are three real roots (multiple roots if $D = 0$). The following algorithms require the special case of a triple root when $Q = R = 0$, and $y_1 = y_2 = y_3 = 0$, to be handled separately.

If $D > 0$ we make the transformation

$$y = 2Q^{1/2} \sinh \frac{\theta}{3},$$

and the cubic reduces to

$$\sinh \theta = \frac{R}{Q^{3/2}}.$$

The standard logarithmic formula for the inverse hyperbolic sine gives

$$\frac{\theta}{3} = \ln \frac{S}{Q^{1/2}},$$

where

$$S = (R + \sqrt{D})^{1/3}.$$

Substituting, this gives the root

$$y_1 = S + T,$$

where

$$T = -Q/S = (R - \sqrt{D})^{1/3}.$$

If $R < 0$ it is best to calculate T first and derive S from it.

If $D < 0$, then we make the transformation

$$y = 2(-Q)^{1/2} \cos \frac{\theta}{3},$$

and the cubic reduces to

$$\cos \theta = \frac{R}{(-Q)^{3/2}}$$

(necessarily $Q < 0$). The solutions are

$$\begin{aligned} y_1 &= 2\sqrt{-Q} \cos \frac{\theta}{3} \\ y_1 &= 2\sqrt{-Q} \cos \left(\frac{\theta}{3} + \frac{2\pi}{3} \right) \\ y_1 &= 2\sqrt{-Q} \cos \left(\frac{\theta}{3} + \frac{4\pi}{3} \right). \end{aligned}$$

orthorhombic case (9 parameters): An orthorhombic medium is characterized by a stiffness Voigt matrix

$$\mathbf{C} = \begin{pmatrix} C_{11} & C_{12} & C_{13} & 0 & 0 & 0 \\ C_{12} & C_{22} & C_{23} & 0 & 0 & 0 \\ C_{13} & C_{23} & C_{33} & 0 & 0 & 0 \\ 0 & 0 & 0 & C_{44} & 0 & 0 \\ 0 & 0 & 0 & 0 & C_{55} & 0 \\ 0 & 0 & 0 & 0 & 0 & C_{66} \end{pmatrix}$$

(Schoenberg and Helbig, 1997, and references therein). This results in some simplification of the monoclinic results above, but in general it is probably best to proceed numerically from the matrices \mathbf{A}'_{12} and \mathbf{A}'_{21} to the solution of the cubic. Only if $p_1 = 0$ or $p_2 = 0$, i.e. on a plane of symmetry, do the results simplify significantly. Then the form simplifies to that in TIV media, and the solution reduces to a simple equation for the qS wave transverse to the symmetry plane, and a quadratic equation for the qP - qS waves in the symmetry plane.

7

Differential systems for stratified media

7.1

Show that the same differential systems (7.1.4) with the definitions (7.1.6), (7.1.33) and (7.1.34) for acoustic or isotropic elastic media, apply in cylindrical coordinates, except that the components of the vector \mathbf{w} are transformed cylindrical components (see Exercise 4.11).

Algebraic details can be found in Takeuchi and Saito (1972). See also Chapman and Orcutt (1985)[†]. We define cylindrical basis functions

$$Y_k^m(r, \phi) = J_m(kr) e^{im\phi},$$

and write the solution as

$$\begin{aligned} v_r &= \frac{1}{i\omega p} \left(w_1 \frac{\partial Y_k^m}{\partial r} + w_2 \frac{1}{r} \frac{\partial Y_k^m}{\partial \phi} \right) e^{i\omega t} \\ v_\phi &= \frac{1}{i\omega p} \left(w_1 \frac{1}{r} \frac{\partial Y_k^m}{\partial \phi} - w_2 \frac{\partial Y_k^m}{\partial r} \right) e^{i\omega t} \\ v_z &= w_3 Y_k^m e^{i\omega t}. \end{aligned}$$

The functions w_i , components of the vector \mathbf{w} , depend on z , ω , p and m ; the r and ϕ dependence is contained in the function $Y_k^m(r, \phi)$. The equations of motion in cylindrical coordinates are given in Exercise 4.11. Following Takeuchi and Saito (1972), together with the constitutive equations, these reduce to (7.1.4)

$$\frac{d}{dz} \mathbf{w} = i\omega \mathbf{A} \mathbf{w},$$

where the matrix \mathbf{A} is given by equation (6.3.47) (which contains the acoustic

[†] Chapman, C.H. and Orcutt, J.A., 1985. The computation of body wave synthetic seismograms in laterally homogeneous media, *Rev. Geophys.*, **23**, 105–63.

(7.1.6), *SH* (7.1.33) and *P-SV* (7.1.34) systems). The development in Chapman and Orcutt (1985) includes the source terms.

7.2

Investigate how the elastic matrix (7.1.34) is modified if buoyancy forces due to gravity are included. This result would be relevant in extremely soft sediments. How are the velocities and eigenvectors modified? A useful publication is Gilbert (1967).

There are two effects due to gravity: there is a buoyancy force due to changes in density from the dilatation; and vertical motion changes the stress due to the hydrostatic pressure gradient. An early publication with the required result is Biot (1940)[†]. A full development can be found in Aki and Richards (1980, pp. 365–7; 2002, pp. 358–60), which includes the effect of self-gravitation which we do not need here.

The equation of hydrostatic equilibrium is

$$-\rho g \hat{\mathbf{k}} = \nabla P = -\nabla \sigma_{zz}$$

(remember $\hat{\mathbf{k}}$ and z are positive *upwards*, and σ_{zz} becomes increasingly negative with depth). The equation of motion (4.5.35) is modified to

$$\rho \frac{\partial \mathbf{v}}{\partial t} = \frac{\partial \mathbf{t}_j}{\partial x_j} + \mathbf{f} + g \nabla \cdot (\rho \mathbf{u}) \hat{\mathbf{k}} - \nabla(\rho g \hat{\mathbf{k}} \cdot \mathbf{u}).$$

The first extra term is the buoyancy force due to the dilatation. The decrease in density is $\nabla \cdot (\rho \mathbf{u})$ giving the vertical buoyancy force. The second extra term is due to the change in σ_{zz} due to the displacement $\hat{\mathbf{k}} \cdot \mathbf{u} = u_z$ in the hydrostatic gradient. Expanding these two terms with the constraint that the pressure gradient is vertical, we obtain

$$g \nabla \cdot (\rho \mathbf{u}) \hat{\mathbf{k}} - \nabla(\rho g \hat{\mathbf{k}} \cdot \mathbf{u}) = \rho g \frac{\partial}{\partial x} (u_x \hat{\mathbf{k}} - u_z \hat{\mathbf{i}}).$$

Thus the transformed equations of motion are modified so

$$\begin{aligned} -i\omega v_x &= f_x + i\omega p \sigma_{xx} + \frac{d\sigma_{xz}}{dz} + p\rho g v_z \\ -i\omega v_z &= f_z + i\omega p \sigma_{xz} + \frac{d\sigma_{zz}}{dz} - p\rho g v_x, \end{aligned}$$

[†] Biot, M.A., 1940. The influence of initial stress on elastic waves, *J. Appl. Phys.*, **11**, 522–30.

(Biot, 1940, equation (22); Aki and Richards, 1980, equation (8.59) and 2002, equation (8.60)) and the differential system (7.1.34) has extra terms

$$A_{61} = -A_{43} = \frac{p\rho g}{i\omega},$$

equivalent to the result in Gilbert (1967).

From the above equations of motion, the effect of gravity is to introduce a term that is equivalent to a body force that is proportional to but perpendicular to the particle velocity. We would therefore expect the rectilinear particle motion of plane waves, i.e. longitudinal for P waves and transverse for SV waves, to be distorted and to become slightly elliptical. This can be analyzed by investigating the perturbations to the eigenvalues and vectors of the matrix \mathbf{A} .

We use normal perturbation theory, e.g. Section 10.2.1. The eigen-equation (6.3.14) becomes

$$(\mathbf{A} + \delta\mathbf{A})(\mathbf{w}_i + \delta\mathbf{w}_i) = (q_i + \delta q_i)(\mathbf{w}_i + \delta\mathbf{w}_i),$$

where the unperturbed matrix \mathbf{A} is given by equation (7.1.34), the perturbation is

$$\delta\mathbf{A} = -\frac{p\rho g}{i\omega} \begin{pmatrix} \mathbf{0} & \mathbf{0} \\ \mathbf{I}_1 & \mathbf{0} \end{pmatrix}$$

(\mathbf{I}_1 is defined in equation (0.1.5)), the unperturbed eigenvalues are given by equations (6.2.8) and (6.2.9), and the unperturbed eigenvectors by equations (6.3.51) and (6.3.53). The small (dimensionless) parameter is pg/ω . The orthonormality relation between the eigenvectors is given by equation (6.3.33). The perturbed eigen-equation gives

$$\delta\mathbf{A} \mathbf{w}_i + \mathbf{A} \delta\mathbf{w}_i = q_i \delta\mathbf{w}_i + \delta q \mathbf{w}_i,$$

to first order.

Pre-multiplying by \mathbf{w}_i^\dagger , we obtain the eigenvalue perturbation

$$\delta w_i = \mathbf{w}_i^\dagger \delta\mathbf{A} \mathbf{w}_i.$$

Because $\delta\mathbf{A} \mathbf{w}_i$ gives a term orthogonal to the particle velocity, this expression reduces to zero, i.e. $\delta w_i = 0$ for all i . Gravity does not affect the wave velocity (to first order).

The eigenvector perturbation can be expanded in terms of the other eigenvectors (as they are orthonormal). Pre-multiplying the perturbation equation

tion by \mathbf{w}_k^\dagger , where $k \neq i$, we obtain

$$\delta \mathbf{w}_i = -\frac{p\rho g}{i\omega} \sum_{k \neq i} \frac{1}{\mathbf{w}_k^\dagger \mathbf{w}_k} \frac{\mathbf{w}_k^\dagger \mathbf{I}_1 \mathbf{w}_i}{q_i - q_k} \mathbf{w}_k.$$

For a up-going SV wave, the polarization of the unperturbed eigenvector is

$$\mathbf{g} = w_1 \begin{pmatrix} q_\beta \\ -p \end{pmatrix}.$$

and the perturbation is

$$\delta \mathbf{g} = w_1 \frac{pg}{2i\omega} \left[\frac{p}{q_\beta} \begin{pmatrix} q_\beta \\ p \end{pmatrix} - \frac{2}{\alpha^2 - \beta^2} \begin{pmatrix} \alpha^2 p \\ \beta^2 q_\beta \end{pmatrix} \right].$$

Similarly for an up-going P wave, the unperturbed polarization is

$$\mathbf{g} = w_3 \begin{pmatrix} p \\ q_\alpha \end{pmatrix}.$$

and the perturbation is

$$\delta \mathbf{g} = w_3 \frac{pg}{2i\omega} \left[\frac{p}{q_\alpha} \begin{pmatrix} -p \\ q_\alpha \end{pmatrix} - \frac{2}{\alpha^2 - \beta^2} \begin{pmatrix} \alpha^2 q_\alpha \\ -\beta^2 p \end{pmatrix} \right].$$

The perturbations tilt the polarization slightly and make it slightly elliptical.

7.3

Investigate how the differential system (7.1.4) behaves for elastic waves, i.e. result (7.1.34), as the shear modulus, μ , tends to zero. How is this compatible with the fluid limit, when the tangential displacement is discontinuous at interfaces? Gilbert (1998) has discussed numerical schemes for solving the differential system as $\mu \rightarrow 0$.

In the limit $\mu \rightarrow 0$, the differential system matrix \mathbf{A} (7.1.34) becomes singular. The eigenvalues $\pm q_\beta$ also become singular. In a transitional region where μ is small, this can lead to numerical difficulties solving differential systems such as (7.1.25) with (7.1.34).

Gilbert (1998) has suggested approximations that give differential systems that can be solved when μ is small. The shear waves are suppressed by imposing the constraint

$$\nabla \times \mathbf{u} = \mathbf{0},$$

so

$$\frac{\partial u_x}{\partial z} = \frac{\partial u_z}{\partial x} = i\omega p u_z.$$

Thus

$$\sigma_{xz} = \mu \left(\frac{\partial u_x}{\partial z} + \frac{\partial u_z}{\partial x} \right) = -2\mu p v_z,$$

so the differential becomes

$$\frac{d}{dz} \begin{pmatrix} v_x \\ v_z \\ \sigma_{zz} \end{pmatrix} = i\omega \mathbf{A} \begin{pmatrix} v_x \\ v_z \\ \sigma_{zz} \end{pmatrix},$$

where

$$\mathbf{A} = \begin{pmatrix} 0 & p & 0 \\ -p\lambda/(\lambda + 2\mu) & 0 & -1/(\lambda + 2\mu) \\ 0 & -\mu\Omega & 0 \end{pmatrix} \begin{pmatrix} v_x \\ v_z \\ \sigma_{zz} \end{pmatrix},$$

with Ω defined in equation (6.3.54). This equation has eigenvalues $\pm q_\alpha$ and 0, i.e.

$$\begin{aligned} \mathbf{A} \begin{pmatrix} p \\ \pm q_\alpha \\ -\mu\Omega \end{pmatrix} &= \pm q_\alpha \begin{pmatrix} p \\ \pm q_\alpha \\ -\mu\Omega \end{pmatrix} \\ \mathbf{A} \begin{pmatrix} 1 \\ 0 \\ -p\lambda \end{pmatrix} &= \mathbf{0}. \end{aligned}$$

A further approximation can be obtained if we take μ as constant. Differentiating $\sigma_{xz} = -2\mu p v_z$ and substituting for both $\partial\sigma_{xz}/\partial z$ and $\partial v_z/\partial z$ from the differential system (7.1.25) with (7.1.34), we obtain

$$p\sigma_{zz} = -\mu\Omega v_x.$$

Then the above differential system reduces to

$$\frac{d}{dz} \begin{pmatrix} v_z \\ \sigma_{zz} \end{pmatrix} = i\omega \mathbf{A} \begin{pmatrix} v_z \\ \sigma_{zz} \end{pmatrix}$$

with

$$\mathbf{A} = \begin{pmatrix} 0 & (p^2\lambda/\mu\Omega - 1)/(\lambda + 2\mu) \\ -\mu\Omega & 0 \end{pmatrix}.$$

Gilbert (1998) has discussed how the boundary conditions must be applied to these reduced differential equations.

In addition, he discusses an alternative using a massive, elastic interface (MEI) (a thin layer, thickness ϵ , with constant parameters. In the solution across the MEI, the displacement is constant and the traction has a discontinuity (saltus)). Combining the first and fourth, and second and third rows of the differential system (7.1.34) we obtain

$$\begin{aligned}\frac{d\sigma_{zz}}{dz} - p\mu\frac{dv_x}{dz} &= i\omega(\mu p^2 - \rho)v_z \\ \frac{d\sigma_{xz}}{dz} - p\lambda\frac{dv_z}{dz} &= i\omega((\lambda + 2\mu)p^2 - \rho)v_x.\end{aligned}$$

Integrating these equations gives

$$\begin{aligned}[\sigma_{zz}] &= i\omega(\bar{\mu}p^2 - \bar{\rho})v_z \\ [\sigma_{xz}] &= i\omega((\bar{\lambda} + 2\bar{\mu})p^2 - \bar{\rho})v_x,\end{aligned}$$

where $\bar{\mu} = \mu\epsilon$, $\bar{\lambda} = \lambda\epsilon$ and $\bar{\rho} = \rho\epsilon$. The virtue of the MEI conditions is that there is no singular behaviour as $\mu \rightarrow 0$. For *SH* waves, the MEI condition becomes a saltus

$$[\sigma_{xy}] = i\omega(\bar{\mu}p^2 - \bar{\rho})v_y.$$

7.4

*Use the propagator method to write down the solution in the transform domain for a homogeneous layer over a homogeneous half-space, without using the ray expansion method, i.e. using the Haskell matrix (7.2.4). Show that the complete response can then be expanded into terms that can be identified as the reverberating rays in the layer. First do this for *SH* waves (relatively simple), and then for *P* – *SV* waves (algebraically messy). The advantages of applying Kennett's ray expansion method to the propagator should now be obvious!*

Using the eigenvectors (6.3.52) for *SH* waves, it is straightforward to form the propagator for the *SH* system (7.1.33)

$$\mathbf{P}(z, z_0) = \begin{pmatrix} \cos \omega q_\beta(z - z_0) & - (i/\mu q_\beta) \sin \omega q_\beta(z - z_0) \\ - (i\mu q_\beta) \sin \omega q_\beta(z - z_0) & \cos \omega q_\beta(z - z_0) \end{pmatrix}$$

(cf. acoustic propagator (7.2.6) — see Exercise 8.5). This is rows and columns 2 and 5 of the full propagator.

Consider a homogeneous layer of thickness d and properties indicated by

a subscript ₁ over a homogeneous half-space indicated by subscript ₂ (for simplicity as we are only considering *SH* waves we drop the subscript _{β} from q). The top of the layer is a free surface at $z = z_1$. In the half-space, the solution must be a down-going wave so just below the interface the transformed solution must be of form (6.3.52)

$$\mathbf{w}(z_2 - 0) = \begin{pmatrix} v_y \\ \sigma_{yz} \end{pmatrix} = aw_2 \begin{pmatrix} 1 \\ \mu_2 q_2 \end{pmatrix},$$

where a is an unknown amplitude. Applying the propagator (C.1.9) with a unit source in the y direction infinitesimally below the free surface ($z_S = z_1 - 0$), the solution at the free surface ($z_R = z_1$) is

$$\begin{pmatrix} v_y \\ 0 \end{pmatrix} = \begin{pmatrix} \cos \omega q_1 d & -(\mathrm{i}/\mu_1 q_1) \sin \omega q_1 d \\ -(\mathrm{i}\mu_1 q_1) \sin \omega q_1 d & \cos \omega q_1 d \end{pmatrix} \\ \times \begin{pmatrix} 1 \\ \mu_2 q_2 \end{pmatrix} \frac{a}{(2\mu_2 q_2)^{1/2}} - \begin{pmatrix} 0 \\ 1 \end{pmatrix}.$$

Eliminating the amplitude a , we obtain

$$v_y = \frac{1}{\mu_1 q_1} \frac{\mu_1 q_1 \cos \omega q_1 d - \mathrm{i}\mu_2 q_2 \sin \omega q_1 d}{\mu_2 q_2 \cos \omega q_1 d - \mathrm{i}\mu_1 q_1 \sin \omega q_1 d} \\ = \frac{1}{\mu_1 q_1} \frac{1 + \mathcal{T}_{22} e^{2\mathrm{i}\omega q_1 d}}{1 - \mathcal{T}_{22} e^{2\mathrm{i}\omega q_1 d}},$$

where \mathcal{T}_{22} is given in equations (6.3.60), (6.3.61) and (6.3.62). Expanding the denominator binomially, we obtain

$$v_y = \frac{1}{\mu_1 q_1} \left(1 + 2 \sum_{n=1}^{\infty} \mathcal{T}_{22} e^{2\mathrm{i}n\omega q_1 d} \right),$$

which can be recognized as the ray expansion in the layer. The first term is the direct ray, and the summation is over reverberations in the layer — the factor 2 occurs because the up- and down-going waves double (6.6.11) as the free surface reflection coefficient is unity (6.4.5).

We leave as a further exercise the more general situation where $z_S \neq z_1$ and/or $z_R \neq z_1$. Then we obtain terms

$$e^{\mathrm{i}\omega q_1 |z_R - z_S|} + \mathcal{T}_{22} e^{\mathrm{i}\omega q_1 (z_R + z_S - 2z_2)} \\ + e^{\mathrm{i}\omega q_1 (2z_1 - z_R - z_S)} + \mathcal{T}_{22} e^{\mathrm{i}\omega q_1 (2d - |z_R - z_S|)},$$

times the reverberation series.

The same problem for *P-SV* waves is similar except 2×2 matrices replace

scalars. For simplicity we consider a point force in the z direction on the surface. Then the solution on the free surface is

$$\begin{pmatrix} \mathbf{v}(z_1) \\ \mathbf{0} \end{pmatrix} = \mathbf{P}(z_1, z_2) \dot{\mathbf{W}}_2 \mathbf{a} - \begin{pmatrix} \mathbf{0} \\ \hat{\mathbf{k}} \end{pmatrix},$$

where $\dot{\mathbf{W}}$ is the 4×2 matrix of down-going eigenvectors from equations (6.3.51) and (6.3.53). The propagator can be calculated from (7.2.4) or more simply from expression (7.2.201). However, the propagator is full and if we expand and substitute the propagator, and then proceed with the algebra to eliminate the unknown 2×1 amplitude vector \mathbf{a} , it is very difficult to recognize the reflection coefficients. Instead we substitute expression (7.2.4) and obtain

$$\begin{pmatrix} \mathbf{v}(z_1) \\ \mathbf{0} \end{pmatrix} = \mathbf{W}_1 e^{i\omega \mathbf{P}_z d} \mathbf{Q} \begin{pmatrix} \mathbf{0} \\ \mathbf{a} \end{pmatrix} - \begin{pmatrix} \mathbf{0} \\ \hat{\mathbf{k}} \end{pmatrix},$$

where the matrix \mathbf{Q} is defined in equation (6.3.22). Substituting expression (6.3.21) for \mathbf{Q} we obtain

$$\begin{pmatrix} \mathbf{v}(z_1) \\ \mathbf{0} \end{pmatrix} = \begin{pmatrix} \mathbf{W}_{11}\Phi_1 & \mathbf{W}_{12}\Phi_1^{-1} \\ \mathbf{W}_{21}\Phi_1 & \mathbf{W}_{22}\Phi_1^{-1} \end{pmatrix} \begin{pmatrix} \mathbf{T}_{11}\mathbf{T}_{21}^{-1}\mathbf{a} \\ \mathbf{T}_{21}^{-1}\mathbf{a} \end{pmatrix} - \begin{pmatrix} \mathbf{0} \\ \hat{\mathbf{k}} \end{pmatrix},$$

where \mathbf{W}_{ij} are the sub-matrices of the eigenvector matrix \mathbf{W}_1 , \mathbf{T}_{ij} are sub-matrices of the coefficient matrix (6.3.23) and the 2×2 diagonal phase matrix is

$$\Phi = \begin{pmatrix} e^{i\omega q_\beta d} & 0 \\ 0 & e^{i\omega q_\alpha d} \end{pmatrix}.$$

Eliminating the vector \mathbf{a} , we obtain

$$\mathbf{v}(z_1) = (\mathbf{W}_{11}\Phi_1\mathbf{T}_{11} + \mathbf{W}_{12}\Phi_1^{-1}) (\mathbf{W}_{21}\Phi_1\mathbf{T}_{11} + \mathbf{W}_{22}\Phi_1^{-1})^{-1} \hat{\mathbf{k}},$$

where \mathbf{T}_{11} is the reflection matrix from the interface at $z = z_2$. The reflection coefficient from the free surface $z = z_1$ is (6.4.4)

$$\mathbf{T}_{22} = -\mathbf{W}_{22}^{-1}\mathbf{W}_{21}$$

(as the two coefficient matrices have different subscripts we do not bother to indicate the interface). Manipulating the above matrix expression (after the binomial expansion, two series are combined into one), we obtain

$$\begin{aligned} \mathbf{v}(z_1) &= (\mathbf{W}_{11}\Phi_1\mathbf{T}_{11} + \mathbf{W}_{12}\Phi_1^{-1}) (\mathbf{I} - \Phi_1\mathbf{T}_{22}\Phi_1\mathbf{T}_{11})^{-1} \Phi_1\mathbf{W}_{22}^{-1}\hat{\mathbf{k}} \\ &= \left(\mathbf{W}_{12} + \mathbf{h} \sum_{n=0}^{\infty} (\Phi_1\mathbf{T}_{11}\Phi_1) (\mathbf{T}_{22}\Phi_1\mathbf{T}_{11}\Phi_1)^n \right) \mathbf{W}_{22}^{-1}\hat{\mathbf{k}}. \end{aligned}$$

where

$$\mathbf{h} = \mathbf{W}_{11} + \mathbf{W}_{12}\mathbf{T}_{22},$$

are the interface polarizations at the free surface (cf. Section 6.6). The terms in this expression can be recognized as all the reverberating rays expected in the layer.

If instead of expanding the inverse matrix binomially, we invert the 2×2 matrix, the denominator of the complete response will contain the determinant

$$\begin{aligned} |\mathbf{I} - \Phi_1 \mathbf{T}_{22} \Phi_1 \mathbf{T}_{11}| = & \\ & 1 - \mathcal{T}_{44} \mathcal{T}_{11} \Phi_\beta^2 - \mathcal{T}_{66} \mathcal{T}_{33} \Phi_\alpha^2 - 2\mathcal{T}_{46} \mathcal{T}_{13} \Phi_\beta \Phi_\alpha \\ & - \left(\mathcal{T}_{44} \mathcal{T}_{66} \mathcal{T}_{13}^2 + \mathcal{T}_{46}^2 \mathcal{T}_{11} \mathcal{T}_{33} - \mathcal{T}_{44} \mathcal{T}_{11} \mathcal{T}_{66} \mathcal{T}_{33} - \mathcal{T}_{46}^2 \mathcal{T}_{13}^2 \right) \Phi_\beta^2 \Phi_\alpha^2. \end{aligned}$$

In this expression, \mathcal{T}_{44} , \mathcal{T}_{46} and \mathcal{T}_{66} are the reflection coefficients from the free surface contained in the sub-matrix \mathbf{T}_{22} , and \mathcal{T}_{11} , \mathcal{T}_{13} and \mathcal{T}_{33} are the reflection coefficients from the interface contained in the sub-matrix \mathbf{T}_{11} — as the coefficient-type indices differ, we have not indicated the different interfaces. We have used the symmetry of these sub-matrices. The phase factors Φ_β and Φ_α are the diagonal elements of the matrix Φ_1 , i.e. $\Phi_\beta = \exp(i\omega q_\beta d)$ and $\Phi_\alpha = \exp(i\omega q_\alpha d)$. The first five terms in this expansion can be recognized as ray reverberations. In order they are: *SSS*, *PPP*, *SPS* (and *PSP*), *SPPSS* and *SSPPS*, where each symbol represents a segment and the first and last partial segments are down-going. The last two terms do not represent ray groups (and have the wrong sign). Only in the complete binomial expansion do these terms cancel (Cisternas, Betancourt and Leiva, 1973). A partial expansion will contain non-physical terms. The determinant is not the proper expression to be expanded into a power series to obtain rays, when two ray types exist.

As already mentioned we have not attempted to expand the propagator matrix and recognize the reflection coefficients. The real algebraic difficulties of obtaining the complete response as a ratio of just single numerator and denominator functions, and expanding to obtain the ray expansion, are encountered with more than one layer.

7.5

Further reading: A differential system similar to the ordinary differential equation (7.1.4) applies in a stratified sphere when the elastic parameters are

a function of the spherical radius. The horizontal derivatives are removed from the partial differential equations by the generalized Legendre transform (see Takeuchi and Saito, 1972, for the derivation of the differential system). A fundamental difference compared with the cartesian system is that the matrix \mathbf{A} depends explicitly on the radius, r , so even in a homogeneous layer, a fundamental solution cannot be written as equation (7.2.2). The fundamental solution can be written in terms of spherical Bessel functions (see Phinney and Alexander, 1966, for the solutions). Although the fundamental matrix is more complicated, the matrix still has symplectic symmetries and the inverse fundamental matrix needed to form the propagator is known without explicitly inverting the fundamental matrix (first given by Teng, 1970, although without using the symplectic symmetries).

For the sake of completeness we give the ordinary differential system for a spherically stratified sphere. The result can be found in Takeuchi and Saito (1972) with the simplification here of ignoring gravity. We define spherical basis functions

$$Y_n^m(\theta, \phi) = P_n^m(\cos \theta) e^{im\phi},$$

where $P_n^m(\cos \theta)$ are the Legendre polynomials. We write the solution as

$$\begin{aligned} v_r &= \frac{1}{r} w_3 Y_n^m \\ v_\theta &= \frac{1}{i\omega p r^2} \left(w_1 \frac{\partial Y_n^m}{\partial \theta} + w_2 \frac{1}{\sin \theta} \frac{\partial Y_n^m}{\partial \phi} \right) \\ v_\phi &= \frac{1}{i\omega p r^2} \left(w_1 \frac{1}{\sin \theta} \frac{\partial Y_n^m}{\partial \phi} - w_2 \frac{\partial Y_n^m}{\partial \theta} \right), \end{aligned}$$

where

$$p = \frac{\sqrt{n(n+1)}}{r\omega}.$$

The functions w_i , components of the vector \mathbf{w} , depend on r , ω , n and m ; the θ and ϕ dependence is contained in the function $Y_n^m(\theta, \phi)$. The equations of motion in spherical coordinates are given in Exercise 4.11. Following Takeuchi and Saito (1972), together with the constitutive equations, these reduce to (7.1.4)

$$\frac{d}{dr} \mathbf{w} = i\omega \mathbf{A} \mathbf{w}.$$

The matrix \mathbf{A} separates into two parts (cf. equations (7.1.33) and (7.1.34)).

These are

$$\mathbf{A}^{(25) \times (25)} = \begin{pmatrix} 2/\mathrm{i}r\omega & -1/\mu \\ \mu p^2 - \rho - 2\mu/r^2\omega^2 & -2/\mathrm{i}r\omega \end{pmatrix},$$

and

$$\mathbf{A}^{(1346) \times (1346)} = \begin{pmatrix} 2/\mathrm{i}r\omega & -p & -1/\mu & 0 \\ -p\xi & -\chi/\mathrm{i}r\omega & 0 & -\psi \\ \eta p^2 - \rho - 2\mu/r^2\omega^2 & 2\zeta p/\mathrm{i}r\omega & -2/\mathrm{i}r\omega & -p\xi \\ -2\zeta p/\mathrm{i}r\omega & -\rho + 4\zeta/r^2\omega^2 & -p & \chi/\mathrm{i}r\omega \end{pmatrix},$$

where

$$\begin{aligned} \psi &= 1/(\lambda + 2\mu) \\ \eta &= 4\mu(\lambda + \mu)/(\lambda + 2\mu) \\ \zeta &= \mu(3\lambda + 2\mu)/(\lambda + 2\mu) \\ \xi &= \lambda/(\lambda + 2\mu) \\ \chi &= (\lambda - 2\mu)/(\lambda + 2\mu). \end{aligned}$$

An early publication with these equations is Alterman, Jarosch and Pekeris (1959)[†] and they have appeared in many subsequent publications, e.g. Aki and Richards (1980, equation (9.56); 2002, equation (9.81)), Chapman and Phinney (1970, 1972), Chapman and Orcutt (1985)[‡]. A most complete derivation is due to Phinney and Burridge (1973)[§]. The terms and factors have been arranged in our equations to emphasize the symmetries and similarities with the matrix (6.3.47), particularly as $r\omega \rightarrow \infty$. It is straightforward to expand the matrix in a series in inverse powers of $r\omega$ and include this in the asymptotic methods, WKBJ (Section 7.2.5) or Langer (Section 7.2.7) (Chapman and Orcutt, 1985).

Note that because of the way v_θ and v_ϕ are defined in terms of w_1 and w_2 , the system separates into a 4×4 P - SV system (known as the spheroidal system) and a 2×2 SH system (known as the toroidal system). The solutions \mathbf{w} have been scaled with radius to make $\mathrm{tr}(\mathbf{A}) = 0$.

As the matrix \mathbf{A} depends on the radius r , its eigenvalues are not of much

[†] Alterman, A., Jarosch, H. and Pekeris, C.L., 1959. Oscillations of the Earth, *Proc. R. Soc.*, **A252**, 80–95.

[‡] Chapman, C.H. and Orcutt, J.A., 1985. The computation of body wave synthetic seismograms in laterally homogeneous media, *Rev. Geophys.*, **23**, 105–63.

[§] Phinney, R.A. and Burridge, R., 1973. Representation of the elasto-gravitational excitation of a spherical Earth model by generalized spherical harmonics, *Geophys. J.R. astr. Soc.*, **34**, 451–87.

interest. Instead, we need the fundamental matrices (or propagator matrices) in homogeneous media. The fundamental solutions for the *SV* waves (columns 1 and 4 in the full 6×6 system) are given by

$$\sqrt{\frac{2n(n+1)}{\rho\beta}} \begin{pmatrix} (h_n(z_\beta)/z_\beta + h'_n(z_\beta))/\beta p \\ 0 \\ -i h_n(z_\beta) \\ -i\mu [(\Omega + 2/r^2\omega^2) h_n(z_\beta) + 2h'_n(z_\beta)/\beta^2 z_\beta]/p \\ 0 \\ 2\mu (h'_n(z_\beta) - h_n(z_\beta)/z_\beta)/\beta \end{pmatrix},$$

where $z_\beta = r\omega/\beta$. In the first column, $h_n(z_\beta) = h_n^{(1)}(z_\beta)$ is the out-going, spherical Hankel function and in the fourth column, $h_n(z_\beta) = h_n^{(2)}(z_\beta)$, the in-going function (with our sign conventions in the Fourier transform (3.1.2)). For the *SH* waves (columns 2 and 5), the solutions are

$$\sqrt{\frac{2}{\rho\beta}} \begin{pmatrix} 0 \\ z_\beta h_n(z_\beta) \\ 0 \\ 0 \\ i\mu (z_\beta h'_n(z_\beta) - h_n(z_\beta))/\beta \\ 0 \end{pmatrix},$$

and for the *P* waves (columns 3 and 6)

$$\sqrt{\frac{2n(n+1)}{\rho\alpha}} \begin{pmatrix} h_n(z_\alpha) \\ 0 \\ i h'_n(z_\alpha)/\alpha p \\ 2i\mu (h'_n(z_\alpha) - h_n(z_\alpha)/z_\alpha)/\alpha \\ 0 \\ \mu (\Omega h_n(z_\alpha) + 4h'_n(z_\alpha)/\alpha^2 z_\alpha)/p \end{pmatrix},$$

where $z_\alpha = r\omega/\alpha$. Apart from the arrangement and normalization factors, these solutions have been given in several of the references cited above. Here they have been orthonormalized so

$$\mathbf{F}^\dagger \mathbf{F} = -\mathbf{I}_3,$$

where $\mathbf{F}(r)$ is the 6×6 fundamental matrix formed with the above columns. Thus the inverse matrix is

$$\mathbf{F}^{-1} = -\mathbf{I}_3 \mathbf{F}^\dagger,$$

equivalent to a result first given by Teng (1970). The existence of these simple results follows from the Hermitian symplectic symmetries of the matrix

\mathbf{A} , and is discussed in Exercise 7.8. The above result can be confirmed using the Wronskian of the spherical Hankel functions (Abramowitz and Stegun, 1965, §10.1.7)

$$W \left\{ h_n^{(1)}(z), h_n^{(2)}(z) \right\} = \frac{1}{2iz^2}.$$

The fundamental matrix, $\mathbf{F}(r)$ can be used to form propagator matrices in homogeneous spherical layers (Phinney and Alexander, 1966), asymptotically equivalent to the Haskell matrix (7.2.4). In a ‘layer’ containing the origin $r = 0$, the in- and out-going solutions must be summed to give the non-singular, spherical Bessel function

$$h_n^{(1)}(z) + h_n^{(2)}(z) = 2j_n(z).$$

Aside: the cylindrical system

As an aside, we give the equivalent results in cylindrically coordinates. These are useful for studying the two-dimensional equivalent of a spherical Earth (Teng and Richards, 1968†, 1969‡), for studying the interaction of seismic waves with a plume structure (Tilman, McKenzie and Priestley, 1998§), and for studying waves in a borehole (Schoenberg, Marzetta, Aron and Porter, 1981¶).

For comparison purposes, we first give the general results in an isotropic medium in cartesian media. The general result was not given in Section 7.1.5, as we immediately rotated to a system aligned with the \mathbf{p} slowness vector. In the general system, the 6×6 matrix \mathbf{A} is

$$\begin{pmatrix} 0 & 0 & -p_1 & -1/\mu & 0 & 0 \\ 0 & 0 & -p_2 & 0 & -1/\mu & 0 \\ -p_1\xi & -p_2\xi & 0 & 0 & 0 & -\psi \\ \eta p_1^2 + \mu p_2^2 - \rho & p_1 p_2 \zeta & 0 & 0 & 0 & -p_1 \xi \\ p_1 p_2 \zeta & \mu p_1^2 + \eta p_2^2 - \rho & 0 & 0 & 0 & -p_2 \xi \\ 0 & 0 & -\rho & -p_1 & -p_2 & 0 \end{pmatrix},$$

where

$$\begin{aligned} \psi &= 1/(\lambda + 2\mu) \\ \eta &= 4\mu(\lambda + \mu)/(\lambda + 2\mu) \\ \zeta &= \mu(3\lambda + 2\mu)/(\lambda + 2\mu) \end{aligned}$$

† Teng, T.-L. and Richards, P.G., 1968. Diffracted SH and SV, *Nature*, **218**, 1154.

‡ Teng, T.-L. and Richards, P.G., 1969. Diffracted *P*, *SV*, and *SH* waves and their shadow-boundary shifts, *J. Geophys. Res.*, **74**, 1537–55.

§ Tilman, F.J., McKenzie, D.P. and Priestley, K.F., 1998. *P* and *S* wave scattering from mantle plumes, *J. Geophys. Res.*, **103**, 21, 145–63.

¶ Schoenberg, M., Marzetta, T., Aron, J. and Porter, R.P., 1981. Space-time dependence of acoustic waves in a borehole, *J. Acous. Soc. Amer.*, **70**, 1496–507.

$$\xi = \lambda/(\lambda + 2\mu).$$

Taking the combinations

$$\begin{aligned} w_1 &= (p_1 v_1 + p_2 v_2)/p \\ w_2 &= (p_2 v_1 - p_1 v_2)/p, \end{aligned}$$

where $p^2 = p_1^2 + p_2^2$, and similarly for σ_{32} and σ_{12} , the matrix \mathbf{A} decomposes into the *SH* and *P-SV* parts, (7.1.33) and (7.1.34), respectively (using the equality $\mu + \zeta = \eta$).

In the cylindrical coordinate system, we order the components ϕ , z and r corresponding to $x = x_1$, $y = x_2$ and $z = x_3$. Assuming the medium only varies in the radial direction, we can use the Fourier series (3.3.1) in the azimuthal direction (so $\partial/\partial\phi \rightarrow i\ell\phi$), and Fourier transform (3.2.4) in the axial direction (so $\partial/\partial z \rightarrow i\omega q$). With the vector

$$\mathbf{w} = r^{1/2} \begin{pmatrix} v_\phi \\ v_z \\ v_r \\ \sigma_{r\phi} \\ \sigma_{zr} \\ \sigma_{rr} \end{pmatrix},$$

and the cylindrical equations of motion and constitutive equations (see Exercise 4.11), the matrix \mathbf{A} is

$$\begin{pmatrix} 3/2i\omega r & 0 & -\ell' \\ 0 & 1/2i\omega r & -q \\ -\ell'\xi & -q\xi & -\chi/2i\omega r & \cdots \\ \eta\ell'^2 + \mu q^2 - \rho & \ell'q\zeta & \ell'\eta/i\omega r & \cdots \\ \ell'q\zeta & \mu\ell'^2 + \eta q^2 - \rho & q\nu/i\omega r & \\ -\ell'\eta/i\omega r & -q\nu/i\omega r & -\rho + \eta/\omega^2 r^2 & \\ & -1/\mu & 0 & 0 \\ & 0 & -1/\mu & 0 \\ & 0 & 0 & -\psi \\ \cdots & -3/2i\omega r & 0 & -\ell'\xi \\ & 0 & -1/2i\omega r & -q\xi \\ & -\ell' & -q & \chi/2i\omega r \end{pmatrix},$$

where

$$\begin{aligned} \ell' &= \ell/\omega r \\ \chi &= (\lambda - 2\mu)/(\lambda + 2\mu) \end{aligned}$$

$$\nu = 2\mu\lambda/(\lambda + 2\mu).$$

The $r^{1/2}$ scaling has been introduced to make $\text{tr}(\mathbf{A}) = 0$. To lowest order, ignoring terms in $1/\omega r$, this matrix is equivalent to the cartesian matrix above with $\ell' \rightarrow p_1$ and $q \rightarrow p_2$, the ‘horizontal’ slownesses, and $r\phi \rightarrow x$ the ‘distance’ travelled in the angular direction. However, in general it appears to be impossible to separate it into 2×2 and 4×4 systems (the diagonal elements and the elements A_{43} , A_{53} , A_{61} and A_{62} cause problems). This restriction is intuitively reasonable as the two ‘horizontal’ components of displacement are not physically equivalent, i.e. v_z does not ‘see’ the curvature of a cylindrical surface, whereas v_ϕ does. In the cartesian and spherical systems that do separate, the two horizontal components are physically equivalent.

A fundamental matrix of the matrix \mathbf{A} can be constructed using a potential representation for the particle displacement. To obtain results close to the cartesian, with approximately P - SV and SH separation, we use

$$\mathbf{u} = \nabla P + \nabla \times (H\hat{\mathbf{r}}) + \nabla \times (\nabla \times (V\hat{\mathbf{r}})).$$

where the potentials P , H and V satisfy the Bessel equation, i.e. $P = J_\ell(\omega r/\alpha)$ and H or $V = J_\ell(\omega r/\beta)$ (others have used the vector $\hat{\mathbf{z}}$ in the shear potentials but this does not emphasize the similarities with the cartesian system). For brevity we have not written out the full fundamental matrix. Although 6×6 , the matrix \mathbf{A} still has Hermitian symplectic symmetries, and the inverse matrix can be obtained simply (see Exercise 7.8).

Although this is a classical problem, a full development with an analysis of the ordinary differential system does not seem to have appeared in the literature, probably because the system does not separate. Most publications assume symmetry so $\ell = 0$ or $q = 0$, and if they do consider the general case only give the solution in homogeneous cylindrical layers to find numerically the reflection/transmission coefficients or scattering by a cylindrical interface. An early paper by Faran (1951)[†] considered the case $q = 0$ and the solutions in homogeneous media. White (1958)[‡] and Pao and Mow (1971)[§] considered the more general case with ℓ and q non-zero with homogeneous media. Similarly Miles (1960)[¶], Baron and Matthews (1961)^{||}, Baron and

[†] Faran, J.J., 1951. Sound scattering by solid cylinders and spheres, *J. Acoust. Soc. Amer.*, **23**, 405–18.

[‡] White, R.M., 1958. Elastic wave scattering at a cylindrical discontinuity in a solid, *J. Acoust. Soc. Amer.*, **30**, 771–85.

[§] Pao, Y.-H. and Mow, C.-C., 1971. *Diffraction of Elastic Waves and Dynamic Stress Concentrations*, New York: Crane, Russak and Company.

[¶] Miles, J.W., 1960. Motion of a rigid cylinder due to a plane elastic wave, *J. Acoust. Soc. Amer.*, **32**, 1656–9.

^{||} Baron, M.L. and Matthews, A.T., 1961. Diffraction of a pressure wave by a cylindrical cavity in an elastic medium, *J. Appl. Mech.*, **28**, 347–54.

Parnes (1962)^{††} and Hinders (1993)^{‡‡} considered the case when $q = 0$, the latter obtaining the full algebraic results for reflection/transmission coefficients from a general cylindrical interface. Schoenberg, Marzetta, Aron and Porter (1991) considered the case when $\ell = 0$ and gave the ordinary 4×4 differential system. Lu and Liu (1995)^{§§} considered the general case with ℓ and q non-zero and gave the solutions in homogeneous layers. Tilman, McKenzie and Priestley (1998) have given the ordinary 6×6 differential system.

7.6

Programming exercise: Confirm numerically that the results from the algorithm given in Section 7.2.8 applied to a single interface, agree with those in programming Exercise 6.3 in Chapter 6 (Matlab code is given in Chapman, 2003, which should be revised according to Chapman, 2005, and the revised algorithm given in the text).

Revised Matlab code from Chapman (2003) implementing the algorithm in Section 7.2.8 is

```
function [ Rvv, Rpv, Rvp, Rpp ] = ...
    Rcoefficients( mat, p, omegas, properties )
% Rcoefficients - P-SV reflection coefficients from layer
%                stack using algorithm in Section 7.2.8

% INPUT:
%      mat          = 'Iso' use Iso_PSV_EigenFactors
%                  = 'TIV' use TIV_PSV_EigenFactors
%      p            = horizontal slowness
%      omegas       = circular frequencies
%
%      if mat = 'Iso':
%      properties(i).Alpha = P velocities
%      properties(i).Beta  = S velocities
%
```

^{††} Baron, M.L. and Parnes, R., 1962. Displacements and velocities produced by the diffraction of a pressure wave by a cylindrical cavity in an elastic medium, *J. Appl. Mech.*, **28**, 385–95.

^{‡‡} Hinders, M.K., 1993. Elastic-wave scattering from an elastic cylinder, *Il Nuovo Cimento*, **108B**, 285–301.

^{§§} Lu, C.-C. and Liu, Q.-H., 1995. A three-dimensional dyadic Green's function for elastic waves in multilayer cylindrical structures, *J. Acoust. Soc. Amer.*, **98**, 2825–35.

```

%      if mat = 'TIV':
%      properties(i).C11    = C11 stiffness
%      properties(i).C33    = C33 stiffness
%      properties(i).C44    = C44 stiffness
%      properties(i).C13    = C13 stiffness
%
%      properties(i).Rho    = densities
%      properties(i).Thick  = layer thickness
%
%      coefficients are properties(1).Thick above
%      interface and properties(nLayers).Thick is
%      ignored
%
%      stiffnesses may be frequency arrays for attenuation which
%      should match omegas array.  They must be row vectors
%      e.g. 1 x nOmega.
%
% OUTPUT:
%      Rvv          = VV coefficient
%      Rpv          = PV coefficient (P incident)
%      Rvp          = VP coefficient (SV incident)
%      Rpp          = PP coefficient
%
% NOTE:
%
% properties(*).Alpha etc. must be scalars or nOmega arrays to
% include frequency-dependent velocities to model attenuation
% (the attenuation model is therefore created externally);
% in this simplified version -
% p=0, Beta=0, p*Alpha=1 or p*Beta=1 are not allowed;
% code is so simply we don't use functions except for
% 'mat'_PSV_EigenFactors and LayerPhase;
% the code is written to allow for frequency arrays of velocity
% or not;
%
% As revised for Addenda and Errata, 25 November 2004
% Revised numerical normalization rather than analytic
% factor, 18 Dec 2005
% Revised to use travelling solutions, with revised
% arguments, 22 January 2007

```

```

%
nLayers = length(properties);
nOmega = length(omegas);
%
% loop from bottom to top
for j = nLayers:-1:1
    %
    % eigenfactors of j-th layer
    eval([ 'qV,qP,ZV,ZP,gV,gP,sV,sP] = ' ...
          mat 'PSVEigenFactors(p,properties(j));' ]);
    %
    % starting condition in lower half space,
    % sixth column of  $Y^{-1} L^{-1} W$  - equation (7.2.223)
    if j == nLayers
        % force correct frequency array size
        x1 = zeros(1,nOmega);
        x2 = x1;
        x3 = x1;
        x4 = x1;
        x5 = ones(1,nOmega);
        x6 = x1;
    %
    % propagate through j-th layer
    else
        %
        % multiply by  $L^{-1}$ 
        % temporary vector is (wa,wb,...,wc,wd)
        % first matrix multiply
        wa = ZV.*x1+x2;
        wb = ZV.*x5+x6;
        wc = -ZP.*x1-x2;
        wd = -ZP.*x5-x6;
        % second matrix multiply
        x1 = -ZP.*wa-wb;
        x2 = -ZP.*wc-wd;
        x5 = ZV.*wa+wb;
        x6 = ZV.*wc+wd;
        % scale (minus sign in theory is not strictly necessary
        % as it cancels with previous scaling in L for (j+1))
        dZ = ZV-ZP;
    end
end

```



```

x3 = dZ.*x3;
x4 = -dZ.*x4;
%
% multiply by Y^-1
% temporary vector is (.,wa,wb,wc,wd,.)
wa = x2+x3./gP;
wb = x3-x2.*gP;
wc = x4+x5./gP;
wd = x5-x4.*gP;
%
x2 = wa+wc./gV;
x3 = wb+wd./gV;
x4 = wc-wa.*gV;
x5 = wd-wb.*gV;
%
x1 = 2*x1; x6 = 2*x6;
%
% multiply by exp(i omega q d) (avoid if only DC)
% equation (7.2.229)
if ( nOmega > 1 || omegas(1) ~= 0 )
    thick = properties(j).Thick;
    % P and SV phases
    PposExp = LayerPhase(omegas,thick,qP);
    VposExp = LayerPhase(omegas,thick,qV);
    wa = PposExp.*VposExp;
    % include phase with 1/(PposExp*VposExp) removed to
    % avoid overflow
    x1 = wa.*x1;
    x2 = wa.*wa.*x2;
    x3 = VposExp.*VposExp.*x3;
    x4 = PposExp.*PposExp.*x4;
    x6 = wa.*x6;
end
end
%
% end condition in first layer
if j == 1
    %
    % form coefficients
    dZ = sqrt(gV.*gP);

```

```

Rvv = -gV.*x3./x5;
Rpv = dZ.*x1./x5;
Rvp = dZ.*x6./x5;
Rpp = gP.*x4./x5;
%
% recombine in j-th layer
else
% multiply by Y - equation (7.2.228)
% temporary vector is (.,wa,wb,wc,wd,.)
wa = x2-x3./gP;
wb = x3+x2.*gP;
wc = x4-x5./gP;
wd = x5+x4.*gP;
%
x2 = wa-wc./gV;
x3 = wb-wd./gV;
x4 = wc+wa.*gV;
x5 = wd+wb.*gV;
%
x1 = 2*x1; x6 = 2*x6;
%
% multiply by L - equation (7.2.226)
% temporary vector is (wa,wb,...,wc,wd)
% first matrix multiply
wa = x1+x5;
wb = -ZV.*x1-ZP.*x5;
wc = x2+x6;
wd = -ZV.*x2-ZP.*x6;
% second matrix multiply
x1 = wc+wa;
x2 = -ZV.*wc-ZP.*wa;
x5 = wd+wb;
x6 = -ZV.*wd-ZP.*wb;
% scale
dZ = ZV-ZP;
x3 = dZ.*x3;
x4 = -dZ.*x4;
%
% Normalize solution independently at each frequency.
% Various factors are ommitted, and ZP and ZV may be

```

```

% large or small depending on p and units.
% Safest solution is to normalize numerically - sqrt
% postponed for efficiency.
wt =      max( real(x1).^2+imag(x1).^2, ...
               real(x2).^2+imag(x2).^2 );
wt =      max( real(x3).^2+imag(x3).^2, wt );
wt =      max( real(x4).^2+imag(x4).^2, wt );
wt =      max( real(x5).^2+imag(x5).^2, wt );
wt = 1./sqrt(max( real(x6).^2+imag(x6).^2, wt ));
x1 = x1.*wt; x2 = x2.*wt; x3 = x3.*wt;
x4 = x4.*wt; x5 = x5.*wt; x6 = x6.*wt;
end
end
return

function [ qV, qP, ZV, ZP, gV, gP, sV, sP ] = ...
    IsoPSVEigenFactors( p, properties )
% return eigen-factors for P and SV waves for isotropic medium

% For internal use in algorithm in Section 7.2.8
% For inelastic, vp and vs may be frequency arrays (for attenuation)
% and then q*, Z* and g* will be arrays (s* is scalar).
% For elastic, all are scalars.
% In calling program assumed that arrays match frequencies.
%
ro = properties.Rho;
vp = properties.Alpha;
vs = properties.Beta;
% vertical slownesses - equations (6.2.8) and (6.2.9)
qV = sqrt((1./vs-p).*(1./vs+p));
qP = sqrt((1./vp-p).*(1./vp+p));
% cross-impedances - equations (7.2.193) and (7.2.194)
ZV = 2*ro*p*(vs.*vs);
ZP = ZV-ro/p;
% polarization (co)tangents - equations (7.2.191)
% and (7.2.192)
gV = -p./qV;
gP = -p./qP;
% scaling factors - equations (7.2.195)
sV = sqrt(p/ro);

```

```
sP = sV;
return
```

```
function posExp = LayerPhase( omegas, thick, q )
% return exponential phase term
```

```
% For internal use in algorithm in Section 7.2.8 for
% terms in matrix  $\exp(i \omega q d)$  (as in equation (7.2.202)).
%
% NOTE:
% valid for q as frequency array and omegas uneven, but
% tries to use recursive formula.
%
%  $\text{Im}(q) > 0$  so this may be exponentially small causing underflow
% and zero (but not overflow and Inf or NaN).
%
nOmega = length(omegas);
iq = i*q;
% if q is array, assumed to be frequency array so
% recursion cannot be used
if length(q) > 0
    posExp = exp(thick*omegas.*iq);
else
% q scalar so try to use recursion formula
    posExp(1) = exp(thick*omegas(1)*iq);
    if ( nOmega > 1 )
        for n = 2:1:nOmega
            % compute delPosExp
            % avoids recomputing for uniform distribution
            if n == 2
                del02 = omegas(2)-omegas(1);
                delPosExp = exp(thick*del02*iq);
            else
                del01 = del02;
                del02 = omegas(n)-omegas(n-1);
                % assumes omegas monotonically increasing
                % frequency increment NOT constant
                if abs(del01-del02) > 1.e-6*(del01+del02)
                    delPosExp = exp(thick*del02*iq);
                end
            end
        end
    end
end
```

```

        end
        %
        posExp(n) = posExp(n-1)*delPosExp;
    end
end
end
return

```

A program computing the same coefficients in the same media as in Exercise 6.3 is

```

function Exercise76
% Exercise 7.6
%
% compute reflection/transmission coefficients using
% algorithm in Section 7.2.8.
%
% a slowness value
px = .2;
% media as in Exercise 6.3
a1 = sqrt(3);
b1 = 1;
r1 = 1;
a2 = 1.270*a1;
b2 = a2/2;
r2 = 1.072*r1;
properties(1) = struct( ...
    'Alpha', a1, 'Beta', b1, 'Rho', r1, 'Thick', 0 );
properties(2) = struct( ...
    'Alpha', a2, 'Beta', b2, 'Rho', r2, 'Thick', 0 );
%
[ Rvv, Rpv, Rvp, Rpp ] = Rcoefficients( 'Iso', px, 0, properties );
Rmatrix = zeros(2,2);
Rmatrix(1,1) = Rvv(1);
Rmatrix(1,2) = Rvp(1);
Rmatrix(2,1) = Rpv(1);
Rmatrix(2,2) = Rpp(1);
Rmatrix
return

```

The results are

```

-0.0629   -0.0413
-0.0413    0.1532

```

which agree with the P - SV coefficients in Exercise 6.3.

7.7

*Programming exercise: Generalize the code used in Exercise 7.6 (from Chapman, 2003) to TIV media by writing a new **EigenFactors** routine. Confirm that numerical results agree with those in programming Exercise 6.3 in Chapter 6.*

The TI version of **EigenFactors** is

```

function [ qV, qP, ZV, ZP, gV, gP, sV, sP ] = ...
    TIVPSVEigenFactors( p, properties )
% return eigen-factors for P and SV waves for TIV medium

% For internal use in algorithm in Section 7.2.8
% Stiffnesses are either scalars or frequency arrays (for
% attenuation).
% Assumption that all are same size so all internal
% variables will be same size.
%
A11 = properties.C11/properties.Rho;
A33 = properties.C33/properties.Rho;
A44 = properties.C44/properties.Rho;
A13 = properties.C13/properties.Rho;
%
ps = p*p;
% terms (5.7.20), (5.7.31) and (5.7.33)
aa = A13+A44;
AA = A11.*A33+A44.*A44-aa.*aa;
BB = A33+A44-ps*AA;
% equation (5.7.32) for the normal component of slowness
A34 =2*A33.*A44;
tmp = sqrt(BB.*BB-2*A34.*(A11*ps-1).*(A44*ps-1));
qVs = (BB+tmp)./A34;
qV = sqrt(qVs);
qPs = (BB-tmp)./A34;

```

```

qP = sqrt(qPs);
% qSV polarizations (5.7.35)
g1 = 2*p*aa.*qV;
tmp = (A33-A44).*qVs-ps*(A11-A44);
g3 = tmp-sqrt(tmp.*tmp+g1.*g1);
% normal component of group velocity (5.7.37)
V3 = qV.*(ps*AA+A34.*qVs-A33-A44)./ ...
      (ps*(A11+A44)+(A33+A44).*qVs-2);
% energy normalize polarizations
gg = sqrt(g1.*g1+g3.*g3).*sqrt(2*properties.Rho*V3);
g1 = g1./gg;
g3 = g3./gg;
% traction components (6.3.66)
t31 = -(p*g3+qV.*g1).*properties.C44;
t33 = -p*g1.*properties.C13-qV.*g3.*properties.C33;
%
ZV = t33./g1;
gV = g3./g1;
sV = sqrt(-2*g1.*g3);
% repeat for qP
g1 = 2*p*aa.*qP;
tmp = (A33-A44).*qPs-ps*(A11-A44);
g3 = tmp+sqrt(tmp.*tmp+g1.*g1);
V3 = qP.*(ps*AA+A34.*qPs-A33-A44)./ ...
      (ps*(A11+A44)+(A33+A44).*qPs-2);
gg = sqrt(g1.*g1+g3.*g3).*sqrt(2*properties.Rho*V3);
g1 = g1./gg;
g3 = g3./gg;
t31 = -(p*g3+qP.*g1).*properties.C44;
t33 = -p*g1.*properties.C13-qP.*g3.*properties.C33;
ZP = t33./g1;
gP = -g1./g3;
sP = sqrt(2*g1.*g3);
return

```

and the main program with the same media as in Exercise 6.3 is

```

function Exercise77
% Exercise 7.7
%
% compute reflection/transmission coefficients using

```

```

% algorithm in Section 7.2.8 for TI media
%
% a slowness value
px = .2;
% media as in Exercise 6.3
a1 = sqrt(3);
b1 = 1;
r1 = 1;
%
c11 = r1*a1*a1;
c44 = r1*b1*b1;
c13 = c11-2*c44;
properties(1) = struct( ...
    'C11',c11, 'C33', c11, 'C44', c44, 'C66', c44, ...
    'C13', c13, 'Rho', r1, 'Thick', 0 );
% a TI medium - Green Horn shale (Jones and Wang, 1981)
% (see Exercise 4.4). Units are Gpa and Mg/m^3
r2 = 2.42;
properties(2) = struct( ...
    'C11',34.3, 'C33', 22.7, 'C44', 5.4, 'C66', 10.6, ...
    'C13', 10.7, 'Rho', r2, 'Thick', 0 );
%
[ Rvv, Rpv, Rvp, Rpp ] = ...
    Rcoefficients( 'TIV', px, 0, properties );
Rmatrix = zeros(2,2);
Rmatrix(1,1) = Rvv(1);
Rmatrix(1,2) = Rvp(1);
Rmatrix(2,1) = Rpv(1);
Rmatrix(2,2) = Rpp(1);
Rmatrix
return

```

which reproduces the results

```

-0.3948    -0.2581
-0.2581     0.5675

```

for the qSV - qP reflection coefficients.

7.8

Investigate the symplectic symmetry properties of the differential system $d\mathbf{w}/dz = i\omega\mathbf{A}\mathbf{w}$ with matrices (7.1.6), (6.3.15)–(6.3.17), (7.1.33) and (7.1.34) (and those in Exercises 7.2 and 7.5). Obtain an expression for the inverse of the propagator matrix using a symplectic transform (cf. Section 6.3.2.1).

Consider the sub-matrices of the matrix \mathbf{A}

$$\mathbf{A} = \begin{pmatrix} \mathbf{A}_{11} & \mathbf{A}_{12} \\ \mathbf{A}_{21} & \mathbf{A}_{22} \end{pmatrix}.$$

All the matrices (7.1.6), (6.3.15)–(6.3.17), (7.1.34) and (7.1.34) satisfy the symmetries

$$\begin{aligned} \mathbf{A}_{22} &= \mathbf{A}_{11}^\dagger \\ \mathbf{A}_{12}^\dagger &= \mathbf{A}_{12} \\ \mathbf{A}_{21}^\dagger &= \mathbf{A}_{21}, \end{aligned}$$

where \mathbf{A}^\dagger is the transpose of the matrix. For the differential systems in Exercises 7.2 and 7.5, it is necessary to generalize this so \mathbf{A}^\dagger is the Hermitian transpose (i.e. conjugate transpose) and require the elastic parameters and transform variables to be real. It is then evident that the matrix $\mathbf{I}_2\mathbf{A}$ (\mathbf{I}_2 defined in equation (0.1.5)) is Hermitian.

Let us now define a symplectic transform of a propagator matrix

$$\mathbf{P}^\dagger = -\mathbf{P}^\dagger\mathbf{I}_2 = -\begin{pmatrix} \mathbf{P}_{21}^\dagger & \mathbf{P}_{11}^\dagger \\ \mathbf{P}_{22}^\dagger & \mathbf{P}_{12}^\dagger \end{pmatrix}.$$

Then

$$\begin{aligned} \frac{d}{dz}(\mathbf{P}^\dagger\mathbf{P}) &= \mathbf{P}^\dagger\frac{d\mathbf{P}}{dz} + \frac{d\mathbf{P}^\dagger}{dz}\mathbf{P} \\ &= -i\omega\mathbf{P}^\dagger\mathbf{I}_2\mathbf{A}\mathbf{P} - \frac{d\mathbf{P}^\dagger}{dz}\mathbf{I}_2\mathbf{P} \\ &= -i\omega\mathbf{P}^\dagger(\mathbf{I}_2\mathbf{A})\mathbf{P} + i\omega\mathbf{P}^\dagger(\mathbf{A}\mathbf{I}_2)\mathbf{P} \\ &= \mathbf{0}, \end{aligned}$$

as $\mathbf{I}_2\mathbf{A}$ is Hermitian. Thus

$$\mathbf{P}^\dagger\mathbf{P} = \text{constant} = -\mathbf{I}_2,$$

from the value $\mathbf{P}(z_0, z_0) = \mathbf{I}$. Thus

$$\mathbf{P}^{-1}(z, z_0) = \mathbf{P}(z_0, z) = -\mathbf{I}_2\mathbf{P}^\dagger(z, z_0) = \mathbf{I}_2\mathbf{P}(z, z_0)\mathbf{I}_2.$$

It is straightforward to obtain expressions for the inverse of fundamental matrices, too.

Although this proof requires the elastic parameters and transform variables to be real, if the propagator is known analytically, then the analytic inverse propagator will also be valid for complex elastic parameters and transform variables.

8

Inverse transforms for stratified media

8.1

Prove result (8.1.35).

The equation (8.1.3) defining the Cagniard contour is

$$\tilde{T}_P = px_R + q_\alpha d.$$

This reduces to the quadratic

$$p^2 R^2 - 2p\tilde{T}_P x_R + (\tilde{T}_P^2 - d^2/\alpha^2) = 0,$$

with solutions

$$\begin{aligned} p &= \frac{\tilde{T}_P x_R \pm \sqrt{\tilde{T}_P^2 x_R^2 - \tilde{T}_P^2 R^2 + d^2 R^2 / \alpha^2}}{R^2} \\ &= \frac{\tilde{T}_P x_R \pm d\sqrt{R^2 / \alpha^2 - \tilde{T}_P^2}}{R^2} \\ &= \frac{\tilde{T}_P}{R} \sin \theta \pm i \left(\frac{\tilde{T}_P^2}{R^2} - \frac{1}{\alpha^2} \right)^{1/2} \cos \theta, \end{aligned}$$

i.e. equation (8.1.11), where $R^2 = x_R^2 + d^2$, $\sin \theta = x_R/R$ and $\cos \theta = d/R$.

The vertical slowness is found from

$$\begin{aligned} q_\alpha &= \frac{\tilde{T}_P - px_R}{d} \\ &= \frac{\tilde{T}_P}{R} \sec \theta - \left[\frac{\tilde{T}_P}{R} \sin \theta \pm i \left(\frac{\tilde{T}_P^2}{R^2} - \frac{1}{\alpha^2} \right)^{1/2} \cos \theta \right] \tan \theta \\ &= \frac{\tilde{T}_P}{R} \cos \theta \mp i \left(\frac{\tilde{T}_P^2}{R^2} - \frac{1}{\alpha^2} \right)^{1/2} \sin \theta. \end{aligned}$$

Differentiating the slowness equation we obtain

$$\begin{aligned}
\frac{\partial p}{\partial \tilde{T}_P} &= \frac{1}{R} \sin \theta \mp i \frac{\tilde{T}_P}{R^2} \left(\frac{\tilde{T}_P^2}{R^2} - \frac{1}{\alpha^2} \right)^{-1/2} \cos \theta \\
&= \left[\left(\frac{\tilde{T}_P^2}{R^2} - \frac{1}{\alpha^2} \right)^{1/2} \sin \theta \mp i \frac{\tilde{T}_P}{R} \cos \theta \right] (\tilde{T}_P^2 - R^2/\alpha^2)^{-1/2} \\
&= \pm \frac{i q_\alpha}{(\tilde{T}_P^2 - R^2/\alpha^2)^{1/2}}.
\end{aligned}$$

In the fourth quadrant, $\text{Im}(\partial p / \partial \tilde{T}_P) < 0$ so we require the negative sign. Hence result (8.1.35).

8.2

The results for the direct rays from a line source in a homogeneous medium, e.g. (4.5.84) and (8.1.36), can be obtained exploiting the cylindrical symmetry about the line source. Using the Fourier-Bessel transforms (Section 3.3) to obtain the result as an inverse Fourier transform of a Hankel function (Appendix B.4).

For simplicity let us consider a force along the line source. We consider cylindrical polar coordinates r , ϕ and z with the source along the z axis. From equation (4.5.84), or as proved in Exercise 4.7, we have the solution

$$\mathbf{u} = \frac{\hat{\mathbf{z}}}{2\pi\rho\beta^2(t^2 - r^2/\beta^2)^{1/2}}.$$

From symmetry, there are no variations in the z or ϕ directions, and the non-zero constitutive equation and equation of motion (from Exercise 4.11) are

$$\begin{aligned}
\sigma_{zr} &= \mu \frac{\partial u_z}{\partial r} \\
-\rho\omega^2 u_z &= f_z + \frac{1}{r} \frac{\partial}{\partial r} (r\sigma_{zr}) \\
&= f_z + \frac{\mu}{r} \frac{\partial}{\partial r} \left(r \frac{\partial u_z}{\partial r} \right),
\end{aligned}$$

in a homogeneous medium. Applying the transform (3.3.3) to this equation, we obtain

$$-\rho\omega^2 u_z = \int_0^{r_0} f_z r J_0(\omega pr) dr + \mu \int_0^\infty \frac{1}{r} \frac{\partial}{\partial r} \left(r \frac{\partial u_z}{\partial r} \right) r J_0(\omega pr) dr$$

$$= \frac{f_z A_0}{2\pi} - \mu \omega^2 p^2 u_z,$$

where u_z is a function of the transformed variables ω and p . The last term has been simplified by integrating by parts and using the differential equation satisfied by the Bessel function $J_0(z)$, i.e. $J_0''(z) + J_0'(z)/z + J_0(z) = 0$. We have taken the source as a constant force over an small cylinder of radius r_0 and cross-sectional area $A_0 = \pi r_0^2$. Solving the above equation, we have

$$u_z(\omega, p) = - \frac{f_z A_0}{2\pi \rho \beta^2 q^2 \omega^2}.$$

The inverse transform (3.3.5) gives

$$\begin{aligned} u_z(\omega, r) &= \frac{f_z A_0}{2\pi \rho \beta^2} \int_0^\infty \frac{p}{q^2} J_0(\omega p r) dp \\ &= \frac{f_z A_0}{4\pi \rho \beta^2} \int_{-\infty}^\infty \frac{p}{q^2} H_0^{(1)}(\omega p r) dp, \end{aligned}$$

using (3.3.7), provided $\omega > 0$. Expanding the integrand

$$u_z(\omega, r) = \frac{f_z A_0}{8\pi \rho \beta^2} \int_{-\infty}^\infty \left(\frac{1}{1/\beta - p} - \frac{1}{1/\beta + p} \right) H_0^{(1)}(\omega p r) dp,$$

where the contour of integration loops above the pole at $p = -1/\beta$ and below the pole at $p = 1/\beta$. Distorting the contour upwards into positive imaginary p plane, we pick up the residue of the pole at $p = 1/\beta$, i.e.

$$u_z(\omega, r) = \frac{i f_z A_0}{4\rho \beta^2} H_0^{(1)}(\omega r/\beta) dp.$$

Using transform result (B.4.13), we obtain

$$u_z(t, r) = \frac{f_z A_0}{2\pi \rho \beta^2} \frac{1}{(t^2 - r^2/\beta^2)^{1/2}},$$

in agreement with the result above.

Results for the other force components or a pressure source can be obtained by similar techniques but are algebraically more complicated.

8.3

Result (4.5.84) for the two-dimensional force Green function can be compared with the Cagniard solution (8.1.36) for the two-dimensional pressure Green function. By differentiating result (4.5.84) to form a force dipole, and summing two orthogonal dipoles to form a pressure source, show that

the two results are equivalent — remember the extra time differential in result (8.1.36) (it is fairly easy to confirm the equivalence of the leading term — rather tedious to do for the complete expression).

The leading term for a unit radial line force from the Green dyadic (4.5.84) is

$$\mathbf{u}_{\text{force delta}}(t, \mathbf{x}_R) \simeq \frac{H(t - r/\alpha)}{2\pi\rho\alpha^2(t^2 - r^2/\alpha^2)^{1/2}} \hat{\mathbf{r}}.$$

For a unit, step-function pressure line source, expression (8.1.36) gives

$$\mathbf{u}_{\text{pressure step}}(t, \mathbf{x}_R) = \frac{1}{2\pi\rho\alpha^2 r} \frac{tH(t - r/\alpha)}{(t^2 - r^2/\alpha^2)^{1/2}} \hat{\mathbf{r}}$$

($A_S P'_S(t) = \delta(t)$). The (almost trivial) problem is to prove that these are equivalent.

If the force is a step function, $H(t)$, we integrate the first result so

$$\mathbf{u}_{\text{force step}}(t, \mathbf{x}_R) \simeq \frac{\hat{\mathbf{r}}}{2\pi\rho\alpha^2} \int_{r/\alpha}^t \frac{dt'}{(t'^2 - r^2/\alpha^2)^{1/2}} = \frac{\hat{\mathbf{r}}}{2\pi\rho\alpha^2} \cosh^{-1}\left(\frac{\alpha t}{r}\right)$$

using standard result (A.0.1). Taking minus the r derivative of this expression forms a dipole in the radial direction, i.e. a negative force at a source-receiver distance of $r + \epsilon$ and a positive force at $r - \epsilon$. The orthogonal dipole (from differentiating a force in the $\hat{\phi}$ direction) contributes nothing to the radial displacement. The radial dipole and the orthogonal dipole together make a pressure source. Thus

$$\mathbf{u}_{\text{pressure step}}(t, \mathbf{x}_R) = -\frac{d}{dr} \mathbf{u}_{\text{force step}}(t, \mathbf{x}_R) \simeq \frac{\hat{\mathbf{r}}}{2\pi\rho\alpha^2 r} \frac{tH(t - r/\alpha)}{(t^2 - r^2/\alpha^2)^{1/2}},$$

in exact agreement with the above result from (8.1.36) (the exact agreement is not guaranteed as we did not include the near-field terms in the force dyadic).

8.4

Exercise 7.4 in Chapter 7 developed the solution for a homogeneous layer over a half-space without the ray expansion. For SH waves, investigate the conditions under which the transformed response has poles in the complex p plane. Assume that the shear velocity of the half-space is greater than that of the layer. Sketch the dispersion behaviour of these poles, first as a plot of ω v. ($k = \omega p$), and then as the phase velocity ($c = p^{-1}$) v. ω . Using the method of

residues, find the spectral response, and then using the method of stationary phase, approximate the time response. Show that these poles give rise to a dispersed signal, where the low frequencies arrive first with the frequency increasing with time. Later the high-frequency signals are superimposed with the frequency decreasing with time. Finally, the two frequencies converge and a large amplitude, known as the Airy phase, is observed. To find the waveform of this signal, you will need the third-order saddle-point results in Appendix D.2. These dispersed waves are known as Love waves. They are locked modes generated by the constructive interference of waves in the surface layer that are totally reflected at the interface.

How does the amplitude of the Airy phase behave compared with the dispersed part of the Love wave? Why?

This problem was described by Knopoff (1958).

How is the solution altered if the velocity in the half-space is lower than that of the layer?

The dispersion of Love waves can be investigated analytically or numerically, but the equivalent waves for the $P - SV$ system will probably need numerical solutions. Show that dispersed waves exist for the $P - SV$ system (assume the shear velocity in the half-space is greater than that of the layer). Show that the lowest-order wave behaves like the Rayleigh wave (see Chapter 9) — at low frequencies it has the behaviour of the Rayleigh wave velocity of the half-space and at high frequencies of the layer. Higher-order waves are dispersed between the shear velocities in the half-space and layer. Again Airy phases exist. This problem was described by Spencer (1965).

The model is as described in Exercise 7.4, i.e. a unit force in the y direction on the free surface of a homogeneous layer with a homogeneous half-space. First we consider the case when $\beta_2 > \beta_1$. From Exercise 7.4, the transformed response is

$$v_y = \frac{1}{\mu_1 q_1} \frac{1 + \mathcal{T}_{22} e^{2i\omega q_1 d}}{1 - \mathcal{T}_{22} e^{2i\omega q_1 d}} = \frac{\mathcal{N}(\omega, p)}{\mathcal{D}(\omega, p)},$$

say. The reflection coefficient, \mathcal{T}_{22} , is given by equation (6.3.60) and in the range $\beta_2^{-1} < p < \beta_1^{-1}$ can be reduced to

$$\mathcal{T}_{22} = e^{-2i \operatorname{sgn}(\omega) \phi},$$

where

$$\tan \phi = \frac{\mu_2 |q_2|}{\mu_1 q_1},$$

cf. equations (6.3.11) and (6.3.12) (as we are only considering SH waves, we

drop the subscript β from q). We define the denominator as

$$\mathcal{D}(\omega, p) = 1 - e^{2i\omega q_1 d - 2i \operatorname{sgn}(\omega) \phi},$$

the (*Love*) *dispersion function*. More general situations with $z_S \neq z_1$ and/or $z_R \neq z_1$ can be written similarly with the same dispersion function but a more complicated numerator.

The dispersion function is zero when $\phi = \omega q_1 d - n\pi$ ($\omega > 0$), which reduces to

$$\omega = \frac{1}{q_1 d} \tan^{-1} \left(\frac{\mu_2 |q_2|}{\mu_1 q_1} \right).$$

Thus for a given slowness p , we can immediately calculate the frequencies, ω_n , at with $\mathcal{D}(\omega, p) = 0$. It is more convenient to plot function, $\omega_n(p)$, as the inverse function for the phase velocity $p^{-1} = c(\omega)$. The following program illustrates the phase and group velocity functions.

```
function Exercise84a
% Exercise 8.4
%
% Love dispersion curves

beta1 = 1;
beta2 = 2;
rho1 = 1;
rho2 = 1.5;
d = 1;
%
omax = 10;
%
mu1 = rho1*beta1*beta1;
mu2 = rho2*beta2*beta2;
%
ps = linspace( 1.000001/beta2, .999/beta1, 1000);
ps2 = ps.*ps;
q1 = sqrt(1/beta1^2-ps2);
q2 = sqrt(ps2-1/beta2^2);
omega0 = atan2( mu2*q2, mu1*q1 )./(d*q1);
% plot c v. omega
figure
hold on
plot( omega0, 1./ps, 'b' )
```



```

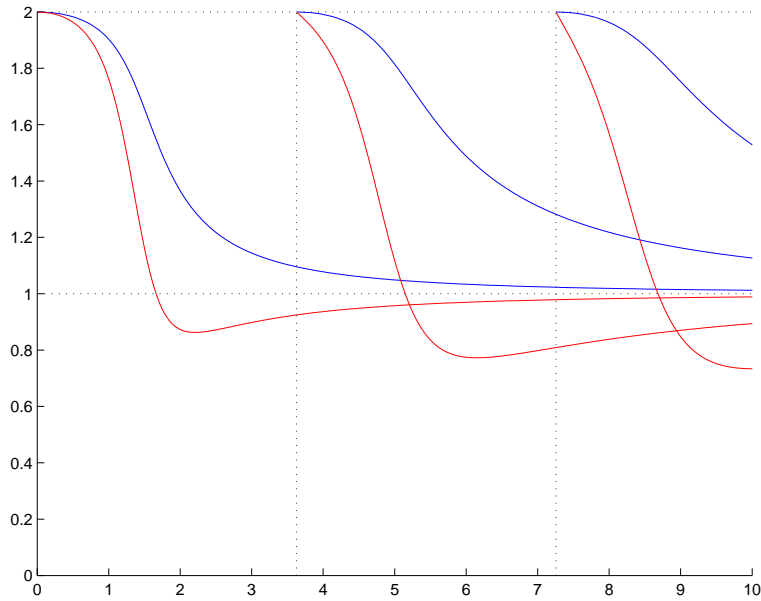
omega1 = omega0 + pi./(d*q1);
plot( omega1, 1./ps, 'b' )
omega2 = omega1 + pi./(d*q1);
plot( omega2, 1./ps, 'b' )
axis([ 0 omax 0 beta2 ])
% plot cutoff
o1 = pi/(d*sqrt(1/beta1^2-1/beta2^2));
o2 = 2*o1;
plot([o1 o1], [0 beta2], 'k:')
plot([o2 o2], [0 beta2], 'k:')
% plot V v. omega
dodp0 = omega0.*ps./(q1.*q1) + ...
        (mu2*rho1-mu1*rho2)./(((mu2*mu2-mu1*mu1)*ps2-...
        mu2*rho2+mu1*rho1).*q1.*q1.*q2*d);
dodk0 = dodp0./(omega0+ps.*dodp0);
plot( omega0, dodk0, 'r')
dodp1 = omega1.*ps./(q1.*q1) + ...
        (mu2*rho1-mu1*rho2)./(((mu2*mu2-mu1*mu1)*ps2-...
        mu2*rho2+mu1*rho1).*q1.*q1.*q2*d);
dodk1 = dodp1./(omega1+ps.*dodp1);
plot( omega1, dodk1, 'r')
dodp2 = omega2.*ps./(q1.*q1) + ...
        (mu2*rho1-mu1*rho2)./(((mu2*mu2-mu1*mu1)*ps2-...
        mu2*rho2+mu1*rho1).*q1.*q1.*q2*d);
dodk2 = dodp2./(omega2+ps.*dodp2);
plot( omega2, dodk2, 'r')
%
plot([ 0 omax], [beta1 beta1], 'k:')
plot([ 0 omax], [beta2 beta2], 'k:')
print -depsc2 exercise8_4a.eps
% plot omega v. k
k0 = omega0.*ps;
k1 = omega1.*ps;
k2 = omega2.*ps;
figure
hold on
plot( k0, omega0, 'k' )
plot( k1, omega1, 'k' )
plot( k2, omega2, 'k' )
% plot beta1 and beta2

```

```

plot([0 omax/beta2], [0 omax], 'k--')
plot([0 omax/beta1], [0 omax], 'k--')
axis([ 0 omax 0 omax/beta1 ])
% plot cutoffs
plot([0 o1/beta2], [o1 o1], 'k:')
plot([0 o2/beta2], [o2 o2], 'k:')
print -depsc2 exercise8_4b.eps
%
return

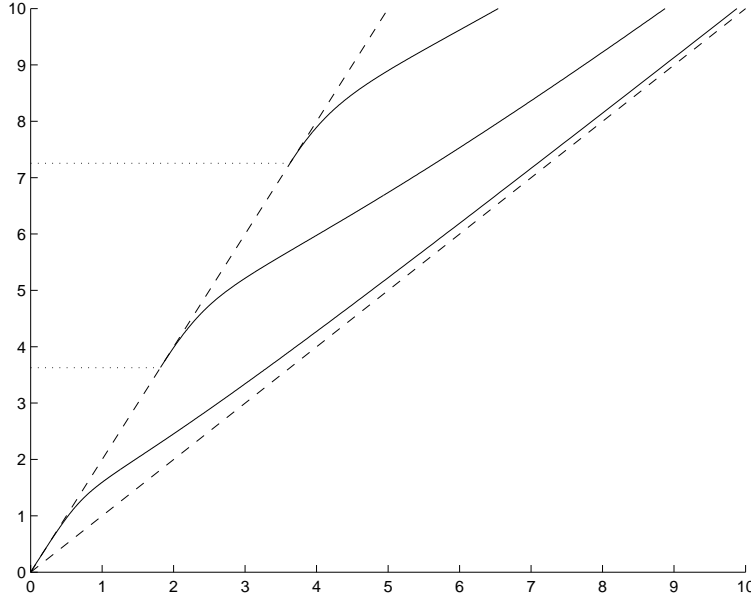
```



The dispersion functions $c_n(\omega)$ (blue) and $V_n(\omega)$ (red) for acoustic modes $n = 0, 1$ and 2 for Love waves in a model with a layer one unit thick, and velocities $\beta_1 = 1$ and $\beta_2 = 2$, and densities $\rho_1 = 1$ and $\rho_2 = 1.5$.

This plot is of c *v.* ω — as $\beta_1 = 1$ and $d = 1$, this is essentially a dimensionless plot. The other parameters are given in the program. An alternative that is very convenient is to plot ω against $k_x = \omega p$ where the slope of straight lines through the origin is the phase velocity, c . The dashed lines indicate these for β_1 and β_2

Note that there are multiple solutions of the dispersion equation due to the inverse trigonometrical function. Each dispersion curve has a low-frequency



The dispersion functions $\omega_n(k)$ for acoustic modes $n = 0, 1$ and 2 for Love waves in a model with a layer one unit thick, and velocities $\beta_1 = 1$ and $\beta_2 = 2$, and densities $\rho_1 = 1$ and $\rho_2 = 1.5$. The velocities $c = \beta_1 = 1$ and $c = \beta_2 = 2$ are illustrated with dashed lines, and the cutoff frequencies Ω_n with dotted lines.

cutoff at

$$\Omega_n = \frac{n\pi}{d(1/\beta_1^2 - 1/\beta_2^2)^{1/2}},$$

where $c = \beta_2$, the half-space velocity. These are indicated with dotted lines in the figures. At high frequencies, the dispersion curves are asymptotic to $c = \beta_1$, the layer velocity.

The inverse slowness integral (3.2.4) passes just below the poles on the real p axis between $p = \beta_2^{-1}$ and $p = \beta_1^{-1}$. By distorting the integration path into the upper p plane, the integral can be reduced to the residues of these poles plus branch cut integrals. We consider just the residues. Thus

$$v_y(\omega, x) = \frac{\omega}{2\pi} \int_{-\infty}^{\infty} \frac{\mathcal{N}(\omega, p)}{\mathcal{D}(\omega, p)} e^{i\omega p x} dp \simeq \sum_{n=0}^{N_\omega-1} \frac{i\omega \mathcal{N}(\omega, p_n) e^{i\omega p_n x}}{\mathcal{D}'(\omega, p_n)},$$

where, for a given ω , $p_n(\omega)$ solves the dispersion equation. We use the notation \mathcal{D}' for $\partial\mathcal{D}/\partial p$. From the figure it is clear that the summation contains only N_ω poles, where $\omega < \Omega_{N_\omega}$, the $(N_\omega + 1)$ -th cutoff. We can

now take the inverse Fourier transform (3.1.10) to obtain

$$v_y(t, x) = -\frac{1}{\pi} \frac{d}{dt} \operatorname{Re} \int_0^\infty \frac{\mathcal{N}(\omega, p_n)}{\mathcal{D}'(\omega, p_n)} e^{ik_n x - i\omega t} d\omega,$$

where $k_n = k_n(\omega) = \omega p_n(\omega)$ are functions of frequency.

The exponential factor in the integrand is highly oscillatory so we evaluate the integral approximately by the saddle-point method (Appendix D). The saddle point exists when

$$\frac{dk_n}{d\omega} x - t = 0.$$

We define a function

$$V_n(\omega) = \frac{d\omega}{dk_n},$$

and for given t and x , solve

$$V_n(\omega) = \frac{x}{t},$$

for the frequency, say ω_n , at the saddle point. We call V_n , the *group velocity* function. The dispersion equation is easily differentiated so

$$\frac{d\omega}{dp} = \frac{k}{q_1^2} + \frac{\mu_2 \rho_1 - \mu_1 \rho_2}{(\mu_2^2 - \mu_1^2)p^2 - \mu_2 \rho_2 + \mu_1 \rho_1} \frac{1}{q_1^2 |q_2| d},$$

and the group velocity calculated from

$$V(\omega) = \frac{d\omega}{dk} = \frac{d\omega/dp}{\omega + p d\omega/dp}.$$

It is clear that at the two limits, the phase and group velocities are equal, i.e. when $p = \beta_1^{-1}$, then $c = V = \beta_1$ and when $p = \beta_2^{-1}$, then $c = V = \beta_2$. The function $V_n(\omega)$ is plotted in the above figure with $c_n(\omega)$. It is the gradient of the dispersion curves in the $\omega - k_x$ plot, so, as these must have an inflexion point between the two limiting gradients β_2 and β_1 , the function $V_n(\omega)$ must have a minimum with $V_n(\omega) < \beta_1$. Let us call the frequency at the minimum $\omega = \omega_{nA}$. For a given n , solving the saddle-point condition $V_n(\omega) = x/t$ may have one or two solutions. Let us denote these by $\omega_{n2} < \omega_{nA}$ and $\omega_{n1} > \omega_{nA}$: for $\beta_2 > x/t = V_n > \beta_1$, only one saddle point with $\omega = \omega_{n2}$ exists; for $\beta_1 > x/t = V_n > V_{nA} = V_n(\omega_{nA})$, two saddle points with $\omega = \omega_{n1}$ and ω_{n2} exist.

To evaluate the second-order saddle-point integral we need the second derivative

$$\frac{d^2 k_n}{d\omega^2} = -V'_n(\omega)/V_n^2(\omega) = U'_n(\omega),$$

where $U_n(\omega) = 1/V_n(\omega)$, the group slowness. From the figure it is clear that

$$\begin{aligned} U'_n(\omega_{n2}) &> 0 \\ U'_n(\omega_{n1}) &< 0. \end{aligned}$$

Then the second-order saddle-point method (D.1.11) gives

$$\begin{aligned} v_y(t, x) = & - \left(\frac{2}{\pi x} \right)^{1/2} \operatorname{Re} \sum_{n=0}^{\infty} \sum_{m=1}^2 \frac{\mathcal{N}(\omega_{nm}, p_{nm})}{\mathcal{D}'(\omega_{nm}, p_{nm})} \\ & \times \frac{1}{|U'_{nm}|^{1/2}} e^{i\omega_{nm}(p_{nm}x-t) \pm i \operatorname{sgn}(U'_{nm})\pi/4}, \end{aligned}$$

where p_{nm} , etc. indicates that the function is evaluated at ω_{nm} . The number of terms in the m summation will depend on the time, t . The signal due to these poles starts with a low frequency signal at $t = x/\beta_2$, from $\omega = 0$ for the $n = 0$ pole, and from the cutoff Ω_n for higher poles. As time increases, the frequency increases in a dispersed wave-train. At any time the frequency arriving is given by the solution of $t = x/V_n$, i.e. $\omega = \omega_{mn}$ (hence V_n is the group velocity). The phase velocity of the waves between different ranges is $\omega/k_n = c_n$. At time $t = x/\beta_1$, a high-frequency signal begins to arrive on the lower-frequency wave. As time increases, the frequency of this high-frequency wave decreases until at $t = x/V_n(\omega_{nA})$ both wave-trains have the same frequency ω_{nA} . At later times, no dispersed waves arrive. The amplitude of the dispersed waves depends on the magnitude of the dispersion. If $|U'_{nm}|$ is large, the velocity varies rapidly with frequency and the dispersion is large and the amplitude small (as energy in a given frequency band is spread out over a larger time interval). The amplitude decays as $x^{-1/2}$ because the waves disperse more with range (we have only solved the two-dimensional problem, so this factor $x^{-1/2}$ is not due to cylindrical spreading, but to the increased dispersion with range). These dispersed waves are known as the *Love* waves.

At times near $t = x/V_n(\omega_{nA})$, the dispersion U'_{nm} is small and the above expressions break down. Two saddle points coalesce and we must use the third-order saddle-point method (Appendix D.2). We approximate the phase by its cubic term about the point where $U'_n(\omega_{nA}) = 0$, so the contribution from the coalescing saddle points is

$$\begin{aligned} v_y(t, x) \simeq & - \frac{1}{\pi} \operatorname{Re} \left(\frac{\mathcal{N}(\omega_{nA}, p_{nA})}{\mathcal{D}'(\omega_{nA}, p_{nA})} e^{ik_{nA}x - i\omega_{nA}t} \right. \\ & \times \left. \int_0^{\infty} e^{i(xU_{nA}-t)(\omega-\omega_{nA}) + iU''_{nA}x(\omega-\omega_{nA})^3/6} d\omega \right) \end{aligned}$$

$$\begin{aligned}
&= -\frac{2^{4/3}}{(x|U''_{nA}|)^{1/3}} \operatorname{Re} \left(\frac{\mathcal{N}(\omega_{nA}, p_{nA})}{\mathcal{D}'(\omega_{nA}, p_{nA})} e^{ik_{nA}x - i\omega_{nA}t} \right) \\
&\quad \times \operatorname{Ai} \left(\frac{t - xU_{nA}}{(x|U''_{nA}|)^{1/3}} \right),
\end{aligned}$$

using (D.2.3) (where again p_{nA} , etc. indicates that the function is evaluated at ω_{nA}). The signal only decays as $x^{-1/3}$ so at large ranges it will dominate the dispersed wave-train (as with a stationary value of the group velocity, a minimum, the waves are not dispersed so much). It is known as the *Airy phase* as the envelope of the waves with frequency ω_{nA} is the Airy function (Figure D.2). Beyond the time $t = x/V_n(\omega_{nA})$, the signal will decay exponentially.

We have only discussed the signal due to the real Love poles between $p = \beta_2^{-1}$ and β_1^{-1} . Near $t = x/\beta_2$, head waves described by the branch cut integral, that we have ignored, will be significant. At the branch point $p = \beta_1^{-1}$, the poles pass through the branch cut and become complex. To describe the complete response, these poles must be investigated further.

If $\beta_2 < \beta_1$, no poles exist on the real p axis as for $p < \beta_1^{-1}$, $|\mathcal{T}_{22}| < 1$ and for $p > \beta_1^{-1}$, q_1 is imaginary so $\exp(2i\omega q_1 d) < 1$ (at $p = \beta_1^{-1}$, $q_1 = 0$ and $\mathcal{T}_{22} = -1$ so the denominator is $\mathcal{D} = 2$). Roots of the dispersion function, $\mathcal{D}(\omega, p)$, exist when

$$q_1 = \frac{i}{2\omega d} \ln \mathcal{T}_{22}.$$

Solutions of this equation can exist on lower Riemann sheets, i.e. $\operatorname{Im}(q) < 0$. Physically, if the contrast between the layers is large, so the coefficient is only slightly less than unity for much of the range $0 < p < \beta_1^{-1}$ (but $\mathcal{T}_{22} = -1$ at $p = \beta_1^{-1}$), then we would expect solutions with a small positive imaginary part to p . The solution from this pole decays slowly with range ($\operatorname{Im}(p) > 0$) as some energy is transmitted out of the waveguide, and grows exponentially with depth ($\operatorname{Im}(q_2) < 0$) below the waveguide due to this energy leakage. These are known as *leaking modes* (as opposed to the *locked modes* of Love waves). In the text we have considered a leaking mode from a single interface (the leaking Rayleigh pulse, Section 9.1.5.3). There is a considerable literature (mainly from the 1960's) concerning leaking modes in layered media, e.g. Phinney (1961), Gilbert (1964)[†], etc. and it is fairly straightforward to analyse the positions and behaviour of the leaking modes further. Nevertheless there is still some confusion about whether leaking modes are useful

[†] Gilbert, F., 1964. Propagation of transient leaking modes in a stratified elastic waveguide, *Rev. Geophys.*, **2**, 123–53.

to describe the response. For a single frequency, the solution increases exponentially with depth which seems to be physically impossible. However, the monochromatic solution is a steady state solution and the exponential growth is due to energy leaking out of the waveguide since $t = -\infty$. For the impulsive solution, this does not occur. The leaking modes are useful to describe the solution at short ranges and depths before the reverberating waves decay.

The dispersion function for P - SV waves is

$$|\mathbf{I} - \Phi \mathbf{T}_{22} \Phi \mathbf{T}_{11}| = 0$$

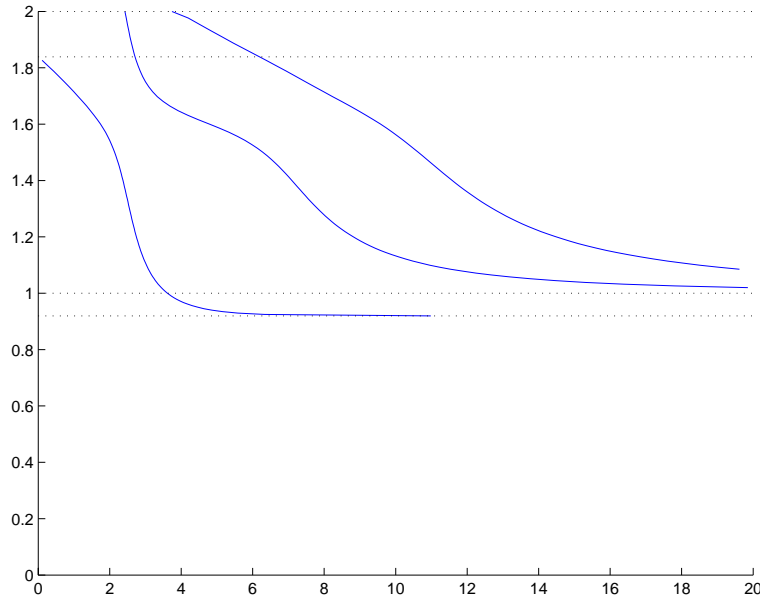
(see Exercise 7.4 for details). The 2×2 matrices \mathbf{T}_{22} and \mathbf{T}_{11} are the reflection coefficient matrices from the free surface and the interface, respectively. Although this equation is significantly more complicated than the Love wave equation, its solutions can be described intuitively.

At high frequencies the wavelengths or exponential decay distances are small. Rayleigh waves can exist on the free surface that decay rapidly with depth (see Section 9.1.5.2 for a description of Rayleigh waves, and Exercise 9.3 for a description of their depth dependence) and do not 'see' the half space. These waves will have velocity $c = \gamma_1 < \beta_1$, the Rayleigh wave velocity in the layer (see Section 9.1.5.2). At low frequencies, the wavelengths are long and the decay rates slow. A wave with the Rayleigh wave velocity of the half-space will exist ($c = \gamma_2 < \beta_2$). This wave may be oscillatory or exponential in the layer depending whether $\gamma_2 > \beta_1$ or $\gamma_2 < \beta_1$, but because the frequency is low the wave does not 'see' the layer. At intermediate frequencies we expected a *Rayleigh mode* to exist with velocities between γ_1 and γ_2 .

In addition, we expect reverberating, interference modes to exist in the layer waveguide. The phase velocities must be in the range $\beta_1 < c < \beta_2$ so the modes are locked with evanescent solutions in the half space. These are known as *shear modes* as the behaviour is mainly controlled by the shear velocities.

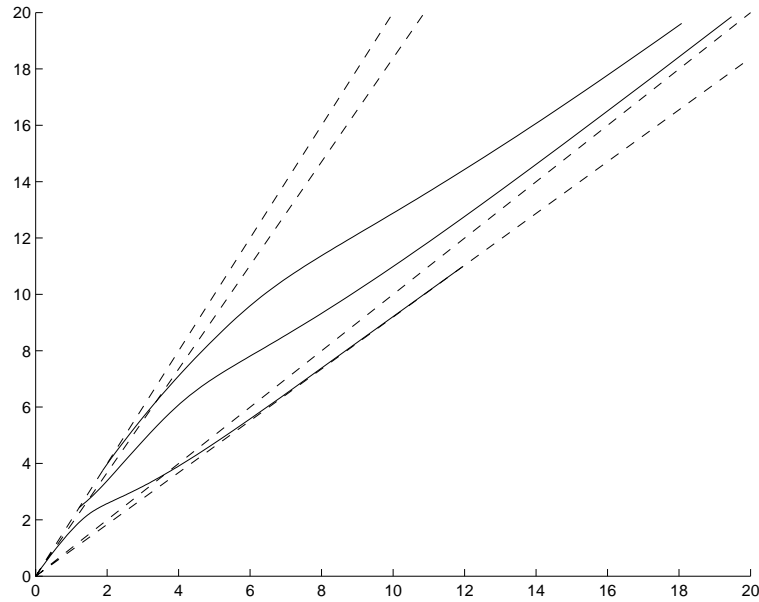
It is possible to analyse the dispersion function (e.g. Ewing, Jardetsky and Press, 1953, p. 192) but numerical solutions are not difficult. The following program and functions compute and plot these modes.

```
function Exercise84c
% Exercise 8.4
%
% Rayleigh and shear dispersion curves
%
```



The dispersion functions $c_n(\omega)$ for the Rayleigh and two shear modes in a model with a layer one unit thick, and velocities $\beta_1 = 1$, $\alpha_1 = \sqrt{3}$, $\beta_2 = 2$ and $\alpha_2 = 2\sqrt{3}$, and densities $\rho_1 = 1$ and $\rho_2 = 1.5$. The velocities $c = \beta_1, \beta_2, \gamma_1$ and γ_2 are illustrated with dotted lines.

```
% Note:
% The algorithm is slightly complicated as:
% (a) the number of roots varies for different slownesses;
% (b) the dispersion function is complex.
% Rather than find zeros of the dispersion function, we
% find minima of the modulus of ShearModeRadix, the
% dispersion function, that are at (or numerically very
% near) the origin of the complex plane.
% For a given slowness the algorithm does a crude search
% for a minimum using frequency steps dmax, and then uses
% the library function fminbnd.
% The algorithm depends on dmax being small enough, and is
% not particularly efficient.
%
global pp
global dd iso0 iso1 iso2
% model
```

The dispersion functions $\omega_n(k)$ for the Rayleigh and two shear modes in a model with a layer one unit thick, and velocities $\beta_1 = 1$, $\alpha_1 = \sqrt{3}$, $\beta_2 = 2$ and $\alpha_2 = 2\sqrt{3}$, and densities $\rho_1 = 1$ and $\rho_2 = 1.5$. The velocities $c = \beta_1, \beta_2, \gamma_1$ and γ_2 are illustrated with dashed lines.

```

beta1 = 1;
alpha1 = sqrt(3)*beta1;
beta2 = 2;
alpha2 = sqrt(3)*beta2;
rho1 = 1;
rho2 = 1.5;
dd = 1;
% frequency range
omax = 20;
nmax = 2001; % increments for root search
dmax = omax/(nmax-1);
%
gamma1 = beta1*RayleighVelocity(.25);
gamma2 = beta2*RayleighVelocity(.25);
%
iso0 = struct( 'Alpha', 0, 'Beta', 0, 'Rho', 0 );
iso1 = struct( 'Alpha', alpha1, 'Beta', beta1, 'Rho', rho1 );

```

```

iso2 = struct( 'Alpha', alpha2, 'Beta', beta2, 'Rho', rho2 );
% complete slowness range
ps = linspace( 1.0001/beta2, .9999/gamma1, 100);
% find 3 modal solutions (index ranges of defined solutions)
strt0 = length(ps)+1; strt1 = strt0; strt2 = strt0;
last0 = 0; last1 = 0; last2 = 0;
for nn=1:length(ps)
    pp = ps(nn);
    % find nmode roots
    if (1/pp > gamma2), nmode = 2;      % just shear
    elseif (1/pp < beta1), nmode = 1;   % just Rayleigh
    else, nmode = 3; end
    ms = 1;      % frequency to start search from
    ks = 0;      % index of root found
    for kk=1:nmode
        % search for minimum amplitude from ms
        for mm=ms:nmax
            omega = dmax*(mm-1);
            absradix(mm) = ShearModeRadix(omega);
            if mm < ms+2, continue, end
            % minimum condition at (mm-1)-frequency near origin
            if ( (absradix(mm) > absradix(mm-1)) && ...
                (absradix(mm-2) > absradix(mm-1)) && ...
                absradix(mm-1) < .1 ), break, end
        end
        if mm == nmax, break, end
        ms = mm;
        ks = ks+1;
        to(ks) = fminbnd( @ShearModeRadix, omega-2*dmax, omega );
    end
    % put solutions in appropriate arrays
    if nmode == 2,      % just shear modes
        if ks > 0,
            omega1(nn) = to(1);
            strt1 = min( strt1, nn ); last1 = max( last1, nn );
        end
    end
    if ks > 1,
        omega2(nn) = to(2);
        strt2 = min( strt2, nn ); last2 = max( last2, nn );
    end
end

```

```

elseif nmode == 1,                % just Rayleigh mode
    if ks > 0,
        omega0(nn) = to(1);
        strt0 = min( strt0, nn ); last0 = max( last0, nn );
    end
else,                             % all modes
    if ks > 0,
        omega0(nn) = to(1);
        strt0 = min( strt0, nn ); last0 = max( last0, nn );
    end
    if ks > 1,
        omega1(nn) = to(2);
        strt1 = min( strt1, nn ); last1 = max( last1, nn );
    end
    if ks > 2,
        omega2(nn) = to(3);
        strt2 = min( strt2, nn ); last2 = max( last2, nn );
    end
end
end
end
% plot c v. omega
figure
hold on
plot( omega0(strt0:last0), 1./ps(strt0:last0), 'b' )
plot( omega1(strt1:last1), 1./ps(strt1:last1), 'b' )
plot( omega2(strt2:last2), 1./ps(strt2:last2), 'b' )
%
axis([ 0 omax 0 beta2 ])
%
plot([ 0 omax], [beta1 beta1], 'k:')
plot([ 0 omax], [beta2 beta2], 'k:')
plot([ 0 omax], [gamma1 gamma1], 'k:')
plot([ 0 omax], [gamma2 gamma2], 'k:')
print -depsc2 exercise8_4c.eps
% plot omega v. k
k0(strt0:last0) = omega0(strt0:last0).*ps(strt0:last0);
k1(strt1:last1) = omega1(strt1:last1).*ps(strt1:last1);
k2(strt2:last2) = omega2(strt2:last2).*ps(strt2:last2);
figure
hold on

```

```

plot( k0(strt0:last0), omega0(strt0:last0), 'k' )
plot( k1(strt1:last1), omega1(strt1:last1), 'k' )
plot( k2(strt2:last2), omega2(strt2:last2), 'k' )
% plot beta1 and beta2, gamma1 and gamma2
plot([0 omax/beta2], [0 omax], 'k--')
plot([0 omax/beta1], [0 omax], 'k--')
plot([0 omax/gamma2], [0 omax], 'k--')
plot([0 omax/gamma1], [0 omax], 'k--')
axis([ 0 omax 0 omax/beta1 ])
print -depsc2 exercise8_4d.eps
%
return

function dispersion = ShearModeRadix( omega )
% ShearModeRadix = dispersion function for P-SV modes in
%                      layer waveguide

% INPUT:
%      omega      = frequency
%
% GLOBAL:
%      pp         = horizontal slowness
%      dd         = layer thickness
%      iso0       = free space properties
%      iso1       = layer properties
%      iso2       = half-space properties
%
% OUTPUT:
%      dispersion = imaginary part of dispersion function
%                  |I-Phi T_22 Phi T_11|=0

% Note: for internal use by Exercise8_4c
global pp
global dd iso0 iso1 iso2
%
Rm1 = Zoeppritz( pp, iso0, iso1 );
Rm2 = Zoeppritz( pp, iso1, iso2 );
PhiA = exp(i*omega*sqrt(1/iso1.Alpha^2-pp^2)*dd);
PhiB = exp(i*omega*sqrt(1/iso1.Beta^2 -pp^2)*dd);
Pa2 = PhiA^2;

```

```

Pb2 = PhiB^2;
Pab = PhiA*PhiB;
%
radix = (1-Rm1(4,4)*Rm2(1,1)*Pb2-Rm1(4,6)*Rm2(1,3)*Pab)*...
        (1-Rm1(4,6)*Rm2(1,3)*Pab-Rm1(6,6)*Rm2(3,3)*Pa2)-...
        (Rm1(4,4)*Rm2(1,3)*Pb2+Rm1(4,6)*Rm2(3,3)*Pab)*...
        (Rm1(4,6)*Rm2(1,1)*Pab+Rm1(6,6)*Rm2(1,3)*Pa2);
% simpler Love dispersion function for testing
%radix = 1-Rm2(2,2)*Pb2;
dispersion = abs(radix);
return

```

This program uses the function `Zoeppritz` from Exercise 6.3 to compute the reflection coefficients, and `RayleighVelocity` from Exercise 9.3 to compute the Rayleigh velocity, γ . Note the basic form of these modes is similar to the Love waves except the lowest mode is asymptotic to the Rayleigh rather than shear velocities. The dispersion curves have more ‘character’ and the ‘horizontal’ feature at an intermediate velocity is due to the existence of an interface or pseudo-interface wave (locked or leaking Stoneley wave — Section 9.1.5.3).

8.5

Show that in a fluid layer over a fluid half-space, dispersive waves exist described by very similar mathematics to the Love waves — acoustic waveguide modes. This problem has been described in the classic paper by Pekeris (1948).

If the fluid layers are replaced by solids with very low shear velocities, what happens to the acoustic modes? Their velocities are outside the range of the shear velocities. Therefore, the waves are not totally reflected at the interface and some shear energy leaks into the half-space. Hence the waves are called leaky modes. What happens to the singularities of the response? But if the shear velocities are very low, the conversion to shear energy is very small, and the leaky mode may propagate significant distances.

Further reading: A related problem is the dispersion of gravity wave waves

or tsunamis. Jeffreys and Jeffreys (1962, Section 17.09) have given the basic theory which gives rise to another Airy phase (see Exercise 8.4).

The acoustic differential system (7.1.6) is

$$\frac{d\mathbf{w}}{dz} = i\omega \begin{pmatrix} 0 & -q_\alpha^2/\rho \\ -\rho & 0 \end{pmatrix} \mathbf{w},$$

with

$$\mathbf{w} = \begin{pmatrix} v_z \\ -P \end{pmatrix}.$$

The *SH* differential system (7.1.33) is

$$\frac{d\mathbf{w}}{dz} = i\omega \begin{pmatrix} 0 & -1/\mu \\ -\mu q_\beta^2 & 0 \end{pmatrix} \mathbf{w},$$

with

$$\mathbf{w} = \begin{pmatrix} v_y \\ \sigma_{yz} \end{pmatrix}.$$

These systems are exactly equivalent provided we interchange parameters and variables. The equivalence is shown in the table. With these changes the

Acoustic	<i>SH</i>
v_z	σ_{yz}
$-P$	v_y
ρ	$1/\mu$
α	β

eigenvectors, (6.3.5) and (6.3.52) (except for the sign), reflection coefficients, (6.3.2) and (6.3.60), propagator matrices, etc. are exactly equivalent. The only differences are in source terms. Thus the results in Exercise 8.4 for Love waves can all be translated into equivalent results for acoustic waves. The model of a fluid layer over a fluid half-space was first investigated in a classic paper by Pekeris (1948) as a model for oceanic, underwater acoustic propagation — the model is now called the *Pekeris waveguide*.

In the fluid model, the acoustic modes exist between the phase velocities $\alpha_1 < c < \alpha_2$. From Exercise 8.4, an elastic model has a Rayleigh mode between $\gamma_1 < c < \gamma_2$ and shear modes between $\beta_1 < c < \beta_2$. The Rayleigh/shear modes are in a completely different velocity range from the acoustic modes if $\beta_1 < \beta_2 \ll \alpha_1 < \alpha_2$. No locked modes can exist with

phase velocity above β_2 as shear energy will propagate into the half-space. However, with the S velocities much smaller than the P velocities, the conversion between P and S waves at the interfaces is small. In the P - SV dispersion function

$$|\mathbf{I} - \Phi \mathbf{T}_{22} \Phi \mathbf{T}_{11}| = 0$$

(see Exercises 7.4 and 8.4 for details), the diagonal elements of the matrices \mathbf{T}_{22} and \mathbf{T}_{11} (the unconverted reflection coefficients) will be larger than the non-diagonal elements (the converted reflection coefficients). To first order, the equation decouples into an acoustic equation and a shear equation. Although further analysis is possible in terms of a small parameter, the ratio of the velocities β/α , it is straightforward to describe intuitively the expected behaviour. The locked, shear modes will exist as described in Exercise 8.4. The acoustic modes, with velocities between $\alpha_1 < c < \alpha_2$ and behaviour like the Love modes described in Exercise 8.4, will exist as leaking modes. The dispersion will be very similar to the purely acoustic, locked modes but the modes will decay slowly with range due to the slight leakage of shear energy into the half-space (the reflection coefficient \mathcal{T}_{33} will be complex for velocities less than α_2 as this is beyond the P critical angle, but have magnitude only slightly less than unity. The conversion transmission coefficient, \mathcal{T}_{31} will be small). Thus when the very low shear velocities are added to the model, the acoustic modes will become leaking waveguide modes with poles at slightly positive imaginary slowness.

This material for *Further reading* was written on 31 December 2004 on returning from Sri Lanka in the immediate aftermath of the Asian tsunami disaster of 26 December 2004.

In terms of a dimensionless frequency, $\Omega = \omega(d/g)^{1/2}$, where d is the water depth and g the acceleration due to gravity, and dimensionless wavenumber, $K = kd$, the dispersion relation for gravity water waves on a flat ocean is

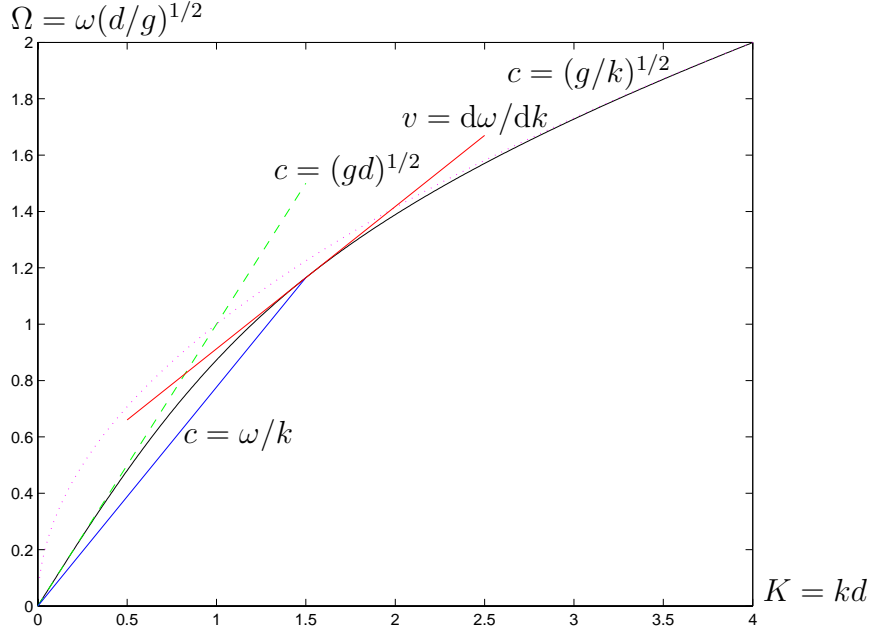
$$\Omega^2 = K \tanh K.$$

This gives dimensionless phase and group velocities of

$$\begin{aligned} C &= c(gd)^{-1/2} = \frac{\Omega}{K} = \left(\frac{\tanh K}{K} \right)^{1/2} \\ V &= v(gd)^{-1/2} = \frac{d\Omega}{dK} = \frac{\tanh K + K \operatorname{sech}^2 K}{2\Omega}, \end{aligned}$$

respectively. The dispersion curves for these functions is shown in the figures.

In fact for tsunami, we only need the long-wavelength limit, $K \ll 1$, when



The dispersion curve for gravity water waves, with the short and long wavelength limits illustrated, and the derivation of the phase c and group v velocity from this curve.

the phase and group velocities can be approximated by the quadratic term, i.e. for dimensionless velocities, these are

$$C \simeq 1 - K^2/6$$

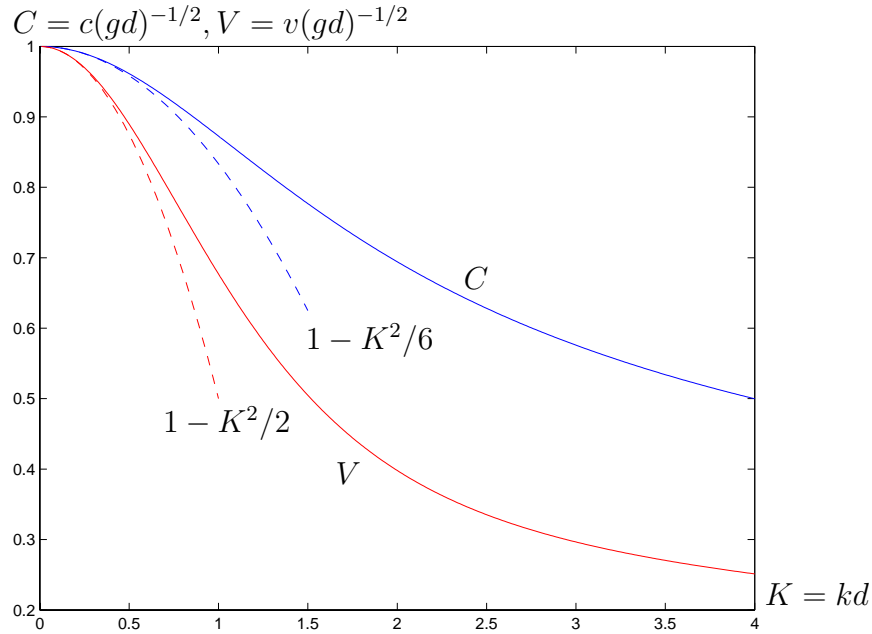
$$V \simeq 1 - K^2/2,$$

respectively. Then a wavenumber integral can be evaluated using the Airy function (D.2.9) to give the wave displacement in the form of the so-called Jeffreys phase (Bullen and Bolt, 1963, p. 465)[†]

$$\begin{aligned} u &= \int_{-\infty}^{\infty} e^{i(\Omega T - K X)} dK \simeq \int_{-\infty}^{\infty} e^{iK(T-X) - iK^3 T/6} dK \\ &= \frac{2\pi}{(T/2)^{1/3}} Ai\left(\frac{X-T}{(T/2)^{1/3}}\right), \end{aligned}$$

where $T = t(g/d)^{1/2}$ is the dimensionless time variable, and $X = x/d$ the dimensionless range. For realistic values for the propagation to Sri Lanka

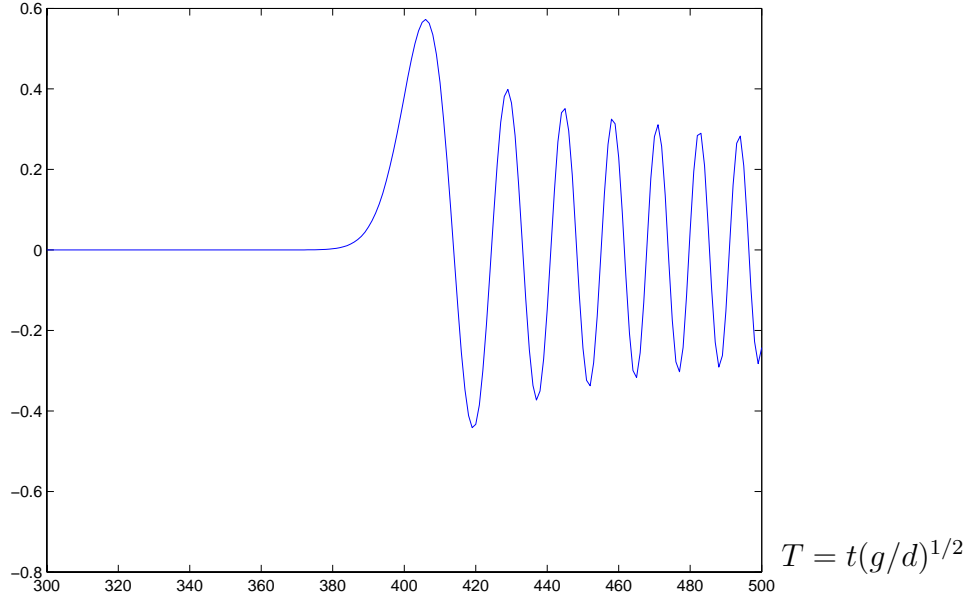
[†] Bullen, K.E. and Bolt, B.A., 1985. *An Introduction to the Theory of Seismology*, 4th edn, Cambridge: Cambridge University Press



The phase and group velocities for gravity water waves, derived from the dispersion curve in previous figure, with the long-wavelength approximations indicated.

of $d = 5$ km and $x = 2000$ km, this gives $X = 400$. The limiting phase and group velocities are $C = V = 1$ or $c = v = 220$ m/s, giving an arrival time of $T = 400$ or $t = 9000$ s = 150 mins. A dimensional time unit is 22.5 s, or 1 hour equals 160 units. The figure illustrates the Jeffreys phase at this range. The important features of the Jeffreys phase, caused by the stationarity of the velocity with respect to wavenumber and frequency, are the slow decay with range, $X^{-1/3}$, due to dispersion (this is the decay due to second-order dispersion only, i.e. one-dimensional wave propagation. Including the geometrical spreading in two dimensions, the decay rate would be increased to $X^{-5/6}$), the build up to an initial, large wave and the slow amplitude decay and decreasing periods at later times.

Although the general form of this waveform corresponds to observations in Sri Lanka, a major discrepancy exists in the period of the oscillations. A small precursor wave observed could probably be modelled easily by including a phase shift in the wavenumber integral. Periods of about 20 dimensionless units correspond to 7.5 mins, whereas observed periods were significantly longer, e.g. 45 mins. This must have been caused by the earth-



The Jeffreys phase for $X = 400$.

quake's mechanism, large magnitude ($M = 9$ on the Richter scale) and dimensions. Normally when a source propagates towards the observer, the Doppler shift increases the frequency (decreases the pulse width), e.g. for a seismic waveforms. But the rupture velocity is supersonic with respect to the tsunami velocity (2000 m/s compared with 220 m/s), so the effect is different. Effectively an observer in Sri Lanka, in the direction of the rupture propagation, sees tsunami waves from the last point of rupture (the nearest point) first, and from the first point of rupture (the furthest point) last. In fact the rupture velocity is so high (as it is in rock), about ten times the tsunami velocity, that the direction of rupture relative to the observation point is not very important. The tsunami from the nearest point of rupture always arrives first, and from the furthest last. For simple numerical calculations, we can assume that all the rupture occurs instantaneously, i.e. an infinite rupture velocity. The pulse can be broadened by the interference of waves generated all along the rupture. This can be simulated by integrating the Jeffreys phase

$$u = \frac{2\pi}{(T/2)^{1/3}} \int w(x) Ai\left(\frac{x-T}{(T/2)^{1/3}}\right) dx,$$

where $w(x)$ is a weighting function indicating the source strength along the rupture. Numerical experiments show that the resultant waveforms are very sensitive to the width and form of this weighting function. Trials have been made with triangular and boxcar weights of various widths. If the weighting function is narrow (a few dimensionless units) the wave shape is close to the Jeffreys phase, of course. With a greater width (say 20 units), the main change is that waves from the two ends of the rupture of slightly different frequencies (because the frequencies in the Jeffreys phase increase with propagation time), interfere and cause beats and a more rapid decay. For long source widths (40 units and greater), the wave begins to have approximately the form of the weighting function with reduced later oscillations (for large integration lengths, the Airy function in the above integral looks more like a Dirac delta function). In reality, it is unlikely that the high-frequency oscillations in the interference beats will propagate coherently due to spatial variations of the source and ocean. If these oscillations are removed, the remaining long-period oscillations from the amplitude of the beats begin to approximate the observations better. Although these numerical simulations are instructive, further numerical experiments with such a simple model seem pointless given the sensitivity of the final waveform to the source weighting function, and the undoubted complexity of such a large earthquake. The varying water depth of the actual ocean will cause further dispersion and focusing of energy. Full numerical simulations for realistic models of tsunami propagation are calculated routinely.

8.6

The two-dimensional Cagniard result (8.1.31) of the far-field approximation for the three-dimensional result (8.2.68) contains singularities. Discuss how the calculations should be performed so they are numerically robust to aliasing problems (cf. the WKBJ seismogram method, Section 8.4.2 — or perform the convolution with the impulse, $\lambda(t)$, in a manner that does not suffer from aliasing problems).

The results of the integrals in the exact, three-dimensional Cagniard method

(8.2.17) and (8.2.59) are not singular, but the integrand has singularities. Discuss numerical methods for evaluating these integrals.

The general expression for the two-dimensional Cagniard response (8.1.31)

$$\underline{\mathbf{u}}_{\text{ray}}(t, \mathbf{x}_R) = -\frac{1}{\pi} \text{Im} \left(\underline{\mathbf{g}}_{\text{ray}}(p) \frac{\partial p}{\partial \tilde{T}_{\text{ray}}} \right)_{p=p(t, \mathbf{x}_R)},$$

contains a singularity at the geometrical arrival time, T_{ray} , where

$$\frac{\partial \tilde{T}_{\text{ray}}}{\partial p} = 0.$$

If the expression is evaluated numerically with a discrete sampling interval of Δt , then the results will be aliased (and unstable if a numerical sample $t_0 + n\Delta t$ happens to correspond to the geometrical arrival time within the numerical rounding error). A solution is to apply the smoothing algorithm used for the WKB seismogram (Section 8.4.2).

Applying the boxcar filter, $B(t/\Delta t)/\Delta t$ (8.4.13), to both sides of the exact response, we obtain

$$\underline{\mathbf{u}}_{\text{ray}}(t, \mathbf{x}_R) = -\frac{1}{2\pi\Delta t} \text{Im} \int_{p(t-\Delta t, \mathbf{x}_R)}^{p(t+\Delta t, \mathbf{x}_R)} \underline{\mathbf{g}}_{\text{ray}}(p) dp.$$

The p integration follows the Cagniard contour but can be distorted to straight segments between the points $p = p(t_0 + n\Delta t, \mathbf{x}_R)$. Provided the function $\underline{\mathbf{g}}_{\text{ray}}$ is varying slowly, the interval integrals can often be approximated by

$$\underline{\mathbf{u}}_{\text{ray}}(t, \mathbf{x}_R) \simeq -\frac{1}{2\pi\Delta t} \text{Im} \left(\underline{\mathbf{g}}_{\text{ray}}(p(t, \mathbf{x}_R)) \Delta p \right),$$

where

$$\Delta p = p(t + \Delta t, \mathbf{x}_R) - p(t - \Delta t, \mathbf{x}_R),$$

or more accurately

$$\begin{aligned} \underline{\mathbf{u}}_{\text{ray}}(t, \mathbf{x}_R) \simeq & -\frac{1}{4\pi\Delta t} \text{Im} \left(\left(\underline{\mathbf{g}}_{\text{ray}}(p(t - \Delta t, \mathbf{x}_R)) + \underline{\mathbf{g}}_{\text{ray}}(p(t, \mathbf{x}_R)) \right) \Delta p_- \right. \\ & \left. + \left(\underline{\mathbf{g}}_{\text{ray}}(p(t, \mathbf{x}_R)) + \underline{\mathbf{g}}_{\text{ray}}(p(t + \Delta t, \mathbf{x}_R)) \right) \Delta p_+ \right), \end{aligned}$$

where

$$\begin{aligned} \Delta p_- &= p(t, \mathbf{x}_R) - p(t - \Delta t, \mathbf{x}_R) \\ \Delta p_+ &= p(t + \Delta t, \mathbf{x}_R) - p(t, \mathbf{x}_R). \end{aligned}$$

Again, provided the intervals are small enough that the function $\underline{\mathbf{g}}_{\text{ray}}$ can be treated as constant or linearly varying, it is not necessary to determine the saddle point, p_{ray} , accurately nor to end intervals containing the geometrical arrival exactly at the saddle point.

The most significant variation of the function $\underline{\mathbf{g}}_{\text{ray}}$ on the contour is usually at branch points giving rise to head waves. In order to obtain numerically accurate results, it is sensible to sub-divide the interval containing t_{head} at p_{head} and evaluate the p integral using the known square root behaviour, e.g.

$$\int_{p_{\text{head}}}^{p(t, \mathbf{x}_R)} g(p) (p - p_{\text{head}})^{1/2} dp \simeq \frac{2}{3} g(p_{\text{head}}) (p(t, \mathbf{x}_R) - p_{\text{head}})^{3/2}.$$

The numerical evaluation of the far-field approximation for the general three-dimensional Cagniard response (8.2.68)

$$\underline{\mathbf{u}}_{\text{ray}}(t, \mathbf{x}_R) \simeq - \frac{1}{\pi^2 (2x_R)^{1/2}} \frac{d}{dt} \lambda(t) * \text{Im} \left(p^{1/2} \underline{\mathbf{g}}_{\text{ray}}(p) \frac{\partial p}{\partial \tilde{T}_{\text{ray}}} \right)_{p=p_{\text{ray}}(t, \mathbf{x}_R)}$$

contains similar problems to the two-dimensional Cagniard result (8.1.31). If a band-limited version of the final term is evaluated as above, the convolution with the operator $d\lambda(t)/dt$ can be performed in the frequency domain, using a rational approximation for the operator as given by Chapman, Chu Jen-Yi and Lyness (1988), or using a numerical robust evaluation of the convolution integral. The frequency domain approach is usually preferred when realistic source and receiver functions are included, which will have band-limited spectra. The numerical issues are just the standard ones encountered approximating Fourier integrals by Fourier series (using a FFT). The rational approximation is efficient and robust, but introduces extra smoothing in the operator (three times the boxcar filter), and is not accurate at very long times/low frequencies. In the numerical evaluation of the convolution, two inverse square root singularities are encountered: from the geometrical arrival and from the function $\lambda(t)$. The convolution integral (3.1.17) can be written

$$\int_T^t \frac{f(t')}{(t' - T)^{1/2} (t - t')^{1/2}} dt' = \int_{-\pi/2}^{\pi/2} f \left(\frac{t+T}{2} - \frac{t-T}{2} \sin \chi \right) d\chi,$$

using the change of variable

$$\sin \chi = \frac{2t' - t - T}{t - T}.$$

As $f(t)$ is a non-singular function, this integral is easily evaluated numerically (even though the χ sampling may be non-uniform). More simply, the

singularities can be evaluated separately, e.g.

$$\int_T \frac{f(t')}{(t' - T)^{1/2}(t - t')^{1/2}} dt' = 2 \int_0 \frac{f(T + y^2)}{(t - T - y^2)^{1/2}} dy,$$

with the change of variable $t' = T + y^2$ for the lower singularity, and similarly $t' = t - y^2$ at the upper singularity, but this does not work well for the first motion.

Finally we consider the exact, three-dimensional Cagniard result (8.2.59)

$$\begin{aligned} u(t, \mathbf{x}_R) &= \frac{1}{\pi^2} \frac{d}{dt} \operatorname{Im} \int_C \mathcal{G}(p) p^{m+1} \frac{((t - \tau(p, z))/px)^m}{\sqrt{(t - \tau(p, z))^2 - p^2 x^2}} dp \\ &= \frac{1}{\pi^2} \frac{d}{dt} \int_0^t \operatorname{Im} \left(\mathcal{G}(p) p^{m+1} \frac{(1 + (t - \tilde{T})/px)^m}{\sqrt{(t - \tilde{T})(t - \tilde{T} + 2px)}} \frac{\partial p}{\partial \tilde{T}} \right) d\tilde{T} \end{aligned}$$

(simplifying the notation slightly by removing subscripts). The final integral has singularities at its upper and lower limits. Changes of variables as above are necessary to evaluate the integral numerically, and for the first motion both singularities should be removed simultaneously. Alternatively, the p integral only has singularities at the upper limit, $\tilde{T} = t$, and only one change of variable is necessary. As before, the p contour can be distorted between the required time points and can be evaluated for a straight-segment contour without error. When a head wave exists, the function $\mathcal{G}(p)$ contains a branch point singularity. This is best handled by the change of variable $y = (p - p_{\text{head}})^{1/2}$ or $y = (t - t_{\text{head}})^{1/2}$ which makes the integrand polynomial. The integral with respect to \tilde{T} along the real axis has an inverse square root singularity at the geometrical arrival, which can either be handled by a change of variable to $y = (T - \tilde{T})^{1/2}$ or to the original p .

8.7

Further reading: So many variants of the Cagniard method have appeared in the literature, that it is probably confusing to study them. However a particularly elegant alternative has been published by Burridge (1968).

8.8

Further reading: The two-dimensional, real slowness inverse method (8.4.1) depends on the inverse spectral Fourier transform of $\exp(i\omega px)$ being the

Dirac delta function $\delta(t - px)$ (cf. the Radon transform (3.4.15)). With the WKB approximation the inverse slowness integral (8.4.4) is trivial to evaluate. In the text we have only developed the far-field approximation for the three-dimensional, real slowness inverse method. Chapman (1978) has shown how using the inverse spectral Fourier transform of the Bessel function, (B.4.7), an exact three-dimensional, real slowness inverse method can be developed, where the slowness integral contains a convolution with the inverse Fourier transform of the Bessel function (cf. the Radon transform (3.4.23)). Approximating the singularities of this function, we can obtain the far-field approximation where the three-dimensional result can be obtained by including some extra factors and a convolution (8.2.66) (cf. Radon transform (3.4.19) and (3.4.28)).

This has been largely covered in Section 3.4.2. In cylindrical coordinates, the inverse transforms (3.1.2), (3.3.2) and (3.3.5) give

$$\underline{\mathbf{u}}(t, \mathbf{x}) = \frac{\omega^2}{2\pi} \sum_{m=-\infty}^{\infty} e^{im\phi} \int_B e^{-i\omega t} \int_0^\infty p J_m(\omega pr) \underline{\mathbf{u}}(\omega, p, m, z) dp d\omega,$$

where $\underline{\mathbf{u}}(\omega, p, m, z)$ is the transformed response found from the solution of an ordinary differential equation (see Exercise 7.1). Taking the inverse Fourier transform first, this reduces to (cf. equation (3.4.23))

$$\underline{\mathbf{u}}(t, \mathbf{x}) = -\frac{1}{\pi} \frac{d^2}{dt^2} \int_{m=-\infty}^{\infty} \int_0^\infty \frac{(-i)^m T_m(t/pr)}{(p^2 r^2 - t^2)^{1/2}} * p \underline{\mathbf{u}}(t, p, m, z) e^{im\phi} dp,$$

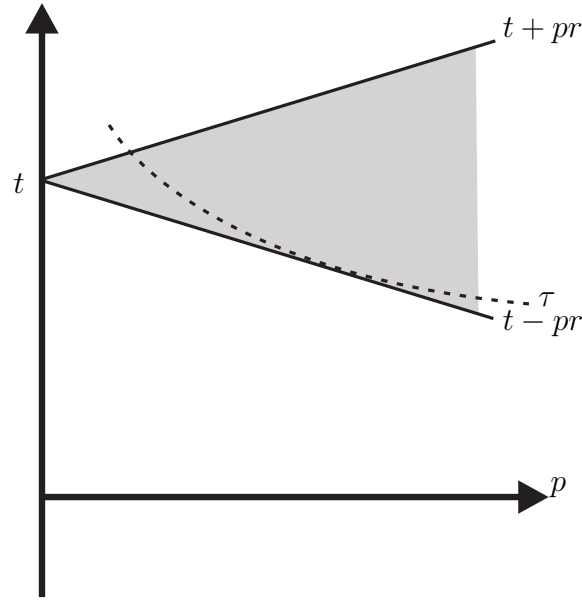
where $\underline{\mathbf{u}}(t, p, m, z)$ is the inverse Fourier transform of $\underline{\mathbf{u}}(\omega, p, m, z)$ and $*$ is a temporal convolution (3.1.18). We have used result (B.4.1) (Abramowitz and Stegun, 1965, §11.4.21). In the t - p domain, the convolution operator acts on $\underline{\mathbf{u}}(t, p, m, z)$ in a sector defined by lines $t \pm pr$. These lines and the sector are illustrated in the figure. In the far field, we use the approximation

$$\frac{(-i)^m T_m(t/pr)}{(p^2 r^2 - t^2)^{1/2}} \simeq \frac{1}{(2pr)^{1/2}} \left((+i)^m \lambda(t + pr) + (-i)^m \lambda(t - pr) \right),$$

and the contribution mainly comes from the singularity along the line $t - pr$ as it may be tangent to a singularity of the function $\underline{\mathbf{u}}(t, p, m, z)$ which typically lie along $\tau(p)$ lines (as illustrated in the figure).

8.9

Further reading: In Exercise 7.5 of Chapter 7, the spherical system was



An illustration in the t - p domain of the sector defined by the lines $t \pm pr$, over which the convolution operator from the inverse Bessel function acts on $\underline{\mathbf{u}}(t, p, m, z)$. Also illustrated with a dashed line is a typical $\tau(p)$ curve where $\underline{\mathbf{u}}(t, p, m, z)$ is singular.

discussed. Performing the inverse transforms at high frequencies is an interesting problem. The summation of modes is converted into an integral using the Watson transform (Watson, 1918). Nussenzveig (1965) has given a thorough analysis for scattering by an impenetrable sphere. In addition to the normal ray expansion at interfaces, we need the so-called rainbow or Debye expansion to expand rays that pass through the centre of the sphere. This has been used extensively in electromagnetic theory by van der Pol and Bremmer (1937a,b) and in seismology by Scholte (1956). A review is contained in Chapman and Phinney (1972). The application of the slowness method to the spherical system is discussed by Chapman (1978, 1979).

Wave propagation in media with cylindrical or spherical stratifications, i.e. when media properties are a function of the cylindrical or spherical radius, presents some interesting physical features and applied mathematical methods. These arise because the ‘horizontal’ angular coordinates are closed, i.e. 0 to π or 2π , and the innermost ‘layer’ contains the radial origin. Physically, the closed angular coordinates mean that signals can propagate around the

cylinder/sphere and pass a receiver multiple times. They can also propagate in either direction to the same receiver. Diametrically opposite the source, signals propagating in either direction arrive at similar times and interfere. In a sphere, this applies to signals propagating with any azimuth and the interesting phenomena of the Poisson spot occurs. The existence of the radial origin means that rays can turn or be ‘reflected’ without a velocity gradient or interface. Mathematically these features are handled by generalizing the ray expansion to include expansions for in- and out-going rays in all layers *including the radial origin*, and for rays with multiple paths around the cylinder or sphere. In order to handle the closed angular coordinates, the discrete transform summations are converted into integrals using the Watson transform or Poisson summation formula.

We first summarize the results in a cylindrical geometry as they are somewhat simpler than in a sphere. We consider a problem where the model properties vary with the cylindrical radius, r , and are independent of the axial variable, z , and angular variable, ϕ . The Fourier series is used to transform the equation with respect to the angular variable, ϕ , so the inverse transform is (3.3.2)

$$u(\phi) = \sum_{\ell=-\infty}^{\infty} u(\ell) e^{i\ell\phi}.$$

We use the Fourier transform with respect to the axial variable, z , so the inverse transform is (3.2.10)

$$u(z) = \frac{|\omega|}{2\pi} \int_{-\infty}^{\infty} u(q) e^{i\omega q z} dz.$$

In Exercise 7.5, we investigate the ordinary differential system with independent variable, r , that is obtained for the transformed solution, $\underline{u}(\omega, \ell, q, r)$.

The Fourier series does not converge rapidly and we convert it into an integral using the Watson transform (Watson, 1918) or equivalently (Nussenzweig, 1969a), the Poisson summation formula (Titchmarsh, 1948†, p. 60; Morse and Feshbach, 1953‡, pp. 466–7, equation (4.8.28)). This gives

$$u(\phi) = \sum_{m=-\infty}^{\infty} \int_{-\infty}^{\infty} u(\ell) e^{i\ell\phi + 2im\ell\pi} d\ell,$$

where now ℓ is a continuous variable (both methods depend on replacing the summation by a contour integral around a string of poles). Letting $\ell = \omega pr$,

† Titchmarsh, E.C., 1948. *Introduction to the Theory of Fourier Integrals*, 2nd edn, Oxford: Clarendon Press.

‡ Morse, P.M. and Feshbach, H., 1953. *Methods of Theoretical Physics*, New-York: McGraw-Hill.

we obtain

$$u(\phi) = r|\omega| \sum_{m=-\infty}^{\infty} \int_{-\infty}^{\infty} u(p) e^{i\omega pr\phi + 2im\omega pr\pi} dp,$$

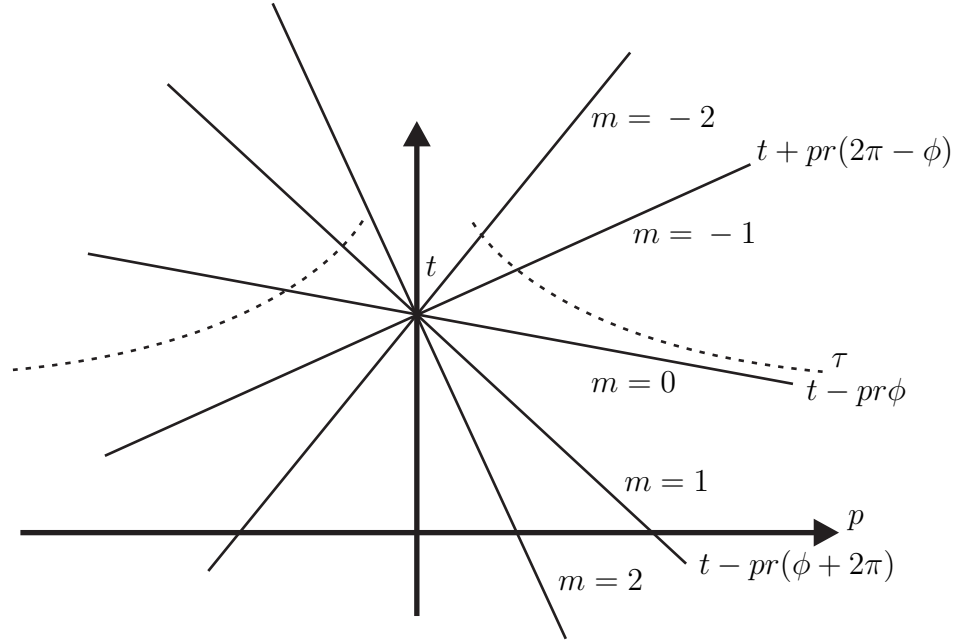
where we follow our standard notation of using the same symbol for the different transformed functions, $u(\ell)$ or $u(p)$. Teng and Richards (1969)[†] have discussed the physical significance of the various terms in this expression. Combining the inverse transforms, we have

$$\begin{aligned} \underline{\mathbf{u}}(t, \mathbf{x}) &= \frac{r\omega^2}{4\pi^2} \sum_{m=-\infty}^{\infty} \int_B \int_{-\infty}^{\infty} \\ &\quad \times e^{i\omega(pr\phi + qz + 2m\pi pr - t)} \underline{\mathbf{u}}(\omega, p, q, r) dp dq d\omega \\ &= -\frac{r}{2\pi} \frac{d^2}{dt^2} \int_{-\infty}^{\infty} \sum_{m=-\infty}^{\infty} \\ &\quad \times \delta(t - pr\phi - qz - 2m\pi pr) * \underline{\mathbf{u}}(t, p, q, r) dp dq \\ &= -\frac{r}{2\pi} \frac{d^2}{dt^2} \int_{-\infty}^{\infty} \sum_{m=-\infty}^{\infty} \\ &\quad \times \underline{\mathbf{u}}(t - pr(\phi + 2m\pi) - qz, p, q, r) dp dq. \end{aligned}$$

Each term in the summation is exactly as a two-dimensional Radon transform. The impulse response in the p - q domain, $\underline{\mathbf{u}}(t, p, q, r)$, is integrated over plane surfaces. This is illustrated in the figure. For simplicity we assume $q = 0$ to reduce the problem to two dimensions. This is for propagation in the toroidal, ϕ , direction around the cylindrical structure, the problem considered by Teng and Richards (1969), with no variations in the axial, z , direction.

The lines $t - pr(\phi + 2m\pi)$ are illustrated. Assuming we arrange the coordinates so $\phi < \pi$, the line with $m = 0$, $t - pr\phi$, will generate signals that have travelled the shorter distance to the receiver. Normally they will be tangent to the $\tau(p)$ curves at the earliest times. At later times, other lines will be tangent to the same curve: the line with $m = 1$, $t - pr(\phi + 2\pi)$, will generate signals that have travelled once around the cylinder, i.e. an angular distance $\phi + 2\pi$; the line with $m = -1$, $t + pr(2\pi - \phi)$, will generate signals that have propagated the opposite way round the cylinder, i.e. an angular distance $\pi < 2\pi - \phi < 2\pi$, when the line is tangent to the $\tau(p)$ curve for $p < 0$, i.e. the opposite propagation direction. As the $\tau(p)$ curves are symmetric about the p origin (although may vary in strength due to direc-

[†] Teng, T. and Richards, P.G., 1969. Diffracted P , SV and SH waves and their shadow boundary shifts, *J. Geophys. Res.*, **74**, 1537-55.

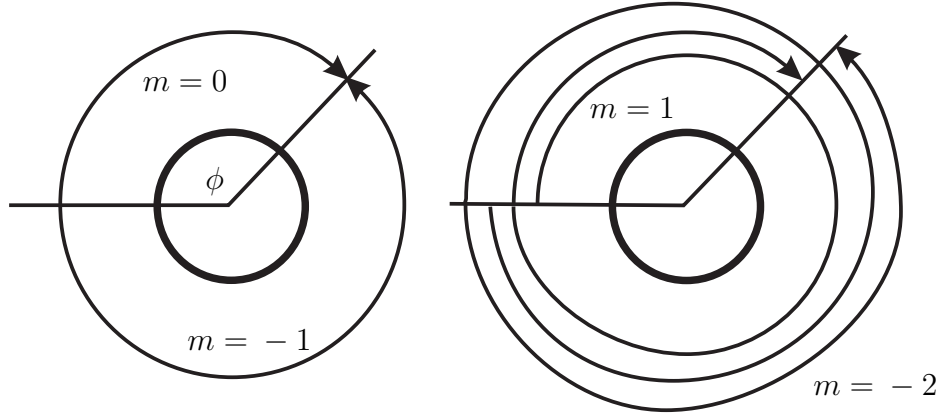


An illustration in the t - p domain of the lines $t \pm pr(\phi + 2m\pi)$ along which the function $\underline{\mathbf{u}}(t, p, 0, r)$ is integrated. Also illustrated with a dashed line is a typical $\tau(p)$ curve where $\underline{\mathbf{u}}(t, p, 0, r)$ is singular.

tional properties of the source), this arrival is normally after the signal that has propagated an angular distance ϕ and earlier than the arrival that has propagated $\phi + 2\pi$. Four terms are illustrated in the figure. If the receiver is at $\phi = \pi$, then the two arrivals will arrive simultaneously and constructively interfere (unless they differ in sign from the source directivity). If $\phi > \pi$, then the identification of the different lines with different signals changes (essentially the figure is reflected in the lines $p = 0$).

Using the slowness method, it is very straightforward to identify the physical significance of the various terms, and only include those required in computations. The equivalent spectral results are easily derived. More details can be found in Chapman (1978).

In addition to the ‘ray expansion’ in the angular direction, i.e. considering the different terms in the m summation separately, it is necessary to generalize the ray expansion in the radial direction. The complete solution must be non-singular at the origin, i.e. it must be of the form $J_\ell(\omega r/c)$ (see Exercise 7.5). However, this represents standing waves and it must be split



An illustration of the direction and angular distance propagated of signals in the cylindrical solution.

into out- and in-going waves in order to separate rays, i.e.

$$2J_\ell(\omega r/c) = H_\ell^{(1)}(\omega r/c) + H_\ell^{(2)}(\omega r/c),$$

even though the Hankel functions are singular at the origin, $r = 0$. The Hankel functions are used in the solutions at interfaces to perform the necessary ray expansions — $H_\ell^{(1)}(\omega r/c)$ is the out-going wave and $H_\ell^{(2)}(\omega r/c)$ is the in-going wave. If a turning point is needed in a layer, then a ‘reflection’ coefficient of

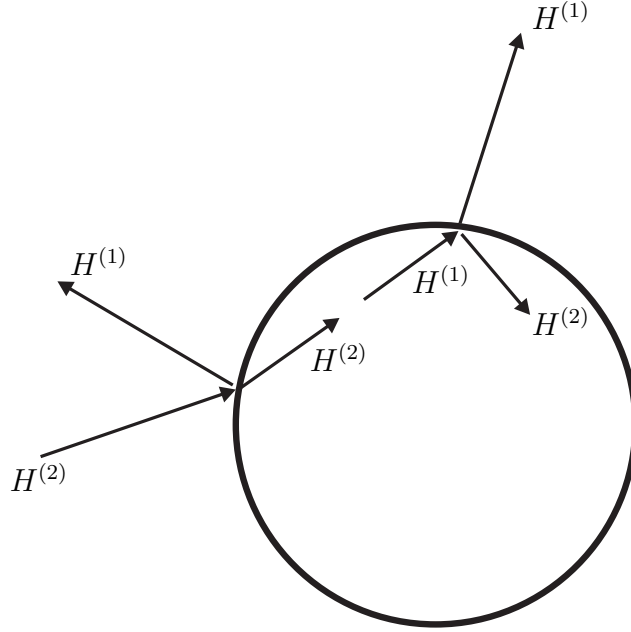
$$\mathcal{T} \sim H_\ell^{(1)}(\omega r/c) / H_\ell^{(2)}(\omega r/c),$$

is obtained. Using the asymptotic forms for the Hankel functions, this reduces to the phase integral to and from the turning point, and the phase shift of a turning point (7.2.162). This expansion is known as the *rainbow* or *Debye expansion*, and is illustrated in the figure.

In a spherically stratified model, the techniques are similar to the cylindrical model, with the complication that the Legendre transform is used in the angular coordinates (see Exercise 7.5). The inverse transform is again a summation which is converted into an integral using the Watson transform or the Poisson summation formula. The inverse transform is naturally more complicated and is a mixture of a finite length convolution operator (as in Exercise 8.8) and the repetitive series in the cylindrical geometry (as above).

The inverse Legendre transform is

$$u(\theta, \phi) = \sum_{n=0}^{\infty} \sum_{m=-n}^n \left(n + \frac{1}{2}\right) P_n^m(\cos \theta) e^{im\phi} u(n, m).$$



An illustration of the in- and out-going waves in a cylindrical model, illustrating the rainbow expansion needed in the ‘central’ layer.

If the source is located on the axis, $\theta = 0$, then the Fourier series in m only contains a few terms (as in plane layered problems using the Bessel function, equation (8.2.60)). For simplicity we take $m = 0$ in the following (an axis-symmetric problem) although the results are easily generalized. In general, it is also necessary to consider terms with the derivative of the Legendre function with respect to angle, θ .

The series in n converges slowly so, as in the cylindrical case, we convert the summation to an integral using the Watson transform or the Poisson summation formula, i.e.

$$\begin{aligned} u(\theta) &= \sum_{n=0}^{\infty} \left(n + \frac{1}{2} \right) P_n(\cos \theta) u(n) \\ &= \sum_{m=-\infty}^{\infty} (-1)^m \int_0^{\infty} u(\nu) \nu P_{\nu-1/2}(\cos \theta) e^{2im\pi\nu} d\nu, \end{aligned}$$

where $\nu = n + 1/2$ is now a continuous variable (we follow our normal convention of using the same notation for the transformed functions $u(n)$ or $u(\nu)$, although obviously they are different functions).

The Legendre functions are standing waves (as are the Bessel functions),

and in the spectral method it is convenient to split them into travelling waves (cf. the Hankel functions). As Nussenzweig (1965), we define travelling waves

$$Q_n^{(1,2)}(\cos \theta) = \frac{1}{2} \left(P_n(\cos \theta) \pm \frac{2i}{\pi} Q_n(\cos \theta) \right).$$

and expand the Legendre function into two travelling waves using

$$P_n(\cos \theta) = Q_n^{(1)}(\cos \theta) + Q_n^{(2)}(\cos \theta).$$

In the slowness method, this split is unnecessary. The physical significance of the above summations and integration are discussed by Nussenzweig (1965), Burridge (1966)[†], Ansell (1973)[‡], Gilbert (1976)[§], etc.

Substituting $\nu = \omega pr$, we obtain

$$u(\theta) = \sum_{m=-\infty}^{\infty} (-1)^m \omega^2 r^2 \int_0^{\infty} u(p) p P_{\omega pr - 1/2}(\cos \theta) e^{2im\pi\omega pr} dp.$$

The similarities with the plane layered result, e.g. Exercise 8.8, can be seen using a uniform asymptotic expansion of the Legendre function given by Szegő (1934)[¶]

$$P_{\nu-1/2}(\cos \theta) \simeq \left(\frac{\theta}{\sin \theta} \right)^{1/2} J_0(\nu\theta),$$

valid for small θ . With this substitution, apart from the summation over m , the inverse transforms are like those in the plane layered problem.

Combining the inverse transforms, we obtain the expression

$$\begin{aligned} u(t, \mathbf{x}) = & \frac{1}{2\pi} \int_B \sum_{m=-\infty}^{\infty} (-1)^m \omega^2 r^2 \int_0^{\infty} \\ & \times u(\omega, p, r) p P_{\omega pr - 1/2}(\cos \theta) e^{2im\pi\omega pr - i\omega t} dp d\omega. \end{aligned}$$

If we change the order of integration, we require the inverse Fourier transform of the Legendre function $P_{\omega pr - 1/2}(\cos \theta)$. This is given by the Mehler-Dirichlet integral formula (Dirichlet, 1837^{||}; Mehler, 1872^{††}, Whittaker and

[†] Burridge, R., 1966. The Legendre functions of the second kind with complex argument in the theory of wave propagation, *J. Meth. Phys.*, **45**, 322–30.

[‡] Ansell, J.H., 1973. Legendre functions, the Hilbert transform and surface waves on a sphere, *Geophys. J.R. astr. Soc.*, **32**, 95–117.

[§] Gilbert, F., 1976. The representation of seismic displacements in terms of travelling waves, *Geophys. J.R. astr. Soc.*, **44**, 275–80.

[¶] Szegő, Von G., 1934. Über Einige Asymptotische Entwicklungen der Legendreschen Funktionen, *Proc. Lond. math. Soc., Ser. 2*, **36**, 427–50.

^{||} Dirichlet, G.L. 1837. Sur les séries dont le terme général dépend de deux angles, et qui servent à exprimer des fonctions arbitraires entre des limites données, *J. reine angew. Math.*, **54**, 33–56.

^{††} Mehler, Von F.G., 1872. Notiz über die Dirichlet'schen Integralausdrücke für die Kugelfunction $P^n(\cos \theta)$ und über eine analoge Integralform für die Cylinderfunction $J(x)$, *Math. Ann.*, **5**, 141–4.

Watson, 1963^{††}, p. 315; and Erdélyi, Magnus, Oberhettinger and Tricomi, 1953^{§§}, equation (3.7 (27)))

$$P_{\omega-1/2}^{\mu}(\cos \theta) = \left(\frac{2}{\pi}\right)^{1/2} \frac{(\sin \theta)^{\mu}}{\Gamma(1/2 - \mu)} \int_0^{\theta} \frac{\cos(\omega t) dt}{(\cos t - \cos \theta)^{\mu+1/2}},$$

valid for $\text{Re}(\mu) < 1/2$. Thus inverse Fourier transform of $P_{\omega-1/2}(\cos \theta)$ is

$$P_{\omega-1/2}(\cos \theta) \rightarrow \frac{2^{1/2} B(t/\theta)}{\pi(\cos t - \cos \theta)^{1/2}},$$

where the normalized boxcar has been defined in equation (8.4.13). Applying this to the above inverse transforms, we obtain

$$\begin{aligned} u(t, \mathbf{x}) = & -\frac{2^{1/2} r}{\pi} \frac{d^2}{dt^2} \sum_{m=-\infty}^{\infty} (-1)^m \int_0^{\infty} \\ & \times \frac{B\left((t/pr - 2m\pi)/\theta\right)}{\left(\cos(t/pr - 2m\pi) - \cos \theta\right)^{1/2}} * u(t, p, r) dp. \end{aligned}$$

The temporal convolution with the impulse response, $u(t, p, r)$, is over bands defined by the lines $t - 2m\pi pr \pm \theta pr$. Each band is like the convolution with the inverse Fourier transform of $J_m(\omega pr)$ in Exercise 8.8 for the plane layered problem, and the repeated bands for different m are like the repeated lines in the cylindrical problem in this exercise (particularly if the negative p values are folded into the positive p values making the integral one-sided). The bands are illustrated in the figure.

More details can be found in Chapman (1978, 1979). Of particular interest are the Hilbert transforms that occur whenever a signal passes through $\theta = 0$ or π , and the interference and combination of two singularities that occur when $\theta \rightarrow \pi$, i.e. the Poisson spot phenomena.

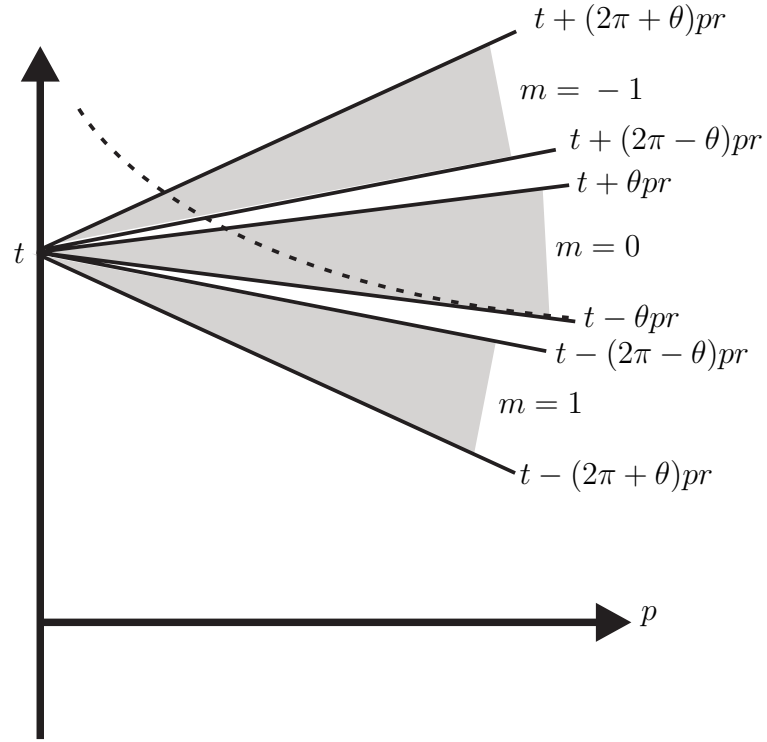
Finally we note that the rainrow or Debye expansion are also used to generalize the ray expansion, with the expansion

$$2j_n(\omega r/c) = h_n^{(1)}(\omega r/c) + h_n^{(2)}(\omega r/c),$$

to decompose the spherical Bessel function into travelling waves.

^{††} Whittaker, E.T. and Watson, G.N., 1963. *A Course in Modern Analysis*, Cambridge: Cambridge University Press.

^{§§} Erdélyi, A., Magnus, W., Oberhettinger, F. and Tricomi, F.G., 1953. *Higher Transcendental Functions, Vol I*, New York: McGraw-Hill.



An illustration in the t - p domain of the sectors defined by the lines $t \pm \theta pr - 2m\pi pr$, over which the convolution operator from the inverse Legendre function acts on $\underline{\mathbf{u}}(t, p, r)$. Also illustrated with a dashed line is a typical $\tau(p)$ curve where $\underline{\mathbf{u}}(t, p, r)$ is singular.

9

Canonical signals

9.1

Head waves can exist on reflected or transmitted waves, with velocities from either side of the interface. There are four kinds of head waves: (1) a reflected wave with velocity from the transmitted medium; (2) a transmitted wave with velocity from the transmitted medium; (3) a transmitted wave with velocity from the incident medium; and (4), a reflected wave with velocity from the incident medium. Which head waves exists depends on the incident wave type, and the arrangement of the velocities. There are six cases for the velocities. In the following table, the six cases are listed together with the number of head waves possible for the two incident rays (in the first medium). Confirm these figures, identifying the kind and the ray notation of the possible head waves.

<i>Case</i>	<i>Velocities</i>	<i>P</i>	<i>S</i>
1	$\alpha_2 > \beta_2 > \alpha_1 > \beta_1$	5	6
2	$\alpha_2 > \alpha_1 > \beta_2 > \beta_1$	3	6
3	$\alpha_2 > \alpha_1 > \beta_1 > \beta_2$	3	5
4	$\alpha_1 > \alpha_2 > \beta_2 > \beta_1$	0	6
5	$\alpha_1 > \alpha_2 > \beta_1 > \beta_2$	0	5
6	$\alpha_1 > \beta_1 > \alpha_2 > \beta_2$	0	3

A head wave can exist for any wave type with velocity greater than the incident and generated wave types. Ordering the head waves by decreasing head-wave velocity and decreasing generated-wave velocity (where the latter varies first so head waves with the same velocity are grouped together), the possible head waves are:

Case 1, P source: $P_1p_2S_2, P_1p_2P_1, P_1p_2S_1, P_1s_2P_1, P_1s_2S_1$;
Case 1, S source: $S_1p_2S_2, S_1p_2P_1, S_1p_2S_1, S_1s_2P_1, S_1s_2S_1, S_1p_1S_1$;
Case 2, P source: $P_1p_2P_1, P_1p_2S_2, P_1p_2S_1$;
Case 2, S source: $S_1p_2P_1, S_1p_2S_2, S_1p_2S_1, S_1p_1S_2, S_1p_1S_1, S_1s_2S_1$;
Case 3, P source: $P_1p_2P_1, P_1p_2S_1, P_1p_2S_2$;
Case 3, S source: $S_1p_2P_1, S_1p_2S_1, S_1p_2S_2, S_1p_1S_1, S_1p_1S_2$;
Case 4, P source: none;
Case 4, S source: $S_1p_1P_2, S_1p_1S_2, S_1p_1S_1, S_1p_2S_2, S_1p_2S_1, S_1s_2S_1$;
Case 5, P source: none;
Case 5, S source: $S_1p_1P_2, S_1p_1S_1, S_1p_1S_2, S_1p_2S_1, S_1p_2S_2$;
Case 6, P source: none;
Case 6, S source: $S_1p_1S_1, S_1p_1P_2, S_1p_1S_2$.

9.2

The first-motion approximation is based on first-order Taylor expansions about the geometrical arrival. Investigate the second-order terms for a point source in a homogeneous medium, and compare the results with the exact result. Do the second-order terms always improve the approximation?

The spectral result corresponding to (8.2.14) is

$$\mathbf{u}(\omega, \mathbf{x}) = \frac{VP(\omega)\omega^2}{4\pi\rho\alpha^2} \int_0^\infty \frac{p}{q} \begin{pmatrix} ipJ_1(\omega px) \\ \pm q_\alpha J_0(\omega px) \end{pmatrix} e^{i\omega\tau} dp,$$

simplifying the notation somewhat. A saddle point exists where

$$\begin{aligned} p &= \frac{\sin \theta}{\alpha} \\ q &= \frac{\cos \theta}{\alpha}. \end{aligned}$$

It is straightforward to evaluate the integral by the second-order saddle-point method (Appendix D.1), to give the first-motion approximation, but surprisingly tedious to find the next terms.

For the Bessel functions we only need

$$\begin{aligned} J_0(z) &\simeq \frac{1}{\sqrt{2\pi z}} \left(1 + \frac{1}{8iz}\right) e^{iz - i\pi/4} \\ J_1(z) &\simeq \frac{1}{\sqrt{2\pi z}} \left(1 - \frac{3}{8iz}\right) e^{iz - 3i\pi/4} \end{aligned}$$

(Abramowitz and Stegun, 1965, §9.2.5). We then need a second-order Taylor expansion about the saddle point, i.e.

$$\begin{aligned}
 pJ_0(\omega px) &\simeq \left(\frac{p}{2\pi\omega x}\right)^{1/2} \left(1 + \frac{1}{8i\omega px}\right) e^{i\omega px - i\pi/4} \\
 &= \frac{1}{(2\pi\omega R \sin \theta)^{1/2}} \left(a_0 + b_0 \delta p + \frac{1}{2}c_0 \delta p^2\right) \\
 &\quad \times e^{i\omega R \sin^2 \theta / \alpha - i\pi/4} \\
 \frac{p^2}{q} J_1(\omega px) &\simeq \left(\frac{p^3}{2\pi\omega x q}\right)^{1/2} \left(1 - \frac{3}{8i\omega px}\right) e^{i\omega px - 3i\pi/4} \\
 &= \frac{1}{(2\pi\omega R \sin \theta)^{1/2}} \left(a_1 + b_1 \delta p + \frac{1}{2}c_1 \delta p^2\right) \\
 &\quad \times e^{i\omega R \sin^2 \theta / \alpha - 3i\pi/4},
 \end{aligned}$$

where

$$\delta p = p - \frac{\sin \theta}{\alpha}.$$

The coefficients are

$$\begin{aligned}
 a_0 &= \left(\frac{\sin \theta}{\alpha}\right)^{1/2} \left(1 + \frac{\alpha}{8i\omega R \sin^2 \theta}\right) \\
 b_0 &= \frac{1}{2} \left(\frac{\alpha}{\sin \theta}\right)^{1/2} \\
 c_0 &= -\frac{1}{4} \left(\frac{\alpha}{\sin \theta}\right)^{3/2},
 \end{aligned}$$

and

$$\begin{aligned}
 a_1 &= \frac{\sin^{3/2} \theta}{\alpha^{1/2} \cos \theta} \left(1 - \frac{3\alpha}{8i\omega R \sin^2 \theta}\right) \\
 b_1 &= \frac{1}{2} \frac{\alpha^{1/2} \sin^{1/2} \theta}{\cos \theta} (3 + 2 \tan^2 \theta) \\
 c_1 &= \frac{1}{4} \frac{\alpha^{3/2}}{\sin^{1/2} \theta \cos \theta} (3 + 16 \tan^2 \theta + 12 \tan^4 \theta),
 \end{aligned}$$

where we have only retained the terms needed.

For the phase function $\tau = qd$, we need terms up to the fourth derivative at the saddle point

$$\begin{aligned}
 \tau &= qd = R \cos^2 \theta / \alpha \\
 \tau' &= -pd/q = R \sin \theta \\
 \tau'' &= -d/\alpha^2 q^3 = -\alpha R / \cos^2 \theta
 \end{aligned}$$

$$\begin{aligned}\tau''' &= -3pd/\alpha^2 q^5 = -3\alpha^2 R \sin \theta / \cos^4 \theta \\ \tau'''' &= -3d/\alpha^2 q^5 - 15p^2 d/\alpha^2 q^7 = -3\alpha^3 R (1 + 5 \tan^2 \theta) / \cos^4 \theta.\end{aligned}$$

Thus

$$\begin{aligned}e^{i\omega\tau} &\simeq \exp\left(\frac{i\omega R \cos^2 \theta}{\alpha} - \frac{i\omega\alpha R}{2\cos^2 \theta} \delta p^2 + B\delta p^3 + C\delta p^4\right) \\ &\simeq \exp\left(\frac{i\omega R \cos^2 \theta}{\alpha} - \frac{i\omega\alpha R}{2\cos^2 \theta} \delta p^2\right) \\ &\quad \times (A + B\delta p^3 + C\delta p^4 + D\delta p^6),\end{aligned}$$

where

$$\begin{aligned}A &= 1 \\ B &= -i\omega \frac{\alpha^2 R \sin \theta}{2\cos^4 \theta} \\ C &= -i\omega \frac{\alpha^3 R \sin \theta}{8\cos^4 \theta} (1 + 5 \tan^2 \theta) \\ D &= \frac{1}{2}B^2 = -\omega^2 \frac{\alpha^4 R^2 \sin^2 \theta}{8\cos^8 \theta}.\end{aligned}$$

Finally we require the saddle-integrals

$$I_n = \int_{-\infty}^{\infty} x^n e^{-iax^2} dx.$$

Integrating by parts it is easily shown that

$$I_{n+2} = \left(\frac{n+1}{2ia}\right) I_n,$$

where

$$I_0 = \sqrt{\frac{\pi}{a}} e^{-i\pi/4},$$

is known (D.1.11) (assuming $a > 0$). With n odd, $I_n = 0$ by the anti-symmetry. The other required, non-zero integrals are

$$\begin{aligned}I_2 &= \frac{\pi^{1/2}}{2a^{3/2}} e^{-3i\pi/4} \\ I_4 &= -\frac{3\pi^{1/2}}{4a^{5/2}} e^{-i\pi/4} \\ I_6 &= -\frac{15\pi^{1/2}}{8a^{7/2}} e^{-3i\pi/4}.\end{aligned}$$

For the u_z integral: the terms a_0 , A and the integral I_0 give

$$-\frac{i \cos \theta}{\alpha \omega R} - \frac{\cos \theta}{8 \omega^2 R^2 \sin^2 \theta};$$

the terms c_0 , A and the integral I_2 give

$$\frac{\cos^3 \theta}{8 \omega^2 R^2 \sin^2 \theta};$$

the terms b_0 , B and the integral I_4 give

$$\frac{3 \cos \theta}{4 \omega^2 R^2};$$

the terms a_0 , C and the integral I_4 give

$$\frac{3(1 + 5 \tan^2 \theta) \cos \theta}{8 \omega^2 R^2};$$

and the terms a_0 , D and the integral I_6 give

$$-\frac{15 \sin^2 \theta}{8 \omega^2 R^2 \cos \theta}.$$

All other terms give odd integrals I_n or are of order ω^{-m} with $m > 2$. Combining all the terms we have

$$-\frac{i \cos \theta}{\alpha \omega R} + \frac{\cos \theta}{\omega^2 R^2}.$$

Similarly for the u_x integral: the terms a_1 , A and the integral I_0 give

$$-\frac{i \sin \theta}{\alpha \omega R} + \frac{3}{8 \omega^2 R^2 \sin \theta};$$

the terms c_1 , A and the integral I_2 give

$$-\frac{3 \cos^4 \theta + 16 \sin^2 \theta \cos^2 \theta + 12 \sin^4 \theta}{8 \omega^2 R^2 \sin \theta \cos^2 \theta};$$

the terms b_1 , B and the integral I_4 give

$$\frac{(9 \cos^2 \theta + 6 \sin^2 \theta) \sin \theta}{4 \omega^2 R^2 \cos^2 \theta};$$

the terms a_1 , C and the integral I_4 give

$$\frac{3(1 + 5 \tan^2 \theta) \sin \theta}{8 \omega^2 R^2};$$

and the terms a_1 , D and the integral I_6 give

$$-\frac{15 \sin^3 \theta}{8 \omega^2 R^2 \cos^2 \theta}.$$

All other terms give odd integrals I_n or are of order ω^{-m} with $m > 2$. Combining all the terms we have

$$-\frac{i \sin \theta}{\alpha \omega R} + \frac{\sin \theta}{\omega^2 R^2}.$$

Combining with the factor outside the spectral integral, we have

$$\mathbf{u}(\omega, \mathbf{x}) = \frac{VP(\omega)}{4\pi\rho\alpha^3 R} \begin{pmatrix} \sin \theta \\ \pm \cos \theta \end{pmatrix} \begin{pmatrix} -i\omega + \frac{\alpha}{R} \end{pmatrix} e^{i\omega R/\alpha},$$

which agrees exactly with result (8.2.70).

The evaluation of the second term, which is of order ω^{-1} compared with the first term, using higher-order, saddle-point methods, is equivalent to the next term in a Taylor expansion about the geometrical arrival in the time domain. In general, the Taylor expansion will not terminate — reflections, etc. will not just be a step and a ramp as the coefficients will vary. Normally the next term in the expansion will improve the approximation, except when the first term is singular. The expansion may have limited validity if the saddle point is near to another singularity, e.g. a branch point or pole.

9.3

Show that at a fixed frequency (e.g. in the spectral domain), the particle motion of a Rayleigh wave is an ellipse. Show that at the free surface it is a retrograde ellipse but that at depth it changes from retrograde to prograde (and at some depth it is vertical). Show that at the free surface the ratio of vertical to horizontal displacement varies from $|u_z/u_x| = 1.83924$ for Poisson's ratio $\nu = 1/2$, to 1.27201 for Poisson's ratio $\nu = 0$.

The spectral result for an interface wave is given by (9.3.22)

$$\underline{\mathbf{u}}_{\text{ray}}(\omega, \mathbf{x}_R) \simeq \frac{i\omega}{\pi} \left(\frac{p_{\text{pole}}}{2x_R} \right)^{1/2} \frac{\tilde{\underline{\mathbf{g}}}_{\text{pole}}(p_{\text{pole}})}{g'(p_{\text{pole}})} e^{i\omega \tilde{T}_{\text{ray}}(p_{\text{pole}}, \mathbf{x}_R)},$$

where $\tilde{\underline{\mathbf{g}}}_{\text{pole}}$ is defined in equation (9.3.21)

$$\underline{\mathbf{g}}_{\text{ray}}(p) \simeq \frac{\tilde{\underline{\mathbf{g}}}_{\text{pole}}(p_{\text{pole}})}{g'(p_{\text{pole}})(p - p_{\text{pole}})}.$$

For a homogeneous half-space, the function $\underline{\mathbf{g}}_{\text{ray}}$ will contain a factor

$$\underline{\mathbf{g}}_P e^{i\omega q_\alpha z_R} + \mathcal{T}_{66} \underline{\mathbf{g}}_P e^{-i\omega q_\alpha z_R} + \mathcal{T}_{46} \underline{\mathbf{g}}_S e^{-i\omega q_\beta z_R},$$

for the source P wave, and

$$\dot{\mathbf{g}}_V e^{i\omega q_\beta z_R} + \mathcal{T}_{64} \dot{\mathbf{g}}_P e^{-i\omega q_\alpha z_R} + \mathcal{T}_{44} \dot{\mathbf{g}}_S e^{-i\omega q_\beta z_R},$$

for the source SV wave, where the free-surface reflection coefficients are given by expressions (6.4.5). These factors are combined with weightings depending on the source excitation, depth, etc. At the Rayleigh pole, the function $g(p)$ can be taken as

$$g(p) = \Delta^{PV} = 4p^2 q_\alpha q_\beta + \Omega^2$$

(definition (6.4.6), dropping the medium subscript). We have used the obvious notation for the up- and down-going, P and SV polarizations from the eigen-matrix \mathbf{W}_2 , (6.3.51) and (6.3.53). The function $\underline{\mathbf{g}}_{\text{pole}}(p_{\text{pole}})$ therefore contains a factor

$$\begin{aligned} & \frac{4p^2 q_\alpha q_\beta - \Omega^2}{(2\rho q_\alpha)^{1/2}} \begin{pmatrix} p \\ -q_\alpha \end{pmatrix} e^{\omega|q_\alpha|z_R} + \frac{4p\Omega(q_\alpha q_\beta)^{1/2}}{(2\rho q_\beta)^{1/2}} \begin{pmatrix} q_\beta \\ p \end{pmatrix} e^{\omega|q_\beta|z_R} \\ & \sim 2pq_\beta \begin{pmatrix} p \\ -q_\alpha \end{pmatrix} e^{\omega|q_\alpha|z_R} + \Omega \begin{pmatrix} q_\beta \\ p \end{pmatrix} e^{\omega|q_\beta|z_R}, \end{aligned}$$

from the P wave source, and

$$\begin{aligned} & \frac{4p\Omega(q_\alpha q_\beta)^{1/2}}{(2\rho q_\alpha)^{1/2}} \begin{pmatrix} p \\ -q_\alpha \end{pmatrix} e^{\omega|q_\alpha|z_R} - \frac{4p^2 q_\alpha q_\beta - \Omega^2}{(2\rho q_\beta)^{1/2}} \begin{pmatrix} q_\beta \\ p \end{pmatrix} e^{\omega|q_\beta|z_R} \\ & \sim \Omega \begin{pmatrix} p \\ -q_\alpha \end{pmatrix} e^{\omega|q_\alpha|z_R} - 2pq_\alpha \begin{pmatrix} q_\beta \\ p \end{pmatrix} e^{\omega|q_\beta|z_R}, \end{aligned}$$

from the SV source (dropping common factors $4p(q/2\rho)^{1/2}$, and using $g(p_{\text{pole}}) = 4p^2 q_\alpha q_\beta + \Omega^2 = 0$).

At the free surface, these expressions reduce to

$$\begin{aligned} 2pq_\beta \begin{pmatrix} p \\ -q_\alpha \end{pmatrix} + \Omega \begin{pmatrix} q_\beta \\ p \end{pmatrix} &= \frac{1}{2p\beta^2} \begin{pmatrix} 2pq_\beta \\ \Omega \end{pmatrix} \\ \Omega \begin{pmatrix} p \\ -q_\alpha \end{pmatrix} - 2pq_\alpha \begin{pmatrix} q_\beta \\ p \end{pmatrix} &= \frac{1}{2p\beta^2} \begin{pmatrix} \Omega \\ -2pq_\alpha \end{pmatrix}, \end{aligned}$$

for the P and SV sources, respectively. The ratio of the displacement components is identical in the two cases

$$\frac{u_z}{u_x} = \frac{\Omega}{2pq_\beta} = -\frac{2pq_\alpha}{\Omega} = -i \frac{2 - \gamma^2/\beta^2}{2(1 - \gamma^2/\beta^2)^{1/2}},$$

as $g(p_{\text{pole}} = 1/\gamma)$ is zero. This ratio is negative imaginary (as $\Omega < 0$). Thus the motion is a retrograde ellipse.

Using the following program we can compute this ratio for Poisson's ratio between $\nu = 0$ and $1/2$

```
function Exercise93
% Exercise 9.3

% surface ratio for Poisson ratio from 0 to 0.5
poisson = linspace(0,.5,100);
for j=1:length(poisson)
    % Rayleigh wave velocity range is 0.8740 to 0.9553
    gamma(j) = RayleighVelocity(poisson(j));
    % magnitude of u_z/u_x range is from 1.27201 to 1.83924
    uzx(j) = .5*(2-gamma(j)^2)/sqrt(1-gamma(j)^2);
end
uzx(1)
uzx(length(poisson))
figure
plot(poisson,uzx)
%
print -depsc2 exercise9_3a.eps

% depth profile for Poisson ratio of 0.25
poisson = 0.25;
beta = 1;
alpha = beta*sqrt(2*(1-poisson)/(1-2*poisson));
gamma = RayleighVelocity(poisson);
p = 1/gamma;
p2 = p^2;
iqa = sqrt(p2-1/alpha^2);
iqb = sqrt(p2-1/beta^2);
Omega = 1/beta^2-2*p2;
%
omegaz = linspace(0,6,100);
for j = 1:length(omegaz)
    % from expression for P source
    % minus imaginary part of u_x
    iux(j) = 2*p2*iqb*exp(-iqa*omegaz(j))...
        +Omega*iqb*exp(-iqb*omegaz(j));
    % real part of u_z
    ruz(j) = -2*p*iqa*iqb*exp(-iqa*omegaz(j))...
```



```

        -Omega*p*exp(-iqb*omegaz(j));
end
figure
hold on
plot(omegaz,iux,'b')
plot(omegaz,rux,'r')
plot([ omegaz(1) omegaz(length(omegaz)) ], [0 0],'k')
%
print -depsc2 exercise9_3b.eps

```

This uses the functions RayleighVelocity and RayleighRadix

```

function gamma = RayleighVelocity( Poisson )
% RayleighVelocity = normalized Rayleigh velocity

% INPUT:
%      Poisson = Poisson's ratio
%
% OUTPUT:
%      gamma    = normalized Rayleigh velocity
%                (gamma/beta)
%
% Algorithm: solve cubic (9.1.60) using fzero
global u
%
u = .5*(1-2*Poisson)/(1-Poisson);
y = fzero(@RayleighRadix,[1 1.4]);
gamma = 1/sqrt(y);
return

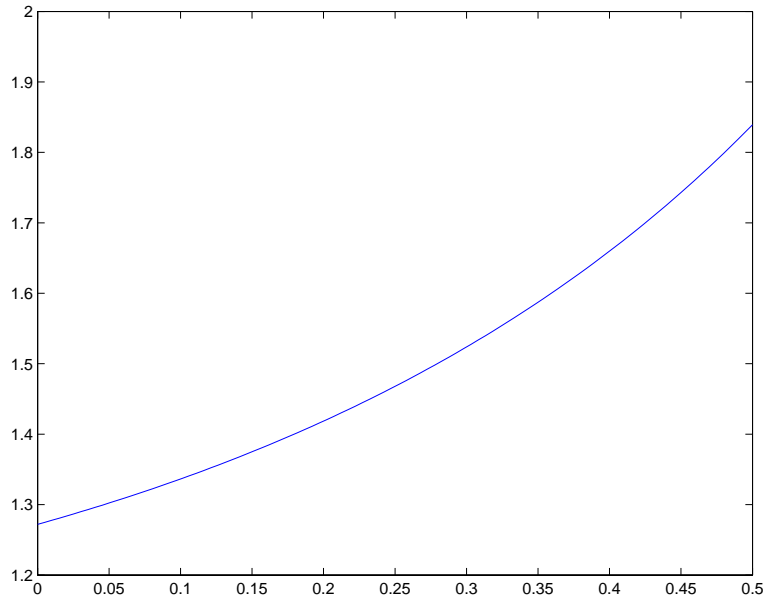
function fy = RayleighRadix( y )
% RayleighRadix = cubic for Rayleigh pole

% INPUT:
%      y        = variable  $p^2 \beta^2$ 
%
% GLOBAL:
%      u        =  $\beta^2 / \alpha^2$ 
% OUTPUT:
%      f(y)     = cubic given by equation (9.1.60)

```

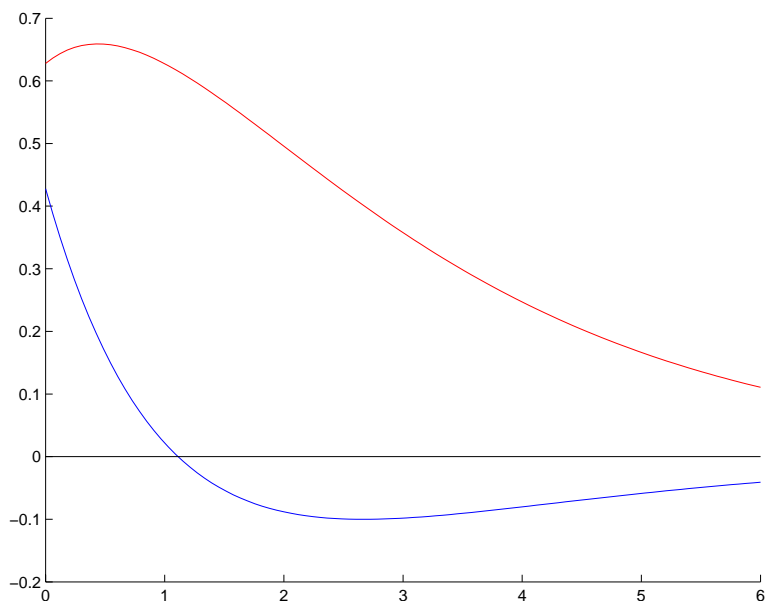
```
% Note: for internal use by RayleighVelocity
global u
%
fy = (1-u)*y^3+(u-3/2)*y^2+y/2-1/16;
return
```

and produces the plot below varying from 1.27201 to 1.83924.



A plot of the magnitude of the vertical to horizontal surface displacement for a monochromatic Rayleigh wave against Poisson's ratio.

It also produces a plot of the displacement as a function of depth for a Poisson ratio $\nu = 1/4$ (a Poisson solid). The imaginary part of u_x and minus u_z are plotted, i.e. $-i u_x$ and $-u_z$ (specifically, we have used the expressions given above for the P wave source, but it doesn't matter which is used — only the relative values are significant). Note that, of course, the displacements decay with depth due to the two negative exponentials. The horizontal displacement changes sign (as the positive P wave term decays more rapidly than the negative SV wave term) so at a certain depth (about $\omega z = -1$), the displacement is vertical, and below this the motion is prograde. This result is often discussed in textbooks but is of limited practical significance as it only applies to monochromatic Rayleigh waves. It does not



A plot of the horizontal (minus imaginary — blue) and vertical (real — red) displacements as a function of depth for a Poisson solid with unit shear velocity and frequency. The magnitude of the vertical axis is not significant.

apply to Rayleigh waves generated by an impulsive source, as discussed in the text (Section 9.1.5.2).

9.4

Further reading: The shadow results, Sections 9.3.6 and 9.3.7, have been extensively studied in a spherical Earth, where even with homogeneous layers, the spherical surfaces cast shadows. Early publications are Duwalo and Jacobs (1959), Gilbert (1960) and Knopoff and Gilbert (1961). Other papers are Phinney and Alexander (1966) and Chapman and Phinney (1972).

9.5

Further reading: The amplitudes of head waves were obtained using the Cagniard and WKB methods and an expansion about the branch points of the reflection/transmission coefficients (9.1.5.2). A completely different

method is used in the textbook by Červený and Ravindra (1971). Show that the two methods agree.

10

Generalizations of ray theory

10.1

In Section 9.2.7, we have investigated the waveforms at Airy caustics in some detail. In three dimensions, more general caustics are possible, e.g. the Pearcey (1946) caustic. Using Maslov asymptotic theory, investigate the waveforms at caustics possible in three dimensions.

A cusp or Pearcey (1946) caustic exists when two Airy caustic surfaces meet at a line (in three dimensions, or a point in two dimensions). An example is visible in Figure 5.5. The wave-function near a cusp was investigated by Pearcey (1946) through the canonical integral

$$Pe(\omega, X, Y) = \lambda(\omega) \int_{-\infty}^{\infty} e^{i\omega(Yp + Xp^2 + p^4)} dp.$$

We define a time function

$$\tilde{T}(p, X, Y) = Yp + Xp^2 + p^4.$$

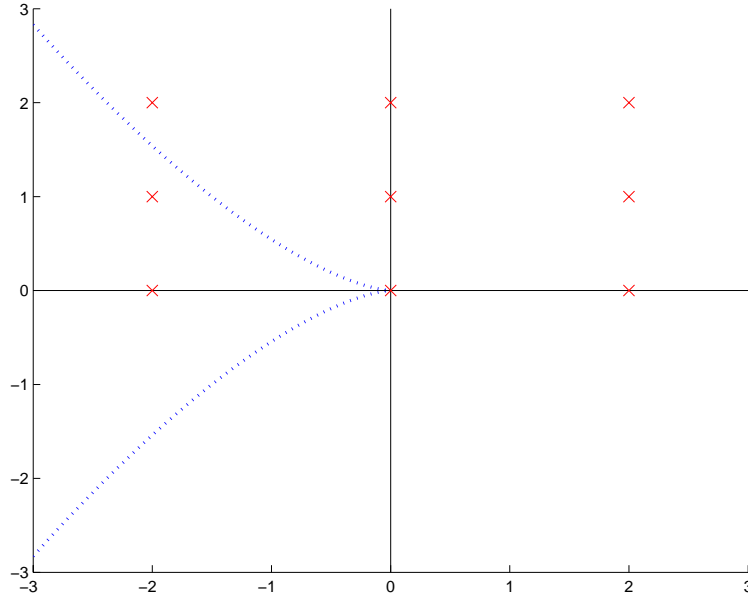
The ‘coordinates’ are arranged so the cusp is at $(X, Y) = (0, 0)$, and at the cusp, the caustic surfaces are tangent to the plane $Y = 0$. Saddle-points corresponding to arrivals exist when

$$\partial\tilde{T}/\partial p = Y + 2Xp + 4p^3 = 0,$$

and caustics when

$$\partial^2\tilde{T}/\partial p^2 = 2X + 12p^2 = 0,$$

i.e. only when $X < 0$ and then at $p = \pm\sqrt{-X/6}$. Substituting back in the saddle-point condition, the caustics are where $Y^2 = -(2X/3)^3$. This is illustrated in the figure of the X – Y domain in the range -3 to 3 . In the next figure, we have plotted the ‘time’ function, \tilde{T} , for the nine values of



The X - Y plane. The dotted lines are caustics, the origin the cusp, and the crosses points where the \tilde{T} function is illustrated in the next plot.

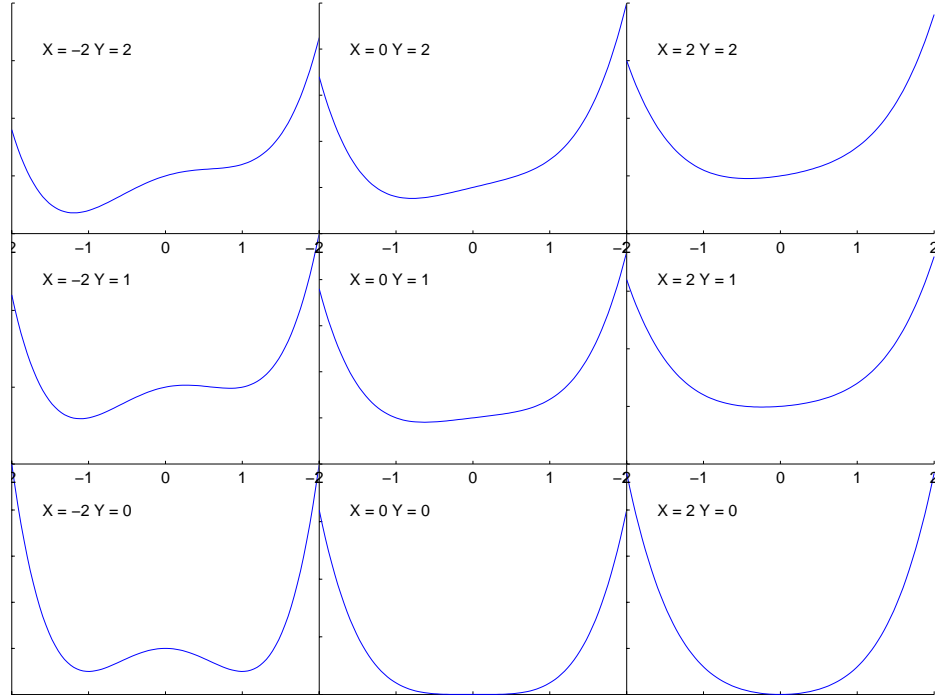
(X, Y) marked in the first figure (these are at $X = -2, 0$ and 2 and $Y = 0, 1$ and 2 — there is symmetry about $Y = 0$).

Between the caustics, with $X < 0$ and $|Y| < (-2X/3)^{3/2}$, three arrivals exist corresponding to stationary values of \tilde{T} . Two arrivals are normal (minima of \tilde{T}), and one is a Hilbert transform (the maximum of \tilde{T}) as it has touched a caustic. Outside this region, only one normal arrival exists which has not touched a caustic (see Figure 5.5).

Pearcey (1948) has presented numerical results for the above function $Pe(\omega, X, Y)$, in the range $X = -8$ to 8 and $Y = 0$ to 8 , i.e. the spectral response near a cusp. The results are of historical interest as they were computed using the differential analyser at Cambridge University, a precursor of modern computers.

The waveforms can be studied using the same techniques as for the Airy caustic (Appendix D.2.2) or the WKB seismogram (8.4.1). The inverse Fourier transform (3.1.2) of the Pearcey integral is

$$Pe(t, X, Y) = \int_{0>0} \frac{dp}{(t - Yp - Xp^2 - p^4)^{1/2}}$$



The function \tilde{T} for the nine values of (X, Y) marked in the first figure (these are at $X = -2, 0$ and 2 and $Y = 0, 1$ and 2).

$$= \lambda(t) * \sum_{\tilde{T}=t} \frac{1}{|\partial \tilde{T} / \partial p|}.$$

It is simple to investigate the singularities using the WKBJ seismogram method (the second expression). The geometrical arrivals and the Airy caustic are as already investigated. The new result is the singularity at cusp. It is given by

$$\frac{\Gamma(1/4)\Gamma(1/2)}{2\Gamma(3/4)} \frac{1}{t^{1/4}} \longleftrightarrow \frac{\Gamma(1/4)\Gamma(1/2)}{2\omega^{3/4}}.$$

This result can be obtained by a variety of means. With $X = Y = 0$, the integral in the first expression above can be reduced to the integral

$$\frac{1}{2} \int_0^{\pi/2} \sin^{-1/2} \theta \, d\theta,$$

with the substitution $p^2 = t^{1/2} \sin \theta$. Solutions of $\tilde{T} = t$ are at $p = \pm t^{1/4}$ so the second expression reduces to the convolution of $t^{-1/2}$ and $t^{-3/4}/2$,

which again can be reduced to the above integral. This integral is the beta function (Abramowitz and Stegun, 1965, §6.2.1 and §6.2.2)

$$B(z, w) = 2 \int_0^{\pi/2} (\sin t)^{2z-1} (\cos t)^{2w-1} dt = \frac{\Gamma(z)\Gamma(w)}{\Gamma(z+w)},$$

which gives the above result. The equivalence of the time and frequency domain results can be obtained using (B.2.6).

A more detailed analysis of the time function near a cusp can be obtained in terms of complete elliptic integrals (Hanyga and Seredyńska, 1991†). We can restrict our discussion to $Y \geq 0$ as by symmetry we have $Pe(t, X, -Y) = Pe(t, X, Y)$. With the substitution $q = Y^{-1/3}p$ ($Y > 0$), we obtain

$$\begin{aligned} Pe(t, X, Y) &= Y^{-1/3} \int_{(0)>0} \frac{dq}{\left(Y^{-4/3}t - q - (XY^{-2/3})q^2 - q^4\right)^{1/2}} \\ &= Y^{-1/3} Pe(Y^{-4/3}t, XY^{-2/3}, 1). \end{aligned}$$

If $Y = 0$, let $q = |X|^{-1/2}p$ and

$$\begin{aligned} Pe(t, X, 0) &= |X|^{-1/2} \int_{(0)>0} \frac{dq}{\left(X^{-2}t - \operatorname{sgn}(X)q^2 - q^4\right)^{1/2}} \\ &= |X|^{-1/2} Pe(X^{-2}t, \operatorname{sgn}(X), 0). \end{aligned}$$

Finally we have the special case (see above) $X = Y = 0$

$$Pe(t, 0, 0) = \int_{(0)>0} \frac{dp}{(t - p^4)^{1/2}}.$$

Thus overall we need to investigate the general case $Pe(t, X, 1)$ and the special cases $Pe(t, \pm 1, 0)$ and $Pe(t, 0, 0)$.

At the cusp, $X = Y = 0$: first we investigate the special cases on the symmetry axis. At the cusp has already been discussed above. Then

$$\begin{aligned} Pe(t, 0, 0) &= 0 \quad \text{if } t < 0 \\ &= \frac{\Gamma(1/4)\Gamma(1/2)}{2\Gamma(3/4)} t^{-1/4} \quad \text{if } t > 0. \end{aligned}$$

Outside the caustics, on the axis, $X = 1$ and $Y = 0$: inside and outside the caustic surface, we use the results (Gradshteyn and Ryzhik, 1980, 3.152 (3) and (9))

$$\int_0^b \frac{dp}{\sqrt{(x^2 + a^2)(b^2 - x^2)}} = \frac{1}{\sqrt{a^2 + b^2}} K\left(\frac{b}{\sqrt{a^2 + b^2}}\right)$$

† Hanyga, A. and Seredyńska, M., 1991. Diffraction of pulses in the vicinity of simple caustics and caustic cusps, *Wave Motion*, **14**, 101–21.

$$\int_b^a \frac{dp}{\sqrt{(a^2 - x^2)(x^2 - b^2)}} = \frac{1}{a} K\left(\frac{\sqrt{a^2 - b^2}}{a}\right),$$

where $K(m)$ is the complete elliptic integral of the first kind (as defined in Abramowitz and Stegun, 1965, §17.3.1). When $X = 1$ and $t > 0$, we use the first result as the denominator has two real roots at $p = \pm b$ with $b^2 = (\sqrt{1+4t} - 1)/2$. With $a^2 = (\sqrt{1+4t} + 1)/2$, the result is

$$\begin{aligned} Pe(t, 1, 0) &= 0 \quad \text{if } t < 0 \\ &= \frac{2}{\sqrt{a^2 + b^2}} K\left(\frac{b}{\sqrt{a^2 + b^2}}\right) \quad \text{if } t > 0. \end{aligned}$$

Inside the caustics, on the axis, $X = -1$ and $Y = 0$: for $t < -1/4$ the denominator has no real roots and the function is zero. For $-1/4 < t < 0$, the denominator has four real roots at $p = \pm a$ and $\pm b$, where $a^2 = (1 + \sqrt{1+4t})/2$ and $b^2 = (1 - \sqrt{1+4t})/2$. We use the second result above. For $t > 0$, the two real roots at $p = \pm a$, and $-b^2$ is positive. We can use the first result above with $b^2 \rightarrow a^2$ and $a^2 \rightarrow -b^2$. Thus

$$\begin{aligned} Pe(t, -1, 0) &= 0 \quad \text{if } t < -1/4 \\ &= \frac{2}{a} K\left(\frac{\sqrt{a^2 - b^2}}{a}\right) \quad \text{if } -1/4 < t < 0 \\ &= \frac{2}{\sqrt{a^2 - b^2}} K\left(\frac{a}{\sqrt{a^2 - b^2}}\right) \quad \text{if } t > 0. \end{aligned}$$

Outside the caustics, off the axis, $X > -3/2$ and $Y = 1$: the equation $\partial\tilde{T}/\partial p = 4p^3 + 2Xp + 1 = 0$ has one real root and at this root $\tilde{T} = T_1$, say. For $t < T_1$, $t = \tilde{T}$ has no real roots and the function is zero. For $t > T_1$, $t = \tilde{T}$ has two real roots, a and b , and a conjugate pair $m \pm in$. We use the result from Gradshteyn and Ryzhik (1980, 3.145 (2))

$$\begin{aligned} \int_b^a \frac{dp}{\sqrt{(a-p)(p-b)((p-m)^2 + n^2)}} &= \\ &= \frac{2}{\sqrt{pq}} K\left(\frac{1}{2} \sqrt{\frac{(a-b)^2 - (p-q)^2}{pq}}\right), \end{aligned}$$

where

$$\begin{aligned} p^2 &= (m-a)^2 + n^2 \\ q^2 &= (m-b)^2 + n^2. \end{aligned}$$

Thus

$$Pe(t, X, 1) = 0 \quad \text{if } t < T_1$$

$$= \frac{2}{\sqrt{pq}} K \left(\frac{1}{2} \sqrt{\frac{(a-b)^2 - (p-q)^2}{pq}} \right) \quad \text{if } t > T_1.$$

The roots can be found analytically (see aside below), or numerically.

Inside the caustics, off the axis, $X < -3/2$ and $Y = 1$: the cubic $\partial\tilde{T}/\partial p = 4p^3 + 2Xp + 1 = 0$ has three real roots with corresponding times in order $T_1 < T_2 \leq T_3$. If $t < T_1$, then $t = \tilde{T}$ has no real roots and the function is zero. For $T_1 < t < T_2$ or $t > T_3$, $t = \tilde{T}$ has two real roots, a and b , and a conjugate pair $m \pm in$. Then we can use the above result. If $T_2 < t < T_3$, then $t = \tilde{T}$ has four roots a, b, c and d (in decreasing order). The integral can be written

$$\begin{aligned} \int_{()>0} \frac{dp}{(t - \tilde{T})^{1/2}} &= \int_d^c \frac{dp}{\sqrt{(a-p)(b-p)(c-p)(p-d)}} \\ &\quad + \int_b^a \frac{dp}{\sqrt{(a-p)(p-b)(p-c)(p-d)}} \\ &= \frac{4}{\sqrt{(a-c)(b-d)}} K \left(\sqrt{\frac{(a-b)(c-d)}{(a-c)(b-d)}} \right), \end{aligned}$$

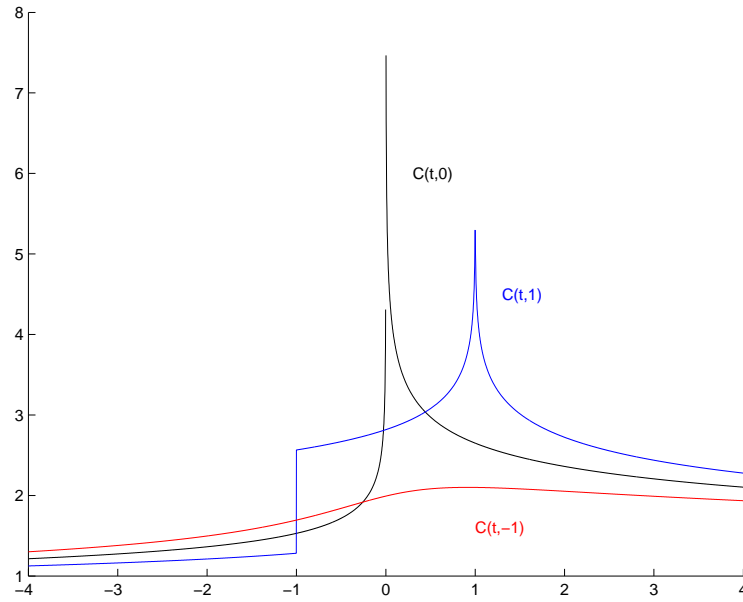
where we have used Gradshteyn and Ryzhik (1980, 3.147 (2) and (7)) for the two integrals. Thus

$$\begin{aligned} Pe(t, X, 1) &= 0 \quad \text{if } t < T_1 \\ &= \frac{2}{\sqrt{pq}} K \left(\frac{1}{2} \sqrt{\frac{(a-b)^2 - (p-q)^2}{pq}} \right) \\ &\quad \text{if } T_1 < t < T_2 \quad \text{or } t > T_3 \\ &= \frac{4}{\sqrt{(a-c)(b-d)}} K \left(\sqrt{\frac{(a-b)(c-d)}{(a-c)(b-d)}} \right) \\ &\quad \text{if } T_2 < t < T_3. \end{aligned}$$

This completes a description of the Pearcey time functions. The same functions can be used if the sign of quartic term is opposite, i.e. $\tilde{T} = Yp + Xp^2 - p^4$, by reversing the signs of ω and t .

It is straightforward to calculate these functions numerically. For the sake of completeness we repeat the results in Figure D.3 for the Airy caustic functions, $C(t, \pm 1)$ and $C(t, 0)$. These have been calculated using the following function

```
function C = AiryTime( t, sign )
% function AiryTime = C(t,sign)
```



The Airy caustic functions $C(t, 1)$ blue, $C(t, -1)$ red and $C(t, 0)$ black.

```
% INPUT:
%      t                = time points
%      sign             = 0, +1 or -1
%
% OUTPUT:
%      C                = function C(t,sign)
%
% Note:
% inverse Airy function time function as defined in
% Appendix D.2.2
%
C=zeros(size(t));
%
% C(t,-1) - (D.2.29) with (D.2.35) and (D.2.36)
if sign == -1
    for j=1:length(t)
        a = -sinh(asinh(t(j))/3);
        p = sqrt(3*a^2+3/4);
        C(j) = ellipke((p-3*a/2)/(2*p))/sqrt(p);
    end
end
```

```

% C(t,0) - result (D.2.21)
elseif sign == 0
    cp = 2^(1/3)*ellipke(1/2+sqrt(3)/4)/3^(1/4);
    cm = 2^(1/3)*ellipke(1/2-sqrt(3)/4)/3^(1/4);
    for j=1:length(t)
        if t(j) > 0.
            C(j) = cp/t(j)^(1/6);
        elseif t(j) < 0.
            C(j) = cm/(-t(j))^(1/6);
        % C(0,0) is singular
        else
            C(j) = Inf;
        end
    end
end
% C(t,1)
elseif sign == 1
    for j=1:length(t)
        % result (D.2.29) with (D.2.27) and (D.2.28)
        if t(j) > 1
            a = real(-cosh(acosh(t(j))/3));
            p = real(sqrt(3*a^2-3/4));
            C(j) = ellipke((p-3*a/2)/(2*p))/sqrt(p);
        % C(1,1) is singular
        elseif t(j) == 1
            C(j) = Inf;
        % result (D.2.29) with (D.2.30)
        elseif t(j) < -1
            a = real(cosh(acosh(-t(j))/3));
            p = real(sqrt(3*a^2-3/4));
            C(j) = ellipke((p-3*a/2)/(2*p))/sqrt(p);
        % result (D.2.26) with (D.2.25)
        else
            aa(1) = real(cos(acos(-t(j))/3));
            aa(2) = real(cos(acos(-t(j))/3+2*pi/3));
            aa(3) = real(cos(acos(-t(j))/3-2*pi/3));
            aa = sort(aa);
            C(j) = 2*ellipke((aa(2)-aa(1))/...
                (aa(3)-aa(1)))/sqrt(aa(3)-aa(1));
        end
    end
end

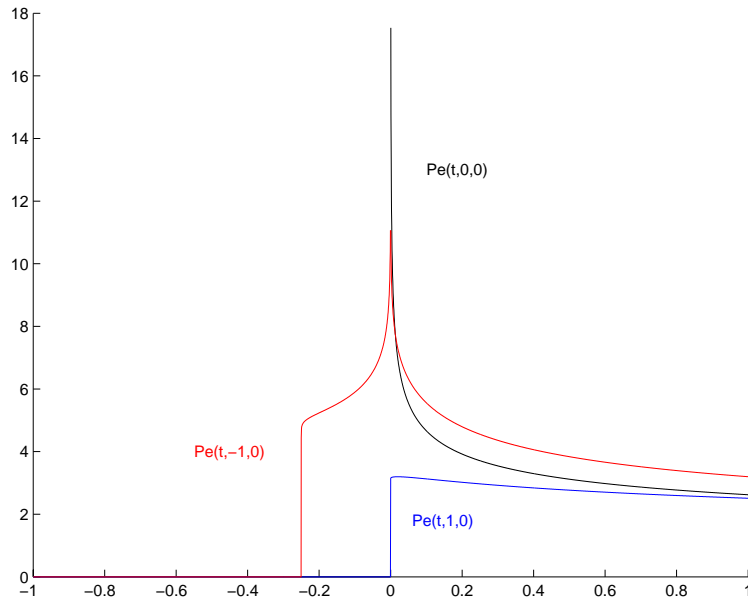
```

```

end
%
return

```

In the next figure, we display the special cases of the Pearcey function on the symmetry axis, i.e. $Pe(t, \pm 1, 0)$ and $Pe(t, 0, 0)$, and in the final figure



The Pearcey caustic functions $Pe(t, 1, 0)$ blue, $Pe(t, -1, 0)$ red and $Pe(t, 0, 0)$ black.

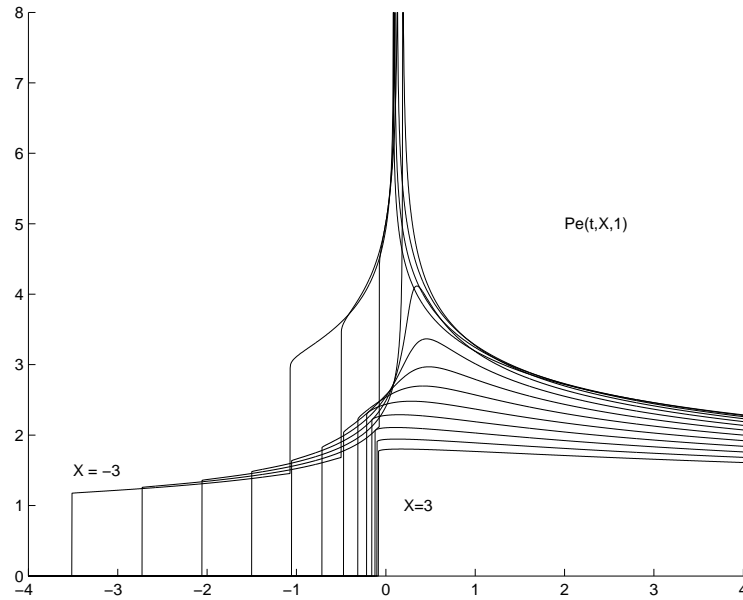
the general function $Pe(t, X, 1)$ for $X = -3$ to 3 in steps of 0.5 . The Pearcey time functions have been calculated with the following function

```

function Pe = PearceyTime( t, x, y )
% function PearceyTime = Pe(t,x,sign)

% INPUT:
%      t      = time points
%      x      = x
%      y      = y parameter 0 or 1
%
% OUTPUT:

```



The Pearcey caustic function $Pe(t, X, 1)$ for $X = -3$ to 3 in steps of 0.5 .

```
%           Pe                      = function Pe(t,x,y)
%
% Note:
% inverse Pearcey function time function as defined in
% Exercise 10.1
% general case Pe(t,x,1)
% special cases Pe(t,-1,0), P(t,0,0) and P(t,1,0)
%
Pe=zeros(size(t));
% special cases on axis
if y== 0
    % Pe(t,-1,0) inside caustic on axis
    if x == -1
        for j=1:length(t)
            if t(j) < -1/4, Pe(j) = 0;
            else % t(j) > -1/4
                z=sqrt(1+4*t(j));
                aa = (1+z)/2;
                bb = (1-z)/2;
                a  = sqrt(aa);
```

```

        if t(j) < 0
            Pe(j) = 2*ellipke(sqrt(aa-bb)/a)/a;
        else % t(j) > 0
            z = sqrt(aa-bb);
            Pe(j) = 2*ellipke(a/z)/z;
        end
    end
end
end
% P(t,0,0) at cusp
elseif x == 0
    for j=1:length(t)
        if t(j) < 0, Pe(j) = 0;
        elseif t(j) == 0, Pe(j) = Inf;
        else % t(j) > 0
            Pe(j) = gamma(1/4)*gamma(1/2)/...
                (2*gamma(3/4)*sqrt(sqrt(t(j))));
        end
    end
end
% P(t,1,0) outside caustic on axis
else
    for j=1:length(t)
        if t(j) < 0, Pe(j) = 0;
        else % t(j) > 0
            z = sqrt(1+4*t(j));
            aa = (z+1)/2;
            bb = (z-1)/2;
            z=sqrt(aa+bb);
            Pe(j) = 2*ellipke(sqrt(bb)/z)/z;
        end
    end
end
end
% P(t,x,1)
else
    % stationary points of quartic
    cubic = [ 4 0 2*x 1 ];
    ps = roots(cubic);
    % outside caustic, off axis
    if x > -3/2
        % one real root
        for k=1:3

```

```

        if imag(ps(k)) == 0, break, end
    end
    p1 = real(ps(k));
    t1 = p1^4+x*p1^2+p1;
    %
    for j=1:length(t)
        if t(j) < t1, Pe(j) = 0;
        else % t(j) > t1
            % 2 real roots
            quartic = [ -1 0 -x -1 t(j) ];
            ps = roots( quartic );
            ll = 0;
            for k=1:4
                if imag(ps(k)) == 0
                    ll = ll+1;
                    ba(ll) = ps(k);
                else
                    mm = real(ps(k));
                    nn = abs(imag(ps(k)));
                end
            end
            ba = sort(ba);
            p = sqrt((mm-ba(2))^2+nn^2);
            q = sqrt((mm-ba(1))^2+nn^2);
            Pe(j) = 2*ellipke(sqrt(((ba(2)-ba(1))^2-...
                (p-q)^2)/(p*q))/2)/sqrt(p*q);
        end
    end
    % inside cusp, off axis
else % X < -3/2
    % 3 real roots
    for k=1:3
        tt(k) = ps(k)^4+x*ps(k)^2+ps(k);
    end
    tt = sort(tt);
    %
    for j=1:length(t)
        if t(j) < tt(1), Pe(j) = 0;
        else % t(j) > tt(1)
            quartic = [ -1 0 -x -1 t(j) ];

```



```

ps = roots( quartic );
if t(j) > tt(2) && t(j) < tt(3)
    % 4 real roots
    ps = sort(ps);
    Pe(j) = 4*ellipke(sqrt((ps(4)-ps(3))*(ps(2)-ps(1))/...
        ((ps(4)-ps(2))*(ps(3)-ps(1)))))/...
        sqrt((ps(4)-ps(2))*(ps(3)-ps(1))));
else % tt(1) < t(j) < tt(2) or t(j) > tt(3)
    % 2 real roots
    ll = 0;
    for k=1:4
        if imag(ps(k)) == 0
            ll = ll+1;
            ba(ll) = ps(k);
        else
            mm = real(ps(k));
            nn = abs(imag(ps(k)));
        end
    end
    ba = sort(ba);
    p = sqrt((mm-ba(2))^2+nn^2);
    q = sqrt((mm-ba(1))^2+nn^2);
    Pe(j) = 2*ellipke(sqrt(((ba(2)-ba(1))^2-...
        (p-q)^2)/(p*q))/2)/sqrt(p*q);
end
end
end
end
end
%
```

These functions use the Matlab routines `roots` to solve the cubic and quartic polynomials. However, these can be solved analytically and for the sake of completeness, the methods are given below in an aside.

Brown (1986a)[†] has investigated the cusp caustic and has analyzed the singularities. As mentioned above, Hanyga and Seredyńska (1991) have analysed the same problem and have obtained the analytic results for the

[†] Brown, M.G., 1986a. The transient wave fields in the vicinity of the cuspid caustics, *J. Acoust. Soc. Amer.*, **79**, 1367–84.

time functions at caustic cusps in terms of complete elliptic integrals (and have confirmed the Airy caustic results of Burridge, 1963*a*, *b*, and Appendix D.2.2). Burridge (1995)[‡] has also analysed the Pearcey cusp problem. He has investigated the inverse Fourier transform of the functions

$$\begin{aligned} \int_{-\infty}^{\infty} p^{\ell} e^{i\omega(Yp+p^3)} dp &\rightarrow \sum_{t=p^3+Yp} \frac{p^{\ell}}{|3p^2+Y|} \\ \int_{-\infty}^{\infty} p^{\ell} e^{i\omega(Yp+Xp^2+p^4)} dp &\rightarrow \sum_{t=p^4+Xp^2+Yp} \frac{p^{\ell}}{|4p^3+2Xp+Y|}, \end{aligned}$$

i.e. without the spectrum $\lambda(\omega)$ (so the result corresponds to the two-dimensional problem). We have used a notation analogous to Pearcey's not quite Burridge's. The first function with $\ell = 0$ corresponds to the function $C(t, y)$ investigated in Appendix D.2.2, without the convolution with $\lambda(t)$. The function with $\ell = 1$ corresponds to the inverse Fourier transform of the derivative of the Airy function, as required by the full asymptotic expansion near an Airy caustic (Chester, Friedman and Ursell, 1959; Ludwig, 1966[†]). The second function is for the Pearcey cusp and for the full asymptotic expansion is required for $\ell = 0, 1$ and 2. Burridge (1995) has investigated it analytically for $Y = 0$ on the symmetry line, and illustrated all functions numerically.

Brown (1986*b*)[‡] has analyzed the singularities of higher-order caustics, and Brown and Tappert (1986)[§] have discussed the general caustic problem.

Aside: roots of cubic or quartic polynomials

A general method of finding the roots of a polynomial is to find the eigenvalues of the companion matrix. For a polynomial

$$a_n x^n + \dots + a_1 x + a_0 = 0,$$

[‡] Burridge, R., 1995. Asymptotic evaluation of integrals related to time-dependent fields near caustics, *SIAM J. Appl. Math.*, **55**, 390–409.

[†] Ludwig, D., 1966. Uniform asymptotic expansions at a caustic, *Comm. Pure Appl. Math.*, **19**, 215–50.

[‡] Brown, M.G., 1986*b*. The transient wave fields in the vicinity of the elliptic, hyperbolic and parabolic umbilic caustics, *J. Acoust. Soc. Amer.*, **79**, 1385–401.

[§] Brown, M.G. and Tappert, F.D., 1986. Causality, caustics, and the structure of transient wave fields, *J. Acoust. Soc. Amer.*, **80**, 251–5.

the companion $n \times n$ matrix is

$$\mathbf{A} = \begin{pmatrix} -a_{n-1}/a_n & -a_{n-2}/a_n & \dots & -a_1/a_n & -a_0/a_n \\ 1 & 0 & \dots & 0 & 0 \\ 0 & 1 & \dots & 0 & 0 \\ \vdots & \vdots & \ddots & \vdots & \vdots \\ 0 & 0 & \dots & 0 & 0 \\ 0 & 0 & \dots & 1 & 0 \end{pmatrix}.$$

The eigen-equation is

$$\mathbf{A} \begin{pmatrix} x^{n-1} \\ x^{n-2} \\ \vdots \\ x \\ 1 \end{pmatrix} = x \begin{pmatrix} x^{n-1} \\ x^{n-2} \\ \vdots \\ x \\ 1 \end{pmatrix},$$

and the eigenvalue is equivalent to the polynomial root. This method is used by the Matlab routine **roots**.

Cubics and quartics can be solved analytically. Consider the cubic in its standard form

$$x^3 + px^2 + qx + r = 0.$$

This can be reduced to

$$y^3 + 3Qy - 2R = 0,$$

where

$$\begin{aligned} y &= x + \frac{p}{3} \\ 3Q &= q - \frac{1}{3}p^2 \\ 2R &= \frac{p}{3} \left(q - \frac{2p^2}{9} \right) - r. \end{aligned}$$

We define a discriminant

$$D = Q^3 + R^2.$$

If $D > 0$, there is one real root, and if $D \leq 0$ there are three real roots (multiple roots if $D = 0$). The following algorithms require the special case of a triple root when $Q = R = 0$, and $y_1 = y_2 = y_3 = 0$, to be handled separately.

If $D > 0$ we make the transformation

$$y = 2Q^{1/2} \sinh \frac{\theta}{3},$$

and the cubic reduces to

$$\sinh \theta = \frac{R}{Q^{3/2}}.$$

The standard logarithmic formula for the inverse hyperbolic sine gives

$$\frac{\theta}{3} = \ln \frac{S}{Q^{1/2}},$$

where

$$S = \left(R + \sqrt{D}\right)^{1/3}.$$

Substituting, this gives the root

$$y_1 = S + T,$$

where

$$T = -Q/S = \left(R - \sqrt{D}\right)^{1/3}.$$

If $R < 0$ it is best to calculate T first and derive S from it.

If $D < 0$, then we make the transformation

$$y = 2(-Q)^{1/2} \cos \frac{\theta}{3},$$

and the cubic reduces to

$$\cos \theta = \frac{R}{(-Q)^{3/2}}$$

(necessarily $Q < 0$). The solutions are

$$\begin{aligned} y_1 &= 2\sqrt{-Q} \cos \frac{\theta}{3} \\ y_1 &= 2\sqrt{-Q} \cos \left(\frac{\theta}{3} + \frac{2\pi}{3}\right) \\ y_1 &= 2\sqrt{-Q} \cos \left(\frac{\theta}{3} + \frac{4\pi}{3}\right). \end{aligned}$$

For a quartic

$$a_4x^4 + a_3x^3 + a_2x^2 + a_1x + a_0 = 0,$$

the transformation

$$y = x + \frac{a_3}{4a_4},$$

reduces it to

$$y^4 + py^2 + qy + r = 0,$$

where

$$\begin{aligned} p &= \frac{a_2}{a_4} - \frac{3a_3^2}{8a_4^2} \\ q &= \frac{a_1}{a_4} - \frac{a_3}{2a_4} \left(\frac{a_2}{a_4} - \frac{a_3^2}{4a_4^2} \right) \\ r &= \frac{a_0}{a_4} - \frac{a_3}{4a_4} \left(\frac{a_1}{a_4} - \frac{a_3}{4a_4} \left(\frac{a_2}{a_4} - \frac{3a_3^2}{16a_4^2} \right) \right). \end{aligned}$$

First we consider the special cases:

- if $q = r = 0$, there are two or four real roots

$$\begin{aligned} y_1 &= y_2 = 0 \\ y_3 &= -y_4 = \sqrt{-p}; \end{aligned}$$

- if $q = 0$, the quartic reduces to a quadratic in y^2 . There will be zero, two or four real roots;
- if $r = 0$, we obtain

$$y(y^3 + py + q) = 0,$$

and we have the root $y_1 = 0$ plus the roots of the cubic. There will be two or four real roots.

Returning to the general quartic. As the cubic term has been removed, it can be factored as

$$(y^2 + vy + z + u)(y^2 - vy + z - u) = 0.$$

Expanding and comparing, we have

$$\begin{aligned} u^2 &= z^2 - r \\ v^2 &= 2z - p \\ 2uv &= -q. \end{aligned}$$

Squaring the last result and substituting, we obtain the reducing cubic

$$z^3 - \frac{p}{2}z^2 - rz + \left(\frac{pr}{2} - \frac{q^2}{8} \right) = 0,$$

from which we can always find at least one real solution for z defining the quadratics. Solving these, we obtain zero, two or four real roots.

10.2

Using transform methods, show that coupling between quasi-shear plane waves exists (using methods similar to Section 7.2.6) and that the form of coupling is similar to the ray result (10.2.56) (see Chapman and Shearer, 1989).

The coupling between the transformed eigen-solutions is given by equation (7.2.122)

$$\frac{d}{dz} \underline{\mathbf{r}}^{(k+1)} = e^{-i\omega\boldsymbol{\tau}(z)} \mathbf{C}(z) e^{i\omega\boldsymbol{\tau}(z)} \underline{\mathbf{r}}^{(k)},$$

dropping the source term, which is used to generate the zeroth iteration (see Section 7.2.6 for more details). The matrix \mathbf{C} is given by (7.2.95)

$$\mathbf{C} = -\mathbf{W}^{-1}\mathbf{W}',$$

where \mathbf{W} is the matrix of eigenvectors. Let us just consider the sub-matrix $\mathbf{C}^{(12)\times(12)}$, i.e. the coupling matrix between qS waves travelling in the positive direction. Using the orthogonal relationship (6.3.33) with the symplectic transform (6.3.31) and the decomposition of the eigenvector \mathbf{w} into the velocity, \mathbf{v} , and traction, \mathbf{t} , vectors, we have

$$\begin{aligned} \mathbf{C}^{(12)\times(12)} &= - \begin{pmatrix} \mathbf{t}_1^T & \mathbf{v}_1^T \\ \mathbf{t}_2^T & \mathbf{v}_2^T \end{pmatrix} \begin{pmatrix} \mathbf{v}'_1 & \mathbf{v}'_2 \\ \mathbf{t}'_1 & \mathbf{t}'_2 \end{pmatrix} \\ &= - \begin{pmatrix} 0 & \mathbf{t}_1 \cdot \mathbf{v}'_2 + \mathbf{v}_1 \cdot \mathbf{t}'_2 \\ \mathbf{t}_2 \cdot \mathbf{v}'_1 + \mathbf{v}_2 \cdot \mathbf{t}'_1 & 0 \end{pmatrix}, \end{aligned}$$

where the subscripts indicate the wave type, i.e. 1 refers to the slower qS_2 , and 2 the faster qS_1 , and the prime, the derivative d/dz . This matrix is known to be anti-symmetric (Section 7.2.5.1).

The traction is defined by (6.3.29)

$$\mathbf{t} = -p_k \mathbf{c}_{3k} \mathbf{v},$$

so

$$\mathbf{t}' = -p'_k \mathbf{c}_{3k} \mathbf{v} - p_k \mathbf{c}'_{3k} \mathbf{v} - p_k \mathbf{c}_{3k} \mathbf{v}'.$$

We are interested in the problem where \mathbf{v} varies rapidly compared with the material properties due to a quasi-shear wave degeneracy. Thus we neglect the derivatives p'_k and \mathbf{c}'_{3k} . Hence

$$\begin{aligned} \mathbf{t}_1 \cdot \mathbf{v}'_2 + \mathbf{v}_1 \cdot \mathbf{t}'_2 &\simeq -\mathbf{v}_1^T (\mathbf{c}_{k3} + \mathbf{c}_{3k}) \mathbf{v}'_2 \\ &\simeq -\frac{p_k \hat{\mathbf{g}}_1^T (\mathbf{c}_{k3} + \mathbf{c}_{3k}) \hat{\mathbf{g}}'_2}{2\rho V_3}, \end{aligned}$$

where the normalizations of the two eigenvectors are approximately equal, $w_1 \simeq w_2 \simeq (2\rho V_3)^{-1/2}$, and we have ignored the derivative of ρV_3 . As $\hat{\mathbf{g}}_1$ and $\hat{\mathbf{g}}_2$ are orthonormal, it is obvious that the matrix $\mathbf{C}^{(12) \times (12)}$ is anti-symmetric, and that the gradient of $\hat{\mathbf{g}}_\nu$ can be described using a rotation angle, ϕ , i.e.

$$\begin{aligned}\hat{\mathbf{g}}'_1 &= \phi' \hat{\mathbf{g}}_2 \\ \hat{\mathbf{g}}'_2 &= -\phi' \hat{\mathbf{g}}_1.\end{aligned}$$

As $p_k \hat{\mathbf{g}}_1^T \mathbf{c}_{3k} \hat{\mathbf{g}}_1 = \rho V_3$ (5.3.20), the quasi-shear coupling matrix becomes

$$\mathbf{C}^{(12) \times (12)} = \begin{pmatrix} 0 & -\phi' \\ \phi' & 0 \end{pmatrix}.$$

Thus the coupling between the transformed eigen-solutions is completely analogous to the quasi-shear ray coupling (10.2.56).

10.3

Using the stationary-phase method to evaluate the Born scattering integral, linearized reflection coefficients can be obtained for a small-contrast interface (Shaw and Sen, 2004). By considering a perturbation to a half-space, show that the coefficients obtained in this matter agree with those in Section 6.7.

For simplicity, we consider a two-dimensional problem with very simple geometry. The algebra is simplified and as the reflection coefficient obtained is independent of the geometry (apart from the angle of incidence, of course), the simplifications are of no consequence. The acoustic model consists of an interface separating two uniform half spaces. The Born perturbation applies to the second half space, i.e.

$$\begin{aligned}\rho^B &= \Delta \rho H(z_2 - z) \\ k^B &= \Delta k H(z_2 - z).\end{aligned}$$

In the notation of Section 6.7, $\Delta \rho = -[\rho]$ and $\Delta k = -[k]$. The source and receiver are at the same depth, $z = z_S = z_R > z_2$.

The acoustic, two-dimensional, perturbation Born result is from (10.3.69)

$$\begin{aligned}\underline{\mathbf{u}}^B(\omega, \mathbf{x}_R; \mathbf{x}_S) &= - \left(-\frac{i\omega\lambda(\omega)}{2^{1/2}\pi} \right)^2 \\ &\times \int_V \Gamma^B(\mathbf{x}, \mathcal{L}_R, \mathcal{L}_S) \underline{\mathbf{D}}^{(2)}(\mathbf{x}, \mathcal{L}_R, \mathcal{L}_S) e^{i\omega \tilde{T}(\mathbf{x}, \mathcal{L}_R, \mathcal{L}_S)} dV,\end{aligned}$$

where from equation (10.3.72)

$$\begin{aligned}\Gamma^{\text{B}}(\mathbf{x}, \mathcal{L}_{\text{R}}, \mathcal{L}_{\text{S}}) &= \frac{1}{2\alpha} \left(\frac{\Delta\rho}{\rho} \hat{\mathbf{p}}(\mathbf{x}, \mathcal{L}_{\text{R}}) \cdot \hat{\mathbf{p}}(\mathbf{x}, \mathcal{L}_{\text{S}}) - \frac{\Delta k}{k} \right) H(z_2 - z) \\ &= \Gamma^{\text{B}} H(z_2 - z),\end{aligned}$$

say, and definition (10.3.54) with the two-dimensional ray results (equations (5.4.34) and (5.2.76)) is

$$\underline{\mathcal{D}}^{(2)}(\mathbf{x}, \mathcal{L}_{\text{R}}, \mathcal{L}_{\text{S}}) = - \frac{\hat{\mathbf{p}}(\mathbf{x}_{\text{R}}, \mathcal{L}_{\text{R}}) \hat{\mathbf{p}}^{\text{T}}(\mathbf{x}_{\text{S}}, \mathcal{L}_{\text{S}})}{2\rho\alpha^2(\mathcal{R}_{\text{R}}\mathcal{R}_{\text{S}})^{1/2}}.$$

The reference media, i.e. the half space $z > z_2$, has constant velocity, α , and density, ρ . The straight source and receiver ray lengths are \mathcal{R}_{S} and \mathcal{R}_{R} so

$$\begin{aligned}\mathbf{x} - \mathbf{x}_{\text{S}} &= \mathcal{R}_{\text{S}} \hat{\mathbf{p}}(\mathbf{x}, \mathcal{L}_{\text{S}}) \\ \mathbf{x} - \mathbf{x}_{\text{R}} &= \mathcal{R}_{\text{R}} \hat{\mathbf{p}}(\mathbf{x}, \mathcal{L}_{\text{R}})\end{aligned}$$

(note the signs of these definitions of $\hat{\mathbf{p}}$), and the travel time is

$$\tilde{T}(\mathbf{x}, \mathcal{L}_{\text{R}}, \mathcal{L}_{\text{S}}) = \tilde{T}_{\text{R}} + \tilde{T}_{\text{S}} = (\mathcal{R}_{\text{R}} + \mathcal{R}_{\text{S}})/\alpha.$$

The Born integral reduces to

$$\underline{\mathbf{u}} = \frac{\text{i}\omega}{2\pi} \int_{-\infty}^{z_2} \int_{-\infty}^{\infty} \Gamma^{\text{B}} \underline{\mathcal{D}}^{(2)} e^{\text{i}\omega\tilde{T}} \text{d}x \text{d}z,$$

omitting the arguments for brevity. The x integral has a saddle point when

$$\frac{\text{d}\tilde{T}}{\text{d}x} = \frac{x - x_{\text{R}}}{\alpha\mathcal{R}_{\text{R}}} + \frac{x}{\alpha\mathcal{R}_{\text{S}}} = 0,$$

i.e. $x = x_{\text{R}}/2$ and $\mathcal{R}_{\text{R}} = \mathcal{R}_{\text{S}}$. The second derivative is

$$\frac{\text{d}^2\tilde{T}}{\text{d}x^2} = \frac{(z - z_{\text{R}})^2}{\alpha\mathcal{R}_{\text{R}}^3} + \frac{(z - z_{\text{S}})^2}{\alpha\mathcal{R}_{\text{S}}^3} > 0,$$

for a given z . The integral is approximated by the second-order saddle-point contribution (D.1.11)

$$\begin{aligned}\underline{\mathbf{u}} &\simeq \frac{\text{i}\omega}{2\pi} \int_{-\infty}^{z_2} \Gamma^{\text{B}} \underline{\mathcal{D}}^{(2)} e^{2\text{i}\omega\mathcal{R}/\alpha} \int_{-\infty}^{\infty} e^{\text{i}\omega(z-z_{\text{S}})^2(x-x_{\text{S}}/2)^2/\alpha\mathcal{R}^3} \text{d}x \text{d}z \\ &= \frac{e^{3\text{i}\pi/4}}{2} \left(\frac{\omega\alpha}{\pi} \right)^{1/2} \int_{-\infty}^{z_2} \Gamma^{\text{B}} \underline{\mathcal{D}}^{(2)} e^{2\text{i}\omega\mathcal{R}/\alpha} \frac{\mathcal{R}^{3/2}}{z_{\text{S}} - z} \text{d}z\end{aligned}$$

(for $\omega > 0$), where the terms in the integrand are evaluated at the saddle point, i.e. with $\mathcal{R}_{\text{S}} = \mathcal{R}_{\text{R}} = \mathcal{R}$, say. This oscillatory integral does not have a

saddle point as \mathcal{R} increases steadily as $z \rightarrow -\infty$, so the major contribution comes the end-point, z_2 . We note that \mathcal{R} is a function of z and write it as

$$\mathcal{R}(z) = (z_S - z) \sec \theta(z),$$

where θ is the angle between a ray through $(x_R/2, z)$ and the vertical. The differentials are connected by $d\mathcal{R} = -\cos \theta dz$, so integrating by parts and dropping terms in $O(1/\omega)$ to obtain the end-point contribution

$$\begin{aligned} \underline{\mathbf{u}} &\simeq \frac{e^{3i\pi/4}}{2} \left(\frac{\omega\alpha}{\pi} \right)^{1/2} \int_{\mathcal{R}(z_2)}^{\infty} \Gamma^B \underline{\mathbf{D}}^{(2)} e^{2i\omega\mathcal{R}/\alpha} \frac{\mathcal{R}^{1/2}}{\cos^2 \theta} d\mathcal{R} \\ &\simeq \frac{e^{3i\pi/4}}{2} \left(\frac{\omega\alpha}{\pi} \right)^{1/2} \frac{\Gamma^B \underline{\mathbf{D}}^{(2)} \mathcal{R}^{1/2}}{\cos^2 \theta} \left(\frac{\alpha}{2i\omega} \right) e^{2i\omega\mathcal{R}/\alpha} \Big|_{\mathcal{R}(z_2)}^{\infty} \\ &= - \frac{\alpha^{3/2} \Gamma^B \underline{\mathbf{D}}^{(2)} \mathcal{R}^{1/2}}{4\pi \cos^2 \theta} \lambda(\omega) e^{2i\omega\mathcal{R}/\alpha}, \end{aligned}$$

where all terms are evaluated at the end-point. Substituting for Γ^B and $\underline{\mathbf{D}}^{(2)}$, the frequency independent coefficient reduces to

$$\frac{\alpha^{3/2} \Gamma^B \underline{\mathbf{D}}^{(2)} \mathcal{R}^{1/2}}{4\pi \cos^2 \theta} = - \frac{\hat{\mathbf{P}}_R \hat{\mathbf{P}}_S^T}{2^{3/2} \pi \alpha^{3/2} (2\mathcal{R})^{1/2}} \left(\cos 2\theta \frac{\Delta\rho}{\rho} - \frac{\Delta k}{k} \right) \frac{\sec^2 \theta}{4}.$$

The acoustic reflection coefficient from an interface is given by (6.3.7)

$$\mathcal{T}_{11} = \frac{\rho_2 q_{\alpha 1} - \rho_1 q_{\alpha 2}}{\rho_2 q_{\alpha 1} + \rho_1 q_{\alpha 2}} \simeq [\gamma_A] = \frac{1}{2} \Delta \left(\frac{\rho\alpha}{\cos \theta} \right) / \left(\frac{\rho\alpha}{\cos \theta} \right),$$

for the linearized coefficient (6.7.23). Using $k = 1/\rho\alpha^2$ for the compressibility (4.4.4), and

$$\Delta\theta = \frac{\Delta\alpha}{\alpha} \tan \theta,$$

from Snell's law, this can be rewritten (to first order in the perturbations) as

$$\mathcal{T}_{11} \simeq \left(\cos 2\theta \frac{\Delta\rho}{\rho} - \frac{\Delta k}{k} \right) \frac{\sec^2 \theta}{4},$$

so (6.7.23)

$$\Gamma^B = \left(\frac{2 \cos^2 \theta}{\alpha} \right) [\gamma_A] \simeq \left(\frac{2 \cos^2 \theta}{\alpha} \right) \mathcal{T}_{11},$$

at the saddle point (remembering that $\Delta\rho = -[\rho]$, etc.). Thus the Born reflected solution reduces to

$$\underline{\mathbf{u}} \simeq \frac{\hat{\mathbf{g}}_R \hat{\mathbf{g}}_S^T}{2^{3/2} \pi \alpha^{3/2} (2\mathcal{R})^{1/2}} \mathcal{T}_{11} \lambda(\omega) e^{i\omega(2\mathcal{R})/\alpha},$$

where a sign change occurs as we have now used the polarizations for the complete ray, i.e. $\hat{\mathbf{g}}_{\mathbf{R}} = \mathbf{g}(\mathbf{x}_{\mathbf{R}}, \mathcal{L}_{\mathbf{S}}) = -\hat{\mathbf{p}}_{\mathbf{R}} = -\mathbf{p}(\mathbf{x}_{\mathbf{R}}, \mathcal{L}_{\mathbf{R}})$. The expression for $\underline{\mathbf{u}}$ can be recognized as the far-field, dyadic two-dimensional Green function (5.2.83) for the reflection with ray length $2\mathcal{R}$.

Thus approximating the Born perturbation volume integral by the second-order, saddle-point contribution in the interface coordinates, and the end-point contribution in the coordinate normal to the interface, we obtain the linearized approximation for the reflection coefficient. For anisotropic media, the operations will be similar although we must be careful to distinguish phase and group velocities, and ray types. The isotropic results can be obtained by specializing the anisotropic results. First we investigate the connection between the linearized coefficients (Section 6.7) and the perturbation Born scattering (Section 10.3.3) for general anisotropic media. As above we consider a perturbation to a half space $z < z_2$

$$\begin{aligned}\rho^{\mathbf{B}} &= \Delta\rho H(z_2 - z) = -[\rho] H(z_2 - z) \\ \mathbf{c}_{jk}^{\mathbf{B}} &= \Delta\mathbf{c}_{jk} H(z_2 - z) = -[\mathbf{c}_{jk}] H(z_2 - z),\end{aligned}$$

so the perturbation Born term is

$$\begin{aligned}\Gamma^{\mathbf{B}'}(\mathbf{x}, \mathcal{L}_{\mathbf{R}}, \mathcal{L}_{\mathbf{S}}) &= \mathbf{g}_{\mathbf{R}}^{\mathbf{T}} (\Delta\rho + p_{\mathbf{R}k} p_{\mathbf{S}j} \Delta\mathbf{c}_{kj}) \mathbf{g}_{\mathbf{S}} H(z_2 - z) \\ &= \Gamma^{\mathbf{B}'} H(z_2 - z),\end{aligned}$$

say, using the abbreviated notation defined above ($\mathbf{p}_{\mathbf{R}} = \mathbf{p}(\mathbf{x}, \mathcal{L}_{\mathbf{R}})$ and $\mathbf{p}_{\mathbf{S}} = \mathbf{p}(\mathbf{x}, \mathcal{L}_{\mathbf{S}})$ for rays to a scattering point, \mathbf{x}) (we use the form of Born scattering with perturbations to the stiffnesses rather than compliances (10.3.78) as this is more common in the literature — to first order, the results are equivalent).

Expanding expression (6.7.21)

$$\delta\mathcal{T} = \mathbf{W}^{\mathbf{T}} \mathbf{I}_2 [\mathbf{W}] \mathbf{I}_2,$$

we can obtain a very simple expression

$$\delta\mathcal{T}_{\mathbf{RS}} = [\gamma_{\mathbf{RS}}] = \mathbf{t}_{\mathbf{R}}^{\mathbf{T}} [\mathbf{g}_{\mathbf{S}}] + \mathbf{g}_{\mathbf{R}}^{\mathbf{T}} [\mathbf{t}_{\mathbf{S}}],$$

for the linearized coefficient from a small-contrast interface with source and receiver types indicated by \mathbf{S} and \mathbf{R} , respectively. However, we would prefer a result in terms of the saltus of the medium rather than the saltus of the eigen-solution. Combining equations (6.7.20) and (6.7.21) for a small-contrast interface, we have

$$\delta\mathcal{T} = -\mathbf{I}_3 [\delta\mathbf{C}] \mathbf{I}_2,$$

where the matrix $\delta\mathbf{C}$ is defined in equation (6.7.16)

$$\text{off-diag}([\mathbf{p}_n, \delta\mathbf{C}]) = \text{off-diag}(\mathbf{I}_3 \mathbf{W}^T \mathbf{I}_2 \delta\mathbf{A} \mathbf{W}).$$

Rearranging the first equation

$$[\delta\mathbf{C}] = -\mathbf{I}_3 \delta\mathbf{T} \mathbf{I}_2,$$

and substituting in the commutator, we have

$$\text{off-diag}(-\mathbf{p}_n \mathbf{I}_3 \delta\mathbf{T} \mathbf{I}_2 + \mathbf{I}_3 \delta\mathbf{T} \mathbf{I}_2 \mathbf{p}_n) = \text{off-diag}(\mathbf{I}_3 \mathbf{W}^T \mathbf{I}_2 [\mathbf{A}] \mathbf{W}).$$

Expanding this, we obtain for any term with $R \neq S$

$$(\mathbf{p}_n)_R \delta\mathcal{T}_{RS} - \delta\mathcal{T}_{RS}(\mathbf{p}_n)_S = -\mathbf{w}_R^\dagger [\mathbf{A}] \mathbf{w}_S,$$

where the subscripts R and S indicate the receiver and source ray types and direction, i.e. RS map into the matrix indices ij . We have the notational complication that in the matrix \mathbf{T} the indexing depends on the *medium* (and ray type), whereas in the above expression it would be more convenient if the indexing depended on the *ray direction* (and ray type). This can be achieved by swapping the columns (corresponding to the source ray) of the matrix \mathbf{T} , i.e.

$$\mathbf{T}^\dagger = \mathbf{T} \mathbf{I}_2,$$

and then in the matrix \mathbf{T}^\dagger the indexing depends on direction. We can then treat R and S as indices, and the above scalar equation can be written in matrix form

$$\text{off-diag}(\mathbf{p}_n \delta\mathbf{T}^\dagger - \delta\mathbf{T}^\dagger \mathbf{p}_n) = -\text{off-diag}(\mathbf{W}^\dagger [\mathbf{A}] \mathbf{W}).$$

Expressions for $\delta\mathbf{A}$ in terms of $\delta\rho$ and $\delta\mathbf{c}_{jk}$ have been given in the text (expressions (6.7.18) and (6.7.19)) — remember that the slowness components, p_ν , contained in \mathbf{A} are in the interface, and are the same for all rays at the interface. The perturbation Born scattering term, $\Gamma^{B'}$, has been given above. Remember that in that expression, the polarizations are normalized with respect to energy flux along the ray, whereas in the coefficients, \mathbf{T} , they are normalized with respect to energy flux normal to the interface (see discussion at the end of Section 6.8.2). Taking the above expression for $\delta\mathcal{T}_{RS}$, we can rewrite it using expressions (6.3.25) and (6.3.31) as

$$(p_{S3} - p_{R3}) \delta\mathcal{T}_{RS} = -\hat{\mathbf{g}}_R^T \begin{pmatrix} -p_{Rj} \mathbf{c}_{j3} & \mathbf{I} \end{pmatrix} [\mathbf{A}] \begin{pmatrix} \mathbf{I} \\ -p_{Sk} \mathbf{c}_{3k} \end{pmatrix} \hat{\mathbf{g}}_S,$$

where in this expression \mathbf{p}_R is in the direction of the reflected ray, not the reversed direction from receiver to scatterer used in the Born scattering term,

$\Gamma^{B'}$. Substituting for $[\mathbf{A}]$, expressions (6.7.18) and (6.7.19), and expanding summations such as

$$p_{Rj}\mathbf{c}_{j3} = p_\eta\mathbf{c}_{\eta3} + p_{R3}\mathbf{c}_{33}$$

(as p_η 's are the same for the source and receiver rays), we obtain

$$\begin{pmatrix} -p_{Rj}\mathbf{c}_{j3} & \mathbf{I} \end{pmatrix} [\mathbf{A}] \begin{pmatrix} \mathbf{I} \\ -p_{Sk}\mathbf{c}_{3k} \end{pmatrix} = \\ p_\eta p_\nu [\mathbf{c}_{\eta\nu}] + p_{R3} p_\nu [\mathbf{c}_{3\nu}] + p_\eta p_{S3} [\mathbf{c}_{\eta3}] + p_{R3} p_{S3} [\mathbf{c}_{33}] - [\rho] \mathbf{I},$$

where many terms cancel in the expansion. Comparing this expression with the expression for the perturbation Born scattering term, $\Gamma^{B'}$, we obtain

$$\delta\mathcal{T}_{RS} = [\gamma_{RS}] = \frac{1}{|\hat{\mathbf{n}} \cdot \hat{\mathbf{V}}_S|^{1/2} |\hat{\mathbf{n}} \cdot \hat{\mathbf{V}}_R|^{1/2}} \cdot \frac{1}{\hat{\mathbf{n}} \cdot (\mathbf{p}_S + \mathbf{p}_R)} \Gamma^{B'},$$

where now \mathbf{p}_R is in the Born direction from receiver to scatterer, and the factors $\hat{\mathbf{n}} \cdot \hat{\mathbf{V}}$ correct for the different normalizations of the polarizations. It is trivial to confirm that this general result for anisotropic, elastic media reduces to the acoustic result

$$\mathcal{T}_{RS} = \frac{\alpha}{2 \cos^2 \theta} \Gamma^{B'},$$

given above.

We now approximate the perturbation Born volume integral by the second-order, saddle-point method to show that the expected reflection is obtained. We summarize the Born integral (10.3.42) with the ray-theory approximation

$$\underline{\mathbf{u}}^{B'} = -\frac{\omega^2}{4\pi^2} \int_V \Gamma^{B'} \mathcal{D}^{(3)} e^{i\omega\tilde{T}} dV,$$

where $\Gamma^{B'}(\mathbf{x}, \mathcal{L}_R, \mathcal{L}_S)$ has been defined above. We first consider the ‘reflections’ from each plane of scatterers with z constant, and evaluate the x - y integral by the method of second-order, saddle-point method. Thus

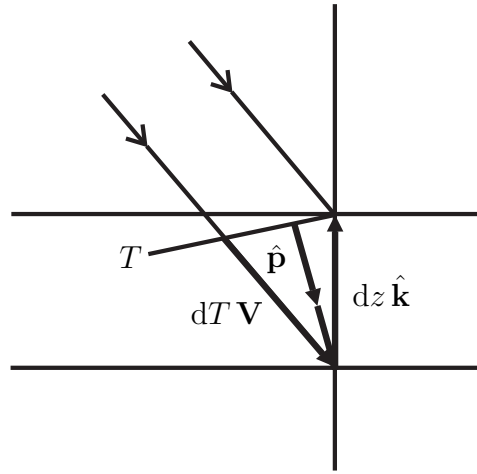
$$\underline{\mathbf{u}}^{B'} \simeq -\frac{i\omega}{2\pi} \int_{-\infty}^{z_2} e^{i\omega T(\mathbf{x}_R, \mathcal{L}_S)} \frac{\Gamma^{B'} \mathcal{D}^{(3)}}{\|\nabla_{\mathbf{q}}(\nabla_{\mathbf{q}} \tilde{T})\|^{1/2}} dz,$$

where the terms in the integrand are functions of z and are evaluated at the saddle point corresponding to the ‘reflection’ from the plane z (we assume $\text{sgn}(\nabla_{\mathbf{q}}(\nabla_{\mathbf{q}} \tilde{T})) = +2$, as usual). In order to evaluate this integral, we change the variable of integration to T and approximate by the end-point

contribution. We need the derivative dz/dT . As $\mathbf{p} = \nabla T$, this is given by

$$\frac{dT}{dz} = \hat{\mathbf{k}} \cdot \nabla T = -\hat{\mathbf{n}} \cdot (\mathbf{p}_S + \mathbf{p}_R) = -|\mathbf{p}_S + \mathbf{p}_R|$$

(note that with the direction of the z axis, dT/dz is negative. The final simplification occurs as the interface components of \mathbf{p}_R and \mathbf{p}_S cancel by Snell's law (10.4.58)). We can confirm this result by a simple geometrical construction. The figure shows the change in rays for a depth change dz . To first order we can assume that the rays are parallel (in direction $\hat{\mathbf{V}}$) and that the spectral reflection point does not move laterally. The diagram is for an anisotropic medium as the phase direction, $\hat{\mathbf{p}}$, perpendicular to the wavefront (T constant) is not in the same direction as $\hat{\mathbf{V}}$. Projecting the ray



Rays with approximately the same direction incident on reflection points dz apart, with a travel-time difference of dT . The slowness direction, $\hat{\mathbf{p}}$, normal to the wavefront, T constant, is also illustrated.

increment $dT \mathbf{V}$ and the vertical increment $dz \hat{\mathbf{k}}$ onto the phase direction $\hat{\mathbf{p}}$, we obtain

$$\hat{\mathbf{p}} \cdot \mathbf{V} dT = \hat{\mathbf{p}} \cdot \hat{\mathbf{k}} dz.$$

Thus

$$\frac{dT}{dz} = \frac{\hat{\mathbf{p}} \cdot \hat{\mathbf{k}}}{\hat{\mathbf{p}} \cdot \mathbf{V}} = \frac{\hat{\mathbf{p}} \cdot \hat{\mathbf{k}}}{V \cos \phi} = \frac{\hat{\mathbf{p}} \cdot \hat{\mathbf{k}}}{c} = \mathbf{p} \cdot \hat{\mathbf{k}},$$

using $\mathbf{p} \cdot \mathbf{V} = 1$ (5.3.32).

Thus the Born integral becomes

$$\underline{\mathbf{u}}^{\text{B}'} \simeq \frac{1}{2\pi} e^{i\omega T(\mathbf{x}_R, \mathcal{L}_S)} \frac{\Gamma^{\text{B}'} \mathcal{D}^{(3)}}{\left\| \nabla_q(\nabla_q \tilde{T}) \right\|^{1/2} \hat{\mathbf{n}} \cdot (\mathbf{p}_S + \mathbf{p}_R)},$$

where the terms are evaluated at the saddle point $\mathbf{x} = \mathbf{x}_{\text{ray}}$ when $z = z_2$. Substituting for $\Gamma^{\text{B}'}$ and $\mathcal{D}^{(3)}$ this becomes

$$\begin{aligned} \underline{\mathbf{u}}^{\text{B}'} &\simeq \frac{1}{2\pi} e^{i\omega T(\mathbf{x}_R, \mathcal{L}_S)} \mathbf{g}(\mathbf{x}_R, \mathcal{L}_S) \mathbf{g}^T(\mathbf{x}_S, \mathcal{L}_S) \mathcal{T}_{\text{RS}} \\ &\quad \times \frac{|\hat{\mathbf{n}} \cdot \hat{\mathbf{V}}_S|^{1/2} |\hat{\mathbf{n}} \cdot \hat{\mathbf{V}}_R|^{1/2} \mathcal{T}^{(3)}(\mathbf{x}_{\text{ray}}, \mathcal{L}_S) \mathcal{T}^{(3)}(\mathbf{x}_{\text{ray}}, \mathcal{L}_R)}{\left\| \nabla_q(\nabla_q \tilde{T}) \right\|^{1/2}} \\ &= \frac{1}{2\pi} e^{i\omega T(\mathbf{x}_R, \mathcal{L}_S)} \mathbf{g}(\mathbf{x}_R, \mathcal{L}_S) \mathbf{g}^T(\mathbf{x}_S, \mathcal{L}_S) \mathcal{T}_{\text{RS}} \mathcal{T}^{(3)}(\mathbf{x}_R, \mathcal{L}_S), \end{aligned}$$

apply the chain rule (5.2.55). The factors $\hat{\mathbf{n}} \cdot \hat{\mathbf{V}}$ are absorbed into the chain rule to include the dynamic effects of the ‘reflection’ at z to connect $\mathcal{T}^{(3)}(\mathbf{x}_{\text{ray}}, \mathcal{L}_S)$ and $\mathcal{T}^{(3)}(\mathbf{x}_{\text{ray}}, \mathcal{L}_R)$ infinitesimally before and after the ‘reflection’ point. Using results (5.4.19) and (6.2.15), the combination $(\hat{\mathbf{n}} \cdot \hat{\mathbf{V}})^{1/2} \mathcal{T}^{(3)} = (\hat{\mathbf{n}} \cdot \hat{\mathbf{V}}/\mathcal{S}^{(3)})^{1/2} \propto (\hat{\mathbf{n}} \cdot \mathbf{V}/cJ)^{1/2}$ is conserved at a ‘reflection’. The relationships between the spreading in the wavefront, perpendicular to the ray, and in the interface are illustrated in the figure.

Thus we obtain the correct reflection from the perturbed half space.

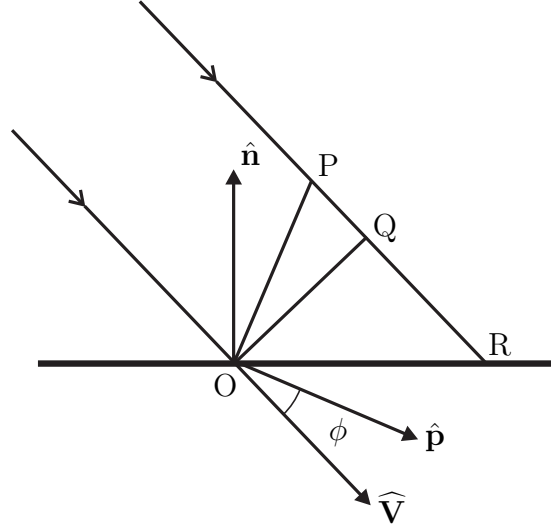
10.4

Further reading: In Section 10.3.5, we have shown that Born perturbation scattering theory predicts to lowest order the travel-time perturbation. Investigate how Born scattering theory predicts other corrections to ray theory (Coates and Chapman, 1990a; Chapman and Coates, 1994).

10.5

Confirm the result (10.3.55) for the acoustic scalar Born error scattering term, Γ^{E} .

Investigate expressions for the spatial derivatives needed in the anisotropic scalar Born error scattering term, Γ^{E} (10.3.68), and how they might be calculated.



Rays with approximately the same direction incident on an interface. The spreading in the wavefront, OP , is proportional to J (definition (5.4.10)); perpendicular to the ray, OQ , is proportional to $J \cos \phi = cJ/V$ which is proportional to $\mathcal{S}^{(3)}$ (definition (5.4.19) and relationship (6.8.7)); and in the interface, OR , is proportional to $J \cos \phi / |\hat{\mathbf{n}} \cdot \hat{\mathbf{V}}| = cJ/|\hat{\mathbf{n}} \cdot \mathbf{V}|$ which is proportional to $\mathcal{S}^{(3)}/|\hat{\mathbf{n}} \cdot \hat{\mathbf{V}}|$ (result (6.2.15)). The ratio of the spreadings OP and OR is $|\hat{\mathbf{n}} \cdot \hat{\mathbf{V}}|/\hat{\mathbf{p}} \cdot \hat{\mathbf{V}}$.

Investigate the simplifications that occur in the Born scattering terms, Γ^E (10.3.68) and Γ^B (10.3.78), in isotropic media.

From equation (10.3.52), we have the definition

$$\underline{\mathcal{K}}^E = -\frac{1}{2} \left(\underline{\mathbf{v}}_R^T \nabla \underline{P}_S - \underline{P}_R^T \nabla \cdot \underline{\mathbf{v}}_S + (\nabla \underline{P}_R)^T \underline{\mathbf{v}}_S - (\nabla \cdot \underline{\mathbf{v}}_R)^T \underline{P}_S \right),$$

where we have simplified the notation by dropping the suffix $^{(0)}$, and replacing the arguments $(\mathbf{x}, \mathcal{L}_S)$ and $(\mathbf{x}, \mathcal{L}_R)$ by subscripts S and R , respectively. The ray amplitude coefficients are given by equation (5.4.31) with (5.4.33) which are notationally simplified to

$$\begin{aligned} \underline{\mathbf{v}}_S &= 2^{-1/2} \hat{\mathbf{g}}_S Z^{-1/2} \left(\mathcal{T}_S \mathbf{g}^T(\mathbf{x}_S, \mathcal{L}_S) \right) \\ \underline{P}_S &= 2^{-1/2} Z^{1/2} \left(\mathcal{T}_S \mathbf{g}^T(\mathbf{x}_S, \mathcal{L}_S) \right). \end{aligned}$$

The required derivatives are

$$\nabla \cdot \underline{\mathbf{v}}_S = 2^{-1/2} \left(\nabla \cdot \hat{\mathbf{g}}_S - \hat{\mathbf{g}}_S^T \nabla (\ln Z)/2 + \hat{\mathbf{g}}_S^T \nabla (\ln \mathcal{T}_S) \right)$$

$$\times Z^{-1/2} \left(\mathcal{T}_S \mathbf{g}^T(\mathbf{x}_S, \mathcal{L}_S) \right) \\ \nabla P_S = 2^{-1/2} \left(\nabla(\ln Z)/2 + \nabla(\ln \mathcal{T}_S) \right) Z^{1/2} \left(\mathcal{T}_S \mathbf{g}^T(\mathbf{x}_S, \mathcal{L}_S) \right),$$

where we have ignored differentials of the source polarization, $\mathbf{g}(\mathbf{x}_S, \mathcal{L}_S)$ (and will also ignore differentials of the receiver polarization). Substituting in the above expression for $\underline{\mathbf{K}}^E$, the factors $2^{-1/2}$ combine to give another $1/2$, the factors $Z^{\pm 1/2}$ cancel, and the factor $\mathcal{T}_S \mathbf{g}^T(\mathbf{x}_S, \mathcal{L}_S)$ goes into the function $\underline{\mathbf{D}}$ (together with the similar factor from the receiver rays). Combining the factors in the brackets for the source and receiver rays, we obtain result (10.3.55)

$$\Gamma^E = \frac{1}{4} \left(\nabla(\ln Z) - \nabla \right) \cdot (\hat{\mathbf{g}}_R + \hat{\mathbf{g}}_S) - \frac{1}{4} \nabla \left(\ln \frac{\mathcal{T}_R}{\mathcal{T}_S} \right) \cdot (\hat{\mathbf{g}}_R - \hat{\mathbf{g}}_S).$$

For acoustic waves the polarizations are the same as the ray direction, i.e. $\hat{\mathbf{g}} = \hat{\mathbf{p}}$, and are obtained directly from the kinematic ray equations. The gradient $\nabla(\ln Z)$ is obtained from the model. The divergence of the polarizations is obtained from the wavefront curvature, K (5.6.11) and Exercise 5.5

$$\nabla \cdot \hat{\mathbf{p}} = K.$$

The final term is normally small. For zero-offset seismograms it is exactly zero as $\mathcal{T}_R = \mathcal{T}_S$ and $\hat{\mathbf{g}}_R = \hat{\mathbf{g}}_S$. In general, we will have to estimate $\nabla \ln(\mathcal{T}_R/\mathcal{T}_S)$ numerically as it depends on higher derivatives of the ray equations. Changes of \mathcal{T} in the wavefront will depend on derivatives of the dynamic ray equations. Changes of \mathcal{T} in the ray direction are described by the dynamic ray equations. \mathcal{T} is proportional to the inverse square-root of the spreading function \mathcal{S} (equation (5.4.34)) which in turn is proportional to cross-section function J (equation (5.2.67)). Exercise 5.5 has given a simple expression for the derivative of J along the ray

$$\frac{dJ}{ds} = JK.$$

Then above expression can be written

$$\begin{aligned} \Gamma^E &= \frac{1}{4} (\hat{\mathbf{p}}_R + \hat{\mathbf{p}}_S) \cdot \nabla \ln Z - \frac{1}{4} (K_R + K_S) \\ &\quad - \frac{1}{8} (\hat{\mathbf{p}}_R - \hat{\mathbf{p}}_S) \cdot \nabla \ln(J_S/J_R) \\ &= \frac{1}{4} (\hat{\mathbf{p}}_R + \hat{\mathbf{p}}_S) \cdot \nabla \ln Z - \frac{1}{8} (K_R + K_S)(1 + c) \\ &\quad - \frac{1}{8} (\hat{\mathbf{p}}_R - \hat{\mathbf{p}}_S) \cdot \left((\mathbf{I} - \hat{\mathbf{p}}_S \hat{\mathbf{p}}_S^T) \nabla \ln J_S - (\mathbf{I} - \hat{\mathbf{p}}_R \hat{\mathbf{p}}_R^T) \nabla \ln J_R \right), \end{aligned}$$

where $c = \hat{\mathbf{p}}_R \cdot \hat{\mathbf{p}}_S$. While the final expression looks more complicated, it has

been written in this manner to separate into the final term, the gradients in the wavefront, $(\mathbf{I} - \hat{\mathbf{p}}\hat{\mathbf{p}}^T)\nabla \ln J$, which without higher-order ray equations, can only be estimated numerically.

To evaluate the general expression for the Born error scattering term in anisotropic media (10.3.68), we need spatial derivatives of the polarizations, \mathbf{g} , the impedances, \mathbf{Z}_j , and the propagation factors, \mathcal{T} . The partial derivatives of the polarizations can be calculated by perturbation theory of the Christoffel equation. Perturbations in the slowness vector can be obtained from the paraxial results (5.2.46) and the kinematic ray equation (5.3.5). Partial derivatives of the ray velocity, needed for the derivatives of the normalized polarizations, can be obtained using the results of Exercise 5.1. Together with the spatial derivatives of the model parameters, density, ρ , and stiffnesses, \mathbf{c}_{jk} , these allow the required derivatives to be calculated although the expressions are sufficiently complicated that we have not attempted to give them here. The derivatives of the propagation factors, \mathcal{T} , can only be estimated numerically unless higher-order ray equations are solved.

In order to efficiently obtain the simplifications of the Born scattering terms, Γ^E (10.3.68) and Γ^B (10.3.78), in isotropic media, we must use vector-matrix notation. In Exercise 5.6, we have proved results (5.5.7) and (5.5.9)

$$\begin{aligned}\mathbf{Z}_j \hat{\mathbf{g}}_3 &= \frac{1}{\alpha} (2\mu \hat{\mathbf{p}} \hat{\mathbf{p}}^T + \lambda \mathbf{I}) \hat{\mathbf{i}}_j \\ \mathbf{Z}_j \hat{\mathbf{g}}_\nu &= \frac{\mu}{\beta} (\hat{\mathbf{p}} \hat{\mathbf{g}}_\nu^T + \hat{\mathbf{g}}_\nu \hat{\mathbf{p}}^T) \hat{\mathbf{i}}_j,\end{aligned}$$

that can be used for the traction vectors. The tractions corresponding the energy-normalized polarizations, \mathbf{g} (5.4.33), can be written

$$\mathbf{t}_j(\mathbf{g}) = -2^{-1/2} Z^{1/2} \mathbf{d}_j,$$

where $Z = \rho\alpha$ or $\rho\beta$, the P or S impedance (5.2.8), and

$$\begin{aligned}\mathbf{d}_j(\hat{\mathbf{p}}, \hat{\mathbf{g}}) &= \left(\mathbf{I} - \frac{2\beta^2}{\alpha^2} (\mathbf{I} - \hat{\mathbf{p}}\hat{\mathbf{p}}^T) \right) \hat{\mathbf{i}}_j \quad \text{for } P \text{ rays} \\ &= (\hat{\mathbf{p}}\hat{\mathbf{g}}^T + \hat{\mathbf{g}}\hat{\mathbf{p}}^T) \hat{\mathbf{i}}_j \quad \text{for } S \text{ rays}.\end{aligned}$$

The Born error scattering kernel, $\underline{\mathbf{K}}^E$ (10.3.67), is compactly written

$$\underline{\mathbf{K}}^E = \frac{1}{2} \left(\mathbf{v}_R^T \frac{\partial \mathbf{t}_{jS}}{\partial x_j} - \mathbf{t}_{jR}^T \frac{\partial \mathbf{v}_S}{\partial x_j} + \frac{\partial \mathbf{t}_{jR}^T}{\partial x_j} \mathbf{v}_S - \frac{\partial \mathbf{v}_R^T}{\partial x_j} \mathbf{t}_{jS} \right),$$

where the arguments $(\mathbf{x}, \mathcal{L}_R)$ and $(\mathbf{x}, \mathcal{L}_S)$ have been abbreviated as subscripts

\mathbf{r} and \mathbf{s} , respectively. Using the above expressions, the Green solutions are

$$\begin{aligned}\mathbf{v}_\mathbf{s} &= 2^{-1/2} Z_\mathbf{s}^{-1/2} \hat{\mathbf{g}}_\mathbf{s} \left(\mathcal{T}_\mathbf{s} \mathbf{g}^\mathbf{T}(\mathbf{x}_\mathbf{s}, \mathcal{L}_\mathbf{s}) \right) \\ \mathbf{t}_{j\mathbf{s}} &= -2^{-1/2} Z_\mathbf{s}^{1/2} \mathbf{d}_{j\mathbf{s}} \left(\mathcal{T}_\mathbf{s} \mathbf{g}^\mathbf{T}(\mathbf{x}_\mathbf{s}, \mathcal{L}_\mathbf{s}) \right),\end{aligned}$$

and similarly for the receiver functions, where the final factor in parentheses will form part of $\mathbf{D}^{(\ell)}$ (10.3.54). Substituting in $\mathbf{K}^\mathbf{E}$, we obtain the scalar Born error scattering term (10.3.68)

$$\begin{aligned}\Gamma^\mathbf{E} = & \frac{1}{4} \left(\left(\frac{Z_\mathbf{R}}{Z_\mathbf{S}} \right)^{1/2} \left((\mathbf{d}_{j\mathbf{R}}^\mathbf{T} \hat{\mathbf{g}}_\mathbf{S}) \frac{\partial}{\partial x_j} \ln(Z_\mathbf{S} Z_\mathbf{R})^{1/2} \frac{\mathcal{T}_\mathbf{R}}{\mathcal{T}_\mathbf{S}} + \frac{\partial \mathbf{d}_{j\mathbf{R}}^\mathbf{T}}{\partial x_j} \hat{\mathbf{g}}_\mathbf{S} - \mathbf{d}_{j\mathbf{R}}^\mathbf{T} \frac{\partial \hat{\mathbf{g}}_\mathbf{S}}{\partial x_j} \right) \right. \\ & \left. + \left(\frac{Z_\mathbf{R}}{Z_\mathbf{S}} \right)^{1/2} \left((\hat{\mathbf{g}}_\mathbf{R}^\mathbf{T} \mathbf{d}_{j\mathbf{S}}) \frac{\partial}{\partial x_j} \ln(Z_\mathbf{S} Z_\mathbf{R})^{1/2} \frac{\mathcal{T}_\mathbf{S}}{\mathcal{T}_\mathbf{R}} + \hat{\mathbf{g}}_\mathbf{R}^\mathbf{T} \frac{\partial \mathbf{d}_{j\mathbf{S}}}{\partial x_j} - \frac{\partial \hat{\mathbf{g}}_\mathbf{R}^\mathbf{T}}{\partial x_j} \mathbf{d}_{j\mathbf{S}} \right) \right).\end{aligned}$$

In order to evaluate this expression, we need spatial derivatives of the ray direction and the polarizations.

The derivatives of the ray direction, $\hat{\mathbf{p}}$ (or longitudinal polarization, $\hat{\mathbf{g}}_3$), are obtained in the ray direction from the kinematic ray equation (5.1.15) or result (5.6.9), and in the wavefront from the paraxial result (5.2.46) with (5.2.47) and (5.2.48). Combining these we have

$$\nabla^\mathbf{T} \hat{\mathbf{p}} = - \left(\hat{\mathbf{g}}_\nu \cdot \nabla \ln c \right) \hat{\mathbf{g}}_\nu \hat{\mathbf{p}}^\mathbf{T} + \mathbf{K},$$

where $\nabla^\mathbf{T} \hat{\mathbf{p}}$ is the 3×3 matrix with ij -th element $\partial \hat{p}_i / \partial x_j$ (strictly in vector-matrix notation, it should be written $(\nabla \hat{\mathbf{p}}^\mathbf{T})^\mathbf{T}$). The j -th column is

$$\frac{\partial \hat{\mathbf{p}}}{\partial x_j} = (\hat{\mathbf{i}}_j \cdot \hat{\mathbf{p}}) (\hat{\mathbf{p}} \hat{\mathbf{p}}^\mathbf{T} - \mathbf{I}) \nabla \ln c + \mathbf{K} \hat{\mathbf{i}}_j,$$

and the trace is

$$\text{tr}(\nabla^\mathbf{T} \hat{\mathbf{p}}) = \nabla \cdot \hat{\mathbf{p}} = K,$$

as given in equation (5.6.11) and proved in Exercise 5.5. We have used the identities

$$\begin{aligned}\hat{\mathbf{p}} \hat{\mathbf{p}}^\mathbf{T} + \hat{\mathbf{g}}_\nu \hat{\mathbf{g}}_\nu^\mathbf{T} &= \mathbf{I} \\ \hat{\mathbf{g}}_\nu \cdot \hat{\mathbf{p}} &= 0.\end{aligned}$$

For the spatial derivatives of the transverse polarizations, $\hat{\mathbf{g}}_\nu$, we have result (5.6.8) for derivatives in the ray direction. In the wavefront, $\hat{\mathbf{g}}_\nu$ changes to remain perpendicular to the ray direction. Combining, we have

$$\nabla^\mathbf{T} \hat{\mathbf{g}}_\nu = \left(\hat{\mathbf{g}}_\nu \cdot \nabla \ln c \right) \hat{\mathbf{p}} \hat{\mathbf{p}}^\mathbf{T} - \hat{\mathbf{p}} \hat{\mathbf{g}}_\nu^\mathbf{T} \mathbf{K}.$$

The j -th column is

$$\frac{\partial \hat{\mathbf{g}}_\nu}{\partial x_j} = (\hat{\mathbf{i}}_j \cdot \hat{\mathbf{p}})(\hat{\mathbf{g}}_\nu \cdot \nabla \ln c) \hat{\mathbf{p}} - \hat{\mathbf{p}} \hat{\mathbf{g}}_\nu^T \mathbf{K} \hat{\mathbf{i}}_j,$$

and the trace is

$$\text{tr}(\nabla^T \hat{\mathbf{g}}_\nu) = \nabla \cdot \hat{\mathbf{g}}_\nu = \hat{\mathbf{g}}_\nu \cdot \nabla \ln c,$$

as given in equation (5.6.10) and proved in Exercise 5.5.

In order to write relatively compact expressions for the scattering term Γ^E , we define

$$\begin{aligned} u &= \beta^2/\alpha^2 \quad \text{cf. equation (9.1.60)} \\ \overline{\mathbf{p}} &= \frac{1}{2}(\hat{\mathbf{p}}_R + \hat{\mathbf{p}}_S) \\ \overline{K} &= \frac{1}{2}(K_R + K_S). \end{aligned}$$

The scattering term, Γ^E , depends on the source and receiver ray types. After considerable algebra we find the scattering for $P \rightarrow P$ is

$$\begin{aligned} \Gamma^E &= \frac{1}{2} \left((1 - 2u + 2uc) \overline{\mathbf{p}} \cdot \nabla \ln Z_\alpha - 4uc \overline{\mathbf{p}} \cdot \nabla \ln \beta \right. \\ &\quad \left. - 2u(1 - 4c + c^2) \overline{\mathbf{p}} \cdot \nabla \ln \alpha - (1 - 2u - 2uc) \overline{\mathbf{p}} \cdot \nabla \ln \frac{T_R}{T_S} \right. \\ &\quad \left. - (1 - 2uc) \overline{K} \right). \end{aligned}$$

It is straightforward to show that this reduces to the acoustic expression (10.3.55) when $u = \beta = 0$.

When shear waves are involved, there are more angle cosines than just $c = \hat{\mathbf{p}}_R \cdot \hat{\mathbf{p}}_S$. We need the scalar products of the direction and polarization of the source and receiver rays. We write these as

$$\begin{pmatrix} \hat{\mathbf{p}}_R^T \\ \hat{\mathbf{g}}_R^T \end{pmatrix} \begin{pmatrix} \hat{\mathbf{p}}_S & \hat{\mathbf{g}}_S \end{pmatrix} = \begin{pmatrix} a & b \\ c & d \end{pmatrix}.$$

In the $P \rightarrow P$ case, $a = b = c = d$. In the $S \rightarrow S$ case, all elements are different although there are only three independent angles (say the opening angle and rotations of the shear polarizations relative to the direction plane). In the $P \rightarrow S$ case, $a = b$ and $c = d$ and there are two independent angles, the opening angle and a rotation angle of the shear polarization from the direction plane. Similarly in the $S \rightarrow P$ case $a = c$ and $b = d$ with two independent angles.

The expression for $S \rightarrow S$ scattering is

$$\begin{aligned}\Gamma^E &= \frac{1}{4} \left(b\hat{\mathbf{g}}_R^T(\mathbf{K}_R\hat{\mathbf{p}}_S + 2(1-a)\nabla \ln \beta) + \hat{\mathbf{g}}_S^T(\mathbf{K}_R + a\mathbf{K}_S)\hat{\mathbf{g}}_R \right. \\ &\quad + c\hat{\mathbf{g}}_S^T(\mathbf{K}_S\hat{\mathbf{p}}_R + 2(1-a)\nabla \ln \beta) + \hat{\mathbf{g}}_R^T(\mathbf{K}_S + a\mathbf{K}_R)\hat{\mathbf{g}}_S \\ &\quad \left. + 2d(\overline{\mathbf{K}} + \overline{\mathbf{p}} \cdot \nabla \ln \beta) \right).\end{aligned}$$

The expression for $P \rightarrow S$ scattering is

$$\begin{aligned}\Gamma^E &= \frac{1}{4} \left(\frac{Z_\beta}{Z_\alpha} \right)^{1/2} \left((c\hat{\mathbf{p}}_R + a\hat{\mathbf{g}}_R) \cdot \nabla \ln(Z_\alpha Z_\beta)^{1/2} \frac{\mathcal{T}_R}{\mathcal{T}_S} \right. \\ &\quad + 2b\hat{\mathbf{g}}_R \cdot \nabla \ln \beta - 2ac\hat{\mathbf{p}}_S \cdot \nabla \ln \alpha \\ &\quad + d\hat{\mathbf{p}}_R \cdot \nabla \ln \beta + a\hat{\mathbf{g}}_R \cdot \nabla \ln \alpha + c\hat{\mathbf{p}}_R \cdot \nabla \ln \alpha \\ &\quad \left. + \hat{\mathbf{g}}_S^T \mathbf{K}_R \hat{\mathbf{g}}_R + dK_R - \hat{\mathbf{g}}_R^T \mathbf{K}_S \hat{\mathbf{p}}_R - \hat{\mathbf{p}}_R^T \mathbf{K}_S \hat{\mathbf{g}}_R \right) \\ &\quad + \frac{1}{4} \left(\frac{Z_\alpha}{Z_\beta} \right)^{1/2} \left(((1-2u)\hat{\mathbf{g}}_R + 2ua\hat{\mathbf{p}}_S) \cdot \nabla \ln(Z_\alpha Z_\beta)^{1/2} \frac{\mathcal{T}_S}{\mathcal{T}_R} \right. \\ &\quad - 2u\hat{\mathbf{g}}_R \cdot \nabla \ln u\alpha + 2uc\hat{\mathbf{p}}_S \cdot \nabla \ln \alpha + 2ucK_S \\ &\quad \left. - (1-2u+2ua^2)\hat{\mathbf{g}}_R \cdot \nabla \ln \beta + 2ua\hat{\mathbf{g}}_R^T \mathbf{K}_R \hat{\mathbf{p}}_S \right)\end{aligned}$$

A similar expression for $S \rightarrow P$ is obtained by interchanging the source and receiver subscripts. It is possible (and desirable) that more compact forms of these expressions can be obtained.

For the Born perturbation result, we need the isotropic stiffness or compliance matrices. In isotropic media, the stiffness matrices, \mathbf{c}_{jk} (4.4.55) and (4.4.56), can be written

$$\mathbf{c}_{jk} = \lambda \hat{\mathbf{i}}_j \hat{\mathbf{i}}_k^T + \mu(\delta_{jk} \mathbf{I} + \hat{\mathbf{i}}_k \hat{\mathbf{i}}_j^T).$$

The corresponding compliance matrices \mathbf{s}_{jk} (4.4.57) and (4.4.58), are

$$\mathbf{s}_{jk} = \ell \hat{\mathbf{i}}_j \hat{\mathbf{i}}_k^T + m(\delta_{jk} \mathbf{I} + \hat{\mathbf{i}}_k \hat{\mathbf{i}}_j^T),$$

where

$$\begin{aligned}\ell &= -\frac{\lambda}{2\mu(3\lambda + 2\mu)} \\ m &= \frac{1}{4\mu}.\end{aligned}$$

Although it is not obvious from these expressions, they can be used in the fluid limit with $\mu = m = 0$ and $\lambda = \kappa$, the bulk modulus, and $\ell = k/9$, where $k = 1/\kappa$, the compressibility (see equation (4.4.4) and Exercise 4.12).

The scalar Born perturbation scattering term, Γ^B (10.3.78), can be compactly written

$$\begin{aligned}\Gamma^B &= \hat{\mathbf{g}}_R^T \left(\rho^B - \mathbf{Z}_{kR}^T \mathbf{s}_{kj}^B \mathbf{Z}_{jS} \right) \hat{\mathbf{g}}_S \\ &= \frac{1}{2} \left(\frac{d\rho^B}{(Z_R Z_S)^{1/2}} - (Z_R Z_S)^{1/2} \mathbf{d}_{kR}^T \mathbf{s}_{kj}^B \mathbf{d}_{jS} \right),\end{aligned}$$

where the subscripts R and S have been used for the arguments $(\mathbf{x}, \mathcal{L}_R)$ and $(\mathbf{x}, \mathcal{L}_S)$, respectively. We have used the above notation for the isotropic expression, where the source and receiver subscripts imply the correct choice of P or S expressions. Using the above expression for \mathbf{s}_{jk}^B , with perturbations ℓ^B and m^B , it is then reasonably easy to simplify these expressions. Different results apply, of course, for different source and receiver ray types:

$$\begin{aligned}\Gamma^B &= \frac{a\rho^B}{4\rho\alpha} - \frac{1}{\rho\alpha^3} \left(\ell^B(3\lambda + 2\mu)^2 \right. \\ &\quad \left. + 2m^B \left(a\mu^2 + 4\mu\lambda + 3\lambda^2 \right) \right) \quad \text{for } P \rightarrow P \\ &= \frac{d\rho^B}{4\rho\beta} - 4\rho\beta m^B(ad + bc) \quad \text{for } S \rightarrow S \\ &= \frac{d\rho^B}{4\rho(\alpha\beta)^{1/2}} - 8\rho(\alpha\beta)^{1/2} \frac{\beta^2}{\alpha^2} abm^B \quad \text{for } S \rightarrow P \\ &= \frac{d\rho^B}{4\rho(\alpha\beta)^{1/2}} - 8\rho(\alpha\beta)^{1/2} \frac{\beta^2}{\alpha^2} acm^B \quad \text{for } P \rightarrow S.\end{aligned}$$

Note that the expression for $P \rightarrow P$ scattering reduces to the acoustic expression (10.3.72) if $m^B = 0$ as $\ell^B = k^B/9$.

10.6

For a free acoustic surface, show that the Kirchhoff surface integral method is robust to the numerical specification of the shape of the interface, i.e. the surface can be represented as a smooth curve or a staircase and provided the steps are small compared with the wavelength, approximately the same results are obtained. This result depends on the reflection coefficient

being independent of angle, and a similar result is not available for general interfaces.

The Kirchhoff integral result is (10.4.9)

$$\mathbf{u}^K = -\frac{i\omega}{4\pi^2} \int_{S'} \Gamma^K \mathbf{D}^{(3)} e^{i\omega\tilde{T}} dS',$$

where for brevity we have omitted the argument $(\mathbf{x}, \mathcal{L}_S, \mathcal{L}_R)$ for Γ^K , $\mathbf{D}^{(3)}$ and \tilde{T} . For an acoustic reflection from a free surface, the scalar Kirchhoff scattering term is (10.4.12)

$$\begin{aligned} \Gamma^K &= \frac{1}{2} \mathcal{T}_{RS} (\cos \theta_R + \cos \theta_S) \\ &= -\frac{1}{2} (\hat{\mathbf{g}}_S(\mathbf{x}, \mathcal{L}_S) + \hat{\mathbf{g}}(\mathbf{x}, \mathcal{L}_R)) \cdot \hat{\mathbf{n}}, \end{aligned}$$

where we have used equations (10.4.13), (10.4.14), $\hat{\mathbf{g}}_R(\mathbf{x}, \mathcal{L}_S) \cdot \hat{\mathbf{n}} = -\hat{\mathbf{g}}_S(\mathbf{x}, \mathcal{L}_S) \cdot \hat{\mathbf{n}}$, and the free-surface reflection coefficient, $\mathcal{T}_{RS} = -1$ (6.4.2). The vectors and angles are illustrated in Figure 10.30. Substituting in the Kirchhoff integral, we obtain

$$\mathbf{u}^K = \frac{i\omega}{8\pi^2} \int_{S'} \mathbf{D}^{(3)} e^{i\omega\tilde{T}} (\hat{\mathbf{g}}_S(\mathbf{x}, \mathcal{L}_S) + \hat{\mathbf{g}}(\mathbf{x}, \mathcal{L}_R)) \cdot d\mathbf{S}',$$

where $d\mathbf{S}' = \hat{\mathbf{n}} dS'$.

Let us now consider a small element of the surface, $\Delta S'$, which may be represented by two slightly different surfaces, $\Delta S'_1$ and $\Delta S'_2$, e.g. one might be a staircase and the other, a linear interpolation (we assume that the two representations share perimeters). We assume that the surfaces are close enough together that the factors $\mathbf{D}^{(3)}$, \tilde{T} , $\hat{\mathbf{g}}_S$ and $\hat{\mathbf{g}}$ can be taken as constant in the volume between the two surfaces (they do not depend on the surfaces). Applying the divergence theorem to this volume, the volume integral is zero so

$$\begin{aligned} \int_{\Delta S'_1} \mathbf{D}^{(3)} e^{i\omega\tilde{T}} (\hat{\mathbf{g}}_S(\mathbf{x}, \mathcal{L}_S) + \hat{\mathbf{g}}(\mathbf{x}, \mathcal{L}_R)) \cdot d\mathbf{S}' = \\ \int_{\Delta S'_2} \mathbf{D}^{(3)} e^{i\omega\tilde{T}} (\hat{\mathbf{g}}_S(\mathbf{x}, \mathcal{L}_S) + \hat{\mathbf{g}}(\mathbf{x}, \mathcal{L}_R)) \cdot d\mathbf{S}' \end{aligned}$$

(the total surface integral is zero with the surface normal defined consistently outwards, but we define \mathbf{S}' from the ray directions — Figure 10.30). Thus the Kirchhoff integral does not depend on geometrical details of the surface, e.g. its slope, but only on its position (provided the volume between different surface representations is small). The significance of this result is that it

means that the Kirchhoff integral result for acoustic reflections from a free surface is numerically robust — very similar results are obtained whether the surface is represented as a staircase, a ramp or something smoother.

The crucial part of this result is that for an acoustic reflection from a free surface, $\mathcal{T}_{\text{RS}} = -1$ (6.4.2), i.e. the reflection coefficient is independent of incident angle, and hence independent of the surface orientation. This is not true for more general reflections and the robustness result appears not to exist.

10.7

Show that expression (10.3.55) for the acoustic Born error term can be reduced to

$$\Gamma^{\text{E}}(\mathbf{x}, \mathcal{L}_{\text{R}}, \mathcal{L}_{\text{S}}) = \frac{1}{4} \left(\hat{\mathbf{g}}(\mathbf{x}, \mathcal{L}_{\text{R}}) + \hat{\mathbf{g}}(\mathbf{x}, \mathcal{L}_{\text{S}}) \right) \nabla \ln \left(Z(\mathbf{x}) \mathcal{T}^{(\ell)}(\mathbf{x}, \mathcal{L}_{\text{R}}) \mathcal{T}^{(\ell)}(\mathbf{x}, \mathcal{L}_{\text{S}}) \right).$$

The scalar Born error acoustic scattering term contains the divergence of the normalized polarizations, $\hat{\mathbf{g}}$, and the gradient of the ray scalar amplitude, \mathcal{T} (5.4.34). These are related.

Poynting's vector (5.2.6) gives

$$\nabla \cdot \left(P^{(0)} \mathbf{v}^{(0)} \right) = 0,$$

and substituting for the ray dyadic (5.4.31) with (5.4.33) this reduces to

$$\nabla \cdot \left(\mathcal{T}^2 \hat{\mathbf{g}} \right) = 0,$$

assuming the source terms are isotropic. As a check, let us expand giving

$$\begin{aligned} \nabla \cdot \hat{\mathbf{g}} &= -\hat{\mathbf{g}} \cdot \nabla (\ln \mathcal{T}^2) \\ &= \hat{\mathbf{g}} \cdot \nabla (\ln \mathcal{R}^2) \\ &= \hat{\mathbf{g}} \cdot \nabla (\ln J). \end{aligned}$$

as the scalar ray amplitude is inversely proportional to the effective ray length, \mathcal{R} (5.4.34) with (5.2.72), and inversely proportional to the square root of the ray tube cross-section, J (5.2.13) (the impedance factor Z in equation (5.2.13) is part of the receiver normalization in \mathbf{g} , (5.4.31) with (5.4.33), not the transmission term, \mathcal{T} (5.4.34)). These results are consistent with those in Exercise 5.5

$$\nabla \cdot \hat{\mathbf{p}} = K,$$

and

$$\frac{dJ}{ds} = JK,$$

where K is the wavefront curvature, i.e.

$$\nabla \cdot \hat{\mathbf{g}} = K = \frac{d}{ds} (\ln J) = \hat{\mathbf{g}} \cdot \nabla (\ln J).$$

They are easily checked for a spherical wavefront in a homogeneous medium with $\mathcal{R} = r$, $\hat{\mathbf{g}} = \hat{\mathbf{r}}$, $K = 2/r$ and $\nabla \cdot \hat{\mathbf{r}} = 2/r$.

The scalar Born error acoustic scattering term (10.3.55) is

$$\Gamma^E = \frac{1}{4} \left(\nabla \ln Z - \nabla \right) \cdot (\hat{\mathbf{g}}^R + \hat{\mathbf{g}}^S) - \frac{1}{4} \left(\nabla \ln \frac{\mathcal{T}^R}{\mathcal{T}^S} \right) \cdot (\hat{\mathbf{g}}^R - \hat{\mathbf{g}}^S).$$

For brevity, we omit the arguments and indicate the source/receiver rays by a superscript, i.e. $\mathbf{g}(\mathbf{x}, \mathcal{L}_S) = \mathbf{g}^S$. Substituting for the divergence of the polarization, this reduces to

$$\Gamma^E = \frac{1}{4} (\hat{\mathbf{g}}^R + \hat{\mathbf{g}}^S) \cdot \nabla \ln(Z \mathcal{T}^R \mathcal{T}^S),$$

the required elegant, symmetric result.

10.8

Show that expression (10.3.78) can be reduced to

$$\begin{aligned} \Gamma^B(\mathbf{x}, \mathcal{L}_R, \mathcal{L}_S) = \\ \mathbf{g}^T(\mathbf{x}, \mathcal{L}_R) \rho^B(\mathbf{x}) \mathbf{g}(\mathbf{x}, \mathcal{L}_S) + \boldsymbol{\Theta}(\mathbf{x}, \mathcal{L}_R) : \mathbf{c}^B(\mathbf{x}) : \boldsymbol{\Theta}(\mathbf{x}, \mathcal{L}_S), \end{aligned}$$

where

$$\boldsymbol{\Theta}(\mathbf{x}, \mathcal{L}) = \frac{1}{2} \left(\mathbf{p}(\mathbf{x}, \mathcal{L}) \mathbf{g}^T(\mathbf{x}, \mathcal{L}) + \mathbf{g}(\mathbf{x}, \mathcal{L}) \mathbf{p}^T(\mathbf{x}, \mathcal{L}) \right),$$

is a symmetric dyadic (related to the time-integral of the energy-normalized strain) formed from the ray slowness and energy-normalized polarization, and the shorthand notation $(:)$ indicates contraction of the fourth-order stiffness perturbation tensor with the dyadics of the source and receiver rays.

The first term involving the density perturbation is identical, so we only consider the second term. For brevity, we omit the arguments and indicate the source/receiver rays by a superscript, i.e. $\mathbf{g}(\mathbf{x}, \mathcal{L}_S) = \mathbf{g}^S$. Using subscript notation, the scalar of interest is

$$-\mathbf{g}^{R^T} \mathbf{Z}_k^{R^T} \mathbf{s}_{kj}^B \mathbf{Z}_j^S \mathbf{g}^S = -g_a^R \left(\mathbf{Z}_k^R \right)_{ba} \left(\mathbf{s}_{kj}^B \right)_{bc} \left(\mathbf{Z}_j^S \right)_{cd} g_d^S$$

$$\begin{aligned}
&= -g_a^R (p_m^R c_{ambk}) s_{bkcj}^B (p_l^S c_{cjd}^S) g_d^S \\
&= -(g_a p_m)^R (p_l g_d)^S (c_{ambk} s_{bkcj}^B c_{cjd}^S),
\end{aligned}$$

where, of course, we have assumed the Einstein summation convention over the repeated indices j and k , and a , b , c and d , and used definitions (5.3.22) and (4.4.37).

We denote the second-order, symmetric tensor by Θ where

$$\Theta_{ij} = \frac{1}{2}(g_i p_j + g_j p_i) \quad \text{or} \quad \Theta = \frac{1}{2}(\mathbf{g} \mathbf{p}^T + \mathbf{p} \mathbf{g}^T)$$

(this symbol is used as overwriting g and p looks like θ , and its trace is related to the dilatation (4.2.8)).

Differentiating expression (4.4.43), we have

$$c_{ijpq}^B s_{pqrs} + c_{ijpq} s_{pqrs}^B = 0,$$

to first-order. Thus

$$\begin{aligned}
c_{ambk} s_{bkcj}^B c_{cjd}^S &= -c_{ambk}^B s_{bkcj} c_{cjd}^S \\
&= -c_{ambk}^B \frac{1}{2} (\delta_{bd} \delta_{kl} + \delta_{bl} \delta_{kd}) \\
&= -c_{amdl}^B,
\end{aligned}$$

using expression (4.4.43) and symmetries again. Thus the term of interest is

$$\begin{aligned}
-\mathbf{g}^{RT} \mathbf{Z}_k^{RT} \mathbf{s}_{kj}^B \mathbf{Z}_j^S \mathbf{g}^S &= \Theta_{am}^R c_{amdl}^B \Theta_{dl}^S \\
&= \Theta^R : \mathbf{c}^B : \Theta^S,
\end{aligned}$$

using the shorthand notation, which is the required result. With this expression, we can easily obtain the special forms in isotropic and TIV media.

The early publications on the Born approximation in elastic media (Bhattachia, 1959; Miles, 1960) only discussed isotropic media. Hudson and Heritage (1981) gave the general anisotropic result, and substituting the ray Green function in their equation (3) would reduce to the above result. Ben-Menahem and Gibson (1990) considered TIV media and Gibson and Ben-Menahem (1991) generalized this. More recently, Burridge, de Hoop, Miller and Spencer (1998) have given an expression very similar to ours, i.e. their equation (3.28) with the dyadics (3.25) and (3.26).

Rather than use the tensor notation, where Θ is 3×3 and \mathbf{c} is $3 \times 3 \times 3 \times 3$, it is convenient to use a vector-matrix notation. Rather than use the usual 6×6 Voigt matrix notation (4.4.13), it is more convenient to use the expanded 9×9 form as this avoids complications with factors of 2, etc.

Francis Muir (FM) has described this as the “Full Monty” (FM) notation! The symmetries that reduce the order of the system to sixth from ninth are implicitly included through equality of terms rather than explicitly through the reduction. See Exercise 4.12 but here we follow Muir’s ordering of the components in order to emphasize the isotropic and TIV symmetries. The 9×9 stiffness matrix is written

$$\mathbf{C} = \begin{pmatrix} C_{11} & C_{12} & C_{13} & \vdots & C_{14} & C_{14} & \vdots & C_{15} & C_{15} & \vdots & C_{16} & C_{16} \\ C_{12} & C_{22} & C_{23} & \vdots & C_{24} & C_{24} & \vdots & C_{25} & C_{25} & \vdots & C_{26} & C_{26} \\ C_{13} & C_{23} & C_{33} & \vdots & C_{34} & C_{34} & \vdots & C_{35} & C_{35} & \vdots & C_{36} & C_{36} \\ \dots & \dots & \dots & \dots & \dots & \dots & \dots & \dots & \dots & \dots & \dots & \dots \\ C_{14} & C_{24} & C_{34} & \vdots & C_{44} & C_{44} & \vdots & C_{45} & C_{45} & \vdots & C_{46} & C_{46} \\ C_{14} & C_{24} & C_{34} & \vdots & C_{44} & C_{44} & \vdots & C_{45} & C_{45} & \vdots & C_{46} & C_{46} \\ \dots & \dots & \dots & \dots & \dots & \dots & \dots & \dots & \dots & \dots & \dots & \dots \\ C_{15} & C_{25} & C_{35} & \vdots & C_{45} & C_{45} & \vdots & C_{55} & C_{55} & \vdots & C_{56} & C_{56} \\ C_{15} & C_{25} & C_{35} & \vdots & C_{45} & C_{45} & \vdots & C_{55} & C_{55} & \vdots & C_{56} & C_{56} \\ \dots & \dots & \dots & \dots & \dots & \dots & \dots & \dots & \dots & \dots & \dots & \dots \\ C_{16} & C_{26} & C_{36} & \vdots & C_{46} & C_{46} & \vdots & C_{56} & C_{56} & \vdots & C_{66} & C_{66} \\ C_{16} & C_{26} & C_{36} & \vdots & C_{46} & C_{46} & \vdots & C_{56} & C_{56} & \vdots & C_{66} & C_{66} \end{pmatrix},$$

and second-order tensors as

$$\boldsymbol{\sigma} = \begin{pmatrix} \sigma_{11} \\ \sigma_{22} \\ \sigma_{33} \\ \dots \\ \sigma_{23} \\ \sigma_{32} \\ \dots \\ \sigma_{31} \\ \sigma_{13} \\ \dots \\ \sigma_{12} \\ \sigma_{21} \end{pmatrix}.$$

In a TIV medium, the stiffness matrix is

$$\mathbf{C} = \begin{pmatrix} \lambda_{\perp} + 2\mu_{\perp} & \lambda_{\perp} & \nu & \vdots & 0 & 0 & \vdots & 0 & 0 & \vdots & 0 & 0 \\ \lambda_{\perp} & \lambda_{\perp} + 2\mu_{\perp} & \nu & \vdots & 0 & 0 & \vdots & 0 & 0 & \vdots & 0 & 0 \\ \nu & \nu & \lambda_{\parallel} + 2\mu_{\parallel} & \vdots & 0 & 0 & \vdots & 0 & 0 & \vdots & 0 & 0 \\ \dots & \dots & \dots & \dots & \dots & \dots & \dots & \dots & \dots & \dots & \dots & \dots \\ 0 & 0 & 0 & \vdots & \mu_{\parallel} & \mu_{\parallel} & \vdots & 0 & 0 & \vdots & 0 & 0 \\ 0 & 0 & 0 & \vdots & \mu_{\parallel} & \mu_{\parallel} & \vdots & 0 & 0 & \vdots & 0 & 0 \\ \dots & \dots & \dots & \dots & \dots & \dots & \dots & \dots & \dots & \dots & \dots & \dots \\ 0 & 0 & 0 & \vdots & 0 & 0 & \vdots & \mu_{\parallel} & \mu_{\parallel} & \vdots & 0 & 0 \\ 0 & 0 & 0 & \vdots & 0 & 0 & \vdots & \mu_{\parallel} & \mu_{\parallel} & \vdots & 0 & 0 \\ \dots & \dots & \dots & \dots & \dots & \dots & \dots & \dots & \dots & \dots & \dots & \dots \\ 0 & 0 & 0 & \vdots & 0 & 0 & \vdots & 0 & 0 & \vdots & \mu_{\perp} & \mu_{\perp} \\ 0 & 0 & 0 & \vdots & 0 & 0 & \vdots & 0 & 0 & \vdots & \mu_{\perp} & \mu_{\perp} \end{pmatrix}$$

(the equivalent matrix for an isotropic medium is a trivial simplification).

The polarization-slowness dyadic is

$$\mathbf{\Theta} = \begin{pmatrix} g_1 p_1 \\ g_2 p_2 \\ g_3 p_3 \\ \dots \\ g_2 p_3 \\ g_3 p_2 \\ \dots \\ g_3 p_1 \\ g_1 p_3 \\ \dots \\ g_1 p_2 \\ g_2 p_1 \end{pmatrix}$$

(it is not important whether we define this symmetrically or not). The required scattering term is then

$$-\mathbf{g}^{\mathbf{R}^T} \mathbf{Z}_k^{\mathbf{R}^T} \mathbf{s}_{kj}^{\mathbf{B}} \mathbf{Z}_j^{\mathbf{S}} \mathbf{g}^{\mathbf{S}} = \mathbf{\Theta}^{\mathbf{R}^T} \mathbf{C}^{\mathbf{B}} \mathbf{\Theta}^{\mathbf{S}},$$

where $\mathbf{C}^{\mathbf{B}}$ is the perturbation of the stiffness matrix above, and in the vector-matrix algebra we have 1×9 times 9×9 times 9×1 reducing to a scalar. Computations are straightforward for isotropic, TIV or even general anisotropic media.